NOTE TO USERS

This reproduction is the best copy available.

UMI

DISSERTATION

MUTAGENIC EFFECTS OF IONIZING RADIATION ON A_L HYBRID CELLS IN DIFFERENT COMPARTMENTS OF THE CELL CYCLE

Submitted by

Holly Ruth Franz

Department of Radiological Health Sciences

In partial fulfillment of the requirements

for the Degree of Doctor of Philosophy

Colorado State University

Fort Collins, Colorado

Summer 2002

ProQuest Information and Learning Company
300 North Zeeb Road
P.O. Box 1346
Ann Arbor, MI 48106-1346

COLORADO STATE UNIVERSITY

April 26, 2002

WE HEREBY RECOMMEND THAT THE DISSERTATION PREPARED UNDER OUR SUPERVISION BY HOLLY RUTH FRANZ ENTITLED MUTAGENIC EFFECTS OF IONIZING RADIATION ON A_L HYBRID CELLS IN DIFFERENT COMPARTMENTS OF THE CELL CYCLE BE ACCEPTED AS FULFILLING IN PART REQUIREMENTS FOR THE DEGREE OF DOCTOR OF PHILOSOPHY.

Committee on Graduate Work

Adviser

Department Head

ABSTRACT OF DISSERTATION

MUTAGENIC EFFECTS OF IONIZING RADIATION ON A_L HYBRID CELLS IN DIFFERENT COMPARTMENTS OF THE CELL CYCLE

I used the A_L assay to investigate mutant induction and spectra during the cell cycle. A_L cells are human X hamster hybrids containing one human chromosome 11 and a normal complement of CHO chromosomes. On the short arm of chromosome 11, at 11p13, is the selection gene for the A_L assay that codes for the CD59 surface antigen. *CD59*$^-$ mutants survive an antibody/complement attack that lysis wild-type cells expressing the antigen. The advantage of the A_L assay is that the human chromosome provides a large non-lethal target allowing analysis of mutational spectra from a few base pairs to 1.6 X 10^8 bases. Centrifugal elutriation was used to collect large populations of A_L cells enriched for early G_1. The resultant elutriated cells were incubated and allowed to progress in phase through the cell cycle. Timing of the replication of the CHO and human chromosomes was analyzed using flow cytometry, bromodeoxyuridine (BrdU) labeling, and fluorescent *in-situ* hybridization (FISH). The analyses showed that S phase and DNA replication of the CHO and human chromosomes began at 5.5 hours after plating the early G_1 cells and continued through 12.5 hours. Most of human chromosome 11 replicated between 6.5 to 8.5 hours, with the remainder replicating from 8.5 to 12.5 hours. Mutation was measured as the loss of expression of the human CD59 antigen. A_L cells were irradiated in specific cell cycle compartments with ^{137}Cs-γ to determine the number and spectra of mutants produced. When irradiated, G_1 cells were most susceptible to killing, followed by S phase cells. G_2 cells were the most resistant to cell killing. Irradiated with 3 Gy and with background subtracted, early G_1 cells produced

426 mutants/10^5/surviving cell (dose/LD_{50}). In S phase, mutant induction dropped to 68 mutants/10^5/ surviving cell, and G_2 phase produced as little as 43 mutants/10^5/surviving cell. Mutant induction was low when the *CD59* gene was replicating. The mutant spectra were determined throughout the cell cycle. Mega-base pair deletions were much more frequent than intragenic mutations in all phases of the cycle. Mutant induction "hot-spots" were discerned on the human chromosome during different phase of the cell cycle.

Holly Ruth Franz
Department of Radiological Health Sciences
Colorado State University
Fort Collins, CO 80523
Summer 2002

ACKNOWLEDGMENTS

In the pursuit of an advanced degree a student never works alone. You learn more from your fellow students; post doctoral researchers and salaried research scientists in the laboratory than from sitting in class. In my degree program for a PhD I learned a great deal from many people and was unselfishly helped by many more.

I would like to thank the people who sponsored me for this degree. To start with the head of the Department of Biology at the United States Air Force Academy, Col. Ron Reed who selected me for the program and Col. Jim Kent and Lt. Col. Jeff Johnston who were my mentors through my degree program. Thanks to Lt. Col. Tom Unangst for his review of my manuscripts. In Florida, thanks to those who looked after me and kept pushing me to get this done: T. Kline, Scott Smith, Scott Ward and Col. David Trask.

The administrative staff and Professors at the Department of Radiological Health Sciences at Colorado State University were always helpful and willing to go an extra mile. Thanks to the front office staff: Julie Asmus, Sandy Wiggen, Linda Jones, Joanne Brown, Lee Wiedeman, and Chuck Sampier. Dr. Michael Fox was very helpful concerning all areas of flow cytometry along with his lab assistant Leslie Armstrong. All I learned--well most of what I learned about radiation therapy I learned from Dr. Susan LaRue. Thanks Dr. LaRue for the insight into treatment planning as well as being one of my committee members. To my outside committee member Dr. Hank Gardner, thank you for joining the team. I look forward to working with you in the future.

The close collaborations between the Waldren Lab and the Bedford Lab was a positive influence on all involved and led to some great times at Pitchers and BW-3. Special thanks to Allen Christian for his help on doing PCR and the special art that is FISH and the Metamorph measurements. Thanks to Tom Fisher for his help on apoptosis measurement. Maria Mühlmann-Diaz was a wonderful mentor on FISH and the preparation of cells spreads. And last but not least, Dr. Joel Bedford for his help and guidance, and his worry for my roller bottles when the power went out, but especially for being on my committee.

As for the Waldren Lab--it's the best. To begin with a clean lab is a happy lab and a lot of the grunt work went to Steven Rappie and Emily Hall. Without their help work stopped, pipettes stagnated, and those traps--oh they got messy. Thanks for all the work on the not so glamorous stuff.

The School Teachers. The summers would not be complete with out my summer students "the school teachers". The first teacher to the plate was Keri Keever. We contaminated more cell lines that summer and grew the most beautiful fungus. The second summer I had help from Rudy Sanchez--the master cell farmer. The cleanup teacher was Tammy Dorsey, the PCR and Southern Queen. All added to the summer ambiance in the lab and to the energy level of a really fun research program. Thanks.

The Fellow Graduate Students. This would be Sue Kramer and Krystal Meyer in the Waldren Lab. Thanks for your help and fellow suffering.

The Young Mysterious Men. Who could forget the computer master Chris Quirk? His riding in with the electronic calvary saved many a sticky computer problem. Then there is Mike White. The slayer of the Frigidair, the keeper of the Bib-3 clones--

where the hell did those clones get to?

The Post Docs. Dr. Elizabeth McNeil it was fun to have you in class and to learn about your dark side. Yes--she parties more than any doctor should. Dr.^{2} McNeil was a mild mannered lab worker by day wild woman by night. Dr. Russell Drabek kept all the little things running in the lab, he can fix anything and was always innovative. I learned more from Dr. Dan Gustafson than anyone with maybe the exception of Diane. Dan was always helpful and occasionally caustic, but he kept every one on their toes in the lab and always pushed us to do the best science possible.

The Hired Hands. Jeanne Robinson is the slide prep queen and the true FISH master, and incredibly helpful. Then there is Megan McGraw the challenge meister, the F12 guru, an amazing selfless and patient help to any and all in the lab. And the winner of the Academy Award picks pool. Dr. Akiko Ueno thanks for your help in wading through the intricacies of challenges.

The Swami. She who must be obeyed. She who knows all. Any question, any procedure, any detail--Diane Vannais of course. The greatest pleasure of working in the Waldren Lab was working with Diane. I learned so much from her-- and she hardly ever looked at you like you were a clueless dweeb--in fact only when you deserved it. Who could forget the Chia head? I also remember Diane's endless details of the food from her travels. The wise words "drop it, it's going to explode". Thanks Diane, I learned so much from you.

The Boss. Charles Waldren thanks for allowing me into your enclave. The lab you run is a challenging and productive working environment but incredibly fun. I am still amazed at how you can pull those references from the thousands right out of your database.

The final thanks are to friends and family. Jim Abraham and Steve Reese made going back to school a blast. What other friends would come up to the lab during an all night experiment and drink beer and eat pizza with you. They are tough guys, and did not complain too much when I took them skiing. There is nothing like a run down Splash Down at 4:00 pm at Loveland when you legs are on fire; nothing that a few Fat Tires couldn't fix.

To my family, thanks for being there. It was incredibly nice to have most of my family within two hours. Thanks to my sisters in Vail, thanks for being there when I called. To my brothers in Denver, it was always nice to stop by and see you, and to have your help when I called. To Aunt Yvonne, the lost Swedish relative--thanks for all your help. Thanks to my Mom and Dad for all the help and support, and the get-a-ways to Vail. And finally, to Adam, Phil, Candy, and Sam for always being there and always being happy.

Thanks,

Holly R. Franz

MUTAGENIC EFFECTS OF IONIZING RADIATION ON A_L HYBRID CELLS IN DIFFERENT COMPARTMENTS OF THE CELL CYCLE

TABLE OF CONTENTS

CHAPTER 1

INTRODUCTION

Cancer arises from mutations (Frieben, 1902; Tyzzler, 1916; Muller, 1956; Eadie et al., 1984; Marx, 1994; Laird et al., 1995; Essers et al., 1997; Huang et al., 1997; Ponnaiya et al., 1997; Tommasi et al., 1997). DNA is constantly attacked and damaged by a number of sources, endogenous and external (Ames, 1989; Waldren et al., 1999). Ionizing radiation, for example, causes base and sugar damage, double strand breaks, and chromosome breaks in DNA leading to deletions, inversions, translocations, and loss of entire chromosomes (Borek, 1981; Waldren et al., 1986; Ames, 1991). Ultraviolet light causes dimers and cyclic rings in the DNA structure leading to deformations in the DNA strand, DNA strand breaks, and base changes. Chemicals can cross-link DNA strands or DNA bases and add bulky adducts that leads to base changes and improper replication of the DNA in transcription and replication (Doll and Peto, 1981). Even the most basic metabolic process, oxygen metabolism, is a danger to DNA (Ames et al., 1987). The oxygen which cells need as the final electron acceptor in the electron transport chain can lead to free radicals of oxygen that wreak havoc on DNA (Ames, 1987; Ames, 1989; Rossman and Goncharova, 1998).

In addition to the relentless attack on DNA from outside sources, the bases of DNA itself are unstable and will naturally degrade over time. Cytosine can deaminate spontaneously to form thymine, leading to mispairings and mistakes in replication. Adenine and Guanine can also deaminate, but at much slower rates than cytosine (Lindahl, 1979). Loss of entire bases can also occur. Depurination and depyrimidination occur under normal physiological conditions (Saul and Ames, 1991; Lindahl, 1993).

With this constant onslaught on DNA, it is amazing that cells survive and function at all. Nevertheless life has evolved in an environment fraught with these challenges to DNA and has developed the means to combat and repair the damage to the genome.

Numerous responses have evolved to repair DNA damage including mismatch repair, base excision repair, and nucleotide excision repair (Friedberg, 1995; Wood, 1996; Wood, 1997; Jeggo, 1998; Yu et al., 1999). These repair processes allow cells to repair DNA damage and ensure that no mistakes, or a minimum of mistakes, are passed on to daughter cells.

The amount of DNA damage and the resulting mutation induction have been studied in many assay systems (Chu and Malling, 1968; Puck et al., 1971; Clive, 1972; Arlett et al., 1975). Generally, mutation assays are applied to a population of cells growing in log phase. Mutagens can be ionizing radiation, ultraviolet radiation (UV), chemicals, or other substances, such as food additives, an anti-cancer drug, or other pharmacological agents. The treatment and testing possibilities cover a myriad of substances that have been implicated in causing malignant transformation in cells. After treatment, the populations of cells are assayed to see how many mutants have been induced. These assays are suited to measuring mutant induction in cycling, log phase cells, but may not reflect what occurs when cells are treated and their DNA is damaged while they are in different stages of the cell cycle. Cells are known to respond differently to killing and ionizing radiation mutagenesis depending upon which cell cycle phase they are in (Sinclair and Morton, 1966; Dewey et al., 1970; Burki, 1980; Leonhardt et al., 1997).

The aim of this dissertation is to apply the A_L mutation assay to cells in different

compartments of the cell cycle and to compare the results obtained for numbers and kinds of mutants with randomly distributed cells. I used the A_L assay to better understand cell sensitivity to mutagens at different phases of the cell cycle. After completing mitosis (M) cells move into life cycle phase G_1 (gap one) where they sequester and manufacture the materials needed for DNA replication. The beginning of replication marks the beginning of S phase, or synthesis phase, followed by G_2 (gap two) where the cells prepare for mitotic division or M phase. In the human body, as in any mammal, there are relatively few cell populations that are rapidly cycling; examples of those include the epithelial layers of the skin, the lining of the gut, the epithelial layer of ducts and glands, the reticuloendothelial system, hair follicles, and the spermatogonia in the testes, but the vast majority of cells are in a state of non-proliferation (Ross and Reith, 1985; Preston-Martin et al., 1990). Such cells are described as being in G_0, not growing or dying, but maintaining a state of homeostasis. Non-cycling cells may accumulate mutations and do not need to be cycling to express these mutations in their genome (O'Neill et al., 1982). My cells were in G_1, not G_0, but provide a close approximation of G_0 cells. I studied these non-cycling cells with a model assay system so as to provide partial answers to questions like: How do these G_0 or G_1 cells respond to DNA damage? How does mutant induction compare in S phase, G_2, or M? What is the spectrum of mutants through the cell cycle?

In Chapter 1, I describe the A_L mutation assay system, which is based on a hybrid human-Chinese hamster ovary (CHO) cell containing a single human chromosome number 11 plus a normal set of CHO chromosomes, and compare it to other gene assays. In addition, I provide a background on the A_L assay system and the gene (*CD59*) used for

mutation selection in the A_L system. I also describe techniques, primarily centrifugal elutriation, used to phase populations of cells. In Chapter 2, I characterize the A_L cells in log phase and described how I synchronized cell populations and treated them with ^{137}Cs gamma radiation to study both the mutant number and type as the cells moved through the cell cycle in a cohort. I also determined when during S phase the gene of interest, *CD59* was replicating, and how or if replication affected mutant induction. In Chapter 3, I measured mutant induction throughout the cell cycle and characterized the spectra of mutants by identifying presence or absence of specific genetic sequences on human chromosome 11 after the A_L cells were treated with ^{137}Cs gamma rays during each phase of the cell cycle.

REVIEW OF MUTATION ASSAYS

Bacterial Assays

The Ames test, named after its developer Bruce Ames, is a widely used mutation assay that measures reversion from requiring histidine to not requiring histidine in the bacteria *Salmonella typhimurium* (Ames, 1971; Ames et al., 1973; Ames et al., 1975; McCann et al., 1975; McCann and Ames, 1976). The Ames test is recommended in a review of assays entitled Department of Health and Human Services, Food and Drug Administration, International Conference on Harmonization; Guidance on Genotoxicity: A standard battery for genotoxicity testing of pharmaceuticals (1997) (subsequently referred to as the 1997 FDA assay paper) as one member of a battery of assays by the Food and Drug Administration (FDA). No single test is adequate to detect all relevant genotoxic agents. The Ames test was recommended as a bacterial mutation assay. The Ames assay uses *Salmonella* that are histidine auxotrophs (*his*$^-$) as the initial bacterial

populations to be treated with a mutagen. The bacteria and the test substance are plated on petri dishes in a medium containing a minimal amount of histidine. Since they are histidine auxotrophs, they will not grow once histidine is depleted, but the small amount of histidine allows the bacteria to survive until some cells have induced mutations that revert the cells from *his*$^-$ to *his*$^+$. The Ames assay is a reverse assay from – to + so it is less sensitive than forward assays, i.e. the mutation must cause reversion back to a functional form of the gene rather than just knocking out the functional gene (Ames et al., 1975). Cells that have reverted to histidine production, by a frame shift mutation for certain strains or by base substitution for other strains of *S. typhimurium*, will grow as colonies on the petri dish (Ames et al., 1975). Modifications to this system have made it more sensitive to certain mutagens.

Many substances are not mutagenic or carcinogenic until metabolized by enzymes such as those in normal liver. By adding rat liver extract, substances can be activated to mutagenic forms much like what occurs in mammalian liver *in vivo* (Malling, 1971; Ames et al., 1973; Matsuoka et al., 1979; O'Neill et al., 1979). Depending on the strain of *S. typhimurium* used, frame shift mutations, base substitutions, and small deletions of up to about 6 base pairs can be detected (Maron and Ames, 1983). The system provides no information about deletions larger than a few base pairs and other types of DNA/chromosomal damage such as translocations, chromosomal deletions, and chromosomal loss. The FDA assay paper recommends other assays to detect larger deletions.

Lower Eukaryote Assays

Other assays have been developed based on fungi, yeast, and other lower

eukaryotes. For example, the fungus *Neurospora crassa* has been used to study photoreactivation and mutagen sensitivity (de Serres et al., 1967; de Serres and Malling, 1971; Ishii and Inoue, 1989; de Serres, 1991; de Serres, 1994). The yeast, *Saccharomyces cerevisiae,* (Zimmerman, 1973; Hartwell, 1992; Hartwell, 1994) and the slime mold, *Dictyostelium discoideum,* (Welker and Deering, 1978; Bronner et al., 1992) have both been used to study the action of DNA-damaging agents. These fungi and slime mold-based systems provide the ability to measure different repair mechanisms and to look at mutation to more complex organisms. Lower animal models have also been useful to study mutation. For example the nematode, *Caenorhabditis elegans,* has been used to study excision repair in response to DNA-damage (Hartman et al., 1989). Many of the earliest mutation induction experiments were carried out with the fruit fly, *Drosophila melanogaster,* (Muller, 1927; Muller, 1939; Muller, 1940) and remain a mainstay for the study of mutant induction and DNA repair. All of these systems provide some information relevant to mutation detection on higher forms of life, but to extrapolate data to human mutagenesis and repair, the best assays are likely based on mammalian systems.

Mammalian Cell Assays

The ouabain resistance mutation assay and the diphtheria toxin resistance mutation assays allow for the measurement of small mutations such as frame-shift, base substitutions, and thymine dimers caused by UV exposure (Colella et al., 1986). Ouabain is a cardiotonic steroid and a potent inhibitor of sodium-potassium ATPase, part of the sodium-potassium pump that maintains electrochemical charge between the inside and outside of the cell membrane as described in Stryer (1988). When bound on the

extracellular face of the cell membrane, ouabain inhibits the dephosphorylation reaction of the Na^+-K^+ ATPase (Stryer, 1988). Ouabain competes for binding with K^+ on the outside of the cell membrane at the Na^+-K^+ ATPase. When ouabain binds to the enzyme, K^+ cannot be transported to the interior of the cell. These cells are "ouabain hypersensitive (OUA^S)" and will be killed by ouabain at concentrations that do not kill wild-type cells. A small change in the base sequence of the sodium-potassium ATPase will allow the potassium to fit in the active site and exclude the ouabain; these cells are ouabain-resistant (OUA^R). Because the change in sequence is small, this forward mutation system is effective for measuring small base changes in the sequence of the ATPase; however, Thacker et al. (1978) showed that the ouabain assay could not detect larger mutations caused by ionizing radiation because the large mutations will delete the entire ATPase gene. Thus, ionizing radiation, a known carcinogen and mutagen, would be erroneously considered a non-mutagen using this assay.

Friedrich and Coffino (1977) found that x-rays would induce mutants at the hypoxanthine-guanine phosphoribosyl transferase *(HPRT)* gene, but not at the gene for ouabain resistance in mouse lymphoma cells. Large deletions in the sodium-potassium ATPase gene led to cell death, which limits the use of this mutation system for measuring damage and mutation due to ionizing radiation. The ineffectiveness of this assay for measuring ionizing radiation, because ionizing radiation tends to cause larger deletions and disruptions to the chromosomes, is well documented (Arlett et al., 1975; Cleaver, 1977; Thacker et al., 1978; Liber et al., 1983). However, the ouabain assay has proved effective measuring radiation induced genetic instability. Little et al. (1998) showed a 3- to 30-fold increase in the frequency of ouabain resistance mutations; however, no

ouabain-resistance mutants were induced directly by x-rays.

In 1977, Moehring and Moehring first described the diphtheria toxin mammalian mutation (DT) assay. DT causes irreversible inhibition of protein syntheses by catalyzing the transfer of ADP-ribose from NAD^+ to a histidine residue of the protein synthesis factor, elongation factor-2 (EF-2), which inactivates the EF-2 and kills the cell (Pappenheimer, 1977; Van Ness et al., 1980; Drinkwater et al., 1982). The DT assay does not exhibit cell-density effects or metabolic-cooperation effects during selection, but it does show a sensitive response to mutation induction by certain mutagens (Gupta and Siminovitch, 1978; Glover et al., 1979). Mutant induction with ethylnitrosourea using the DT assay was about 10^{-3} mutants/viable cell at D_0, which is the log linear portion of the survival curve (Drinkwater et al., 1982). When the DT cells are targeted under the appropriate selection conditions, most of the DT resistant mutants contain small mutations to the EF-2 structural gene that causes the protein synthesis factor EF-2 to be resistant to DT (Moehring and Moehring, 1977, 1979; Gupta and Siminovitch, 1978). Drinkwater et al. (1982) found that membrane-receptor mutants would be eliminated by the high concentration of DT used in assay selection. In addition, they found that recessive post-translational mutants occur in low frequency in the diploid target cells. The primary mutations measured by this assay are base substitutions. This mutation system does not detect deletions and most frame shift mutations that cause the EF-2 to be inactive in protein synthesis, and thus, be lethal (Drinkwater et al., 1982). The DT mutation assay system is, therefore, useful for measuring small mutations, but not the entire spectrum of mutations, such as deletions, translocations and complex mutations that would be expected with ionizing radiation.

Mammalian Mutation Assays Useful for Measuring Ionizing Radiation

The adenine phosphoribosyl transferase (APRT) assay allows for molecular analysis of induced mutations in mammalian cells (Adair, 1987). The *APRT* gene used for selection is a constitutive enzyme in the purine salvage pathway. *APRT* is an autosomal locus located at 3p2, a very distal region of chromosome 3 in CHO cells (Adair et al., 1983). The size of the gene is 3.3 kilobases (kb) (Grosovsky et al., 1986), as compared to the 30 kb for the *HPRT* gene in CHO (Melton et al., 1984) described in a later section (see Table 1). The CHO cells used for mutant induction measurement are hemizygous for *APRT*, either $APRT^{+/-}$ or $APRT^{+/0}$. The $APRT^{+/-}$ cells are selected from an unmutagenized CHO cell population. The $APRT^{+/-}$ has intermediate levels of APRT activity, compared to the high level found in $APRT^{+/+}$. $APRT^{+/-}$ cells are selected based on their resistance to low concentrations of the adenine analog, 8-azaadenine; the $APRT^{+/+}$ cells are killed by low concentrations of 8-azaadenine (Adair et al., 1980). The selected $APRT^{+/-}$ cells are then exposed to a mutagen and are kept in log phase growth to allow expression of induced mutants. In the mutation assay, the $APRT^{-}$ mutant cells are selected by using 8-azaadenine or 2, 6-diaminopurine which are toxic, suicide adenine analogues that kill the cells when incorporated by the $APRT^{+}$ cells. The $APRT^{+}$ mutants are selected by blocking the *de novo* purine biosynthesis with amethopterine, azaserine, or alanosine while concurrently supplying adenine (Adair, 1987). The spontaneous mutation rate for the APRT assay is about 1.8×10^{-6} per cell/generation; the fraction is 23×10^{-6} per surviving cell induced by 5 Gy (Adair, 1987). This mutation assay in CHO cells is useful for measuring base substitutions, frame shifts, and small deletions caused by ionizing radiation (Grosovsky et al., 1988). This assay also detects larger mutations

commonly seen with ionizing radiation (Breimer et al., 1986; Turker et al., 1997). The APRT assay has been used very successfully with CHO cells. Bradley et al., (1988) found that CHO cells treated with ionizing radiation had complete deletions of *APRT*-linked sequences among APRT$^-$ mutants. Turker et al., (1995) used a mouse APRT mutation assay and were able to measure the large deletions caused by ionizing radiation. The APRT assay in CHO is peculiarly size limited; the assay in mice or rats detects much larger mutations (Turker et al., 1994).

Locus	**Protein Encoded**	**Size of Detectable Deletion**	**Map Site**
APRT	adenine phosphoribosyl transferase	2.6 kb	CHO 3p2 Human 16q24
TK	thymidine kinase	11-14 kb	Mouse 11 Human 17p21
HPRT	hypoxanthine-guanine phosphoribosyl transferase	~1 Mbp	Human Xq26
CD59	CD59	~160 Mbp	Mouse 2 Human 11p13.5

Table 1. Map location of genes used in various mammalian mutation assays and sizes of the detectable deletions.

The APRT assay does have several limitations for use with clastogens. The *APRT* gene used for selection is on an autosome and a normal cell usually carries two copies of the gene. When an *APRT*$^{+/-}$ cell is selected prior to assay development, the extent of the loss of any sequences adjacent to the gene is unknown. When the *APRT*$^{-/-}$ cells are selected after treatment with a mutagen, the loss of DNA sequences beyond the *APRT* mutant-selection gene is not usually lethal because the other autosome may provide

essential gene products. This assay is similar to the TK assay described next. Both assays use genes that lie on autosomes, and therefore, mapping the loss of chromosomal material past the selection gene is difficult because there may be one or two copies of neighboring genes.

The thymidine kinase (TK) assay is used with the mouse lymphoma line L5178Y developed into the TK mutation assay by Clive et al., (1972), or in diploid human lymphoblasts (Thilly et al., 1980; Liber and Thilly, 1982; Evans et al., 1986). The *TK* gene is between 11-14 kb in length and is located on mouse chromosome 11 and in human chromosome 17p21 (Evens et al., 1987; Meuth, 1990). The TK assay has been recommended as a system that detects gene mutations and clastogenic effects for pharmaceutical screening (mouse lymphoma TK assay) in the 1997 FDA assay paper described earlier. A heterozygous TK cell line must be constructed, generally from a homozygous $TK^{-/-}$ by selecting for a revertant of one allele in hypoxanthine, aminopterin, and thymidine (HAT) media to get a ($TK^{+/-}$). HAT media will kill any $TK^{-/-}$ cells but $TK^{+/-}$ cells will survive. The TK assay has been used to test diverse mutagens including ionizing radiation, UV light, ethyl methanesulfonate, butyl methanesulfonate, nitrosomethylurea, ICR-191, 4-nitroquinoline oxide, benzo[a]pyrene, fluorodeoxyuridine, mitomycin C, aflatoxin B_1, and even caffeine (Liber and Thilly, 1982; Evans et al., 1986; Clive et al., 1990; Davies et al., 1993). Prior to treatment with a mutagen, the $TK^{-/-}$ cells are removed from the population by growing in HAT or THMG media (3μg/ml thymidine + 5μg/ml hypoxanthine + 0.1 μg/ml methotrexate + 7.5 μg/ml glycine) (Clive, 1987). In a typical TK mutation assay, thymidine kinase competent hemizygous cells ($TK^{+/-}$) are exposed to a mutagen in growth media, and then incubated in a soft-agar

medium with trifluorothymidine (TFT) to select mutagen induced thymidine kinase-deficient ($TK^{-/-}$) clones (Amacher, 1984). The TK assay is very sensitive and can detect mutations for 6 Gy of X-rays at a level of 83 x 10^{-6} for large colonies, 314 x 10^{-6} for very large colonies, and a total of 397 x 10^{-6} (Clive, 1987). The two colony sizes suggest that there are either two genes involved giving multilocus deletions in the TK mutant, or alternate forms of alleles (Evens et al., 1990; Amundson and Liber, 1992; Evans, 1994). Molecular analysis has shown that small mutations usually result in large colonies and big mutations result in small phenotypic colonies (Oberly et al., 1986; Applegate et al., 1990; Davies et al., 1993). The small colonies have multi-locus mutations such as deletions that affect the TK gene and a gene involved in normal growth, however the correlation between colony size and the deletion size is very poor (Clive, 1987; Moore and Doerr, 1990). Balzac et al. (1989) observed, "not all small colonies are caused by the induction of large deletions of translocations of genomic material in the vicinity of the tk allele". Evans (1994) describes the complexity of the TK assay regarding differences between a heterozygous and hemizygous TK assay. She found ionizing radiation-induced mutant frequencies were dramatically higher in L1578Y mouse lymphoblasts when the genetic marker analyzed was heterozygous (TK^{+}, LTK^{+}) than when hemizygous (TK^{+}, LTK^{+}, or *HPRT*). In contrast, mutagens that cause small mutations like base-changes induce similar mutant frequencies at hetero- or hemizygous loci. Their results indicate the mutagens that cause large deletions, such as radiation, induced mutants that harbor multilocus lesions. Furthermore, these large mutations are poorly recovered when the target gene is in a hemizygous chromosomal region.

The TK assay's strength lies in the fact that it measures mutation at only one

locus but can tolerate the loss of many loci, it can be used to measure point mutations as well as large clastogens (Davies et al., 1993). TK can be used as both a forward and reverse mutation system. In the forward mutation, $TK^{+/-}$ cells are exposed to a mutagen and the $TK^{-/-}$ mutants are selected with TFT media. For the reverse assay, $TK^{-/-}$ cells are exposed to a mutagen and the $TK^{+/-}$ cells are selected in HAT or THMG media (Clive, 1987). There is a 300-fold difference in the rates of the forward and reverse mutation system, with the forward system, $TK^{+/-} \rightarrow TK^{-/-}$ selected in TFT being 300 times more sensitive than the $TK^{-/-} \rightarrow TK^{+/-}$ selected in THMG (Clive, 1975). Spontaneous mutation of the $TK^{+/-}$ to $TK^{-/-}$ is about 2×10^{-6} mutations/focus/generation (Clive, 1975). Compared to other assay systems, the mutant induction frequencies are much higher at the TK locus (Table 2) than at the HPRT locus and Na^+, K^+ -ATPase loci (ouabain) for both ionizing and UV radiation (Evans et al., 1986). The TK assay and the APRT assay have been used to show that large kinds of damage to the chromosome that are produced by ionizing radiation are fixed in viable mutated cells (Evens, 1994). The limit of the TK heterozygous assay (and the APRT assay) is that outside of the TK locus (APRT locus) there are two copies of each gene, which makes it difficult to characterize large deletions by mapping markers downstream or upstream of the lesion produced, and the mutants are poorly recovered in the hemizygous region (Evans, 1994).

The hypoxanthine guanine phosphoribosyl transferase (HPRT) assay is the most commonly used mammalian locus for mutation assays. It is used in human, mouse, and Chinese hamster cells. Its chief advantage is that it can be applied *in vivo*. The HPRT assay has been used to measure the mutagenicity of a hundreds of chemicals including alkylating agents, quinones, metal compounds, aromatic hydrocarbons, and aromatic

Cell Line	Radiation Type	Locus	Mutant Fraction Per 10^{-6}/ Gy/survivor	Reference
CHO D422	^{60}Co γ-rays	aprt	4.0	Breimer et al., 1986
CHO D422	^{137}Cs γ-rays	aprt	4.0	Grosovsky et al., 1986
mouse P19H22	^{137}Cs γ-rays	aprt	60	Turker et al., 1995
CHO D422	^{60}Co γ-rays	hprt	7	Breimer et al., 1986
L5178Y	^{60}Co γ-rays	hprt	13	Furuno-Fukushi et al., 1988
L5178YS1	250 kVp x-rays	hprt	5	Evans, et al., 1986
L5178YR83	250 kVp x-rays	hprt	7.5	Evans, et al., 1986
L5178YR16	250 kVp x-rays	hprt	15	Evans, et al., 1986
hB-cell TK6	80 kVp x-rays	hprt	5	Nelson et al., 1994
hB-cell TK6	100 kVp x-rays	hprt	6.5	Amundson et al., 1993
WI-L2-NS	100 kVp x-rays	hprt	24	Amundson et al., 1993
A_L	230 kVp x-rays	hprt	20	Waldren et al., 1986
HF12	x-rays	hprt	0.075	Morris et al., 1993
L5178YS1	250 kVp x-rays	tk	3200	Evans, et al., 1986
L5178YR83	250 kVp x-rays	tk	10	Evans, et al., 1986
L5178YR16	250 kVp x-rays	tk	2000	Evans, et al., 1986
TK6	100 kVp x-rays	tk	30	Amundson et al., 1993
WI-L2-NS	100 kVp x-rays	tk	300-800	Amundson et al., 1993
A_L	230 kVp x-rays	CD59	2000	Waldren et al., 1986
A_L	^{137}Cs γ-rays	CD59	750	Waldren et al., 1992

Kramer, 1996

Table 2. Comparison of mutant fraction for ionizing radiation in various mammalian mutation assays. This table compares the mutant fraction induced per 10^{-6}/Gy/clonable cell. The TK and CD59 assays give more mutants/Gy than the other assays.

amines (Li et al., 1988), as well as ionizing radiation (Cox and Masson, 1978). The *HPRT* gene codes for the purine salvage pathway enzyme hypoxanthine-guanine phosphoribosyl transferase found on the X chromosome; thus only one active copy is available for transcription, even in female cells, because one X chromosome is active while the other is a barr body and is inactivated (Chu and Malling, 1968; Albertini and deMars, 1973; Thilly et al., 1976; O'Neill et al., 1977). The size of the *HPRT* gene is approximately 34 kb in CHO cells and about 40 kb in human cells with an effective target size of 1 Mbp (Nicklas et al., 1991; Leonhardt, et al., 1997). Before treatment, the population can be cleared of preexisting HPRT$^-$ cells by growing the cells in HAT media (hypoxanthine, aminopterin, and thymidine). To measure mutant induction, the cells are treated with a mutagen and then allowed to express the loss of the *HPRT* marker by incubating them for 7-9 days. HPRT$^-$ mutants are then selected with 6-thioguanine, which kills wild type cells that have an intact *HPRT* gene. The HPRT assay is not as sensitive as the TK assay, but it is useful because it can be applied *in vivo*. The HPRT assay's lower mutant yield per survivor is most likely due to the presence of essential genes on both sides of the *HPRT* gene (Evens, 1991; Hei et al., 1994). With the HPRT assay large mutations are often lethal mutations. The HPRT assay has only one active copy of the X chromosome, so measuring large deletions and mapping mutant spectra is easier than with TK or APRT assays. The HPRT mutation assay is not well suited for low ionizing radiation (O'Neill et al., 1977). However, Thacker (1986) described how HPRT could be useful for measuring gamma radiation, because greater than 70% of the radiation induced HPRT$^-$ mutants were large genetic lesions (1 kb or greater) including deletions of part or the entire *hprt* gene.

The A_L Assay

The mutation assays described above provide various techniques and have various sensitivities to measure mutation. The gene targets for mutant-induction assays vary from a few base pairs to several kilobases. The target sizes range from very small for ouabain and DT, which measure small frame shifts and base pair deletions, to assays that can lose the entire gene and range in size from 2.6 kb for APRT, 11-14 kb for the thymidine kinase TK gene to 1 Mbp for the HPRT gene (Table 1). The A_L assay has the advantages of both the TK and HPRT assay systems; it is sensitive and is useful for measuring both small and large mutations. Furthermore, as shown below, the A_L assay detects ~100 more ionizing radiation induced mutants per unit dose per survivor than does the HPRT assay (Table 3). In the APRT and HPRT assays, if the mutation extends beyond the target gene, it is likely that the cell will die because of the loss of neighboring essential genes on the chromosome needed for cell survival. The A_L assay sidesteps this cell death by loss of essential genes, because the selection marker is on a fundamentally non-essential human chromosome 11.

When both the HPRT and the *CD59* are measured in A_L cells, the number of mutants measured at the CD59 locus is 30 to 60-fold greater than at the HPRT locus (Waldren et al., 1979; Zhu et al., 1996). The CD59 assay is as sensitive as the TK assay (Table 2), but like the HPRT assay, has only one copy of the chromosome with the selection marker, CD59, in each cell. The advantages provided by the A_L cell using the CD59 assay include sensitivity, gene location on a large target chromosome (~160 Mbp target provided by human chromosome 11), and the ability to measure both large and small genetic changes. These attributes make the A_L CD59 assay suitable for use as a

sensitive test for mutagenesis by ionizing radiation.

Agent	Mutants/10^5clonable cells/D_0[a]		Reference
	HPRT$^-$	A_LCD59$^-$	
X-ray	~1	>100	Waldren et al., 1986
UV (254 nm)	15	40	Waldren, 1983
MNNG	30	600	Waldren et al., 1986
EMS	20	250	Waldren et al., 1986
Benzo(a)pyrene	70	200	Waldren et al., 1986
Methyl cholanthrene	40	120	Waldren et al., 1999
Diagnostic ultrasound	0	0	Ritenour et al., 1991
Arsenite	20	220	Hei et al., 1998; Liu et al., 2001
Asbestos (chryostile)	0	175	Hei et al., 1992
Amsacrine[b]	0	150	Shibuya et al., 1994
MeIQ, PhIP[c]	0	~15	Waldren et al., 1999
Cigarette Smoke Condensate	0	~20	Matsukura et al., 1991

Table 3. Comparison of mutant yields at HPRT and A_L CD59 locus for various agents. A_L cells are not inherently hypermutagenic. The differences in yield for HPRT$^-$ and CD59$^-$ mutants are due to differences in the sizes of the mutations (effective target size) detectable at the two loci, approximately 1 x 10^6 for HPRT and 160 x 10^6 for CD59. [a] D_0 = mean lethal dose. [b] Amsacrine is a chemotherapeutic drug that inhibits DNA topoisomerase II. [c] MeIQ and PhIp are found in cooked meats.

The CD59 assay was used in my research. The cell line used is referred to as A_L, or the lethal antigen line (Puck et al., 1958; Puck et al., 1971; Waldren and Jones, 1981; Waldren, 1983). The A_L hybrid cell contains a standard set of CHO-K1 chromosomes (CHO, Chinese hamster ovary) and a single copy of human chromosome 11 derived from human amniotic fluid fibroblasts (Waldren, 1983). A_L cells are easy to grow, have a cell cycle time of 12-13 hours, a plating efficiency of 80% or better, and a small chromosome number--20 total chromosomes, 19 CHO and one human chromosome 11 (Jones et al., 1975). Three versions of A_L cells were used in this study (Waldren et al., 1992). They

were either the AH1-9 cells that have the hygromycin-resistance gene (G418) inserted only into human chromosome 11 as a selection feature, or AND-6 that are resistant to neomyosin, and also inserted in the human chromosome 11 (Waldren et al., 1992). The genes for hygromycin and neomyosin resistance were site directed into chromosome 11 by DNA transfection in the presence of human ALU sequences. This allows for selection of either cell line of cells that have retained the human chromosome by growing in the appropriate antibiotic. AM2 cells were also used; these cells are AND-6 cells containing a single copy of human O-6 methylguanine methyl transferase gene in a hygromycin construct lipofected into the cells (Gustafson et al., 1997). All three versions of A_L cells have the same growth characteristics, including a cell cycle time of about 13 hours. The primary strain used was the AM2 cells, which tended to have lower levels of background mutants.

The A_L CD59 assay is different from the other assays in that the target, the entire human chromosome 11, is approximately 160 Mbp (Figure 1) and only a tiny portion of human chromosome 11 is needed for cell survival of the A_L cells (Waldren et al., 1979; Waldren, 1983; Hei et al., 1992; McGuinness et al., 1995). The gene with which the mutation is selected is the *CD59* gene, formally known as *MIC1, S1 and* a_1 in A_L (Kao et al., 1977; Davies et al., 1989; Glaser 1989, Wilson et al., 1999). Expression of the CD59 antigen also depends on the correct function of about 10 CHO genes that are also targets for mutation (Kinoshita et al., 1997). *CD59* consists of four exons, three that are translated. It spans approximately 20kb of DNA (Petranka et al., 1992) see Figure 2. CD59 encodes a cell surface antigen, CD59 (described in detail later) that is lost, as measured by fluctuation analysis, at a rate of 4×10^{-6} to 15×10^{-6} per generation per cell

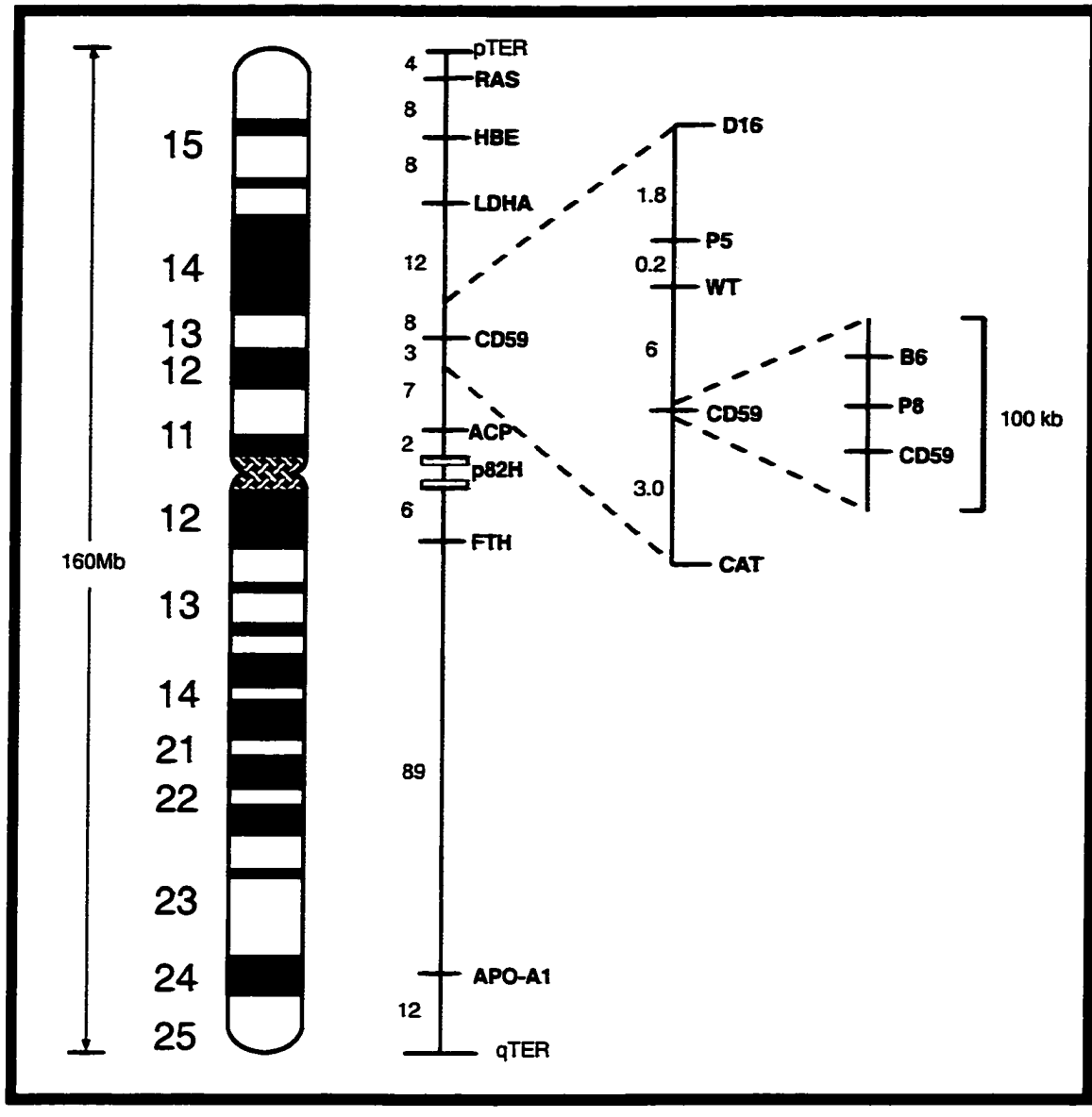

Figure 1. Diagram of human chromosome 11. CD59 is located at 11p13.5. The vital hostage locus is located near RAS. The length of human chromosome 11 is 160 Mb. The other markers are shown in relation to CD59. D16, P5, P8, WT (Wilms' tumor), B6, and CAT (catalase) are all located at 11p13. LDHA (lactate dehydrogenase-A) is at 11p14-p15; HBE (hemoglobin) is located at 11p15, while RAS (H-*ras*) is at 11p15.5. ACP (acid phosphatase-2) is located at 11p11. P82H is an alphoid repeat found at the centromeres of all human chromosomes. FTH (ferretin) is found at 11q13 with APO-A1 (apolipoprotein A1) found at 11q24 (Mitchell et al., 1985; Hei et al., 1992; Shibuya et al., 1994; McGuinness et al., 1995; Waldren et al., 1999). Note: this chromosome 11 has not rearranged during its time in the A_L hybrid and was in fact chosen as the reference human chromosome 11 for the human genome project (Shows et al., 1996). The A_L human chromosome 11 also repairs ionizing induced damage as effectively as chromosome 11 in normal human cells (Fouladi et al., 2000).

in A_L cells (Hinkle, 1980; Waldren, 1983; Kraemer and Waldren, 1997). This fluctuation rate is roughly 20 times greater than for HPRT and reflects the fact that more kinds of damage can produce viable CD59$^-$ mutants than HPRT$^-$ mutants (Waldren, 1983). The rest of the human chromosome, except for a small portion at the tip of the q arm of human chromosome 11 at 11p15.5 is not necessary for the normal function of the cell (Gerhard et al., 1987; Glaser et al., 1989). The unknown, vital gene that encodes this hostage locus is located near the *RAS* locus, but is not *RAS* (Figure 1). It has not been identified. In addition, the human chromosome 11 target of 160 Mbp provides the ability to measure large deletions that are commonly caused by ionizing radiation and other clastogenic agents (Waldren et al., 1979; Waldren, 1983; Puck and Waldren, 1987; Waldren and Puck, 1987; Matsukura et al., 1991; Waldren et al., 1999).

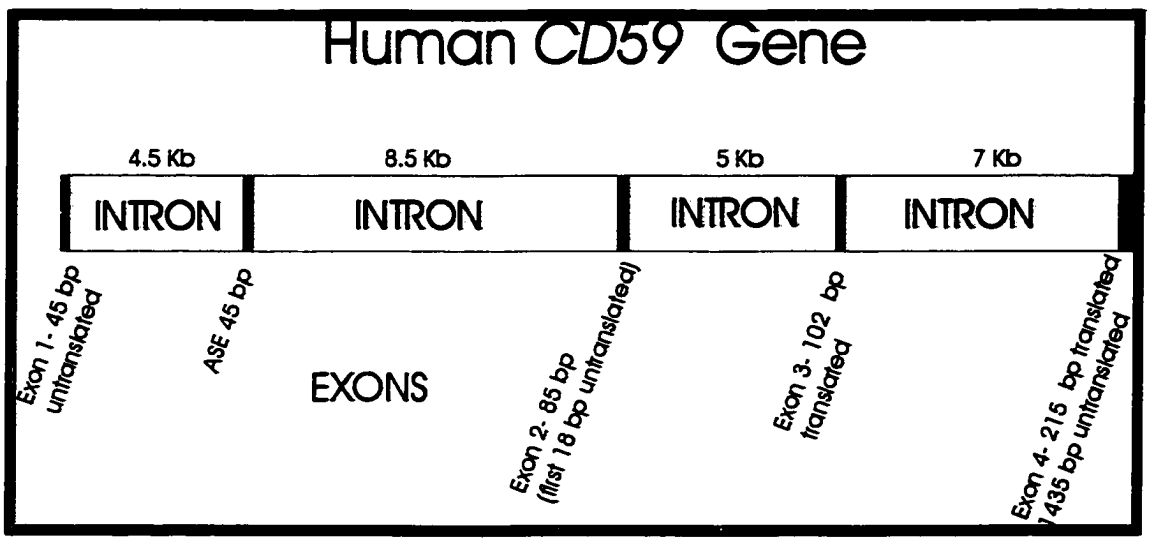

Figure 2. Human *CD59* has four exons and one alternative spliced exon (ASE). The four exons span about 20 kb (Tone et al., 1992; Petranka et al., 1992; Wilson et al., 1999)

The CD59 gene has been sequenced and PCR primers have been constructed which allows the analysis of intragenic mutations by polymerase chain reaction (PCR) or

by sequencing (Figure 3) (Wilson et al., 1999). The binding sites for CD59 to the cell and for complement to CD59 are located in exon 4. Thus, exon 4 is a principal region of mutation. The A_L assay has been used to measure mutant induction by ionizing radiation including x-rays, gamma rays, neutrons, and α particles, high HZE carbon and iron nuclei, as well as N-methyl-N'-nitro-N-nitrosoguanidine, ethylmethane sulfonate, ultraviolet light, colcemid, cigarette smoke condensate, ultrasound, asbestos, amsacrine, and various mutagens created by cooking certain foods (Table 2) (Waldren and Jones, 1981; Hei et al., 1988; Matsukura et al., 1991; Ritenour et al., 1991, Hei et al., 1992, Waldren et al., 1992; Shibuya et al., 1994; Hei, et al., 1997; Waldren et al., 1999).

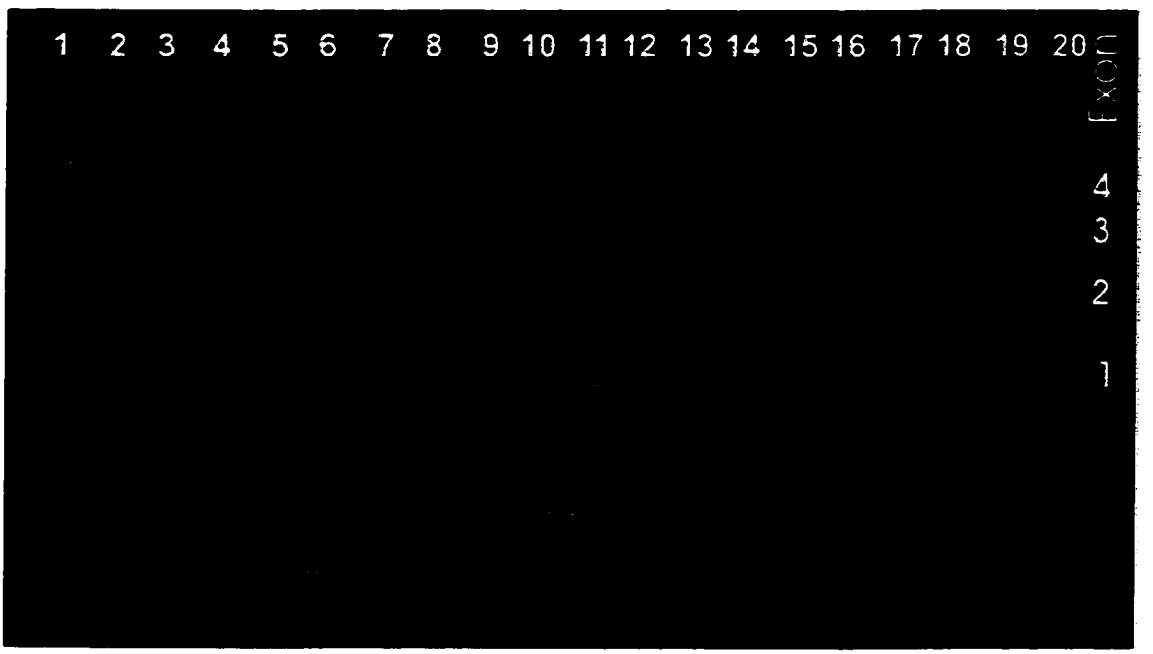

Figure 3. PCR analysis of mutations affecting the *CD59* gene in A_L cells. Molecular weight markers (100 bp ladder) were run in lane 1. A_L cell DNA was extracted and run in lane 2 showing CD59 exons 1-4 (87 bp, 205 bp, 300 bp and 401 bp respectively). CHO cell DNA was run in lane 3 and a negative control (no template) in lane 4. Lanes 5-20 were mutagen treated A_L cells selected with the E7.1 antibody in the A_L assay, each of these cell populations was *CD59*$^-$ but not missing other markers. (Data discussed in Chapter 3)

CD59 was formerly known as S1, and before that a1 (Puck et al., 1971; Jones et al., 1975; Ritenour et al., 1991; Wilson et al., 1999). *CD59* has been mapped to the 11p13.5 locus of human chromosome 11 (Glaser, 1989; Holguin et al., 1996) (Figure 1). Cells that lose the *CD59* locus of chromosome 11 survive in the presence of a monoclonal antibody E7.1 directed against the CD59 antigen and rabbit serum complement (Carey et al., 1976; Waldren et al., 1986; Shibuya et al., 1994; Wilson et al., 1999). When a monoclonal or polyclonal anti-human CD59 antibody is added to A_L cells, the complement cascade is initiated on cells that express CD59, enabling rabbit serum complement to lyse the cells. Mutant (*CD59*$^-$) cells not expressing CD59 are spared because the complement is not activated. The CD59 encoded by CHO genes may provide protection from the rabbit serum complement-mediated lysis (Braoveanu et al., 1995; Braoveanu et al., 1996). Because there is only one copy of the human *CD59* gene, and one copy of human chromosome 11 in A_L cells, this assay allows for the measurement of mutant spectra to include the entire length of human chromosome 11. The next section provides a background on CD59.

CD59 - Normal Function in Human Cells

The CD in CD59 stands for cluster of differentiation in the nomenclature system used to identify differentiation antigens recognized by particular monoclonal antibodies on the surface of human leukocytes (Barclay, 1993). CD59 is an 18-20 kDa membrane protein attached to the cell membrane by a glycosylphosphatidylinosotol (GPI) anchor. CD59 is constitutively expressed in numerous tissues including hematopoietic cells, platelets, and numerous non-hematopoietic cells such as the vasculature of the heart, kidney and liver (Davies et al., 1989; Meri et al., 1991; Maciejewski et al., 1996; Byrne et

al., 1997). CD59 has also been found in exogenous bodily fluids including breast milk, and seminal fluid (Rooney et al., 1993; Bjorge et al., 1996). In breast milk, Bjorge hypothesized that CD59 may provide protection for an infant from complement activation of the serum complement proteins found in breast milk. In the female reproductive tract after coitus, CD59 in the seminal fluid prevents complement activation and helps the sperm survive. CD59 is also expressed on spermatozoa; antibody blocking of this Membrane Attack Complex (MAC) inhibitor increases lysis of sperm *in vitro* (Rooney et al., 1993). CD59 is also known in the literature as Membrane Inhibitor of Reactive Lysis (MIRL), protectin, H19, MEM-43, Membrane Attack Complex Inhibitory Factor (MACIF), and HRF-20 (Davies and Lachmann, 1993).

The phosphatidylinositol-glycan class A (PIG-A) gene is necessary for the synthesis of early intermediates in the GPI anchor, and this gene is usually the one missing or mutated in the genetic disease Paroxysmal Nocturnal Hemoglobinuria PNH (Holguin et al., 1996; Hatanaka et al., 1996; Tomita, 1999; Nishimura, 1999). CD59 cell-surface expression can be completely abolished by treating the cells with 5 U/ml of phosphatidylinositol-specific phospholipase C (Brasoveanu et al., 1995). GPI anchored proteins are attached to the cells as membrane spanning cell surface proteins that have been demonstrated to be signal transduction molecules (Van den Berg et al., 1995). GPI-anchored proteins can induce strong signal transduction that may be related to their association with *src* kinases and G protein α subunits (Solomon et al., 1996). With the initiation of activation of lymphocytes, GPI -anchored proteins are associated with α subunits of heterotrimeric GTP binding proteins (G proteins) in human lymphocytes.

Solomon et al., (1996) found that the CD59 co-immunoprecipitated with G protein α subunits and that there was GTP activity associated with this molecule. CD59 can induce the activation of T cells and neutrophils; this can be done by using a monoclonal antibody that causes cross-linking of the CD59. Cross-linking induces a large Ca^{2+} flux and allows CD59 to act as a signal-transducing molecule (Van den Berg et al., 1995).

The primary function of CD59 is to inhibit the activity of complement. Complement is the collective term for an assembly of enzymes, proenzymes, and other proteins that form the principal effector mechanism of immunity in extracellular body fluids such as blood plasma (Kuby, 1994). Complement is antigen nonspecific, but is active in the final process of antibody-mediated immune response. During an immune response, an antibody binds to an epitope and forms an immune complex, the Membrane Attack Complex, which activates the complement to form a pore in the cell membrane causing lysis. CD59 prevents the MAC from forming in homologous tissue (Braoveanu, et al., 1995; Braoveanu, et al., 1996; Bodian, et al., 1997). CD59 stops the cytolytic membrane attack complex of components C5b through C9 by restricting the polymerization of C9 (Figure 4a and b). The lysis of cells by complement requires the proteins C5, C6, C7, C8, and C9. C5 is cleaved to C5b, which leads to formation of the MAC, by the sequential addition of C6-C9 (Lachmann and Thompson, 1970). The polymerization of C9 forms a transmembrane pore which lysis the cell. CD59 binds to the α-chain subunit of human C8 and blocks the initiation of polymerization of the C9 protein by binding to amino acid residues 245-538 on the C9b domain (Chang et al., 1994; Lockert et al., 1995; Zhang et al., 1999). C8's binding to CD59 prevents the formation of the MAC and cell lysing.

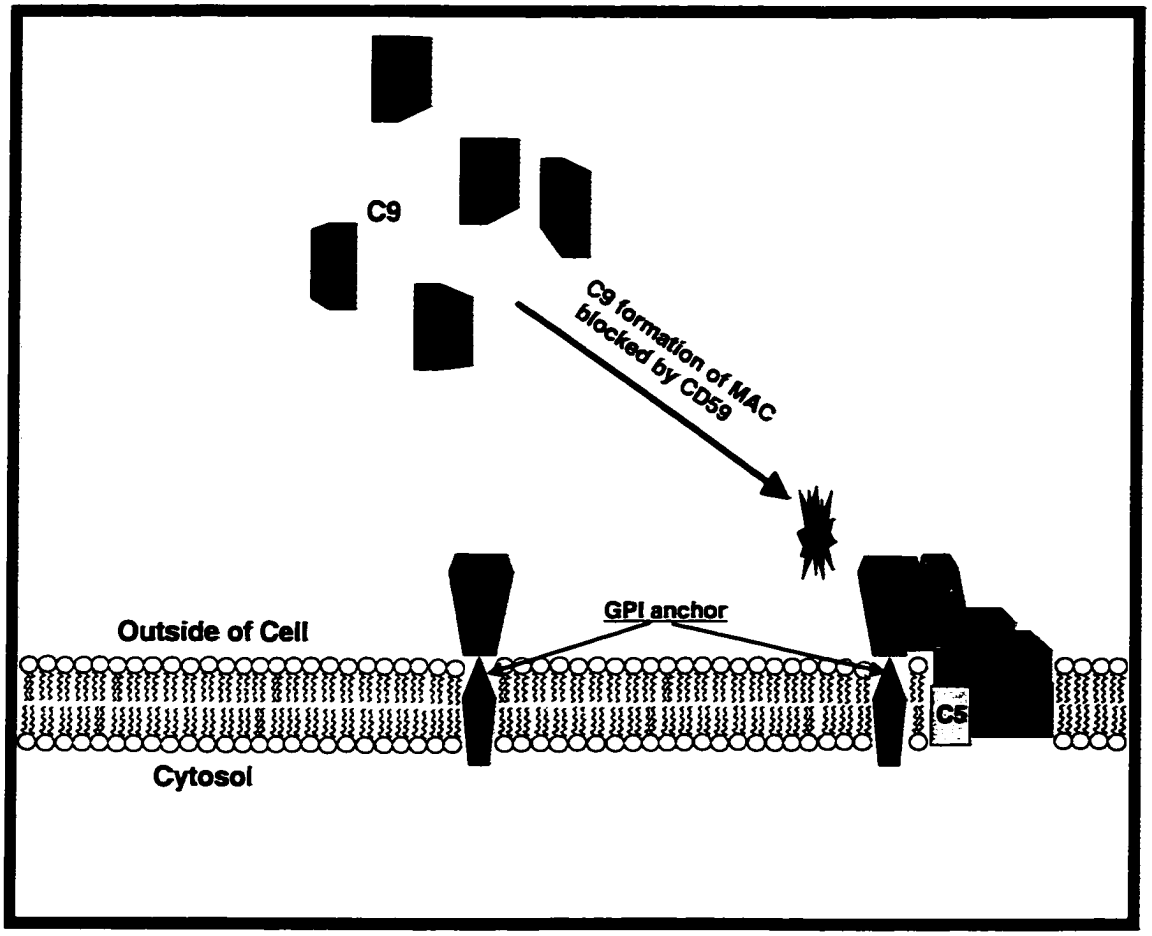

Figure 4a. The function of CD59 on the cell surface. CD59 is attached to the cell via a glycophosphoinosotol (GPI) anchored protein. The function of CD59 is to prevent self-lysis of cells by complement-mediated destruction. The complement cascade involves the assembly of the complement proteins in the cell membrane. Complement protein C5 is cleaved inserts into the cell membrane. C5 is followed by C6, C7, and C8. C8 would then initiate the polymerization of the C9 protein to form a pore in the cell membrane. CD59 prevents cell lysis by binding to the complement protein C8 in the C5-8 complex. When CD59 is attached to the C8 protein the formation of the Membrane Attack Complex is prevented. If CD59 is not present the C9 proteins will form the MAC, which is a pore structure that causes lysis of the cell. (Meri et al., 1990; Kuby, 1994; Liszewski et al., 1996; Morgan, 1999)

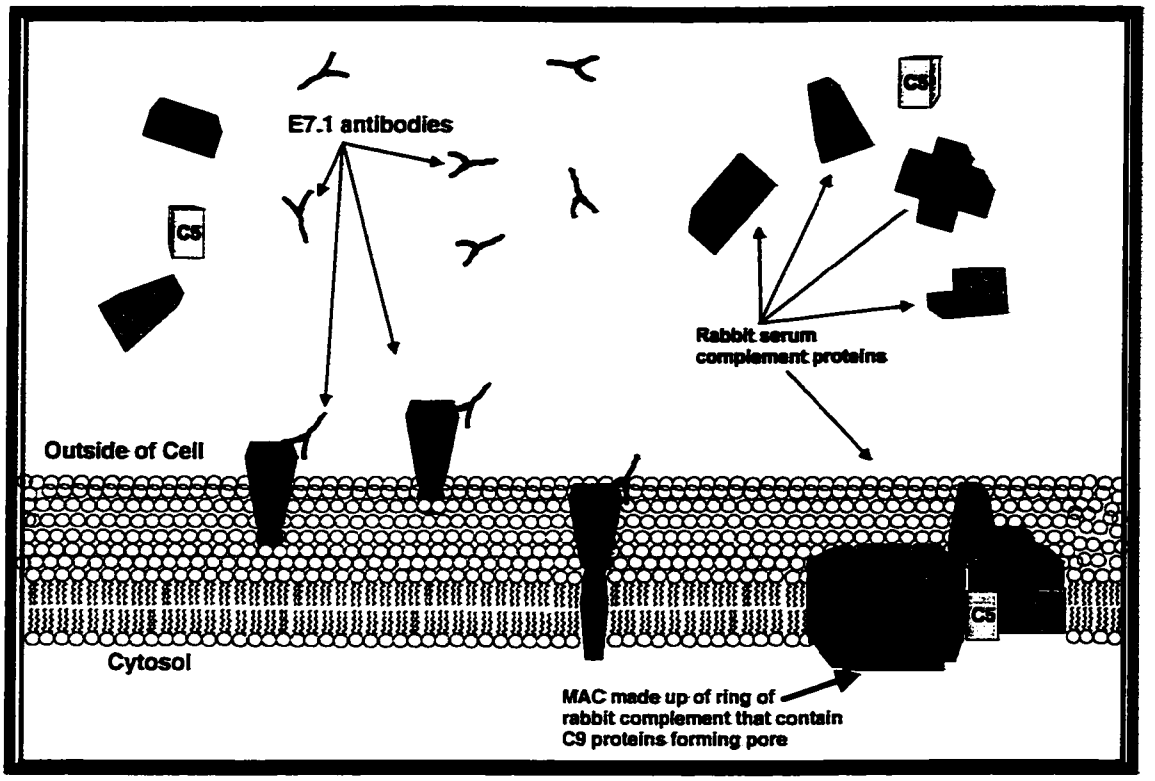

Figure 4b. Complement-mediated cell lysis as it is exploited in the A_L assay system. After treatment with a mutagen the A_L cells are allowed to "express" the induced mutations for 10 days. Thus if CD59 is damaged or lost the CD59 cannot be replace and the cell membrane becomes depleted of CD59. The A_L cells are then "challenged" with the monoclonal anti-CD59 antibody E7.1 and rabbit serum complement. The anti-CD59 E7.1 antibodies bind to the CD59 and prevent the CD59 from binding to the C8 protein, allowing the formation of the Membrane Attack Complex. The monoclonal E7.1 antibody is an IgM that will initiate the complement cascade. In $CD59^+$ cells the addition of heterologous complement causes the formation of large pores, made from polymerized rings of the C9 protein, lysing the cells. Any cell that expresses the human CD59 will be killed. Cells that have lost the expression of the human CD59 antigen will not activate the complement. Besides the CD59 gene on human chromosome 11, approximately 10 CHO genes are required for expression of the CD59 antigen. Mutations in any of these can produce the $CD59^-$ phenotype. In addition, the hamster CD59 may provide protection from lysis by the rabbit serum complement to the cells that do not express human CD59. (Meri et al., 1990; Kuby, 1994; Liszewski et al., 1996; Morgan, 1999)

In addition to complement mediated cell death, CD59 is thought to play a role in the regulation of complement-mediated platelet activation during wound repair (Sims et al., 1989; Morgan, 1992). CD59 has also been identified as ligand for CD2 in T cell adhesion and may have potentializing effects in T cell and B cell adhesion and activation (Deckert et al., 1992a; Deckert et al., 1992b; Korty et al., 1992). CD59 has a number of functions in cell-surface recognition and its absence causes detrimental effects.

A congenital lack of the CD59 protein causes the genetic disease Paroxysmal Nocturnal Hemoglobinuria (PNH) (Yamashina et al., 1990). Clinically PNH is characterized by recurrent episodes of complement-mediated intravascular hemolysis. PNH can be caused by the loss of the *CD59* gene or by loss or a deficiency in the expression of the GPI-anchor that holds the CD59 antigen to the outer leaflet of the cell membrane (Telen, 1995). These two mechanisms; 1) the loss of the complementation group for human *CD59*, and 2) the loss of the hamster *PIG-A* gene (phosphatidylinositol-glycan class A, an intermediary in the formation of the GPI anchor), provide a plausible explanation for two of the four complementation groups for $CD59^-$ mutants in the A_L assay (Jones et al., 1979; Nishimura et al., 1999). In 1979, Jones described that $CD59^-$ ($a1^-$) variants behave in a recessive manner and that at least 10 genes have now been identified that are involved in the synthesis of the GPI-anchor in mammalian cells (Kinoshita et al., 1997). Tomita (1999) described that of 200 patients with PNH the deficiency of CD59 is derived from inability of GPI-anchored synthesis. He described at least 10 proteins involved in the GPI-anchor synthesis, but PIG-A tends to cause the disease state because it is located on the human X chromosome, and therefore, only one copy is active.

The most effective test for PNH involves flow cytometry of blood cells using anti-CD59 monoclonal antibodies. This technique is more quantitative, sensitive, and rapid than hemolysis by complement (Hall and Rosse, 1996). Fluoresce assisted cell sorting (FACS) analysis of the presence or absence CD59 on individual cells may also lead to a faster screening technique for detecting mutants of the A_L system (Shibata and Kohsaka, 1995; McNiel et al., 2000).

Exon		Intron
1	45 bp-untranslated	13 kb–between exon 1 and 2
ASE	45 bp	4.5 kb downstream from exon 1
2	85 bp (first 18 bp untranslated)	5 kb
3	102 bp translated	7 kb
4	215 bp translated/1435 untranslated	(Holguin et al., 1996)

Table 4. The size of exons and introns of the human *CD59* gene.

The *CD59* gene maps at 11p13.5 (Figure 1 and 2) (Philbrick et al., 1990). The *CD59* gene produces five different mRNA transcripts. The lengths of the transcripts are 6, 2.2, 1.9, 1.2, and 0.6 kb (Davies et al., 1989; Tone et al., 1992; Holguin et al., 1993). The 5' untranslated region and the coding sequence of the transcripts are identical for all five transcripts, but the length of the 3' untranslated regions varies because of alternative polyadenylation signals. The different transcripts are translated into proteins that are found in different populations of hematopoietic cells (Hill et al., 1996). The *CD59* gene has four exons (segments of coding sequence) spanning about 20 kb and an alternative spliced exon (ASE) (Table 4) (Petranka et al., 1992; Holguin et al., 1996). The alternatively spliced exon is 2.2 kb, and the transcript is found in a ratio of 1:10 compared

to other CD59 transcripts. The transcripts have the same start site and similar regulation, most likely by the same promoter site (Holguin et al., 1996). The active site for CD59 and a binding site for a stalk of 7 amino acids is located in exon 4, and is probably the site where is where most mutations occur (Bodian et al., 1997).

The promoter region of *CD59* is G+C rich; it contains two consensus Sp1 binding sites, but no TATA and CAAT consensus sequences (Petranka et al., 1992). This is the same type of promoter feature found in a number of eukaryotic genes including *HPRT* (Holguin et al., 1996). CD59 is normally expressed at constitutive low levels. Very few substances have been found that either up-regulate or down-regulate CD59. However, in some cells CD59 mRNA expression can be up-regulated 15-fold in cells by using phorbol 12-myristate 13-acetate, leading to a four-fold increase in CD59 protein expression on the surface of the cell and a seven-fold increase in the amount of CD59 released into the supernatant (Marchbank et al., 1995). In A_L cells, the same gene regulation should hold true because the entire chromosome 11 was inserted into the CHO cells and the human CD59 is expressed on the surface of the CHO cells (Davis et al., 2000).

CD59 is similar to several proteins that make up a superfamily of related proteins. The amino acid sequence has 24-30% similarity to a group of murine proteins called Ly-6, a T cell acting protein (Davies et al., 1989), and mouse thymocyte B–cell antigen (Gumley et al., 1992). Other proteins in this super family include urokinase plasminogen-activator receptor (uPAR) (Roldan et al., 1990). The uPAR is also a GPI membrane anchored protein and uPAR is also not expressed in patients with PNH (Casey et al., 1994). The overall structure of the human uPAR gene is more similar to human CD59 than to the Ly-6 family of murine proteins (Wang et al., 1995). These proteins

have a high content of cysteine that forms a hydrophobic core around which loops are arranged in a triplicate pattern to define three homologous domains (Casey et al., 1994). This same structure is also found in several elapid snake venom toxins (erabutoxin and bungarotoxin) (Fleming et al., 1993), in herpes virus saimiri-15 (Albrecht et al., 1992), and a squid glycoprotein Spg-2 of unknown function (Williams et al., 1988).

CD59 is important in regulating the MAC. By increasing or decreasing the expression of CD59, cells survivability may be increased or decreased. Many cancer cells and a few viruses mimic or actually use CD59 to enhance their survivability. Montefiori et al. (1994) found CD59 expressed on HIV virons after the virus has been released from the surface of affected cells. In addition, CD59 is decreased on lymphocytes during HIV-1 infection (Schmitz et al., 1995). This creates a two-sided problem; 1) an increased sensitivity of lymphocytes from HIV-1 infected patients to lysis by monoclonal antibodies and the MAC, and 2) the HIV virus is protected by lysis because it incorporates CD59, CD46, and CD55 into the outer viral coat (Montefiori et al., 1994). Saifuddin et al. (1997) showed that HIV virons that incorporated CD46, CD55, and CD59 were significantly more resistant to complement lysis than a control virus. The HIV virus does not make these proteins, but incorporates them from the cell membrane of infected cells. Herpes simplex virus has been shown to mimic complement regulatory proteins but HIV, SIV, and *Vaccinia* are the first shown to use the actual human protein in their viral coat (Fries et al., 1986; Kotwal et al., 1990; Nakamura et al., 1996). Vanderplassche et al. (1998) found that *Vaccinia* incorporates CD46, CD55, CD59, CD71, CD81 and major histocompatibility complex class I antigen into the extracellular enveloped virus form of *Vaccinia*.

In addition to viruses, several cancers also employ the CD59 antigen to their selective advantage. Expression of CD59 was found in numerous cancers including colon carcinomas, breast carcinomas, and renal cell carcinomas (Neihans et al., 1996; Gorter et al., 1996). Hakulinen and Meri (1994) found CD59 to be strongly expressed in all tested human solid breast cancers. Complement killing of breast cancer cells was also enhanced after the cells were treated with an anti-CD59 monoclonal antibody. Expression of CD59 has been found to be over expressed in melanoma, thus regulating the host-tumor interaction in favor of the tumor by protecting tumor cells from complement mediated lysis (Brasoveanu et al., 1995; Simon, et al., 1996). Maenpaa et al. (1996) found CD59 strongly expressed in malignant glioma cell lines and tumors. Malignant glioma cells were extremely resistant to complement mediated cell lysis; several of the malignant glioma cell lines resisted complement lysis at higher levels than any other tested cells. Bjorge et al., (1994) showed that the expression of CD59 is enhanced in colorectal adenocarcinoma cells as compared to normal colon epithelial cells, and this expression provides protection to the cell from activation of the MAC. In addition, CD59 has been found in the surrounding matrix around the tumors suggesting that CD59 is released in soluble forms from the tumor cells (Niehans et al., 1996).

CD59 provides a tool for a cancer cell to use in natural selection to enhance survival, however, it also provides a tool to control cancers or help with their treatment. CD59 could be used as a target for anti cancer treatment for a number of cancers. In colorectal adenocarcinoma, treatment relapse has been decrease by using the immune system booster levamisole. CD59 is down regulated by treatment with levamisole. The reduced CD59 levels caused an increase in vulnerability of the colorectal

adenocarcinoma cells to complement mediated lysis. Levamisole is an anti-helminthic drug, and combined with 5-fluorouracil can be used as adjuvant therapy to treat colorectal cancer. This combined treatment reduced the rate of cancer recurrence by approximately 40% (Bjorge and Matre, 1995).

CD59 is important in a host of immune functions. CD59 prevents self-lysis of cells by a host's complement system. Xenotypic cells and tissue are particularly susceptible to complement-mediated destruction due to the unregulated activity of the Membrane Attack Complex (MAC). This phenomenon is the basis for hyperacute immune rejection after xenotransplantation (Dalmasso et al., 1991). The addition of human *CD59* to non-human tissue may enable the transplant of xenograph tissues into humans. Byrne et al., (1997) theorized that transgenic organs with high levels of human CD59 would allow the use of xenotransplantation from other animals, such as pig into humans. They have demonstrated this theory by using pig to baboon heterotopic heart transplants that express human CD59. The protection given was sufficient to block complement-mediated damage that is normally seen in xenographs when non-transgenic organs are used. By transfecting human *CD59* into pig embryos and then using the transgenic pigs for donor organs, the transplanted organs would be better protected against self-lysis. Holguin et al., (1996) have shown that transgenic expression of human CD59 in pigs allows a longer graft survival in primate cardiac transplants. However, Van den Berg et al., (1995) found that native pig CD59 inhibited human complement, as well and questioned the tactics of trying to use transgenic pig organs to protect against hyperacute rejection. The challenge of avoiding complement-mediated destruction in xenotransplantation will most likely need more than the insertion of a single gene to solve

the problem.

The human complement system is effective in protecting against bacteria, parasites, and heterologous cells. Normal and malignant cells are usually resistant to lysis by homologous complement (Maenpaa et al., 1996). CD59 provides protection from the MAC complex of same species complement; however, Hüsler found that if you have one species of cell or tissue and another species of complement then CD59 exerts little or no inhibitory activity toward C8 or C9 of most other species (Hüsler et al., 1995). Researchers have found that the complement inhibitory activity is species specific. The use of rabbit C9, which can substitute for human C9 in the MAC leads to unrestricted lysis in human cells (Hüsler et al., 1995). The gene for mouse *CD59* has been mapped to the E2-E4 region of mouse chromosome 2, which is syntenous with the location of *hCD59* on chromosome 11p13. Mouse CD59 expressed in a CD59 negative human cell line imparts protection against lysis by complement from rodent, human, and several other species (Powell et al., 1997). However, Van den Berg et al. (1995) found that neither rat nor sheep CD59 showed any difference in protection with homologous versus heterologous complement. When pig CD59 was incorporated into guinea pig erythrocytes, protection from lysis from a wide variety of species was imparted; there was no homologous restriction (Van den Berg et al., 1995). The human CD59 binds human C9 at residues 359-391 and this area probably gives the species selectivity for complement mediated lysis (Hüsler et al., 1996). Human CD59 and the other species analogs that have been tested inhibit complement from many different species, which suggests that the active sites of attachment for the C8 and C9 proteins are conserved (Rushmere et al., 1994). Human CD59 binds to human C9 and to peptides derived from

human C9 but not to rabbit C9, and leads to unrestricted lysis. Rollins et al. (1991) found that inhibition of C5b-9 mediated hemolysis was maximal when C8 and C9 came from human or baboon serum. In contrast, CD59 provided reduced protection from lysis when C8 and C9 were derived from dog or sheep serum and no protection when C8 and C9 were derived from rabbit of guinea pig serum. Therefore, rabbit complement will cause unrestricted lysis with the presence of human CD59. This gives the A_L assay the sensitivity level to select for mutants that have lost hCD59 because any cells with hCD59 will be destroyed by antibody-rabbit complement interaction.

The A_L CD59 assay and the some other assays described provide sensitive methods for looking at mutant induction in cycling mammalian cells. I used the A_L assay to look at cells in various parts of their cell cycle. I had to synchronize the cells so that I could work with large cohorts of cells in the same phase of the cell cycle. The following is a review of synchronization methods describing especially centrifugal elutriation that I used to isolate cells in different phases of the cell cycle.

METHODS OF SYNCHRONIZING CELLS

There are many different methods of synchronizing cells, which can be divided into two classes: chemical and physical (Grdina et al., 1984; Grdina et al., 1987). Some chemical methods are harsh and affect normal cell metabolism and structure. Most chemical synchronizing methods either inhibit DNA synthesis or starve the cell of essential nutrients. Chemicals that inhibit DNA usually cause unbalanced growth (Rice et al., 1984) where RNA and protein synthesis continue at normal rates but the DNA synthesis is halted. The cells may take several hours to recover completely from the use of DNA inhibitors. Nutrient-deprivation Synchronization methods such as imposing

isoleucine deficiency is effective but is not the best method because the cells may have uneven growth when given the complete media (Enger and Tobey, 1972). Physical separation methods, such as selection based on reduced adherence of cells to their growth surface during mitosis, can be effective but yields are often relatively small. Mitotic shake off allows for the collection of cells that are physically rounded up in mitosis so that they and are easier to shear off the tissue culture plate (Griffith and Adams, 1982; Grdina et al., 1984). The cells are collected in time increments of approximately one hour and are kept on ice until enough are collected. This method is time consuming and takes hours to get enough cells, about 2×10^6 for an experiment. Because of these limitations, I chose to use centrifugal elutriation, which can provide large numbers ($\geq 6 \times 10^6$) of highly synchronized cells.

Centrifugal Elutriation

Centrifugal elutriation is an excellent method for obtaining synchronized cells because it is gentle and provides cells in specific phases of the cycle are obtained (Griffith and Adams, 1982). The cells are separated with small changes in fluid flow opposing the centrifugal force, thus avoiding deleterious effects from pelleting the cells or from using osmotic gradients (Applications Data, Beckmen Instruments, 1990). Centrifugal elutriation has proven effective in separating cells based on their position through the cell cycle (Rice et al. 1984). Cell volume increases during the cell cycle from mitosis to mitosis, so that it is possible to separate cells in different stages by changes in their sedimentation rate, which depends on their volume (Applications Data, Beckmen Instruments, 1990). For centrifugal elutriation, a population of cells is injected into an elutriation chamber of special geometry (Figure 5) that is spun at approximately 2000

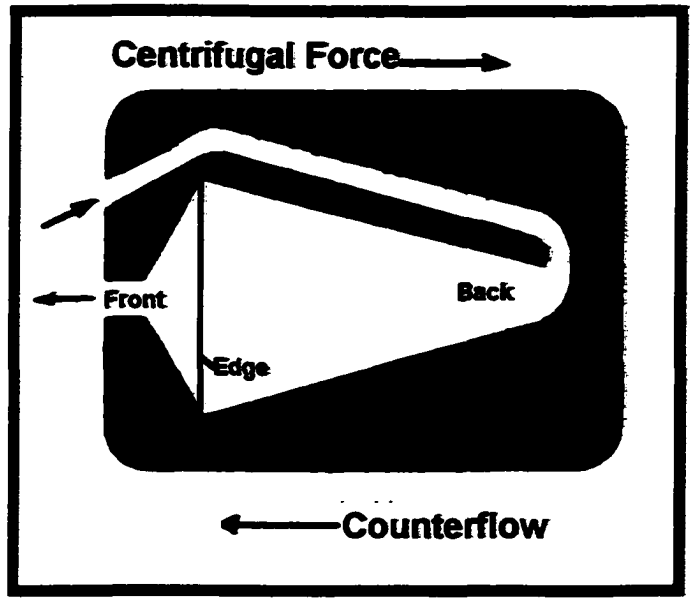

Figure 5. Elutriation Chamber. The elutriation chamber is spun at a constant 2000 rotations per minute. Cells are forced into the back of the chamber. As the flow is increased smaller cells are forced to the front of the chamber and eluted thru the front of the elutriation chamber. With each incremental increase in buffer flow, (counterflow against the centrifugal force) larger and larger cells are eluted.

RPM. Two opposing forces, the buffer flow towards the center and the centrifugal force in the opposite direction cause to separate into layers based on volume differences. The centrifugal force drives the cells away from the center of rotation of the elutriation chamber; thus, causing the cells to collect at the base of the funnel inside the chamber based on their volume. Buffer is simultaneously pumped into the chamber to produce a counter-flow, forcing the cells towards the center where they exit the elutriation chamber. Because the cells of the same volume all have the same density, this centrifugal force causes them to separate according to volume. The smallest cells are forced out of the elutriation chamber first and are collected. This procedure has proven effective in separating cells based on their position in the cell cycle because cells are smaller just

after mitosis than are cells at later stages of the cell cycle. Centrifugal elutriation can quickly provide large yields (1-5 x 10^6 cells) of highly phased cells for study (Meistrich et al., 1977). Centrifugal elutriation allows cells to be studied and comparisons made based on which part of the cell cycle is most affected by an agent.

In this chapter, I have reviewed mutation assay systems and described advantages of the A_L system for measuring small and large mutations. The sensitivity of the A_L assay allowed me to study the mutation induction rate of the *CD59* locus through the various phases of the cell cycle, to determine differences in mutant yield, and to examine the mutation spectra from the loss of *CD59* exons to the loss of almost all of human chromosome 11. In chapter 2, I describe levels of mutation induction by ionizing radiation in A_L cells at different times in the cell cycle. In chapter 3, I show how the mutation spectra vary through the cell cycle. These data may further shed light on relationships of repair and mutation.

References

Applications Data. Centrifugal elutriation of living cells. An annotoated bibliography. (DS-534E). 1990. Palo Alto, CA, Beckman Instruments, Inc. Ref Type: Pamphlet

Department of Health and Human Services, Food and Drug Administration, International Conference on Harmonization; Guidance on Genotoxicity: A standard battery for genotoxicity testing of pharmaceuticals. Federal Register 62, No. 225, Friday, November, 62472-62475. 1997. Ref Type: Report

Adair, G. M., Carver, J. H., & Wandres, D. L. (1980) Mutagenicity testing in mammalian cells. I. Derivation of a Chinese hamster ovary cell line heterozygous for the adenine phosphoribosyltransferase and thymidine kinase loci. Mutat.Res. 72: 187-205.

Adair, G. M., Stallings, R. L., Nairn, R. S., & Siciliano, M. J. (1983) High-frequency structural gene deletion as the basis for functional hemizygosity of the adenine phosphoribosyltransferase locus in Chinese hamster ovary cells. Proc.Natl.Acad.Sci.USA 80: 5961-5964.

Adair, G. M. (1987) Analysis of mutation at the Chinese hamster APRT locus. In: Mammalian Cell Mutagenesis: Banbury Report No. 28 (Moore, M. M., DeMarini, D. M., de Serres, F. J., & Tindall, K. R., eds.), pp. 183-191. Cold Spring Harbor Press, Cold Spring Harbor, NY.

Albertini, R. J. & DeMars, R. (1973) Somatic cell mutation, detection, and quantification of x-ray induced mutation in cultured diploid human fibroblasts. Mutat.Res. 18: 199-224.

Albrecht, J. C., Nicholas, J., Cameron, K., Newman, C., Fleckenstein, B., & Honess, R. S. (1992) Herpesvirus Saimiri has a gene specifying a homologue of the cellular membrane glycoprotein CD59. Virology 190: 527-530.

Amacher, D. E. (1984) The L5178Y/TK gene mutation assay system. In: Chemical mutagens. Principles and methods for their detection (deSerres, F. J., ed.), vol. 9, pp. 183-212. Plenum Press, New York.

Ames, B. N., Durston, W. E., Yamasaki, I., & Lee, F. D. (1973) Carcinogens are mutagens: a simple test system combining liver homogenates for activation and bacteria for detection. Proc.Natl.Acad.Sci.USA 70: 2281-2285.

Ames, B. N. (1971) The detection of chemical mutagens with enteric bacteria. In: Chemical Mutagens: Principles and Methods for Their Detection (Vol. 1) (Hollaender, A., ed.), pp. 267-288. Plenum Press, New York.

Ames, B. N., McCann, J., & Yamasaki, E. (1975) Methods for detecting carcinogens and mutagens with the *Salmonella*/mammalian-microsome mutagenicity test. Mutat.Res. 31: 347-364.

Ames, B. N., Magaw, R., & Gold, L. S. (1987) Ranking possible carcinogenic hazards. Science 236: 271-280.

Ames, B. N. (1989) Mutagenesis and carcinogenesis: Endogenous and exogenous factors. Environ.Molec.Mutagen. 14 (suppl 16): 66-77.

Ames, B. N. (1989) Endogenous DNA damage as related to cancer and aging. Mutat.Res. 214: 41-46.

Ames, B. N. & Gold, L. S. (1991) Carcinogenesis mechanisms: The debate continues. Science 252: 902-904.

Amundson, S. A. & Liber, H. L. (1992) A comparison of induced mutation at homologous alleles of the *tk* locus in human cells. II. Molecular analysis of mutants. Mutat.Res. 267: 89-95.

Amundson, S. A., Xia, F., Wolfson, K., & Liber, H. L. (1993) Different cytotoxic and mutagenic responses by X-rays in two human lymphoblastoid cell lines derived from a single donor. Mutat.Res. 286: 233-241.

Applegate, M. L., Moore, M. M., Broder, C. B., Burrell, A., Juhn, G., Kasweck, K. L., Lin, P.-F., Wadhams, A., & Hozier, J. C. (1990) Molecular dissection of mutations at the heterozygous thymidine kinase locus in mouse lymphoma cells. Proc.Natl.Acad.Sci.USA 87: 1583-1587.

Arlett, C. F., Turnbull, D., Harcourt, S. A., Lehman, A. R., & Colella, C. M. (1975) A comparison of the 8-azaguanine and oubain-resistance systems for the selection of induced mutant Chinese hamster cells. Mutat.Res. 33: 262-278.

Barclay, A. N. (1993) The Leucocyte Antigen Facts Book Academic Press, London.

Bjorge, L., Vedeler, C. A., Ulvestad, T. E., & Matre, R. (1994) Expression and function of CD59 on colonic adenocarcinoma cells. Eur.J.Immunol. 24: 1598-1603.

Bjorge, L. & Matre, R. (1995) Down-regulation of CD59 (Protectin) expression on Human colorectal adenocarcinoma cell lines by levamisole. Scand.J.Immunol. 42: 512-516.

Bjorge, L., Jensen, T. S., Kristoffersen, E. K., Ulstein, M., & Matre, R. (1996) Identification of the complement regulatory protein CD59 in human colostrum and milk. Am.J.Reprod.Immunol. 35: 43-50.

Blazak, W., Stewart, B., Galperin, I., Allen, K., Rudd, C., Mitchell, A., & Caspary, W. (1989) Chromosome analysis of small and large L5178Y mouse lymphoma cell colonies. Comparison of trifluorothymidine-resistant and unselected cell colonies from mutagen-treated and control cultures. Mutat.Res. 224: 197-208.

Bodian, D. L., Davis, S. J., Morgan P.B., & Rushmere, N. K. (1997) Mutational analysis of the active site and antibody epitopes of the complement-inhibitory glycoprotein, CD59. J.Exp.Med. 185: 507-516.

Borek, C. (1981) The induction, expression and modulation of radiation induced oncogenesis *in vitro* in diploid human and rodent cells. In: Carcinogenesis: Fundamental Mechanisms and Environmental Effects (Pullman, B., Ts'o, P., & Belboin, H., eds.), pp. 590-616. Reidel, Dordrecht.

Bradley, W. E., Belouchi, A., & Messing, K. (1988) The aprt heterozygote/hemizygote system for screening mutagenic agents allows detection of large deletions. Mutat.Res. 199: 131-138.

Brasoveanu, L. I., Altomonte, M., Gloghini, A., Fonsatti, E., Coral, S., Gasparollo, A., Montagner, R., Cattarossi, I., Simonelli, C., Cattelan, A., & et, a. (1995) Expression of protectin (CD59) in human melanoma and its functional role in cell- and complement-mediated cytotoxicity. Int.J.Cancer 61: 548-556.

Brasoveanu, L. I., Altomonte, M., Fonsatti, E., Colizzi, F., Coral, S., Nicotra, M. R., Cattarossi, I., Cattelan, A., Natali, P. G., & Maio, M. (1996) Levels of cell membrane CD59 regulate the extent of complement-mediated lysis of human melanoma cells. Laboratory Investigation 74: 33-42.

Breimer, L. H., Nalbantoglu, J., & Meuth, M. (1986) Structure and sequnce of mutations induced by ionizing radiation at selectable loci in Chinese Hamster ovary cells. J.Mol.Biol. 192: 669-674.

Bronner, C. E., Welker, D. L., & Deering, R. A. (1992) Mutations affecting sensitivity of the cellular slime mold *Dictyostelium discoideum* to DNA-damaging agents. Mutat.Res. 274: 187-200.

Burki, H. J. (1980) Ionizing radiation-induced 6-thioguanine-resistant clones in synchronous CHO cells. Radiat.Res. 81: 76-84.

Byrne, G. W., McCurry, K. R., Martin, M. J., McClellan, S. M., Platt, J. L., & Logan, J. S. (1997) Transgenic pigs expressing human CD59 and decay-accelerating factor produce an intrinsic barrier to complement-mediated damage. Transplantation 63: 149-155.

Carey, T. E., Takahashi, T., Resnick, L. A., Oettgen, H. F., & Old, L. J. (1976) Cell surface antigens of human malignant melanoma: mixed hemadsorption assays for humoral immunity to cultured autologous melanoma cells. Proc.Natl.Acad.Sci.USA 73: 3278-3282.

Casey, J. R., Petranka, J. G., Kottra, J., Fleenor, D. E., & Rosse, W. F. (1994) The structure of the urokinase-type plasminogen activator receptor gene. Blood 84: 1151-1156.

Chang, C., Husler, T., Zhao, J., Wiedmer, T., & Sims, P. J. (1994) Identity of a peptide domain of Human C9 that is bound by the cell-surface complement inhibitor, CD59. J.Biol.Chem. 269: 26424-26430.

Chu, E. H. Y. & Malling, H. V. (1968) Mammalian cell genetics, II. Chemical induction of specific locus mutations in Chinese hamster cells *in vitro*. Proc.Natl.Acad.Sci.USA 61: 1306-1312.

Cleaver, J. E. (1977) Induction of thioguanine- and ouabain-resistant mutants and single strand breaks in the DNA of Chinese hamster ovary cells by 3H-thymidine. Genetics 87: 129-138.

Clive, D., Flamm, W. G., Machesko, W. G., & Bernheim, N. J. (1972) A mutational assay system using the thymidine kinase locus in mouse lymphoma cells. Mutat.Res. 16: 77-87.

Clive, D. & Spector, J. F. S. (1975) Laboratory procedure for assessing specific locus mutations at the TK locus in cultured L5178Y mouse lymphoma cells. Mutat.Res. 31: 17-29.

Clive, D. (1987) Historical overview of the mouse lymphoma $TK^{+/-}$ assay. In: Mammalian Cell Mutagenesis: Banbury Report 28 (Moore, M. M., DeMarini, D. M., de Serres, F. J., & Tindall, K. R., eds.), pp. 25-36. Cold Spring Harbor Laboratory, Cold Spring Harbor.

Clive, D., Glover, P., Applegate, M., & Hozier, J. (1990) Molecular aspects of chemical mutagenesis in L5178Y/tk+/- mouse lymphoma cells. Mutagenesis 5: 191-197.

Colella, C. M., Bogani, P., Agati, G., & Fusi, F. (1986) Genetic effects of UV-B: Mutagenicity of 308 nm light in Chinese hamster V79 cells. Photochem.Photobiol. 43: 437-442.

Cox, R. & Masson, W. K. (1978) Do radiation-induced thioguanine-resistant mutants of cultured mammalian cells arise by HGPRT gene mutation or X-chromosome rearrangement? Nature 276: 629-630.

Dalmasso, A. P., Platt, J. L., & Bach, F. H. (1991) Reaction of complement with endothelial cells in a model of xenotransplantation. Clin.Exp.Immunol. 86: 31-43.

Davies, A., Simmons, D. L., Hale, G., Harrison, R. A., Tighe, H., Lachmann, P. J., & Waldmann, H. (1989) CD59, an LY-6-like protein expressed in human lymphoid cells, regulates the action of the complement membrane attack complex on homologous cells. J.Exp.Med. 170: 637-654.

Davies, A. & Lachmann, P. J. (1993) Membrane defence against complement lysis: the structure and biological properties of CD59. Immunol.Res. 12: 258-275.

Davies, M. J., Phillips, B. J., & Rumsby, P. C. (1993) Molecular analysis of mutations at the tk locus of L5178Y mouse-lymphoma cells induced by ethyl methane sulfonate and mitomycin C. Mutat.Res. 290: 145-153.

de Serres, F. J., Malling, H. V., & Weber, B. B. (1967) Dose-rate effects on inactivation and mutation induction in *Neurospora crassa*. Brookhaven Symp.Biol. 20: 56-75.

de Serres, F. J. & Malling, H. V. (1971) Measurement of recessive lethal damage over the entire genome and at two specific loci in the *ad-3* region of a two-component heterokaryon of *Neurospora crassa*. In: Chemical Mutagens: Principles and Methods for their Detection (Hollaender, A., ed.), vol. 2, pp. 311-342. Plenum, New York.

de Serres, F. J. (1991) X-ray-induced specific-locus mutations in the *ad-3* region of two-component heterokaryons of *Neurospora crassa*, IX. Mutational spectra as a function of X-ray dose. Mutat.Res. 246: 15-30.

de Serres, F. J. (1994) X-ray-induced specific-locus mutations in the *ad-3* region of two-component heterokaryons of *Neurospora crassa*. XII. Analysis of multiple-locus *ad-3* mutations reveals a nonrandom distribution of the separate sites of recessive lethal damage throughout the genome. Mutat.Res. 307: 175-184.

Deckert, M., Kubar, J., & Didier, Z. (1992) CD59 molecule: A second ligand for CD2 in T cell adhesion. Eur.J.Immunol. 22: 2943-2947.

Deckert, M., Kubar, J., & Benard, A. (1992) CD58 and CD59 molecules exhibit potentializing effects in T cell adhesion and activation. J.Immunol. 148: 672-677.

Dewey, W. C., Furman, S. C., & Miller, H. H. (1970) Comparison of lethality and chromosomal damage induced by X-rays in synchronized Chinese hamster cells *in vitro*. Radiat.Res. 43: 561-581.

Doll, R. & Peto, R. (1981) The causes of cancer: Qualitative estimate of avoidable risks of cancer in the United States today. J.Natl.Cancer Inst. 68: 1191-1308.

Drinkwater, N. R., Corner, R. C., McCormick, J. J., & Maher, V. M. (1982) An *in situ* assay for induced diptheria-toxin-resistant mutants of diploid human fibroblasts. Mutat.Res. 106: 277-289.

Eadie, J. S., Conrad, M., Toorchen, D., & Topal, M. D. (1984) Mechanism of mutagenesis by O6-methylguanine. Nature 308: 201-203.

Enger, M. D. & Tobey, R. A. (1972) Effects of isoleucine deficiency on nucleic acid and protein metabolism in cultured Chinese hamster cell. Continued ribonucleic acid and protein synthesis in the absence of deoxyribonucleic acid synthesis. Biochemistry 11: 269-278.

Essers, J., Hendriks, R. W., Swagemakers, S. M. A., Troelstra, C., de Wit, J., Bootsma, D., Hoeijmakers, J. H. J., & Kanaar, R. (1997) Disruption of mouse RAD54 reduces ionizing radiation resistance and homologous recombination. Cell 89: 195-204.

Evans, H. H., Mencl, J., Horng, M.-F., Ricanati, M., Sanchez, C., & Hozier, J. (1986) Locus specificity in the mutability of L5178Y mouse lymphoma cells: the role of multilocus lesions. Proc.Natl.Acad.Sci.USA 83: 4379-4383.

Evans, H. H., Ricanati, M., & Horng, M. F. (1987) Deficiency in DNA repair in mouse lymphoma strain L5178Y-S. Proc.Natl.Acad.Sci.USA 84: 7562-7566.

Evans, H. H., Nielsen, M., Mencl, J., Horng, M.-F., & Ricanati, M. (1990) The effect of dose rate on X-radiation-induced mutant frequency and the nature of DNA lesions in mouse L5178Y cells. Radiat.Res. 122: 316-325.

Evans, H. H. (1991) Cellular and molecular effects of radon and other alpha particle emitters. Adv.Mutat.Res. 3: 28-52.

Evans, H. H. (1994) The prevalence of multilocus lesions in radiation-induced mutants. Radiat.Res. 137: 131-144.

Fleming, T. J., O'hUigin, C., & Malek, T. R. (1993) Characterization of two novel Ly-6 genes: Protein sequence and potential structural similarity to α-Bungarotoxin and other neurotoxins. J.Imminol. 150: 5379-5390.

Fouladi, B., Waldren, C. A., Rydberg, B., & Cooper, P. K. (2000) Comparison of repair of DNA double-strand breaks in identical sequences in primary human fibroblast and immortal hamster-human hybrid cells harboring a single copy of human chromosome 11. Radiat.Res. 153: 795-804.

Frieben, E. (1902) Demonstration eines carcroids des rechten handruckens, das sich nach langdauernder einwirkung von roentgenstrahlen entwickelt hatte. Fortsch Roentgenstr 6: 106.

Friedberg, E. C., Walker, G. C., & Siede, W. (1995) DNA Repair and Mutagenesis. ASM Press, Washington, D.C.

Friedrich, V. & Coffino, P. (1977) Mutagenesis in S49 mouse lymphoma cell; induction of resistance to ouabain, 6-thioguanine, and dibutyryl cyclic AMP. Proc.Natl.Acad.Sci.USA 74: 679-683.

Fries, L. F., Friedman, H. M., Cohen, G. H., Eisenberg, R. J., Hammer, C. H., & Frank, M. M. (1986) Glycoprotein C of Herpes simplex virus type 1 is an inhibitor of the complement cascade. J.Immunol. 137: 1636-1640.

Furuno-Fukushi, I., Ueno, A., & Matsudaira, H. (1988) Mutation induction by very low dose rate gamma rays in cultured mouse leukemia cells L5178Y. Radiat.Res. 115: 273-280.

Gerhard, D. S., Jones, C., Morse, H. G., Handelin, B., Weeks, V., & Housman, D. (1987) Analysis of human chromosome 11 by somatic cell genetics: Reexamination of derivatives of human hamster cell line J1. Somat.Cell Mol.Genet. 13: 293-304.

Glaser, T., Housman, D., Lewis, W. H., Gerhard, D., & Jones, C. (1989) Fine structure deletion map of human chromosome 11p: Analysis of J1 series hybrids. Somat.Cell Mol.Genet. 15: 477-501.

Glaser, T., Jones, C., Douglass, E. C., & Housman, D. (1989) Constitutional and somatic mutations of chromosome 11p in Wilm's tumor. In: Cancer Cells 7: Molecular Diagnostics of Human Cancer (Furth, M. & Greaves, M., eds.), pp. 253-279. Cold Spring Harbor Laboratory Press, Cold Spring Harbor, NY.

Glover, T. W., Chang, C. C., Trosko, J. E., & Liu, S. S. (1979) Ultraviolet light induction of diptheria toxin-resistant mutants of normal and xeroderma pigmentosum human fibroblasts. Proc.Natl.Acad.Sci.USA 76: 3982-3986.

Gorter, A., Blok, V. T., Haasnoot, W. H., Ensink, N. G., Daha, M. R., & Fleuren, G. J. (1996) Expression of CD46, CD55, and CD59 on renal tumor cell lines and their role in preventing complement-mediated tumor cell lysis. Lab.Invest. 74: 1039-1049.

Grdina, D. J., Meistrich, M. L., Meyn, R. E., Johnson, T. S., & White, R. A. (1984) Cell synchrony techniques. I. A comparison of methods. Cell Tissue Kinet. 17: 223-236.

Grdina, D. J., Meistrich, M. L., Meyn, R. E., Johnson, T. S., & White, R. A. (1987) Cell synchrony techniques. I. A comparison of methods. In: Techniques in Cell Cycle Analysis (Gray, J. W. & Darzynkiewicz, Z., eds.), pp. 367-402. Humana Press, Clifton, NJ.

Griffith, O. M. and Adams, E. G. A method for obtaining synchronous cells by centrifugal elutriation. DS-594A. 1982. Palo Alto, CA, Beckman Instruments, Inc. Ref Type: Pamphlet

Grosovsky, A. J., Drobetsky, E. A., deJong, P. J., & Glickman, B. W. (1986) Southern analysis of genomic alterations in gamma-ray-induced *aprt* hamster cell mutants. Genetics 113: 405-415.

Grosovsky, A. J., de Boer, G., De Jong, P. J., Drobetsky, E. A., & Glickman, B. W. (1988) Base substitutions, frameshifts, and small deletions constitute ionizing radiation-induced point mutations in mammalian cells. Proc.Natl.Acad.Sci.USA 85: 185-188.

Gumley, T. P., McKenzie, I. F., Kozak, C., & Sandrin, M. (1992) Isolation and characterization of cDNA clones for the mouse thymocyte B cell antigen (ThB). J.Immunol. 149: 2615-2618.

Gupta, R. S. & Simonovitch, L. (1978) Isolation and characterization of mutants of diploid human fibroblasts resistant to diptheria toxin. Proc.Natl.Acad.Sci.USA 75: 3337-3340.

Gupta, R. S. & Siminovitch, L. (1978) Diptheria-toxin-resistant mutants of CHO cells affected in protein synthesis: A novel phenotype. Somat.Cell Genet. 4: 553-571.

Gustafson, D., Trotter, B., Snead, D., & Waldren, C. (1997) Expression of human O^6-methyl guanine methyl transferase (MGMT) in post replication repair (PRR) deficient CHO-UV-1 cells: compensation for hypersensitivity to methylating and ethylating agents but not to mitomycin C. Somat.Cell Mol.Genet. 23: 9-17.

Hüsler, T., Lockert, D. H., Kafman, K. M., Sodetz, M., & Sims, P. J. (1995) Chimeras of Human complement C9 reveal the site recognized by complement regulatory protein CD59. J.Biol.Chem. 270: 3483-3486.

Hüsler, T., Lockert, D. H., & Sims, P. J. (1996) Role of a disulfide-bonded peptide loop within Human complement C9 in the species-selectibity of complement inhibitor CD59. Biochemistry 35: 3263-3269.

Hakulinen, J. & Meri, S. (1994) Expression and function of the complement membrane attack complex inhibitor protectin (CD59) on human breast cancer cells. Lab.Invest. 71: 820-827.

Hall, S. E. & Rosse, W. F. (1996) The use of monoclonal antibodies and flow cytometry in the diagnosis of paroxysmal nocturnal hemoglobinuria. Blood 87: 5332-5340.

Hartman, P. S., Hevelone, J., Dwarakanath, V., & Mitchell, D. L. (1989) Excision repair of UV radiation-induced DNA damage in *Caenorhabditis elegans*. Genetics 122: 379-385.

Hartwell, L. (1992) Defects in a cell cycle checkpoint may be responsible for the genomic instability of cancer cells. Cell 71: 543-546.

Hartwell, L. (1994) Camping out. Nature 371: 286.

Hatanaka, M., Seya, T., Matsumoto, M., Hara, T., Nonaka, M., Inoue, N., Takeda, J., & Shimizu, A. (1996) Mechanisms by which the surface expression of the glycosylphosphatidylinositol-anchored complemant regulatory proteins decay-accererating factor (CD55) and CD59 is lost in human leukaemia cell lines. Biochem.J. 314: 969-976.

Hei, T., Piao, C. Q., He, Z. Y., Vannais, D., & Waldren, C. A. (1992) Chrysotile fiber is a strong mutagen in mammalian cells. Cancer Res. 52: 6305-6309.

Hei, T. K., Hall, E. J., & Waldren, C. A. (1988) Mutation induction and relative biological effectiveness of neutrons in mammalian cells. Radiat.Res. 115: 281-291.

Hei, T. K., Zhu, L. X., Vannais, D., & Waldren, C. (1994) Molecular analysis of mutagenesis by high LET radiation. Adv.Space Res. 14: 355-361.

Hei, T. K., Wu, L.-J., Liu, S.-X., Vannais, D., Waldren, C., & Randers-Pehrson, G. (1997) Mutagenic effects of a single and an exact number of alpha particles in mammalian cells. Proc.Natl.Acad.Sci.USA 94: 3765-3769.

Hei, T. K., Liu, S. X., & Waldren, C. (1998) Mutagenicity of arsenic in mammalian cells: role of reactive oxygen species. Proc.Natl.Acad.Sci.USA 95: 8103-8107.

Hill, B., Rozler, E., Travis, M., Chen, S., Zannetino, A., Simmons, P., Galy, A., Chen, B., & Hoffman, R. (1996) High-level espression of a novel epitope of CD59 identifies a subset of CD34+ bone marrow cells highly enriched for pluripotent stem cells. Exp.Hematol. 24: 936-943.

Hinkle, L. L. (1980) Mutagenesis and Genome Repair in Mammalian Cells. Thesis, M.S., University of Colorado.

Holguin, M. H., Martin, C. B., Weis, J. H., & Parker, C. J. (1993) Enhanced expression of the complement regulatory protein, membrane inhibitor of reactive lysis (CD59), is regulated at the level of transcription. Blood 82: 968-977.

Holguin, M. H., Martin, C. B., Eggett, T., & Parker, C. J. (1996) Analysis of the gene that encodes the complement regulatory protein, membrane inhibitor of reactive lysis (CD59). J.Immunol. 157: 1659-1668.

Huang, M.-T., Xie, J.-G., Wang, Z. Y., Ho, C. T., Lou, Y.-R., Wang, C.-X., Hard, G. C., & Conney, A. H. (1997) Effects of tea, decafinated tea, and caffeine on UVB light-induced complete carcinogenesis in SKH-1 mice: demonstration of caffeine as a biologically important constituent of tea. Cancer Res. 57: 2623-2629.

Ishii, C. & Inoue, H. (1989) Epistasis, photoreactivation and mutagen sensitivity of DNA repair mutants *upr-1* and *mus-26* in *Neurospora crassa*. Mutat.Res. 218: 95-103.

Jeggo, P. A. (1998) DNA breakage and repair. Advances in Genetics 38: 185-218.

Jones, C., Wuthier, P., & Puck, T. T. (1975) Genetics of somatic cell surface antigens, III. Further analysis of the A_L marker. Somat.Cell Mol.Genet. 1: 235-246.

Jones, C., Moore, E. E., & Lehman, D. W. (1979) Genetic and biochemical analysis of the a1 cell-surface antigen associated with human chromosome 11. Proc.Natl.Acad.Sci.USA 76: 6491-6495.

Kao, F.-T., Jones, C., & Puck, T. T. (1977) Genetics of cell-surface antigens: regional mapping of three components of the human cell-surface antigen complex, A_L, on chromosome 11. Somat.Cell Mol.Genet. 3: 421-429.

Kinoshita, T., Ohishi, K., & Takeda, J. (1997) GPI-anchor synthesis in mammalian cells: genes, their products, and a deficiency. Journal of Biochemistry 122: 251-257.

Korty, P. E., Tedder, T. F., & Shevach, E. M. (1992) Identification of the ligands for the CD59 and Ly-6A.2 cell surface antigens. Fed.Am.Soc.Exp.Biol.J. 62: 1224-1228.

Kotwal, G. J., Isaacs, S. N., McKenzie, R., Frank, M. M., & Moss, B. (1990) Inhibition of the complement cascade by the major secretory protein of *Vaccinia* virus. Science 250: 827-830.

Kraemer, S. M. & Waldren, C. A. (1997) Chromosomal mutations and chromosome loss measured in a human-hamster hybrid cell line, A_LC: studies with colcemid, ultraviolet irradiation, and ^{137}Cs-gamma rays. Mutat.Res. 379: 151-166.

Kramer, S. (1996) Mutation studies in two newly constructed hamster-human hybrid cells lines. Colorado State University.

Kuby, J. (1994) Immunology. WH Freeman and Company, New York.

Lachmann, P. J. & Thompson, R. A. (1970) The complement-mediated lysis of unsensitized cells II. The characterisation of activated reactor as C5b and the participation of C8 and C9. J.Exp.Med. 131: 643-650.

Laird, P. W., Jackson-Grusby, L., Fazeli, A., Dickinson, S. L., Jung, W. E., Li, E., Weinberg, R. A., & Jaenisch, R. (1995) Suppression of intestinal neoplasia by DNA hypomethylation. Cell 81: 197-205.

Leonhardt, E. A., Trinh, M., Forrester, H. B., Johnson, R. T., & Dewey, W. C. (1997) Comparisons of the frequencies and molecular spectra of HPRT mutants when human cancer cells were X-irradiated during G1 or S phase. Radiat.Res. 148: 548-560.

Li, A. P., Gupta, R. S., Heflich, R. H., & Wassom, J. S. (1988) A review and analysis of the Chinese hamster ovary/hypoxanthine guanine phosphoriobyl transferase assay to determine the mutagenicity of chemical agents. Mutat.Res. 196: 17-36.

Liber, H. L. & Thilly, W. G. (1982) Mutation assay at the thymidine kinase locus in diploid human lymphoblasts. Mutat.Res. 94: 467-485.

Liber, H. L., LeMotte, P. K., & Little, J. B. (1983) Toxicity and mutgenicity of X-rays and (125-I)dUrd or (3-H)TdR incorporated in the DNA of human lymphoblast cells. Mutat.Res. 111: 387-404.

Lindahl, T. (1979) DNA glycosylases, endonucleases for apurinic/apyrimidinic sites and base excision repair. Prog.Nucleic Acid Res.Mol.Biol. 22: 135-192.

Lindahl, T. (1993) Instability and decay of the primary structure of DNA. Nature 352: 709-715.

Liszewski, M. K., Farries, T. C., Lublin, D. M., Rooney, I. A., & Atkinson, J. P. (1996) Control of the complement system. Adv.Immunol. 61: 201-283.

Little, J. B., Nagasawa, H., Pfenning, T., & Vetrovs, H. (1998) Radiation-induced genomic instablity: delayed mutagenic and cytogenic effects of X rays and alpha particles. Radiat.Res. 148: 299-307.

Liu, S. X., Athar, M., Lippai, I., Waldren, C. A., & Hei, T. K. (2001) Induction of oxyradicals by arsenic: Implication for mechanism of genotoxicity. Proc.Natl.Acad.Sci.USA 98: 1643-1648.

Lockert, D. H., Kaufman, K. M., Chang, C., Husler, T., Sodetz, J. M., & Sims, P. J. (1995) Identity of the segment of Human complement C8 recognized by complement regularoty protein CD59. J.Biol.Chem. 270: 19723-19728.

Maciejewski, J. P., Young, N. S., Yu, M., Anderson, S. M., & Sloand, E. M. (1996) Analysis of the expression of glycosylphosphatidylinositol anchored proteins on platelets from patients with paroxysmal nocturnal hemoglobinuria. Thromb.Res. 83: 433-447.

Maenpaa, A., Junnikkala, S., Hakulinen, J., Timonen, T., & Meri, S. (1996) Expression of complement membrane regulators membrane cofactor protein (CD46), Decay Accelerating Factor (CD55), and Protectin (CD59) in Human malignant gliomas. American Journal of Pathology 148: 1139-1152.

Malling, H. (1971) Dimethylnitrosamine: Formation of mutagenic compounds by interaction with mouse liver microsomes. Mutat.Res. 13: 425-429.

Marchbank, K. J., Morgan, B. P., & Van den Berg, C. W. (1995) Regulation of CD59 expression on K562 calls: effects of phorbol myristate acetate, cross-linking antibody and non-leathal complement attack. Immunology 85: 146-152.

Maron, D. & Ames, B. N. (1983) Revised methods for the Salmonella mutagenicity test. Mutat.Res. 113: 172-215.

Marx, J. (1994) Oncogenes reach a milestone. Science 266: 1942-1944.

Matsukura, N., Willey, J., Miyashita, M., Taffe, B., Hoffmann, D., Waldren, C., Puck, T. T., & Harris, C. C. (1991) Detection of direct mutagenicity of cigarette smoke condensate in mammalian cells. Carcinogenesis 12: 685-689.

Matsuoka, A., Hayashi, M., & Ishidate, M. Jr. (1979) Chromosomal aberration tests on 29 chemicals combined with S9 mix *in vitro*. Mutat.Res. 66: 277-290.

McCann, J., Choi, E., Yamasaki, E., & Ames, B. N. (1975) Detection of carcinogens as mutagens in the *Salmonella*/microsome test: Assay of 300 chemicals. Proc.Natl.Acad.Sci.USA 72: 5135-5139.

McCann, J. & Ames, B. N. (1976) Detection of carcinogens as mutagens in the *Salmonella*/microsome test: Assay of 300 chemicals: Discussion. Proc.Natl.Acad.Sci.USA 73: 950-954.

McGuiness, S., Shibuya, M., Ueno, A., Vannais, D., & Waldren, C. (1995) Mutant quantity and quality in mammalian cells (A_L) exposed to ^{137} gamma radiation: effect of caffeine. Radiat.Res. 142: 247-255.

McNiel, E. A., Waldren, C. A., Vannais, D. B., Holmes, A. A., Avery, A. C., Tatsumi, K., & Fox, M. H. (2000) Flow cytometric analysis of mutation in A_L cells. Radiation Research Society 47th Annual Meeting, Poster Session, P285: 138.

Meistrich, M. L., Meyn, R. E., & Barlogie, B. (1977) Synchronization of mouse L-P59 cells by centrifugal elutriation separation. Exp.Cell Res. 105: 169-177.

Melton, D. W., Konecki, D. S., Brennand, J., & Caskey, C. T. (1984) Structure, expression, and mutation of the hypoxanthine phosphoribosyltransferase gene. Proc.Natl.Acad.Sci.USA 81: 2147-2151.

Meri, S., Morgan, B. P., Davies, A., Daniels, R. H., Olavesen, M. G., Waldmann, H., & Lachmann, P. J. (1990) Human protectin (CD59), an 18,000-20,000 MW complement lysis restricting factor, inhibits C5b-8 catalysed insertion of C9 into lipid bilayers. Immunology 71: 1-9.

Meri, S., Waldmann, H., & Lachmann, P. J. (1991) Distribution of protectin (CD59), a complement membrane attack inhibitor, in normal human tissues. Lab.Invest. 65: 532-537.

Meuth, M. (1990) The structure of mutation in mammalian cells. Biochim.Biophys.Acta. 1032: 1-17.

Mitchell, A. R., Gosden, J. R., & Miller, D. A. (1985) A cloned sequence, p82H, of the alphoid repeated DNA family found at the centromeres of all human chromosomes. Chromosoma 92: 369-377.

Moehring, J. M. & Moehring, T. J. (1979) Characterization of the diphtheria toxin resistance system in Chinese hamster ovary cells. Somat.Cell Genet. 5: 453-468.

Moehring, T. J. & Moehring, J. M. (1977) Selection and characterization of cells resistant to diptheria toxin and *Pseudomonas* exotoxin A: Presumptive translational mutants. Cell 11: 447-454.

Montefiori, D. C., Cornell, R. J., Zhou, J. Y., Zhou, J. T., Hirsch, V. M., & Johnson, P. R. (1994) Complement control proteins, CD46, CD55, and CD59, as common surface constituents of human and simian immunodeficiency virus and possible targets for vaccine protection. Virology 205: 82-92.

Moore, M. M. & Doerr, C. L. (1990) Comparison of chromosome aberration frequency and small-colony TK-deficient mutant frequency in L5178Y/TK+/--3.7.2C mouse lymphoma cells. Mutagenesis 5: 609-614.

Morgan, B. P. (1992) Isolation and characterization of the complement-inhibiting protein CD59 antigen from platelet membranes. Biochem.J. 282: 409-413.

Morgan, B. P. (1999) Regulation of the complement membrane attack pathway. Crit.Rev.Immunol. 19: 173-198.

Morris, T., Masson, W., Singleton, B., & Thacker, J. (1993) Analysis of large deletions in the *HPRT* gene of primary human fibroblasts using the polymerase chain reaction. Somat.Cell Mol.Genet. 19: 9-19.

Muller, H. J. (1927) Artificial transmutation of the gene. Science 66: 84-87.

Muller, H. J. (1939) The mechanism of structural change in chromosomes of *Drosophila*. Proc.7th Int.Congr.Genet. J. Genet. Suppl. 221.

Muller, H. J. (1940) An analysis of the process of structural change in chromosomes of *Drosophila*. J.of Genet. 40: 1.

Muller, H. J. (1956) The relation between chromosome changes and gene mutations. Brookhaven Symp.Biol. 8: 126.

Nakamura, M., Okada, H., Sasaki, H., Yoshida, K., Kamada, M., Okada, N., Terada, M., & Ohno, T. (1996) Quantification of the CD55 and CD59, membrane inhibitors of complement on HIV-1 particles as a function of complement-mediated virolysis. Microbiol.Immunol. 40: 561-567.

Nelson, S. L., Giver, C. R., & Grosovsky, A. J. (1994) Spectrum of X-ray-induced mutation in the human *hprt* gene. Carcinogenesis 15: 495-502.

Nicklas, J. A., Hunter, T. C., O'Neill, J. P., & Albertini, R. J. (1991) Fine structure mapping of the hypoxanthine-guanine phosphoribosyltransferase (HPRT) gene region of the human X chromosome (Xq26). Am.J.Hum.Genet. 49: 267-278.

Niehans, G. A., Cherwitz, D. L., Staley, N. A., Knapp, D. J., & Dalmasso, A. P. (1996) Human carcinomas variably express the complement inhibitory proteins CD46 (membrane cofactor protein), CD55 (decay-accelerating factor), and CD59 (protectin). Am.J.Pathol. 149: 129-142.

Nishimura, J., Murakami, Y., & Kinoshita, T. (1999) Paroxysmal nocturnal hemoglobinuria: An acquired genetic disease. Am.J.Hematol. 62: 175-182.

O'Neill, J. P., Machanoff, R., & Hsie, A. W. (1982) Phenotypic expression time of mutagen-induced 6-thioguanine resistance in Chinese hamster ovary cells (CHO/HGPRT system): expression in division-arrested cell cultures. Environ.Mutagenesis 4: 421-434.

O'Neill, J. P., Brimer, P. A., Machanoff, R., Hirsch, G. P., & Hsie, A. W. (1977) A quantitative assay of mutation induction at the hypoxanthine- guanine phosphoribisyltransferase locus in Chinese hamster ovary cells (CHO/HPRT system): Development and definition of the system. Mutat.Res. 45: 91-101.

O'Neill, J. P., Machanoff, R., & Hsie, A. W. (1979) The use of a rat liver S9 activation system in the CHO/HGPRT mutation induction assay. Environ.Mutagenesis 2.

Oberly, T. J., Bewsey, B. J., & Probst, G. S. (1986) Thymidine kinase activity and trifluorothymidine resistance of spontaneous and mutagen-induced L5178Y cells in RPMI 1640 medium. Mutat.Res. 161: 165-171.

Pappenheimer, A. M. (1977) Diphtheria toxin. Annu.Rev.Biochemistry 46: 69-94.

Petranka, J. G., Fleenor, D. E., Sykes, K., Kaufman, R. E., & Rosse, W. F. (1992) Structure of the CD59-encoding gene: Further evidence of a relationship to murine lymphocyte antigen Ly-6 protein. Proc.Natl.Acad.Sci.USA 89: 7876-7879.

Philbrick, W. M., Palfree, R., Maher, S. E., Bridgett, M. M., Sirlin, S., & Bothwell, A. L. M. (1990) The CD59 antigen is a structural homologue of murine Ly-6 antigens but lacks interferon inducibility. Eur.J.Immmunol. 20: 87-92.

Ponnaiya, B., Cornforth, M. N., & Ullrich, R. L. (1997) Radiation-induced chromosomal instability in BALB/c and C57BL/6 mice: the difference is as clear as black and white. Radiat.Res. 147: 121-125.

Powell, M. B., Marchbank, K. J., Rushmere, N. K., Van den Berg, C. W., & Morgan, B. P. (1997) Molecular cloning, chromosomal localization, expression, and functional characterization of th mouse analogue of human CD59. J.Immunol. 158: 1692-1702.

Preston-Martin, S., Pike, M. C., Ross, R. K., Jones, P. A., & Henderson, B. E. (1990) Increased cell division as a cause of human cancer. Cancer Res. 50: 7415-7421.

Puck, T. T., Ciecuira, S. J., & Robinson, A. (1958) Genetics of somatic mammalian cells. III. Long-term cultivation of euploid cells from human and animal subjects. J.Exp.Med. 108: 945-955.

Puck, T. T., Wuthier, P., Jones, C., & Kao, F. T. (1971) Lethal antigens as genetic markers for study of human linkage groups. Proc.Natl.Acad.Sci.USA 68: 3102-3106.

Puck, T. T. & Waldren, C. A. (1987) Mutation in mammalian cells: Theory and implications. Somat.Cell Mol.Genet. 13: 405-409.

Rice, G. C., Dean, P. N., Gray, J. W., & Dewey, W. C. (1984) An ultra-pure *in vitro* phase synchrony method employing centrifugal elutriation and viable flow cytometric cell sorting. Cytometry 5: 289-298.

Ritenour, E. R., Braaton, M., Harrison, G. H., Ueno, A., Gadd, M., Manco-Johnson, M., Parker, R. D., Shih, S., & Waldren, C. A. (1991) Absence of mutagenic effects of continuous and pulsed ultrasound in cultured (A_L) human-hamster hybrid cells. Ultrasound in Med.& Biol. 17: 921-930.

Roldan, A. L., Cubellis, M. V., Masucci, M. T., Behrendt, N., Lund, L. R., Dano, K., Appella, E., & Blasi, R. (1990) Cloning and expression of the receptor for human urokinase plasminogen activator, a central molecule in cell surface, plasmin dependent proteolysis. EMBO J. 9: 467-474.

Rollins, S. A., Zhao, J., Ninomiya, H., & Sims, P. J. (1991) Inhibition of homologous complement by CD59 is mediated by a species-selective recognition conferred through binding to C8 within C5b-8 or C9 within C5b-9. J.Immunol. 146: 2345-2351.

Rooney, I. A., Atkinson, J. P., Krul, E. S., Schonfeld, G., Polakoski, K., Saffitz, J. E., & Morgan, B. P. (1993) Physiologic relevance of the membrane attack complex inhibitory protein CD59 in human seminal plasma: CD59 is present on extracellular organelles (prostasomes), binds cell membranes, and inhibits complement-mediated lysis. J.Exp.Med. 177: 1409-1420.

Ross, M. H. & Reith, E. J. (1985) Histology A Text and Atlas. Harper and Row, New York.

Rossman, T. G. & Goncharova, E. I. (1998) Spontaneous mutagenesis in mammalian cells is caused mainly by oxidative events and can be blocked by antioxidants and metallothionein. Mutat.Res. 402: 103-110.

Rushmere, N. K., Harrison, R. A., Van den Berg, C. W., & Morgan, B. P. (1994) Molecular cloning of the rat analogue of human CD59: structural comparison with human CD59 and identification of a putative active site. Biochem J. 304: 595-601.

Saifuddin, M., Hedayati, T., Atkinson, J. P., Holguin, M. H., Parker, C. J., & Spear, G. T. (1997) Human immunodeficiency virus type 1 incorporates both glycosyl phosphatidylinositol-anchored CD55 and CD59 and integral membrane CD46 at levels that protect from complement-mediated destruction. J.Gen.Virol. 78 (Pt 8): 1907-1911.

Saul, R. L. & Ames, B. N. (1991) Background levels of DNA damage in the population. In: Mechanisms of DNA damage and repair: Implications for Carcinogenesis and risk assessment (Simic, M. G., Grossman, L., & Upton, A. C., eds.), pp. 529-535. Plenum, NY.

Schmitz, J., Zimmer, J. P., Kluxen, B., Aries, S., Bogel, M., Gigli, I., & Schmitz, H. (1995) Antibody-dependent complement-mediated cytotoxicity in sera from Patients with HIV-1 infection is controlled by CD55 and CD59. J.Clin.Invest. 96: 1520-1526.

Shibata, T. & Kohsaka, T. (1995) Effects of complement activation on the expression of CD59 by human mesangial cells. J.Immunol. 155: 403-409.

Shibuya, M. L., Ueno, A. M., Vannais, D. B., Craven, P. A., & Waldren, C. A. (1994) Megabase pair deletions in mutant mammalian cells following exposure to Amsacrine, an Inhibitor of DNA Topoisomerase II. Cancer Res. 1092-1097.

Shows, T. B., Alders, M., Bennett, S., Burbee, P., Cartwright, P., Chandrasekharappa, S., Cooper, P., Courseaux, A., Davies, C., Devignes, M.-D., Devilee, P., Elliott, R., Evans, G., Fantes, J., Garner, H., Gaudray, P., Gerhard, D. S., Gessler, M., Higgins, H., Hummerich, H., James, M., Lagercrantz, J., Litt, M., Little, P., Mannens, M., Munroe, D., Nowak, N., O'Brien, S., Parker, N., Perlin, N., Reid, L., Richard, C., Sawicki, M., Swallow, D., Thakker, R., Van Heyningen, V., van Schothorst, E., Vorechovsky, I., Wadelius, B., Weber, B., & Zabel, B. (1996) Report of the fifth international workshop on human chromosome 11 mapping (1996). Cytogenet.Cell Genet. 74: 1-56.

Simon, H., Risse, B., Jost, M., Oppenheimer, S., Kari, C., & Rodeck, U. (1996) Identification of differentially expressed messenger RNAs in human melanocytes and melanoma cells. Cancer Res. 56: 3112-3117.

Sims, P. J., Rollins, S. A., & Wiedmer, T. (1989) Regulatory control of complement on blood platelets. J.Biol.Chem. 264: 19228-19235.

Sinclair, W. K. & Morton, R. A. (1966) X-ray sensitivity during the cell generation cycle of cultured Chinese hamster cells. Radiat.Res. 29: 450-474.

Solomon, K. R., Rudd, C. E., & Finberg, R. W. (1996) The association between glycosylphosphatidylinositol-anchored proteins and heterotrimeric G protein α subunits in lymphocytes. Proc.Natl.Acad.Sci.USA 93: 6053-6058.

Stryer, L. (1988) Biochemistry. WH Freeman and Co., New York.

Telen, M. J. (1995) Glycosyl phosphatidylinositol-linked blood group antigens and paroxysmal nocturnal hemoglobinuria. Transfus.Clin.Biol. 2: 277-290.

Thacker, J., Stephans, M. A., & Stretch, A. (1978) Mutation to ouabain resistance in Chinese hamster cells: Induction by ethyl methanesulphonate and lack of induction by ionizing radiation. Mutat.Res. 51: 255-270.

Thacker, J. (1986) The nature of mutants induced by ionizing radiation in cultured hamster cells. III. Molecular characterization of HPRT-deficient mutants induced by gamma rays or alpha particles showing that the majority have deletions of all or part of the hprt gene. Mutat.Res. 160: 267-275.

Thilly, W. G., Deluca, J. G., Furth, E. E., Hoppe, H., & Penman, B. W. (1976) Mutation of human lymphoblasts by methylnitrosourea. Chem.-Biol.Interact. 15: 33-50.

Thilly, W. G., Deluca, J. G., Furth, E. E., Hoppe, E. I., Kaden, D. a., Krolewski, J. J., Skopek, t. r., Slapikoff, S., Tixard, R. J., & Penman, B. W. (1980) Chemical Mutagens VI, pp. 331-360. Plenum, New York.

Tomita, M. (1999) Biochemical background of paroxysmal nocturnal hemoglobinuria. Biochim.Biophys.Acta. 1455: 269-286.

Tommasi, S., Denissenko, M. F., & Pfeifer, G. P. (1997) Sunlight induces pyrimidine dimers preferentially at 5-methylcytosine bases. Cancer Res. 57: 4727-4730.

Tone, M., Walsh, L. A., & Waldman, H. (1992) Gene structure of human CD59 and demonstration that discrete mRNAs are generated by alternative polyadenylation. J.Mol.Biol. 227: 971-976.

Turker, M., Walker, K. A., Jennings, C. D., Mellon, I., Yusufji, A., & Urano, M. (1995) Spontaneous and ionizing radiation induced mutations involve large events when selecting for loss of an autosomal locus. Mutat.Res. 329: 97-105.

Turker, M. S., Mummaneni, P., & Cooper, G. E. (1994) The mouse APRT gene as a model for studying epigenetic gene inactivation. Adv.Exp.Med.Biol. 370: 647-652.

Turker, M. S., Pieretti, M., & Kumar, S. (1997) Molecular evidence for the induction of large interstitial deletions on mouse chromosome 8 by ionizing radiation. Mutat.Res. 374: 201-208.

Tyzzler, E. E. (1916) Tumour immunology. Journal of Cancer Research 1: 125-155.

Van den Berg, C. W., Cinek, T., Hallett, M. B., Horejsi, V., & Morgan, B. P. (1995) Exogenous glycosyl phosphatidylinositol-anchored CD59 associates with kinases in membrane clusters on U937 cells and becomes Ca^{2+} -signaling competent. Journal of Cell Biology 131: 669-677.

Van den Berg, C. W., Harrison, R. A., & Morgan, B. P. (1995) A rapid method for the isolation of analogues of human CD59 by preparative SDS-PAGE: application to pig CD59. Journal of Immunological Methods 179: 223-231.

Van Ness, B. G., Howard, J. B., & Bodley, J. W. (1980) ADP-ribosylation of elongation factor 2 by diphtheria toxin: NMR spectra and proposed structures of ribosyl-diphthamide and its hydrolysis products. J.Biol.Chem. 225: 10710-19716.

Vanderplasschen, A., Mathew, E., Hollinshead, M., Sim, R. B., & Smith, G. L. (1998) Extracellular enveloped *Vaccinia* virus is resistant to complement because of incorporation of host complement control proteins into its envelope. Proc.Natl.Acad.Sci.U.S.A 95: 7544-7549.

Waldren, C., Correll, L., Sognier, M. A., & Puck, T. T. (1986) Measurement of low levels of x-ray mutagenesis in relation to human disease. Proc.Natl.Acad.Sci.USA 83: 4839-4843.

Waldren, C. & Puck, T. T. (1987) Steps toward experimental measurement of total mutations relevant to human disease. Somat.Cell Mol.Genet. 13: 411-414.

Waldren, C., Ueno, A., Vannais, D., Bedford, J. S., & Hei, T. (1992) Molecular analysis of chromosomal mutations induced in mammalian cells by high and low dose rate ^{137}Cs gamma rays. In: Low Dose Irradiation and Biological Defense Mechanisms (Sugihara, T., Sagan, L. A., & Aoyama, T., eds.), pp. 339-342. Elsevier Science Publishers B.V., Amsterdam.

Waldren, C. A., Jones, C., & Puck, T. T. (1979) Measurement of mutagenesis in mammalian cells. Proc.Natl.Acad.Sci.USA 76: 1358-1362.

Waldren, C. A. & Jones, C. (1981) Chromosome loss and damage as measured by biological markers. In: Health Risk Analysis: Proceedings of The Third Life Sciences Symposium (Richmond, C. R., Walsh, P. J., & Copenhaver, E. D., eds.), pp. 333-343. The Franklin Press, Philadelphia.

Waldren, C. A. (1983) Mutational analysis in cultured human-hamster hybrid cells. In: Chemical Mutagens: Principles and Methods for Their Detection, Vol. 8 (de Serres, F. J., ed.), pp. 235-260. Plenum Publishing Corp., New York.

Waldren, C. A., Fouladi, B., Braaton, M., Parker, R. D., & Vannais, D. (1992) The use of human repetitive DNA to target selectable markers into only the human chromosome of a human/hamster hybrid cell Line (A_L). Somat.Cell Mol.Genet. 18: 417-422.

Waldren, C. A., Ueno, A. M., Schaeffer, B. K., Wood, S. G., Sinclair, P. R., Doolittle, D. J., Smith, C. J., Harvey, W. F., Shibuya, M. L., Gustafson, D. L., Vannais, D. B., Puck, T. T., & Sinclair, J. F. (1999) Mutant yields and mutational spectra of heterocyclic amines MeIQ and PhIP at the S1 locus of human-hamster A_L cells with activated by chick embryo liver (CELC) co-cultures. Mutat.Res. 425: 29-46.

Wang, Y., Dang, J., Johnson, L. K., Selhamer, J. J., & Doe, W. F. (1995) Structure of the human urokinase receptor gene and its similarity to CD59 and the Ly-6 family. Eur.J.Biochem. 227: 116-122.

Welker, D. L. & Deering, R. A. (1978) Genetics of radiation sensitivity in the slime mold *Dictyostelium discoideum*. J.Gen.Microbiol. 109: 11-23.

Williams, A. F., Tse, A., & Gagnon, J. (1988) Squid glycoproteins with structural similarity to Thy-1 and Ly-6 antigens. Immunogenetics 27: 265-272.

Wilson, A. B., Seilly, D., Willers, C., Vannais, D. B., McGraw, M., Waldren, C. A., Hei, T. K., & Davies, A. (1999) Antigen S1, encoded by the MIC1 gene, is characterized as an epitope of human CD59, enabling measurement of mutagen-induced intragenic deletions in the AL cell system. Somat.Cell Mol.Genet. 25: 147-157.

Wood, R. D. (1996) DNA repair in eukaryotes. Annu.Rev.Biochem. 65: 135-167.

Wood, R. D. (1997) Nucleotide excision repair in mammalian cells. J.Biol.Chem. 272: 23465-23468.

Yamashina, M., Ueda, E., Kinoshita, T., Takami, T., Ojima, A., Ono, H., Tanaka, H., Kondo, N., Orii, T., Okada, H., Okada, N., Inoue, K., & Kitani, T. (1990) Inherited complete deficiency of 20-kilodalton homologous restriction factor (CD59) as a cause of paroxysmal nocturnal hemoglobinuria. N.Engl.J.Med. 323: 1184-1194.

Yu, Z., Chen, J., Ford, B. N., Brackley, M. E., & Glickman, B. W. (1999) Human DNA repair systems: an overview. Environ.Molec.Mutagen. 33: 3-20.

Zhang, H. F., Yu, J., Chen, S., Morgan, B. P., Abagyan, R., & Tomlinson, S. (1999) Identification of the individual residues that determine human CD59 species selective activity. J.Biol.Chem. 274: 10969-10974.

Zhu, L. X., Waldren, C. A., Vannais, D., & Hei, T. K. (1996) Cellular and molecular analysis of mutagenesis induced by charged particles of defined LET. Radiat.Res. 145: 251-259.

Zimmerman, F. K. (1973) Detection of genetically active chemicals using various yeast systems. In: Chemical Mutagens: Principles and Methods for Their Detection (Hollaender, A., ed.), vol. 3, pp. 209-258. Plenum, New York.

CHAPTER 2

TIMING OF REPLICATION OF CD59 ON HUMAN CHROMOSOME 11, CELL KILLING, AND MUTANT INDUCTION IN THE A_L HYBRID

ABSTRACT

My goal was to determine, as precisely as possible, when during "S" phase the *CD59* gene in human chromosome 11 was replicated, and to relate mutability of the *CD59* gene to its replication.

The outline of the protocol is as follows (see Chapter 2, Figure 1). I determined the timing of the replication of the CHO and human chromosomes in the human X hamster hybrid cell line A_L using DNA pulse labeling. A_L cells contain one human chromosome 11 and a normal complement of CHO chromosomes. Mutation is measured as the loss of expression of the human CD59 antigen. Centrifugal elutriation was used to collect A_L cells in the G_1 phase of the cell cycle. The resultant elutriated cells were incubated and allowed to progress through the cell cycle from G_1 into S, and G_2. Cell cycle phases were analyzed using flow cytometry and bromodeoxyuridine (BrdU) labeling. The timing of DNA replication was measured by pulse labeling with BrdU, which incorporates in the place of thymidine in the DNA double helix during DNA replication. Pulse labeling and fluorescent *in-situ* hybridization (FISH) was then used to determine when the human chromosome was replicating. The A_L hybrid cells were inoculated onto plates in BrdU labeling groups, incubated to initiate cell cycle progression and sequentially labeled with BrdU in one-hour relays starting at 4.5 hours post-plating. Labeling was started at 4.5 hours because flow cytometry analysis showed

that replication did not begin until 5 to 6 hours after inoculation of cells on the plates. Control plates were labeled from 4.5 to 10.5 hours. Cells were then prepared for Fluorescent In-Situ Hybridization (FISH) as follows: all chromosomes were labeled with the blue stain 4, 6-diamino-2-phenyl-indol (DAPI); the human chromosome was specifically tagged with fluorescein isothiocyanate (FITC) bound to human centromere probe D11Z1 (Mitchell et al., 1985), which is specific to the human chromosome. Regions of DNA replication on the chromosomes were visualized with a Zeiss Axioskop (Thornwood, NY) fluorescent microscope by the incorporation of BrdU labeled with a Texas Red® fluorochrome on an anti-BrdU antibody. Progression of the cells through the cell cycle was elucidated by determining which regions of the chromosome had replicated using a fluorescent microscope with a triple band pass filter, and a digital analysis program (Metamorph, Universal Imaging Corp., Westchester, PA). Cell cycle progression was measured by flow cytometry fluorescence assisted cell sorting (FACS). This analysis was consistent with the data from the pulse labeling. Both analyses showed that replication of CHO chromosomes began at 5.5 hours post-plating and continued through 10.5 hours. Eighty percent of human chromosome 11 replicated between 6.5 to 8.5 hrs, with the remainder replicating at 8.5 to 12 hrs.

Mutational studies were done with cells irradiated with 1.5 and 3 Gy of ^{137}Cs gamma rays in early G_1, and at 8 hours after plating, when human chromosome 11 was replicating. Cell killing and mutant induction were highest in early G_1 cells; cells in S phase were more resistant to killing and mutant induction than those in early G_1 at the equal irradiation doses. The induced mutant fraction by 3 Gy of ^{137}Cs gamma per LD_{50}

was $160/10^5$ in G_1 and $92/10^5$ in S phase respectively. Mutant induction was lowest when the *CD59* gene was replicating.

INTRODUCTION

My purpose was to study the mutant induction at two different phases of the cell cycle in the A_L human X hamster hybrid cell line. Thus, I had to carefully characterize A_L progression thru the cell cycle. Figure 1 is a flow-diagram of the protocol used which includes the process to plate and incubate cells, separate the G_1 cells by centrifugal elutriation, and characterize the cell position in the cell cycle by flow cytometry or pulse labeling with BrdU and FISH analysis. Other populations of elutriated cells were plated, irradiated with ^{137}Cs gamma rays and analyzed for survival and mutant induction at G_1 and S phase.

Most *in vitro* studies of mutation, including those using the A_L assay were done on dividing cells (Adair et al., 1980; Waldren, 1983; Clive, 1987). Various mutation assays have been characterized and used to study mutant induction by agents such as ultraviolet (UV) light, gamma-rays, X-rays, chemicals, and metals in dividing cells (Liber and Thilly, 1982; Evans et al., 1986; Waldren and Jones, 1981; Waldren et al., 1999). However, in adult humans, rapidly dividing (cells dividing every few hours to weeks) are found primarily restricted to certain organs and locations such as cells in the alimentary tract, the skin, the reticuloendothelial system, and in males, the germ cells involved in spermatogenesis. These rapidly dividing cells arise from long-lived stem cells and generally have a short life span in the body: 2-3 days for the gut, two weeks for the skin, a month for the blood cells, and about two months for sperm (Clermont, 1963; Ross and

Flow Chart for A_L Cell Cycle Characterization and Mutant Induction Experiment

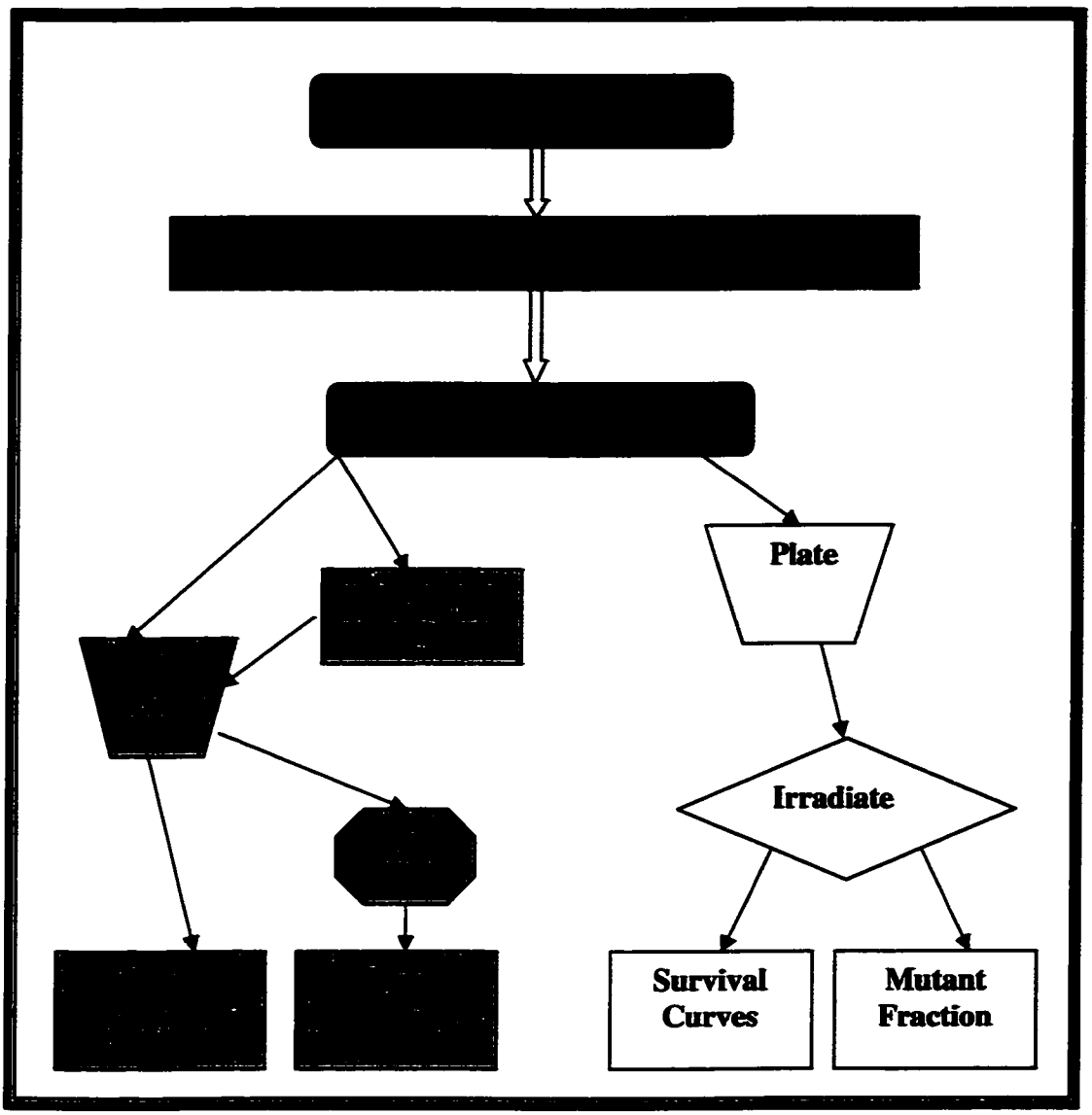

Figure 1. A_L cells were grown up to the numbers needed for effective centrifugal elutriation and harvested. Cells were elutriated and used to perform chromosome studies and conduct irradiation experiments. Those cells used for chromosome studies were fixed and analyzed by a flow cytometer to characterize the cell cycle, others were pulse labeled with BrdU as they progressed through the cell cycle and labeled for FISH analysis. Line-scans were used to quantify FISH labeling. Cells for irradiation experiments were plated and allowed to progress through the cell cycle, and then irradiated at the appropriate time. Survival and induced mutant fraction were measured.

Reith, 1985). The cells of several other body tissues have longer proliferation cycles, such as monthly for the uterine lining and the female breast, and even longer for bone (Ross and Reith, 1985). However, most of the human body's cells at risk for DNA damage are not rapidly dividing, but are non-cycling or quiescent. The majority of tissue cells in the body are defined as being in G_0, not proliferating, and not cycling, just performing the function of the tissue that they belong. These include connective tissue, muscle, lymphatic, adipose, and central nervous system tissue, which make up the body's larger systems such as the digestive system, skeletal system, musculature, the brain and nervous system.

Mutant induction estimates for humans and other animals have been based primarily on results from *in vitro* mutation assays with rapidly cycling cells. My purpose was to better predict how non-cycling cells react to mutant induction by comparing the mutant induction in early G_1 cells, S phase cells, and log phase cells. One method to measure mutant induction in non-cycling cells is to modify standard assays to detect mutants in cells at different times in the cycle. My assumption is that the G_1 cells provide a reasonable mimic to G_0 cells. Both have a 1 n amount of DNA, and G_0 cells are G_1 cells that have stopped cycling. Comparing the G_1/G_0 cells to cells in other compartments of the cell cycle should give an estimate for the susceptibility to killing and mutant induction by ^{137}Cs gamma for quiescent cells compared to cycling cells in specific phases of the cell cycle. The A_L mutation assay proved to be an excellent model to examine cells in different compartments of the cell cycle, because I could measure both large and small deletions and mutations.

The A_L Cell for Mutation Measurement

Many *in vitro* mutation assays using cultured mammalian cells have been described (DeMarini et al., 1989; Cotton, 1993; Ashby et al., 1994). All of these can measure small intragenic mutations that are characteristic of UV irradiation and alkylating agents, but most are less well suited to measure large, multilocus mutations (Waldren et al., 1979; Waldren et al., 1986; DeMarini et al., 1989). Small mutations are defined as those that affect only a specific gene, and may be as small as a single base change. Most of the mutation assays described in Chapter I cannot measure large deletions that involve vital genes whose loss destroys cell viability. However, large chromosomal deletions and rearrangements have been implicated in the cancer process as well as smaller types of mutations (Croce and Klein, 1985; Bishop, 1987; White and Caskey, 1988; Lothe et al., 1989; Josyln et al., 1991). The power of the A_L *in vitro* assay system is that it detects both small and large mutations with great sensitivity. The A_L assay is at least 100 fold more sensitive to the mutagenic activity of ionizing radiation than standard assays such as the Chinese hamster ovary (CHO) hypoxanthine guanine phosphoribosyl transferase (HPRT) assay, and 1000 times more sensitive than the bacterial Ames test (Waldren et al., 1986; Waldren et al., 1992). Although the A_L assay is as sensitive as the mouse lymphoma L5178Y $TK^{+/-}$, the A_L assay has a large 160 Mbp human chromosome target for mutant induction and measuring of mutant spectra that is not required for cell viability (Waldren, 1983; Evans et al., 1986). This sensitivity makes it possible to quantify mutagenic effects at the lower exposure levels where most human exposures occur. The assay sensitivity also makes it possible to study the efficacy of

radio-protectants and other anti-mutagens. These qualities also enable the use of the A_L assay to quantify changes in mutant induction by ionizing radiation when cells are mutated at different phases of the cell cycle.

The A_L hybrid cell line contains a normal set of CHO chromosomes, plus a single copy of human chromosome 11. The A_L cell line was made by fusion of a CHO double auxotrophic mutant and a normal human amniotic fluid fibroblast. Its properties and use in mutation assays has been described (Waldren, 1983; Waldren et al., 1986; Puck and Waldren, 1987; Matsukura et al., 1991; Shibuya et al., 1994; Waldren et al., 1998; Waldren et al., 1999; Kraemer et al., 2001). Human chromosome 11 encodes a series of human cell surface antigens that provide excellent markers for mutations. I primarily used the CD59 antigen, formally known as S1, for mutation studies. The *CD59* gene is located at 11p13, and formally known as *MIC1*, encodes the CD59 surface protein (Davis et al., 1995; Wilson et al., 1999; Kraemer et al., 2001). Wild type A_L cells that express CD59 are quantitatively killed when exposed to a monoclonal anti-CD59 antibody and rabbit serum complement. Mutations of any kind (intragenic or multilocus) involving the *CD59* gene usually causes loss of expression of CD59. Mutant cells survive and grow to form colonies when exposed to the E7.1 anti-CD59 antibody and rabbit serum complement (Carey et al., 1976; Waldren et al., 1999). Thus, mutant induction is scored by counting mutant colonies as a function of the mutagen dose. Mutant clones can then be selected and their genotype investigated by using southern or polymerase chain reaction (PCR) analysis with the mapped probes available for human chromosome 11 (Shibuya, et al. 1994; McGuiness et al., 1995; Kraemer and Waldren, 1997; Waldren et

al., 1998; Waldren et al., 1999; Wilson et al., 1999; Gustafson et al., 2000; Kraemer et al., 2001). The analysis of mutational spectra using southern and PCR analysis is covered in Chapter 3.

Mutation in the Cell Cycle

Under normal conditions, the error rate for human DNA synthesis is very small, i.e. 1 X 10^{-9}/base pair. For example, DNA replication in human cells is estimated to make mistakes in only three base pairs when copying the 3 billion base pairs in the human genome (Lindahl, 1979). The National Academy of Sciences (1972) estimates a spontaneous mutation rate per human generation in the range of 5 X 10^{-7} to 5 X 10^{-6} per gamete. However, when cells are exposed to mutagenic agents, the rate of introduction of mistakes increases considerably (Goodman, 1988; Ames, 1989). Ionizing radiation, specifically X-ray radiation, was the first agent shown to induce mutations in Drosophila and in corn (Muller, 1927; Stadler, 1928). The spontaneous rate of mutation in CHO cells has been measured as being 5 X 10^{-7} per viable cell per cell generation, with an induced mutation rate per cGy of about 2 X 10^{-7} per viable cell per cell generation (Carver et al., 1976). Carver did not find a significant difference in mutant induction between G_1 and S phase. Later works showed that cell survival and mutant induction vary during different phases of the cell cycle, depending on the mutagen used and on the cell type (Burki and Aebersold, 1978; Olive and Balnath, 1993; Leonhardt et al., 1997; Tauchi et al., 1999). Tables 1 thru 5 summarize previous results of mutant induction during various phases of the cell cycle with different mutagens.

Sinclair and Morton (1966) showed for CHO cells that X-rays are most lethal in

G_1 and G_2/M, with the greatest resistance in S phase (up to 100 times greater than for the G_1 cells determined by single cell survival derived from micro-colony survival; colonies of 50 cells or less). This pattern is similar to the results for mutation assays such as HPRT and TK (Table 1). Carver (1976), in contrast, did not see a difference between G_1 and S phase cells for mutant induction when hprt mutants were selected with 8-azaguanine.

For HPRT$^-$ mutants, Watanabe and Horikawa (1977) found no significant differences in the level of single strand breaks induced in cellular DNA and their rejoining through out the cell cycle. The G_1, S and G_2 phase radiation induced mutants were the same level and kind as log phase induced mutants. However, more radiation-induced mutants resistant to 8-azaguanine occurred in the radiation-sensitive G_1 -S boundary phase. Jostes et al., (1980) found that the mutant frequencies were much higher than in log phase cells, when the cells were irradiated in mitosis or at the G_1/S border. For studies using 8-azaguanine, S phase is the most resistant to mutant induction per survivor. G_1 is the same or slightly more sensitive to mutant induction than S, with the most sensitive phase at the G_1/S boundary. Burki, (1980) reported greater mutant induction in the G_1 stage of the cell cycle with maximum induction near the end of the G_1 period. His were among the first experiments to obtain a population of cells synchronized without the use of drugs and to measure mutation in these cells.

Chuang and Liber (1996) compared mutant induction for two loci, thymidine kinase (TK) and HPRT. They showed that the TK locus was most sensitive to radiation-induced mutants during G_1 through mid-S phase, whereas the HPRT locus was most

X-ray Mutation

Reference (Investigator)	Cell Type	Selection Method/ locus	Cell Killing, from highest to	Mutant Induction, from highest to lowest
Sinclair and Morton, 1966	CHO	N/A	G_1, G_2/M	N/A
Dewey et al., 1970	CHO	N/A	G_1/S, G_2/M	N/A
Carver et al., 1976	CHO	HPRT[1]/8AG[2]	same in all	same in all
Watanabe and Horikawa, 1977	HeLa S3	HPRT/8AG ASDG[3]	G_1/S	G_1/S>G_2
Jostes et al., 1980	CHO	HPRT/8AG	early G_1>G_1>S	M, G_1, G_1/S
Burki, 1980	CHO	HPRT/6TG[4]	G_1>G_2/M>S	G_1/S>G_1
O'Neill and Flint, 1985	CHO	HPRT	N/A	G_1
Miller et al., 1992	CH3 10T1/2 mouse	oncogenic transformation	G_2>eG_1>S	late S/G_2
Cao et al., 1993	CH3 10T1/2 mouse	oncogenic transformation	M>S	M>S
Olive and Balnath, 1993	CHO/V79	comet assay	N/A	earlyG_1>G_2/M> mid S>early S
Cheong et al., 1994	V79 *irs-1*	N/A	G_1/S all phases	N/A N/A
Evens et al., 1996	L5178Y mouse	TK	G_1, G_2/M	G_2/M>G_1
Chuang and Liber, 1996	WTK1 human WTK1 human	TK HPRT	G_1, early S G_1, early S	G_1, early S G_1
Leonhardt et al., 1997	EJ30-15 human	HPRT	G_1>S	G_1>S
Leonhardt et al., 2000	EJ30-15 human	HPRT	G_1>S	G_1>S

Table 1. Cell cycle position of maximum cell killing and mutant induction for cell exposed to X-rays, measured by various methods and loci. ([1]hypoxanthine-guanine-phosphoribosyl-transferase, [2] 8-azaguanine, [3]alkaline sucrose density gradients, [4]6-thioguanine.)

sensitive during G_1. The general pattern of induced mutations through the cell cycle using X-rays is shown in Table 1: for X-rays, G_1 is the most sensitive for cell killing and

mutant induction; although slight differences are seen when different end points assays are measured such as oncogenic transformation and comet assays, rather than mutation.

Many of the investigations in Table I were evaluating differences in DNA repair capability as a factor involved in differences in mutant induction thru the cell cycle. Cheong et al., (1994) compared mutant induction via X-rays in radiosensitive irs-1 (V79$^-$) cells with the parental V79 cells, and showed that the irs-1 cells had a relatively flat response for mutant induction thru the cell cycle, and a lack of radio-resistance during S phase. Results from this study suggest that an inability to repair damage in the irs-1, but not in the parental V79 cells, causes fluctuations in radio-sensitivity to X-rays, and possibly other ionizing radiation. Leonhardt et al., (1997) hypothesized that the reason they found more mutants/viable cell in G_1 was because there is more error-free repair of double strand breaks during S than G_1. They looked at three classes of induced mutants; class one had base pair changes or small deletions, class two had deletions of greater than 20 base pair, and class three was missing the entire *HPRT* gene. They showed that the induction frequency for all three classes of mutants was at least threefold lower in cells irradiated in S phase than for cells irradiated in G_1. Further research by Leonhardt et al., (1998) indicate that although survival was the same for G_1 and S the residual DNA damage lasted twice as long when the cells were irradiated in G_1 than when irradiated in S phase. The irradiated G_1 cells took longer to regain plating efficiencies and multiplied at lower rates than those in S phase. Expanding on their research, Leonhard et al. (2000) compared the frequencies of mutants yielding RT-PCR products of cells irradiated in G_1 and S phase. Sequencing of RT-PCR products and the associated genomic DNA showed

that 40% of the RT-PCR products had splice errors. The G_1 cells had 10 times less RT-PCR products, indicating that the low yield of mRNA was due to splice errors from deletions induced during G_1. They postulated that the preferential induction of mutants not yielding mRNA was due to splice errors from deletions preferentially induced in G_1.

Other methodologies of measuring DNA damage and cellular response caused by X-irradiation, such as oncogenic transformation or the comet assay, showed cell cycle dependent responses similar to those found by mutation assays. Watanabe et al., (1984) using hamster embryo cells and Redpath and Sun (1990) using a human-hybrid cell line showed cell-cycle-dependent induction of oncogenic transformation thru the cell cycle, (these two studies did not show the same pattern of transformation induction). Miller et al., (1992) used 10T1/2 cells to measure oncogenic transformation in synchronized cells collected using mitotic shake-off. They found the greatest transformation at G_2, but their measurement of where the cells were in the cell cycle was not reliable. Some CH2 10T1/2 cell populations have proven difficult to synchronize. Using the same type of CH2 10T1/2 cells, Cao et al., (1993) demonstrated the transformation frequency per viable cells was five times greater in M than in S phase. Differences could also be due to the species from which cells were obtained.

When comparing X-ray mutant induction assays, Table 1 shows the greatest cell killing per Gy is during G_1 or at the G_1/S border, and the highest mutant induction is generally in G_1. However, the highest levels of oncogenic transformation are found in M and G_2/M phases. Olive and Blanth, (1993) used comet assays to show that Chinese hamster V79 cells in S phase had about 2-3 times less induced damage in the form of

double strand breaks (DSBs) than G_1 or G_2/M phase cells exposed to X-rays. The researchers suggested that differences in DNA structure were responsible for reduced sensitivity for detecting DSBs in S phase. Most of the research to look at effects of ionizing radiation thru the cell cycle has been done using X-rays, although gamma rays have also been used. X-rays and gamma rays are both photons and cause very similar cell cycle responses as shown in Table 2, but they have slightly different linear energy transfer (LET) (Hall, 1994).

Gamma-ray Mutation

Reference (Investigator)	Cell Type	Selection Method/ locus	Cell Killing, from highest to lowest	Mutant Induction, from highest to lowest
Redpath and Sun, 1990	HeLa X skin hybrid	induced antigen	G_2 to M	G_2 to M
Grdina and Sigdestad, 1992	CHO	HPRT	G_1>G_2>S	G_1>G_2>S
Cao et al., 1992	CH3 10T1/2 mouse	trans-formation	late G_2 to M	late G_2 to M
Tauchi et al., 1993	L5178Y mouse	HPRT	G_1	G_1
Chuang and Liber, 1996	WTK1 human WTK1 human	TK HPRT	G_1, early S G_1, early S	G_1, early S G_1

Table 2. Cell cycle phase of maximal killing and mutant induction or cell transformation for cells exposed to gamma radiation.

Gamma-ray effects on cells in different phases of the cell cycle are very similar to those of X-rays. Grdina and Sigdestad (1992) found that regardless of the radiation quality used (they used ^{60}Co and fission-spectrum neutrons), cells in G_1 were the most sensitive to radiation-induced mutagenesis at the HPRT locus. Gamma ray assays that

use *in vitro* neoplastic transformation as the end point have results similar to those with X-rays; G_2 and mitosis are highly sensitive for transformation (Redpath and Sun, 1990; Cao et al., 1992). Data from Tauchi et al. (1993), using L5178Y mouse cells, and Chuang and Liber (1996), using WTK1 human cells, demonstrated that both HPRT and TK assays are most sensitive for mutant induction in G_1 and both kinds of cells were more sensitive to killing from gamma-rays in G_1 and early S phase. The greatest amount of data on cell cycle cell killing and mutant induction for ionizing radiation is for to X-rays followed by gamma rays, which produced similar cell effects. In contrast, very little data exists for neutron or most other kinds of radiation effects on mutant induction through the cell cycle.

Neutron Mutation

Reference (Investigator)	Cell Type	Selection Method/ locus	Cell Killing, from highest to lowest	Mutant Induction, from highest to lowest
Grdina and Sigdestad, 1992	CHO	HPRT	G_1>S	G_1>G_2/M
Tauchi et al., 1993	L5178Y mouse	HPRT	G_1/S>G_2/M>S	G_2/M>S>late S

Table 3. Cell cycle phase of maximal cell killing and mutant induction for cells exposed to neutrons.

Few reports on effects of neutrons on mutant induction during the cell cycle are available. Grdina and Sigdestad, (1992) found that CHO cells the G_1 phase were most sensitive for mutant induction at the HPRT locus for both the ^{60}Co and the fission-spectrum neutrons (Table 3). Tauchi et al., (1993) found in the L5178Y mouse cell that ^{252}Cf neutron radiation was more effective in inducing mutations at the same cell survival levels than

^{60}Co, and that G_2/M was particularly sensitive to mutant induction by ^{252}Cf. Essentially the same basic cell cycle sensitivity to cell killing and the mutant induction is seen for X-rays, gamma rays, and neutrons. In contrast, results for ionizing radiation compared with ultraviolet and chemical mutant induction are significantly different in that S phase tends to be more sensitive to mutant induction and cell killing (Table 4 and 5).

UV Mutation

Reference (Investigator)	Cell Type	Selection Method/ locus	Cell Killing, from highest to lowest	Mutant Induction, from highest to lowest
Han and Sinclair, 1969	CHO	NA	S>G_1>G_2	N/A
Riddle and Hsie, 1978	CHO	HPRT	S>G_1>G_2	S
Burki et al., 1980	CHO CHO CHO	HPRT Ouabain^R Diphtheria^R	G_1, early S G_1, early S G_1, early S	G1, early S G_1, early S G_1, early S
Wood and Burki, 1982	CHO	Diphtheria^R	early S>G	late G_1, early S
Enninga et al., 1985	Human fibroblasts	N/A	no difference	S
Kaufmann and Wilson, 1994	Human fibroblasts	chrom. aberrations	N/A	G_1/S border

Table 4. Cell cycle phase for maximum cell killing and mutant induction or induction of chromosomal aberrations for cells exposed to ultraviolet radiation.

Germicidal UV irradiation (254 nm) induces different kinds of mutants than and has different cell killing sensitivity than X-rays, gamma rays and neutrons. Figure 2 is a compilation of data from Sinclair and colleagues (Sinclair and Morton, 1966; Han and Sinclair, 1969) that compares killing curves from X-rays and UV in CHO cells, under

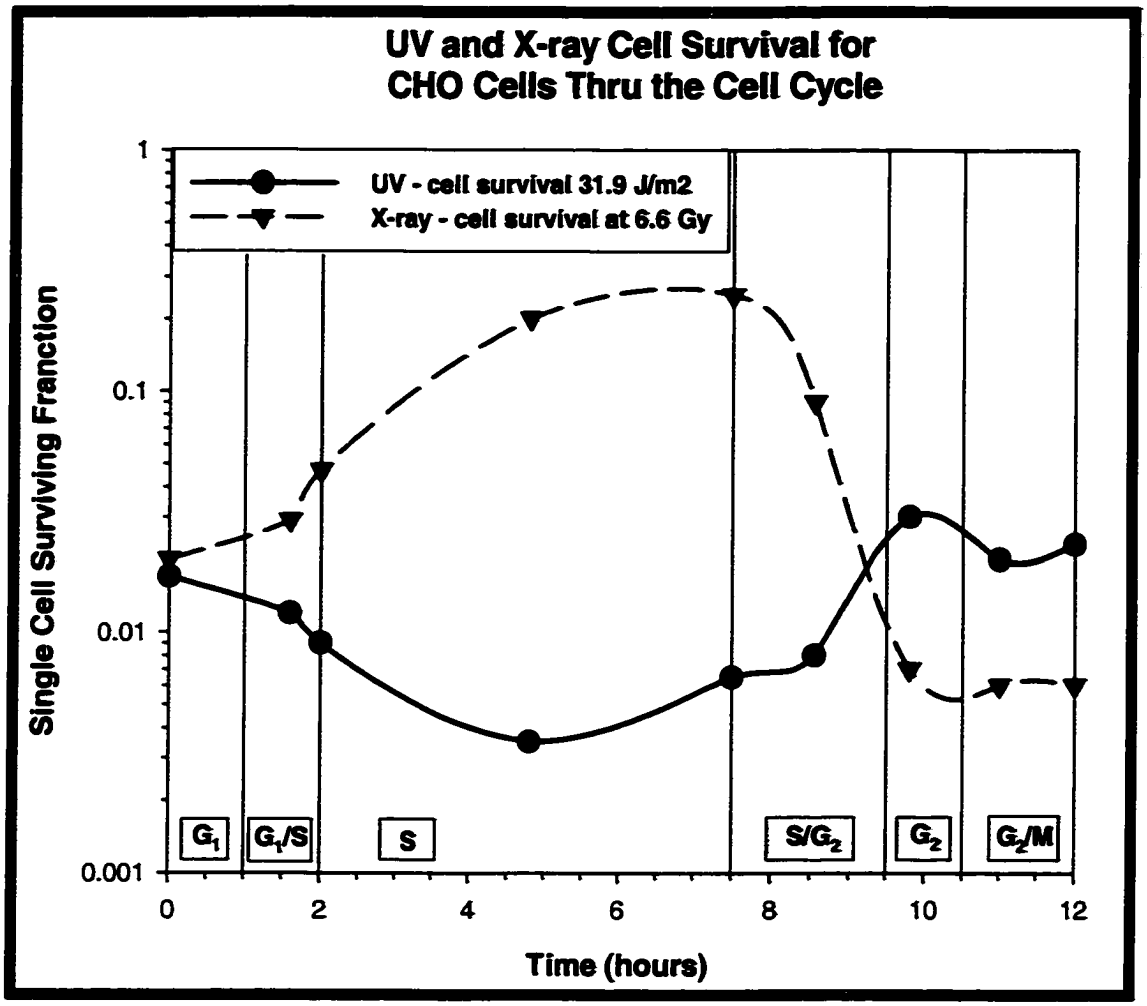

Figure 2. Survival for CHO cells irradiated with ultraviolet and X-ray thru the cell cycle. This comparison of survival curves for germicidal UV (254 nm) and 250 keV X-rays was done in the Sinclair lab in the late 1960's. UV caused relatively more cell killing in S phase, whereas killing with X-rays is greatest in G_1 and G_2/M (Redrawn from: Sinclair and Morton, 1966; Han and Sinclair, 1969).

identical conditions in the same laboratory, using the same methods for synchronization and cell growth. The UV irradiated CHO cells have a lower surviving fraction in S phase than the X-ray irradiated cells, but a greater surviving fraction in G_2 and G_2/M.

CHO cells respond differently to UV than to X-rays for cell killing and mutation. Riddle and Hsie (1978) demonstrated that the maximum mutant induction for UV is in S phase. Burki compared mutant induction by UV (Burki et al., 1980), X-rays (Burki, 1980) and chemicals (Burki and Aebersold, 1978). His results suggested different cell cycle phase-specific mutant induction for these agents. Burki also looked at different mutagenic endpoints including HPRT$^-$, ouabain^R, and diphtheria toxin^R for UV (Burki, 1980; Wood and Burki, 1982). They report increased diphtheria toxin resistance in late G_1 and early-S, but little variation at different cell cycle phases for HPRT$^-$ and ouabain^R mutant induction. Kaufmann and Wilson (1994) suggested that UV is an S phase dependent clastogen. They found that UV induced the most possible chromosomal aberration at the G_1/S border in synchronized human fibroblasts; cells in early G_1 or G_2 were less sensitive. The probable response differences in response between UV and ionizing radiation stems from differences in the specific damage caused with the induction of thymine-thymine dimers and different repair responses that are initiated by UV.

Cell cycle related mutant induction by chemicals is much different than by ionizing radiation with the primary mutant induction in S phase. Burki and Aebersold (1978) found that incorporation of 5-bromo-2'-deoxyuridine (BrdU) induces mutants during S phase. For HPRT, maximum mutant induction occurs 2 hours into S phase, and

Chemical Mutation

Reference (Investigator)	Mutagen	Cell Type	Selection Method/ locus	Cell Killing, From highest to	Mutant Induction, highest to lowest
Burki and Aebersold, 1978	5-bromo-2'-deoxyuridine	CHO	HPRT ouabain		early S mid S
Aebersold, 1979	5-fluoro-2'-deoxy-uridine (FldU)	CHO	HPRT	N/A	early S
Tong et al., 1980	methyl methanesulfonate N-methyl-N'-nitro-N-nitrosoguanidine(MNNG)	rat liver	HPRT HPRT	S S	S S
Goth-Goldstein and Burki, 1980	N-ethyl-N-nitrosourea (ENU)	CHO	HPRT ouabain	early S early S	no difference G_1
Crespi and Thilly, 1982	5-bromo-2'-deoxyuridine 5-bromo-2'-deoxyuridine ethyl methanesulfonate ethyl methanesulfonate	CHO	HPRT ouabain HPRT ouabain	S S S S	early S mid S no difference no difference
McCormick and Bertram, 1982	N-methyl-N'-nitro-N-nitrosoguanidine	C3H10T1/2	ouabain transform	late S	late S G_1/S
Yang et al., 1993	N-methyl-N'-nitro-N-nitrosoguanidine	CHO	HPRT	same	G_1/S> late S
Kaufmann, 1995	benzo [a] pyrene diolepoxide I	rat liver	Chromo. Abber.	N/A	G_1/S

Table 5. Cell cycle phase of maximum mutant induction and transformation for cells exposed to chemical mutagens.

for ouabain, the sensitive period for mutant induction is 2-4 hours into S phase. Aebersold (1979) used 5-fluro-2'-deoxyuridine (FldU), which generated induced mutants, but did not cause killing. Goth-Goldstein and Burki (1980) found no increase in mutant induction for HPRT using N-ethyl-N-nitrosourea (ENU), but did report more mutants in G_1 for ouabain^R. Tong et al., (1980) showed that mammalian cells (rat liver) in S phase have more mutant induction than other phases of the cell cycle for MNNG using the

HPRT⁻ assay. Differences in transformation and mutant induction assay results were demonstrated by McCormick and Bertram, (1982), although transformation was markedly different than the ouabain mutant induction. The mutant induction assays showed maximum induction in G_1 whereas the maximum oncogenic transformation was in mitosis. The anti-cancer drug, Cisplatin showed primarily chromatid-type deletions. Cells in G_1 were 1.5 times more sensitive to cell killing than those in S phase (Krishnaswamy and Dewey, 1993). Data for chemical mutagens strongly suggests that their primary mutant induction is during S phase as seen in Table 5.

Mutation by Gamma rays of A_L Thru the Cell Cycle

I evaluated how the mutant fraction varies from early G_1 and S phase in A_L cells exposed to ^{137}Cs gamma radiation. This raised a number of additional questions, partially addressed in this research: If a gene is damaged while it is replicating, how will that affect the mutant induction for that gene? Or on a larger scale, if a portion of a chromosome is damaged while it is replicating, how will this affect mutant induction, and how will mutant induction vary. I found, as have others, differences in rates of mutant induction, and cell killing, between cells in early G_1 and in S phase. For A_L cells, the mutant fraction was lower in the S phase than in G_1 phase. The cells in S phase must either be more resistant to mutagenic agents, or the DNA within these cells is undergoing considerably more repair. The latter explanation is more likely the case.

I characterized the mutant frequency differences by isolating a cohort of A_L cells and following their progression through the cell cycle. The G_1 cells were collected by elutriation, inoculated into plates, and allowed to progress as a cohort through the cell

cycle. A_L cells irradiated with gamma rays in G_1 phase had higher mutant fractions and lower cell survival than log phase A_L cells. On the other hand, in S phase, the mutant fraction and cell survival was similar to that for cells in log phase cells. A weakness of previous mutant induction studies during the cell cycle was collecting large numbers of cells in each phase and in accurately determining what phase of the cell cycle the cells were residing.

To determine cell cycle phase times in the A_L cells, I performed an in-depth study to determine the time of replication the human chromosome 11 during S phase of the cell cycle relative to its replication time i.e. early/mid/late S phase, and the replication of the CHO chromosomes. I used centrifugal elutriation and a large number of A_L cells (1-2 X 10^8 cells) to isolate G_1 cells to determine replication timing of the human chromosome 11 in the A_L cells. Earlier studies have shown that chromosome 11 replicated early in S phase in human cells (Bickmore and Carothers, 1995). I needed to determine when in S phase the human chromosome replicated in relation to the CHO chromosomes in A_L cells. The human chromosome replicates early in S phase when it is placed in A_L cells.

I chose centrifugal elutriation to isolate phased cells, because I could run a large number of cells through the elutriator and obtain large numbers of early G_1 cells to conduct flow cytometry, FISH, survival curves, and mutation challenges (Figure 1). Populations of 1-2 X 10^8 cells were necessary to allow collection of several million cells in early G_1. Centrifugal elutriation is gentle on cells. However, Rice et al. (1984) found that elutriation consistently reduced G_1 plating efficiencies by 20%, but the plating efficiencies of the S and G_2-M phase were unchanged. Centrifugal elutriation also

requires no drugs or cell cycle blockers that may change cellular physiology (Turman et al., 1979; Griffith and Adams, 1982; Rice et al., 1984). Once the cells were collected and re-incubated, they resume their progression through the cell cycle without significant lag. This agrees with the results of Mitchell and Tupper (1977), who demonstrated that centrifugally elutriated cells were returned to normal growth without a significant lag time. I showed that incubated cells began to traverse the cell cycle after about a 2 to 3 hour delay following plating. Another advantage of elutriation is that it is very time efficient. Cells can be collected and prepared for elutriation in about an hour, and the actual elutriation process takes about 20 minutes, compared to mitotic shake-off which requires hours to gather the same number of cells. I typically collected 6 X 10^6 G_1 cells in 60-90 minutes from a starting population of over 10^8 cells.

The next step was using flow cytometry analysis to characterize the progression of cells obtained by elutriation through the cell cycle. To do this G_1 cells were inoculated into dishes, incubated, and pulse labeled with BrdU. BrdU is incorporated into DNA because it assumes the place of thymidine during DNA replication. Additional populations were prepared for FISH and mutant induction analysis.

The primary question I addressed in this chapter was how do mutant induction and survival vary in the G_1 and S phase? To accomplish this I determined in S phase the time of replication of the region of the chromosome in which the *CD59* gene is located, and determined if the mutant induction in *CD59* is affected by irradiating during this replication. I also measured the mutant induction at early G_1 and S phase.

MATERIALS AND METHODS

Experimental Design

A flow chart for these experiments is shown in Figure 1. A_L cells were grown in 100 mm tissue culture plates and harvested to obtain the 1-2 X 10^8 cells needed for centrifugal elutriation. After centrifugal elutriation the cells were processed for fluorescent *in-situ* hybridization (FISH), flow cytometry, or plated on tissue culture plates and irradiated with ^{137}Cs gamma for cell killing and mutant induction.

Cell Culture Techniques

Effective centrifugal elutriation requires between 2 X 10^7 to 10^9 cells in the 5 ml elutriation chamber (Beckman Pamphlet SB-574H, 1992). I determined that obtaining A_L cells by centrifugal elutriation is most efficient with 1 X 10^8 to 2 X 10^8 cells in the elutriation chamber. A minimum of 2 X 10^7 cells is needed to develop an elutriation gradient, but more cells were needed to get a large population of G_1 cells. To obtain 1 X 10^8 to 2 X 10^8 cells, fifteen 150 mm cell culture plates were seeded with 2 X 10^6 A_L cells in 20 ml of Hams F-12 growth media (Atlanta Biologicals, Norcross, GA), supplemented with 4% newborn calf serum (Summit, Ft Collins, CO), 3% fetal calf serum (Gemini Bio-Products, Calabasas, CA), 0.02 M HEPES, ph 7.4 (Amersham Life Sciences, Cleveland, OH), 50 u/ml penicillin, and 50 mcg/ml streptomycin (Gemini Bio-Products, Calabasas, CA), and 0.001 M L-glutamine (Sigma, St. Louis, MO) forty eight hours prior to the elutriation. Cells were grown in log phase and incubated at 37°C in an atmosphere of 95% air and 5% CO_2.

Harvesting Cells

After 48-hours of incubation, the cells reached an approximant number of 1-2 X 10^8, with 10^7 cells per plate. To harvest cells, the media was removed from each plate and put into a 50 ml centrifuge tube; this ensured that any unattached newly divided cells could be collected. The 50 ml tubes were kept on ice to prevent the cells from proceeding through the cell cycle. The plates were rinsed with 7 ml of 0.5% trypsin in Hank's Balanced Salt Solution (HBSS, Sigma, Gathersberg, MD) and the rinse was transferred to the same 50 ml tube. The cells on the tissue culture plate were then covered with 8 ml of 0.5% trypsin in HBSS and incubated at 37°C for 5 minutes. The surface of the plate was sprayed with the trypsin rinse until all of the cells were dislodged and this rinse was also placed in the same 50 ml tube. The tubes were centrifuged for 4 minutes at 400 g and the supernatant was aspirated from each of the tubes. The cells in the pellets were broken-up and resuspended by gentle tapping, combined with the cells from other tubes in a total volume of 4 ml supplemented Hams F12 media, and kept on ice until elutriation. This processing was shown to reduce plating efficiency by less than 10%.

Centrifugal Elutriation

A Beckman J-6 elutriator (Palo Alto, CA) was set to run at 2000 RPM at 4^0 C using rotor JE-5.0 and a standard chamber, Figures 3 and 4. The elutriator was sterilized by running 150 ml of a solution of ice-cold 95% ethanol through the elutriation pathway at a pump speed of 25 ml/min, followed by 150 ml ice-cold sterile water. Finally 100 ml of ice cold Ham's F_{12} media was run thru the apparatus, the speed of the pump was reduced to 7 ml/min and Hams F_{12} was continually run thru the elutriator until the cells

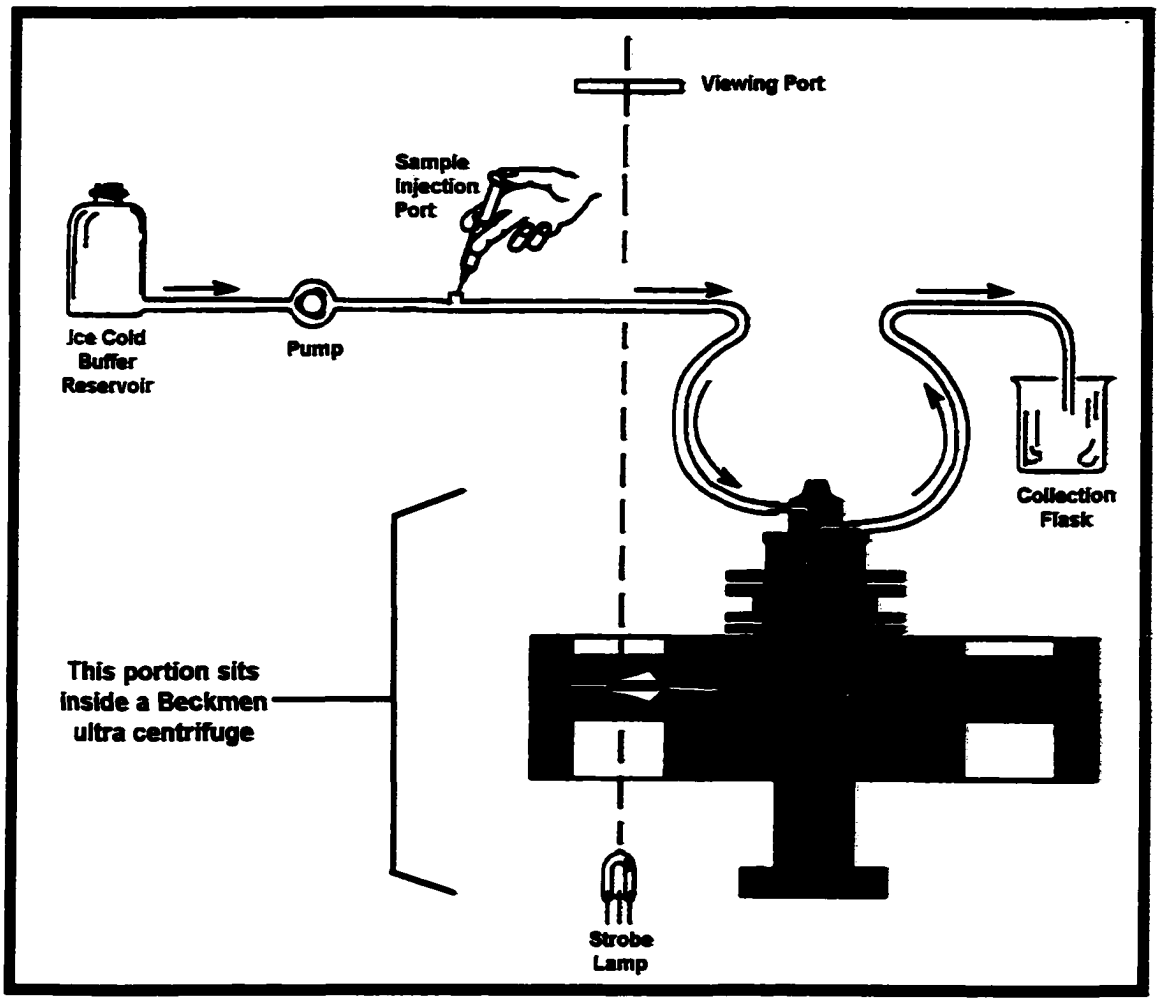

Figure 3. Diagram of centrifugal elutriation set up. The centrifugal elutriator apparatus was housed in a Beckman ultra-centrifuge. The system was sterilized with 95% ethanol. Ice-cold buffer was used to elutriate the cells. Samples were introduced through the sample injection port into the elutriator with a 10cc syringe. The elutriator was set at 2000 RPM and 4^0C. Approximately 1 to 2 x10^8 ice-cold cells in suspension were introduced at a pump speed of 7 ml per min and the pump speed was slowly increased to 10 ml/min then increased in increments of 1 ml/min. The elutriation chamber could be viewed through the viewing port when a strobe lamp illuminated the chamber. As the pump speed was increased the cells were forced out of the elutriation chamber and collected in a 50 ml centrifuge tube.

Figure 4. Diagram of centrifugal elutriation chamber. The elutriation chamber is cut out of a solid block of Lucite. The cells in buffer enter the chamber from the back. The cells remain in the chamber because of the centrifugal force pushing them to the back of the chamber. As the counter flow provided by the pump increases, the cells are forced toward the front edge of the chamber. After the cells go past the edge they elute out of the front of the chamber with the buffer because the chamber starts to narrow and the counterflow velocity increases.

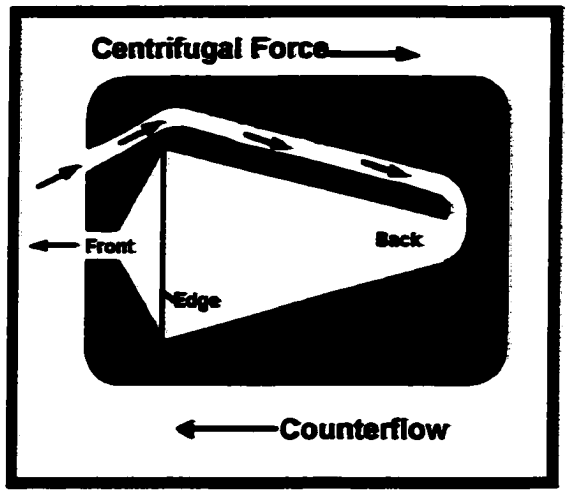

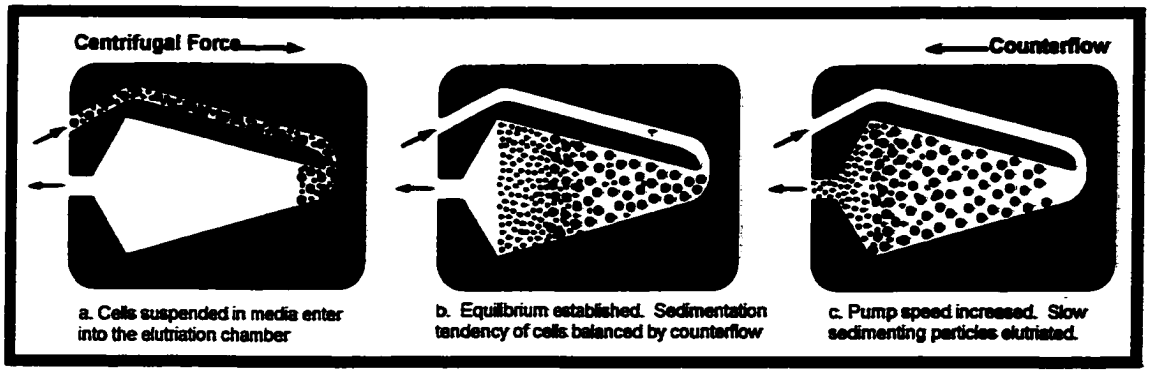

Figure 5. Centrifugal elutriation chamber. The cells enter the elutriation chamber after injection into the centrifugal elutriator. a.) At a pump speed of 7 ml/min the cells reach an equilibrium about half way up the chamber. b.) The cells in the chamber assemble with the smallest, slowest sedimenting particles towards the front of the chamber. Larger particles are forced to the back of the chamber by centrifugal force. As the speed of the pump is increased, the equilibrium balanced cells move to the outlet of the chamber. c.) For an A_L centrifugal elutriation, the cells are forced out of the chamber when the pump speed reaches about 13 ml/min. The smallest cells, the newly divided G_1 cells, are the first cells out and are collected in the elutriate.

were injected.

A MasterFlex (Chicago, IL) peristaltic pump was used to control the rate of flow at which the buffer solution passed through the chamber of the elutriator (Figure 4). The pump was set at 7 ml/min and the cells were injected slowly into the elutriator over a period of 1-2 minutes, making sure that the combined pump speed and injection pressure did not cause the cells to exceed the escape velocity of the elutriation chamber. After the cells were injected and reached the elutriation chamber, they could be visualized thru the strobe window in the elutriation chamber with a well-demarcated equilibrium boundary like that shown in Figure 5b. The equilibrium gradient caused the cells to form in zones with the smallest of the cells (early G_1) at the front of the chamber closer to the edge (Figure 4), and the larger cells (S, then G_2, then M) towards the back of the elutriation chamber. The pump speed was then slowly increased to 12 ml/min to move the cell boundary closer to the edge of the elutriation chamber. The pump speed was increased at increments of 0.5 ml/min, 1.0 ml/min, or 2.0 ml/min depending on the needs of particular experiments. At each velocity setting, 50 ml of media was elutriated and collected in conical 50 ml centrifuge tubes. Based on the balance of forces acting upon the cells during the centrifugal elutriation, cells of approximately the same volume (and, therefore in the same cell-cycle position) were forced out of the chamber with the buffer solution.

Stokes' Law describes sedimentation velocity of particles in a non-compressible fluid using six variables: SV is the sedimentation velocity; d is the diameter of the particle; ρ_p is the density of the particle; ρ_m is the density of the medium; μ is the viscosity of the medium; r is the radial position of the particle; and ω is the angular

velocity in radians/seconds:

$$SV = \left(\frac{d^2 (\rho_p - \rho_m)}{18 \mu} \right) \omega^2 r$$

Two properties of a cell affect its sedimentation velocity, its size and density. The size of a cell is a more important component in the equation since the diameter of the particle is raised to the second power and the density of cells do not vary much. Thus, the sedimentation velocity is a separation based on cell size differences (Beckman Instruments, 1990).

For the mutation and cell labeling studies, six to ten-50 ml samples were collected over a period of 15 minutes as the pump speed was increased to eject larger and larger cells. The elution volumes were centrifuged, aspirated, resuspended in 2 to 4 ml of supplemented F12 media (ice-cold), and counted. Only the first 5-6 million cells collected (these cells were the smallest G_1 cells that had just gone through mitosis) were retained for the mutation, FISH, and pulse labeling experiments (Griffith and Adams, 1982). For the flow cytometry characterization of the entire population, cells from G_1, S, and G_2/M phases were collected by pump speed increments ranging from 14 ml/min to 26 ml/min.

Fixation and Labeling for Flow Cytometry

Flow cytometry was used to determine how the cells progressed over time through the cell cycle as a cohort. Cells used for flow cytometry analysis were collected at each

pump speed and a maximum of 1 million cells were retained and resuspended in 2 ml of ice-cold PBS. Cells were collected at pump volume settings of 14, 15, 16, 17, 18, 22 and 26 ml/min, a log phase control sample was also collected and all were analyzed. The cells were fixed by adding ice-cold 100% EtOH drop-wise until a total volume of 7 ml was reached (70% EtOH). The cells were then centrifuged at 400g for 5 min and the supernatant was decanted. The pellet of cells was resuspended in 1 ml of propidium iodide (10 μg/ml) in PBS and incubated for 20 minutes at room temperature (Fox, 1994).

An Epics flow cytometer (Beckman Coulter, Fullerton, CA) was used for the flow cytometry analysis. The laser was set at 488 nm. Filters included a 515 interference filter, 590 dichroic, 590 longpass, and a 530 shortpass filter (Fox, 1994). The measurements taken on the propidium iodide labeled cells included the forward angle light scatter, the integral red fluorescence, and integral green fluorescence. The forward angle light scatter (FALS) measured low angle light scattered in the forward direction as laser light hit the particles in the flow cell; this gave a count of the particles in the flow stream. The integral red fluorescence (IRF) measured the light that was emitted by the propidium iodide molecule when it was hit with the 488 nm laser, and after it had passed thru the red, 590 nm longpass filter. Propidium iodide is an intercalating dye that is weakly fluorescence until it binds to DNA; it is a large planar molecule that enters the cells only after the cell membrane is damaged. Because propidium iodide is an intercalating die, it gives a quantitative measurement of the amount of DNA in the cell. The fluorescence/per cell is directly proportional to the amount of DNA per cell. The green fluorescence measured fluorescein isothiocynate (FITC) after the emitted

fluorescent green light passed through the 530 nm shortpass filter. To obtain cell cycle histograms, the two measurements, IRF and FALS, were used to determine the amount of DNA in each cell. All three measurements, IRF, IGF, and FALS, were combined in one histogram to identify the fraction of apoptotic cells in the population.

Measurement of Apoptotic Cells Created by Centrifugal Elutriation

Apoptosis is programmed cell death characterized by fragmentation of the DNA and blebbing of the cells so they "fall apart" and can be easily engulfed by macrophages (Fadok et al., 1992). An extra peak at the small end of the spectrum in the flow cytometry (Figure 8-1 to 8-5) indicated the possibility that some cells may have undergone apoptosis. To determine if this was the case, apoptotic cells were looked for using a Trevigen® (Gaithersberg, MD) TACS™ Annexin V-FITC apoptosis detection kit. Annexin V, a calcium-dependent phospholipid binding protein, binds tightly to phosphatidylserine in a reversible manner (Meers and Mealy, 1993). This binding enables detection of phosphatidylserine that has moved from the inner leaflet of the cell membrane to the outer leaflet, which is one of the earliest events in apoptosis (Fadok, et al., 1992).

To collect cells that might be apoptotic (and not G_1), cells were grown as previously described. During the elutriation, cells were injected at the sample injection port (Figure 3) at an initial pump speed of 7 ml/min that was increased to an elutriation speed of 10 ml/min to move the cells closer to the elutriation edge. The cells collected from 10 ml/min to 13.5 ml/min were suspected to be a population containing both G_1 and apoptotic cells, because the cell histograms analyzed for the elutriated cells had a DNA

peak for less than a 1 n amount of DNA. These cells were collected before the cell demarcation line had reached the edge of the elutriation chamber (Figure 5b), so they are not the normal G_1 cell population collected at higher pump speeds but, they had a smaller volume than normal G_1 cells.

These cells obtained early in elutriation were tested for apoptosis by incubating them with an optimized binding buffer, Trevigen® (Gaithersburg, MD) plus propidium iodide, then analyzing the cells further by flow cytometry. Cells were collected as described, centrifuged at 400g for 4 min and resuspended in 100 ml Trevigen binding buffer to a final concentration of 0.50 μg/ml of annexin V-FITC for 15 min at room temperature in the dark. The final binding buffer consisted of 10 μl of 10X binding buffer, 10 μl propidium iodide (10 μg/ml), 1 μl annexin V-FITC conjugate (50 μg/ml), and 79 μl of deionized, distilled water to a total volume of 100 μl. After incubation, 400 μl of 1X binding buffer was added to the tubes and the samples were analyzed on the flow cytometer using the setup as described.

Pulse Labeling with BrdU to Determine Cell Cycle Position

After the cells were elutriated, centrifuged, and counted, they were plated in standard F12 media in eight each 100 mm tissue culture plates and prepared for pulse labeling with BrdU. Only cells in S phase incorporate BrdU into their DNA and can be identified by labeling incorporated BrdU with a fluorescent antibody. Six of the 100 mm plates (numbered 1- 6) were inoculated with 1 X 10^6 cells in early G_1. The two control plates (C-1 and C-2) were inoculated with 2 X 10^6 cells from a population of A_L cells in log phase growth. The control cells were maintained in the same environment as the

elutriated cells. At 4.5 hr after plating, and every hour thereafter, in relay fashion, one of the treatment plates was pulse labeled for one hour with BrdU(+)/thymidine(-) media (labeling schedule Figure 6). Before a plate was treated with the BrdU pulse media, it was first rinsed twice with 7 ml of 37^{0}C Hank's Balanced Salt Solution (HBSS) to ensure that any free thymidine was rinsed off the plate. Each plate of cells was covered with 7 ml of BrdU pulse media. This media consisted of 60 ml of F12(-) media (minus thymidine and hypoxanthine), supplemented with 600 µl of hypoxanthine (3 X 10^{-3}M), 600 µl of L-Glutamine (0.1 M), and 4.62 ml of fetal calf serum. The plates were returned to the incubator. After one hour of incubation and incorporation of BrdU into DNA, the cells were rinsed with 37^{0}C HBSS and standard F12 media at 37^{0}C was added to the plates. The cells were then returned to the incubator. BrdU media was added to the two control plates at 4.5 hr post plating and the BrdU media was removed and replaced with regular media at 10.5 hr post plating (Figure 6). Next, 70 µl of Colcimid solution, 10 g/ml (Karyomax, Life Technologies, Rockville, MD) was added to all plates at 10.5 hr post plating to prevent the cells from going through mitosis. The cells in all plates were fixed 18.5 hr post plating.

Cell Fixation and Chromosome Spread Preparation

At 18.5 hr post-plating, the cells were removed from the six relay plates and the two control plates using the Ham's trypsin method, with all the media and rinses saved in 15 ml centrifuge tubes. The eight 15 ml tubes were centrifuged at 400 g for 4 minutes. The supernatant was aspirated and the cell pellet was re-suspended by gentle tapping.

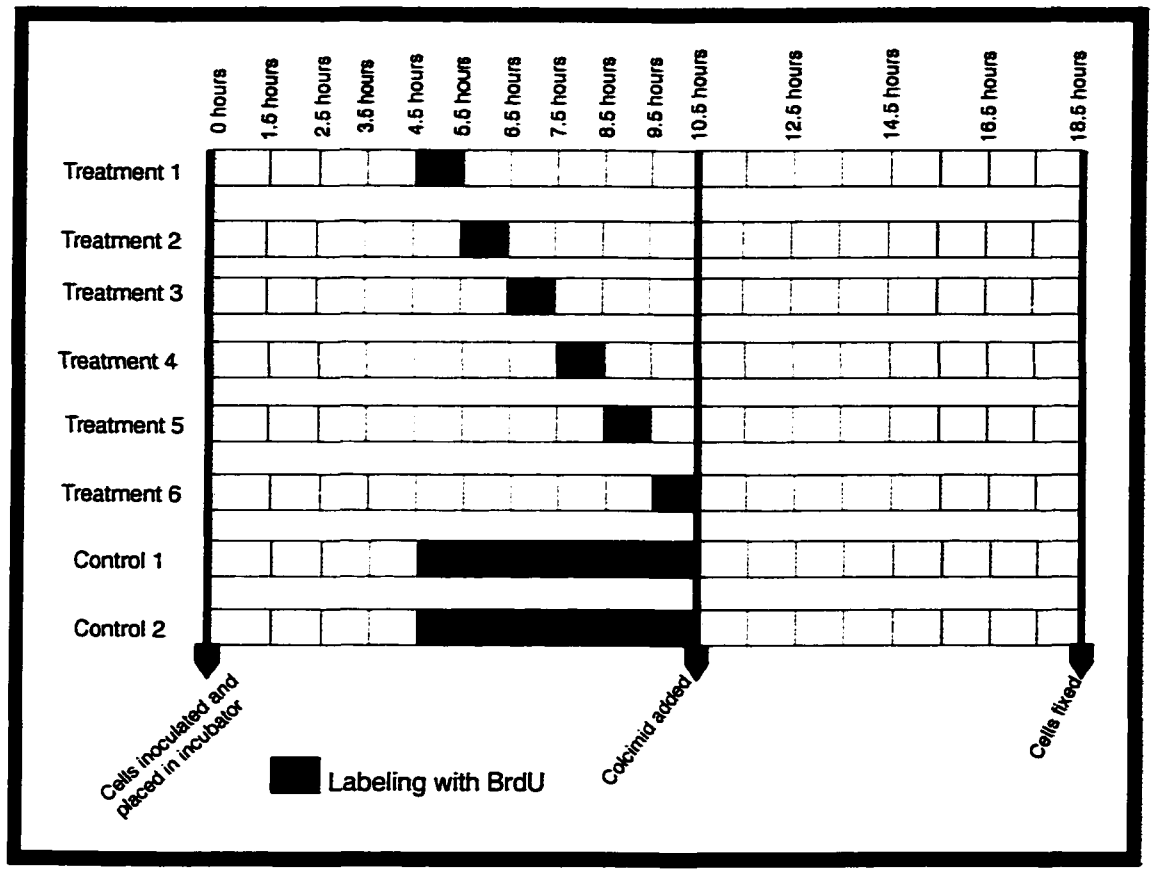

Figure 6. Time line for pulse labeling A_L cells with BrdU. The BrdU treatment groups were pulse labeled in a relay fashion starting at 4.5 hours. Pulse labeling was not started until 4.5 hours because the cells were still in G_1 as determined by flow cytometry. The relay method of pulse labeling was used to pinpoint the time when the cells entered S phase. Treatment groups were pulse labeled with BrdU for one hour at progressively later times after elutriation. The control groups were labeled for six hours. Colcimid was added to all plates at 10.5 hours and the cells were fixed for FISH at 18.5 hours

Seven ml of 0.075 M KCl hypotonic solution was added drop-wise to each of the tubes followed by incubation in a 37°C water bath for 15-20 minutes to pull excess water out of the cells. Three ml of fresh fixative (methanol: acidic acid, 3:1) was added to each tube. The tubes were re-centrifuged again at 400g for 4 min and the supernatant was discarded. The cell pellet was again re-suspended in fresh fixative added drop-wise with vortexing to a volume of 4 ml. After 5 min, the tubes were centrifuged at 400g for 5 min and the supernatant was again discarded. The fixative rinse was repeated 2 more times, with 5 min between rinses.

After the final rinse, the cells were prepared for chromosome analysis. The cell pellet was re-suspended by adding approximately 20 drops of fresh fixative to the tubes. To prepare the slides, Fisher's finest premium microscope slides (Hampton, NH), were soaked in 95% EtOH for two hours and then rinsed with deionized water for several hours, and the slides were covered and kept at 4^0C until ready to use. Chromosome spreads of the cells were prepared by dropping two to three drops of the cell suspension in fixative onto the drained cold wet slides. After the chromosomes spreads were dried the slides were kept in a vacuum jar for at least two days until used for fluorescent *in-situ* hybridization (FISH) studies.

Identifying the Human Centromere by Probe Labeling

The human chromosome in the A_L chromosome spreads was identified using labeled probes specific to human chromosomes. Human centromere probe D11Z1 was used to identify p82H; an alphoid repeated DNA family found at the centromere of all human chromosomes (Mitchell et al., 1985). The probe D11Z1 was labeled with biotin

using an Ambion Random Prime Labeling Kit (Austin, TX), or by nick translation with a Gibco/BRL Nick Translation Kit (Grand Island, NY). The DNA for the probe was prepared by adding 3 µl of D11Z1 (a 2.5 kb DNA fragment at a concentration of 25 mg/µl), 7 µl of deionized water, and 5 µl of decamer random primers to a microfuge tube, the tube was vortexed and heated in a sand block for 8 min at 100°C. After heating, 10 µl of dNTPs (The dCTP was labeled with biotin), 24 µl of water, and 1 µl of Klenow fragment was added to the microfuge tube, vortexed, and the tube allowed to sit for four hours at room temperature. Finally, 1 µl of 0.5 M EDTA was added to stop the reaction.

Fluorescence *In-Situ* Hybridization (FISH)

FISH studies were used to analyze both the human centromere and the BrdU that incorporated into the DNA during replication of the A_L cells. The day prior to FISH, 30 μl of hybridization mix was prepared for each slide by mixing 2.1 μl of D11Z1 Human centromere probe as described above, 3.5 μl of sonicated salmon sperm and 30 μl of hybridization buffer. The buffer contained: 2.5 ml formamide (Gibco-BRL, Ultra pure, Grand Island, NY), 50% final volume; 1.0 ml of 50% dextran sulfate, 10% final volume; and 1.5 ml 2 X SSC (saturated sodium citrate), final concentration of 0.6 X SSC. The 5.0 ml total volume was frozen in 1 ml aliquots at -20° C. The probe/hybridization mix was vortexed, centrifuged, and pipetted onto a slide, which was then covered with a 50 mm coverslip. Care was taken to ensure that the probe/hybridization mix was spread evenly and all air bubbles were removed. The coverslip was sealed to the slide with rubber cement and placed on a hot plate for 10 min at 75°C. The slides were then removed, placed in a moist slide box and incubated overnight at 37°C.

After the incubation period, the rubber cement was removed and the slides were placed in a Coplin jar containing 50% formamide and 2 X SSC at 42°C for 5 minutes. The coverslips were removed and the slides were then placed in the same jar of formamide/2 X SSC for 10 additional minutes. The slides were then moved to a second Coplin jar containing formamide/2 X SSC at 42°C for 10 more minutes. The slides were then placed sequentially into 3 Coplin jars of 2 X SSC at 37°C for five minutes each, followed by room temperature 2 X SSC for 5 minutes to reduce non-specific binding of the probe. The next step was to add an aviden-fluorescein isothiocyanate conjugate to the biotin labeled probe and an anti-BrdU IgG antibody to label the incorporated BrdU. Non-specific binding of the anti-BrdU antibody was reduced by placing 30 μl of 1% bovine serum albumin (BSA) in 4 X SSC with 0.1% triton on each slide, a 50 mm coverslip was placed over the slides for 5 minutes, and then removed.

The following steps were done in the dark to prevent bleaching the fluorochromes. The human centromere probe and the BrdU were labeled by adding a 30 μl of a mixture of aviden-fluorescein isothiocyanate conjugate and mouse IgG anti-BrdU to the chromosome spread and a coverslip was placed on each slide. The labeling mix was made by adding 1 μl of mouse IgG anti-BrdU (Sigma B2531, Gathersberg, MD) per 50 μl of 0.6 µg/ml aviden-FITC (AV-FITC, Molecular Probes, Eugene, OR). The aviden binds non-covalently to the biotin on the dCTP that had been incorporated in the hybridized probe on the human centromere. The mouse IgG anti-BrdU binds to the BrdU that had incorporated in the chromosomes during pulse labeling. The slides were then incubated in a moist box at 37°C for a minimum of 30 minutes. After incubation, each

slide was washed 3 times in 4 X SSC with 0.1 % triton at 43°C. The slides were allowed to stand in the first Coplin jar for 5 minutes, and the coverslips were removed, then the slides were transferred to the second and third Coplin jars for five minutes each.

The next layer of the antibody "sandwich" was applied to the chromosome spreads by pipetting 30 μl of biotin-labeled rabbit anti-FITC IgG antibody (AB-biotin, Molecular Probes, Eugene, OR), final concentration 0.6 µg/ml on each slide and covering each with a 50 mm coverslip. The slides were incubated in a moist box at 37°C for 30 min, followed by three washes in the 4 X SSC/triton solutions at 43°C, as above.

The final layer of each fluorochrome was added by putting 30 μl of a mix of AV-FITC and goat anti-mouse IgG Texas Red-X®, (Molecular Probes, Eugene, OR; 1 μl of goat anti-mouse IgG Texas Red- X® per 50 μl of mix) on each slide that was then covered with a 50 mm coverslip. The slides were incubated in a moist box at 37°C for a minimum of 30 minutes and then washed in the 4 X SSC/triton solutions following the same procedure stated above.

After the last wash, each slide was labeled with 30 μl of "counter" stain from a master mix consisting of 500 μl of anti-fade (Slowfade, Molecular Probes, Eugene OR) and 5μl of 5μg/ml of 4,6-diamino-2-phenyl-indol (DAPI, Molecular Probes, Eugene, OR). Coverslips were placed on the slides in preparation for microscopic examination.

Photograph and Image Analysis

Photos of the FISH preparation were taken with a 35 mm camera using Kodak (Rochester, NY) ASA400 color slide film viewed on a Zeiss Axioskop (Thornwood, NY) fluorescent microscope at 1000 X under oil, through four different filter sets. Excitation

wavelengths were 380 nm for DAPI, 495 nm for fluorescein isothiocynate, and 570 nm for Texas Red®. Photos of DAPI labeled spreads were taken with a blue pass filter, FITC was taken with a green pass filter and Texas Red® photos were taken through a red pass filter. All three colors could be seen in photos taken with a triple band pass filter. All filters were from Chroma (Battleboro, VT).

Image analysis was done using a Leitz Ortholux II fluorescent microscope (Wetzlar, Germany). The images were captured and analyzed with Metamorph Image Processor (Universal Imaging Corp., Westchester, PA). After the image was captured through the three different band-pass filters, the image was combined and extraneous background signals were eliminated by digitally subtracting out the background noise. Line-scans of Metamorph images of chromosomes were done to determine levels of labeling with the different fluorochromes along the entire length of the chromosome 11. A digital line was drawn through the chromosome on the computer screen and the gray scale value (light level) for the three different wavelengths red, green, and blue were measured along the length of the chromosome. The intensity measurements were entered into a spreadsheet for analysis and plotting. High light emission levels at a particular wavelength represent the binding of the fluorochrome label to the chromosome structure. Red shows location of BrdU incorporation, green was used to label the centromere probe on chromosome 11, and blue was used to label all of the chromosomes in the spread.

Cell Survival Curves

Survival curves and mutant induction in cells prepared for centrifugal elutriation were done as follows, and as depicted in Figure 7. The cells irradiated for survival curves

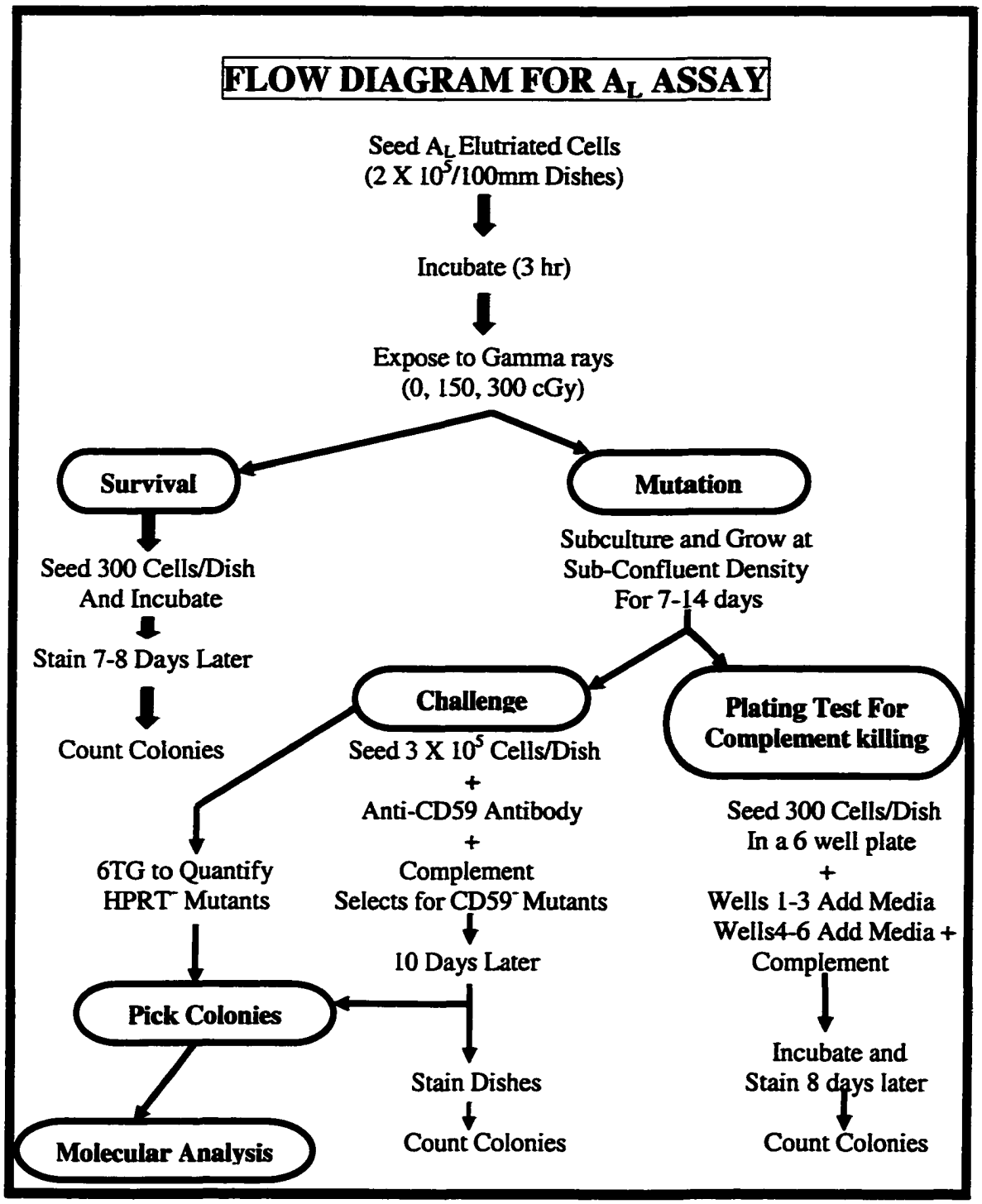

Figure 7. Flow diagram of the A_L assay.

were plated in 60 mm tissue culture plates containing 4 ml of supplemented F12 media as described. The 0 Gy treatment had 300 cells/plate, the 1.5 Gy treatment had 600 cells/plate, the 3 Gy treatment had 1000 cells/plate, and the 4 Gy treatment had 1500 cells/plate. Three replicate plates were irradiated for each dose. The cells were irradiated with a J. L. Shepherd and Associates Mark I Model 68A cavity irradiator containing 6000 Ci of ^{137}Cs (Glendale, CA) at a dose rate of approximately 0.85 Gy/min. Dosimetry was performed by T. C. Patel using a Victoreen Condenser R-meter and Harshaw TLD-100 lithium fluoride chips. The cells were in F12 media in the tissue culture plates and were placed on a rotating platform to ensure even exposure in the irradiator four inches off the floor of the irradiation chamber. After irradiation, the plates were put into the incubator for 8-10 days for colony formation, then fixed with a mixture of 7.5 % glacial acetic acid and 20 % EtOH in H_2O, and stained with crystal violet. Four different killing curves were constructed by plotting the surviving fraction (number of colonies/cells plated) on the y-axis vs. the dose on the x-axis (Puck, 1956; Waldren et al., 1986). The first curve for the log phase cells at 0, 1,1.5, 2, 3, 4 Gy, the second for G_1 cells that were obtained by elutriation at a pump speed of 13-15 ml/min; a third for the S phase cells obtained from elutriation at a pump speed of 22 ml/min. The cells position in the cell cycle was verified by flow cytometry analysis. The fourth killing curve was carried out on the cells from the G_1 elutriate that had been plated, placed in the incubator, and allowed to progress through the cell cycle for 8 hours to move into S phase.

Mutation Measurement

Survival

The elutriated G_1 cells were separated into two populations for mutant induction measurement; the first group (G_1) was plated and irradiated immediately with 0, 1.5, or 3 Gy of ^{137}Cs gamma rays. Non-irradiated cells were plated with 2 X 10^5 cells per 100 mm tissue culture plate. The G_1 and S cells irradiated with 1.5 Gy were plated at 3 X 10^5 cells/100 mm tissue culture plate; cells irradiated with 3 Gy were plated at 5 X 10^5 cells per 100 mm tissue culture plate. The cells were irradiated with ^{137}Cs gamma rays as described above. The other half of the population was plated, incubated and allowed to progress through the cell cycle for eight hours into S phase and then irradiated at the same doses. Another population of cells was collected from the centrifugal elutriator at a pump speed of 22 ml/min to collect S phase cells (cell position shown in Figure 8-6). This was done to compare cell survival curves and mutant induction in the elutriated S phase cells with cells that had been collected in G_1 and allowed to progress into S phase. This enables a comparison of newly elutriated cells with cells that were allowed to stabilize in the incubator and to observe any negative effects of elutriation on cell survival. After irradiation, the cells were returned to the incubator and kept in log phase growth with sub-culturing as needed for 10 days to allow for expression of mutations.

Determination of Fractions of $CD59^-$ Mutants

Mutant fraction was determined with the following formula:

$$M_f = (\text{number of colonies}/10^5) \text{ X } (1/PE) = \text{mutants}/ 10^5 \text{ clonable cells}$$

Where M_f = mutant fraction, and PE = plating efficiency in complement. After 10 days for expression of mutation and recovery, $CD59^-$ mutant cells were selected with a complement mediated cytotoxicity assay (Waldren, 1983; Waldren et al., 1986; Shibuya

et al., 1994; McGuiness et al., 1995; Waldren et al., 1999). Briefly, for each G_1 and S control and G_1 and S radiation treatment, mutant fractions were determined by plating 2 X 10^5 A_L cells into each of 3 100 mm tissue culture plates in 7 ml of 'challenge media' consisting of Ham's F12 (Atlanta Biologicals, Norcross GA) plus 7% fetal calf serum heat inactivated to get rid of endogenous complement activity (Gemini Bio-Products, Calabasis, CA), 0.02 M HEPES (Amersham Life Sciences, Cleveland, OH), and 0.001 M L-glutamine (Sigma, St Louis, MO) (Figure 7). The plates were incubated for 3-4 hours to allow the cells to adhere to the tissue culture plates and recover from trypinsinization, the media was removed and replaced with the 'challenge media' described above with the addition of 2% final volume rabbit serum complement (Dutchland Laboratory, Denver, PA) (the rabbit serum complement contained 5% heat inactivated human serum which was added to the rabbit serum before it was put into the challenge media to reduce complement only killing), plus 0.2% v/v anti-CD59 monoclonal antibody E7.1. The monoclonal antibody against CD59 was prepared as described (Carey et al, 1976; Waldren et al., 1979; Waldren, 1983). After 10 days incubation for colony formation, the plates were fixed and colonies stained as above. Cells that express CD59 are killed by complement mediated cells lysis. Cells with mutation at *CD59* formed a colony.

To detect any non-specific killing by complement, six-well tissue culture plates were seeded with 300 cells in each well in 3 ml of the challenge media. The cells were serially diluted from the same irradiation treatment and control groups as the mutant induction challenge cells. After 3-4 hr, the media was carefully aspirated from three of the wells of the 6 well plates that had been previously seeded. The media was replaced

with challenge media containing 2% final volume rabbit serum complement (with 5% heat inactivated human serum and no complement or with challenge medium alone). The other three wells were left undisturbed to give plating efficiency data for each data point. All plates were returned to the incubator at 37^0C. After eight days, the 6-well plates were removed from the incubator, the media was aspirated off, the cells were fixed and stained, and colonies were counted.

The mutant fraction (M_f) was calculated by counting the number of colonies (C) that arise in anti-CD59 serum plus complement divided by the number of cells inoculated (I) X 1/cloning efficiency in just complement (E).

$$M_f = C/(I \times 1/E)$$

The induce mutant fraction $M_{F(I)} = M_{F(Total)}$ - the preexisting M_F. The mutant yield M_y is the slope of the mutant dose response curve. It's value is independent of the level of pre-existing mutants in the population.

RESULTS

Flow Cytometry

Flow Cytometry was applied to populations of cells obtained by elutriation to determine their position in the cell cycle. Two protocols were employed. The first method involved collecting cells during centrifugal elutriation at increasing pump speeds to obtain cells in different specific phases of the cell cycle. The smaller cells elutriate first, followed by progressively larger cells. As cells grow from division thru G_1, S, and G_2, the smallest cells are the newly divided cells and the largest are the late G_2 cells that about twice the volume and have twice the DNA content of newly divided G_1 cells.

Thus, the first cells collected should be early G_1, then S phase, and finally G_2/M. In the second method, cells were collected only in G_1 and incubated to allow them to progress into later phases, then collected and analyzed with flow cytometry. These two approaches were tried to verify that the elutriation had worked properly and to determine cell cycle position.

Flow Cytometry Analysis of Cells Collected at Incremental Pump Speeds

In the first method, the centrifugal elutriated cells were collected at pump speeds of 14 to 26 ml/min (Tables 6 and 7). The flow cytometry histograms for these populations are shown in Figures 8-2 through 8-8. A flow cytometry histogram for un-phased A_L cells is shown in Figure 8-1. This histogram has a typical logarithmic cell cycle shape. The G_1 peak is centered on a relative DNA content of 70; the 2 n DNA amount is 140. Cells in all phases of the cell cycle appear in the histogram, from G_1 cells at about 70 to S phase cells from 75 through 135, and G_2/M cells around 140 relative DNA units. No apoptotic cells were seen. The control cells were taken out of the incubator, collected off a single tissue culture plate, fixed, and stained. These cells were never exposed to the ice-cold temperature to that centrifugal elutriation cells were exposed, which accounts for the lack of an apoptotic population. Apoptosis has been described in CHO V79 at the transition from logarithmic to stationary growth in cells exposed to ice-cold temperatures (Soloff et al., 1987; Nagle et al., 1990).

The distribution of cells collected at 14 ml/min is shown in Figure 8-2. The peak on the right contained 61% of the cells in the population and had a relative DNA content of 95 (Table 6) and was in G_1. In this experiment the flow cytometry measured the

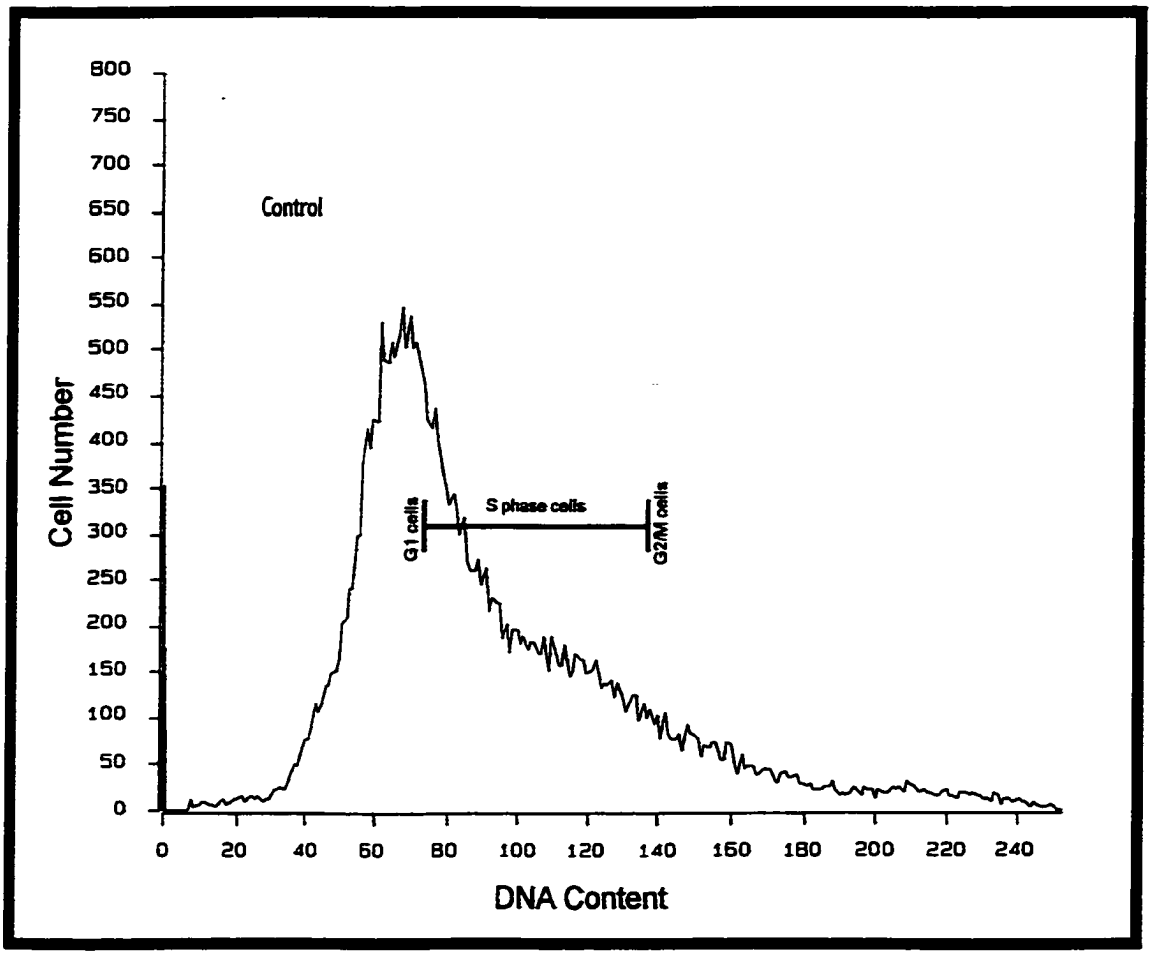

Figure 8-1. Flow cytometry histogram of A_L log phase cells that were subjected to centrifugal elutriation. The DNA content of the cells in the population is shown on the X-axis by measuring the relative amount of the DNA intercalating dye, propidium iodide, in each A_L cell and assigning it to "bin" numbers from 0 to 256. The Y-axis gives the number of cells assigned to each data bin. For this histogram the G_1 cells have a relative DNA content of 70, G_2/M cells a relative DNA content of 140, and S phase cells have between 70 and 140 relative units depending on average the fraction of the genome that has been replicated. A total of 30,000 cells were analyzed by the flow cytometer. This histogram shows a typical profile for A_L cells in log phase growth. The majority of the population in the large peak consists of G_1 cells at a relative DNA measurement of 70. The shoulder to the right consists of S phase and G_2/M cells. These A_L cells came from a single 100 mm tissue culture plate, not the large population that was prepared for elutriation. This population of cells did not have the apoptotic peak seen in the elutriated population in Figures 8-2 thru 8-6. The control log phase population and the elutriated population were treated the same.

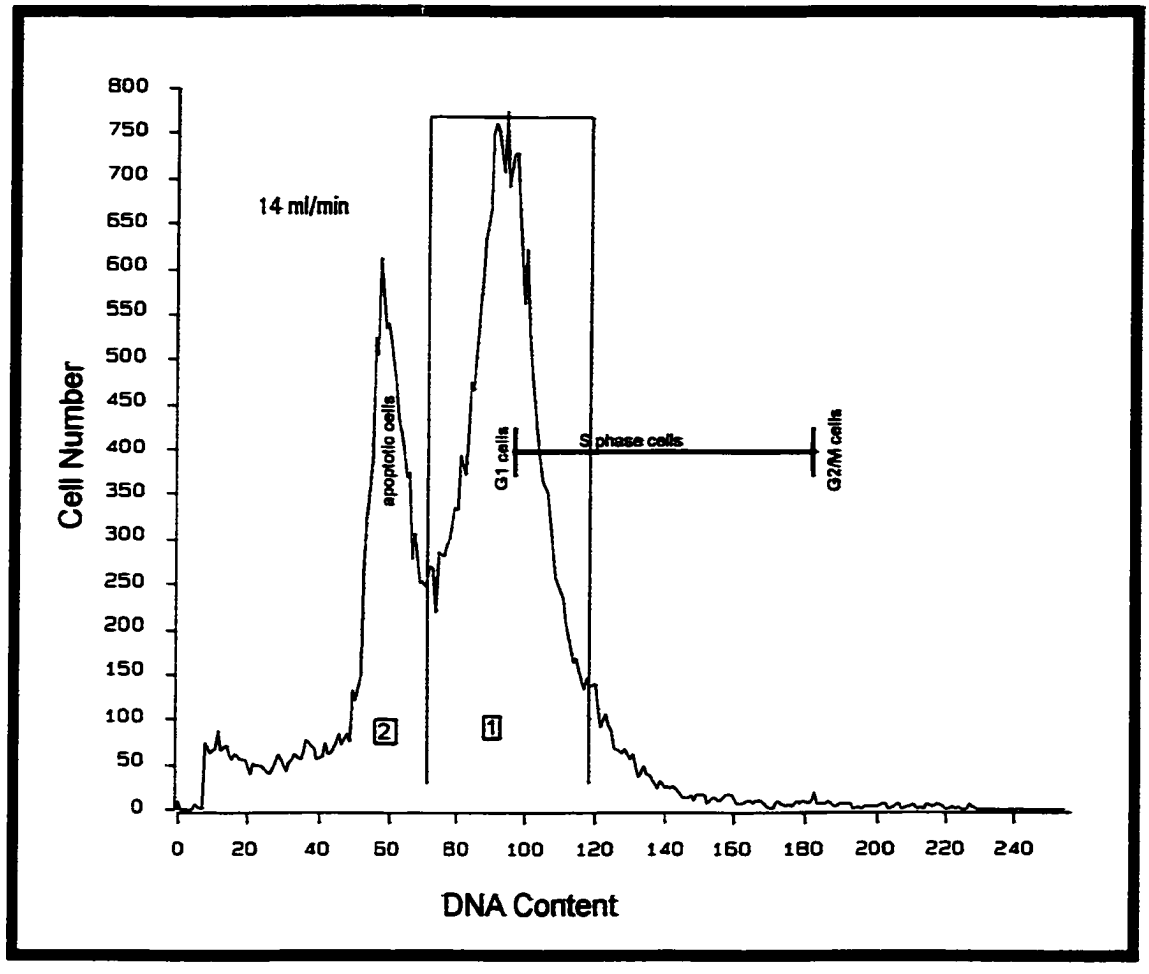

Figure 8-2. Histogram of cells collected at a flow rate of 14 ml/min. The X and Y-axis are as in figure 8-1. A total of 36,679 cells were analyzed. Region 1 contains 20,095 cells or about 61% of the total cells of which approximately 95% are in G_1 with a relative DNA content of 95 and a coefficient of variance (CV) of 12, modal value of 95. G_2/M cells have double the DNA content of the G_1 cells with 190 relative units. S phase cells have between 95 and 190 of the DNA content depending on how much DNA has replicated. The peak in region 2 contains approximately 30% of the cells and consists of apoptotic cells, with relative DNA content of 56. The cells were determined to be apoptotic by using a Trevigen® TACS™ Annexin V-FITC apoptosis detection kit.

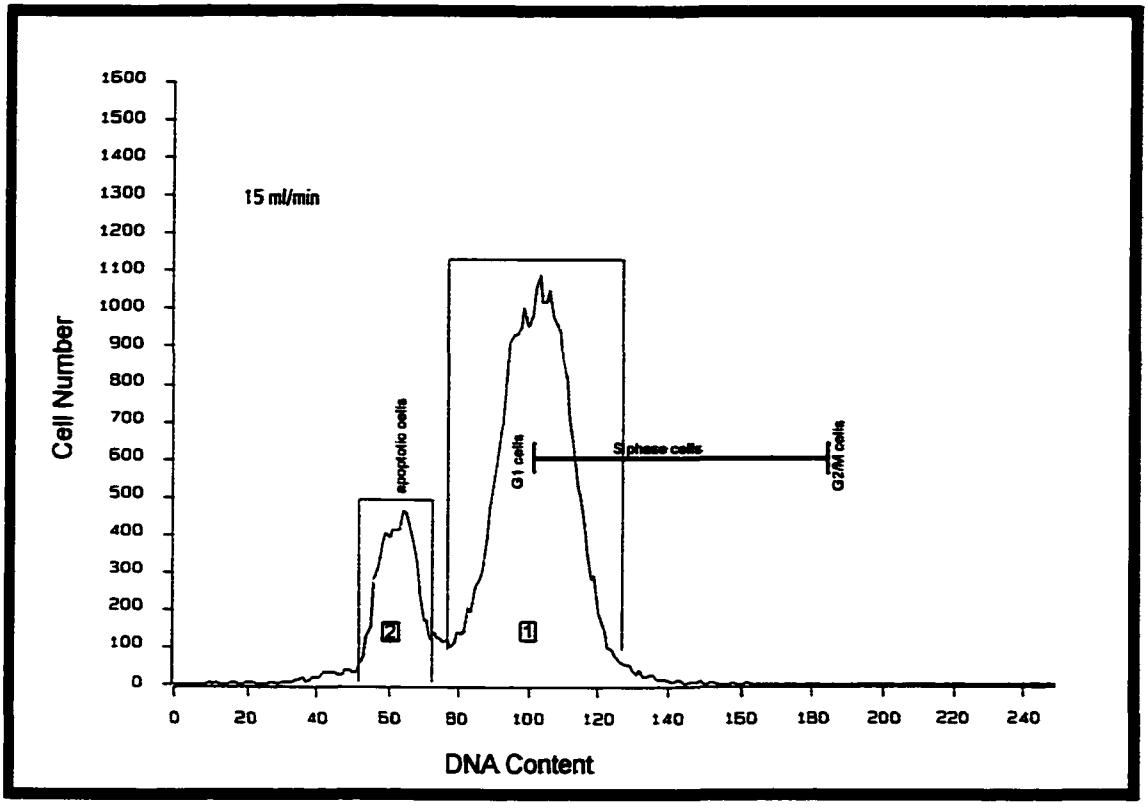

Figure 8-3. Histogram of cells collected at a flow rate of 15 ml/min. The X and Y-axis are as in Figure 8-1. A total of 36,935 cells were analyzed. Region 1 contains 27,410 cells (77% of the total). The peak on the right (region 1) contains cells with a relative DNA content of 103 and a CV of 9.6, the modal value is 104. These cells are slightly larger than the cells collected at a pump speed of 14 ml/min (Figure 8-2) and have more DNA since the X value is 103 vs. 95 in Figure 8-2. These cells have approximately 8.5% more DNA than G_1 cells in Figure 8-2. The peak on the left (region 2) contains about 6500 cells (18% of the total) with a relative DNA content of 64. These cells have less than a 1n amount of DNA and consist of apoptotic cells.

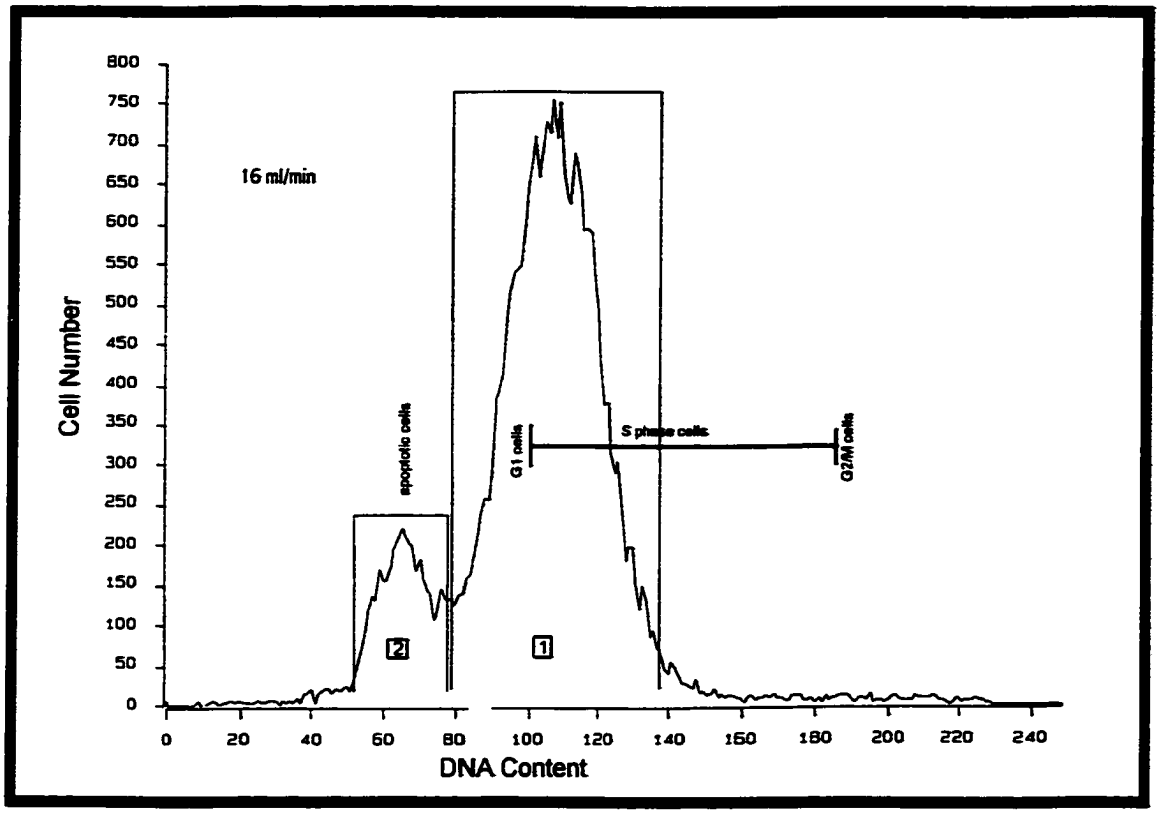

Figure 8-4. Histogram of cells collected at a pump speed of 16 ml/min, which is used to obtain cells that are later in G1 than those in Figures 8-2 and 8-3. The X and Y-axis are as in Figure 8-1. A total of 30,000 cells were analyzed. Region 1 contained 24,254 cells (81% of the total cells). The peak on the right (region 1) has a relative DNA content of 108 and a CV of 12, modal value is 108. This peak is situated farther to the right than the peaks in Figures 8-2 and 8-3. This population contains larger cells than the previous figures with more DNA, 14.5% more than the G_1 cells in Figure 8-2. The peak on the left (region 2), with a relative DNA content of 66 contains about 13% apoptotic cells.

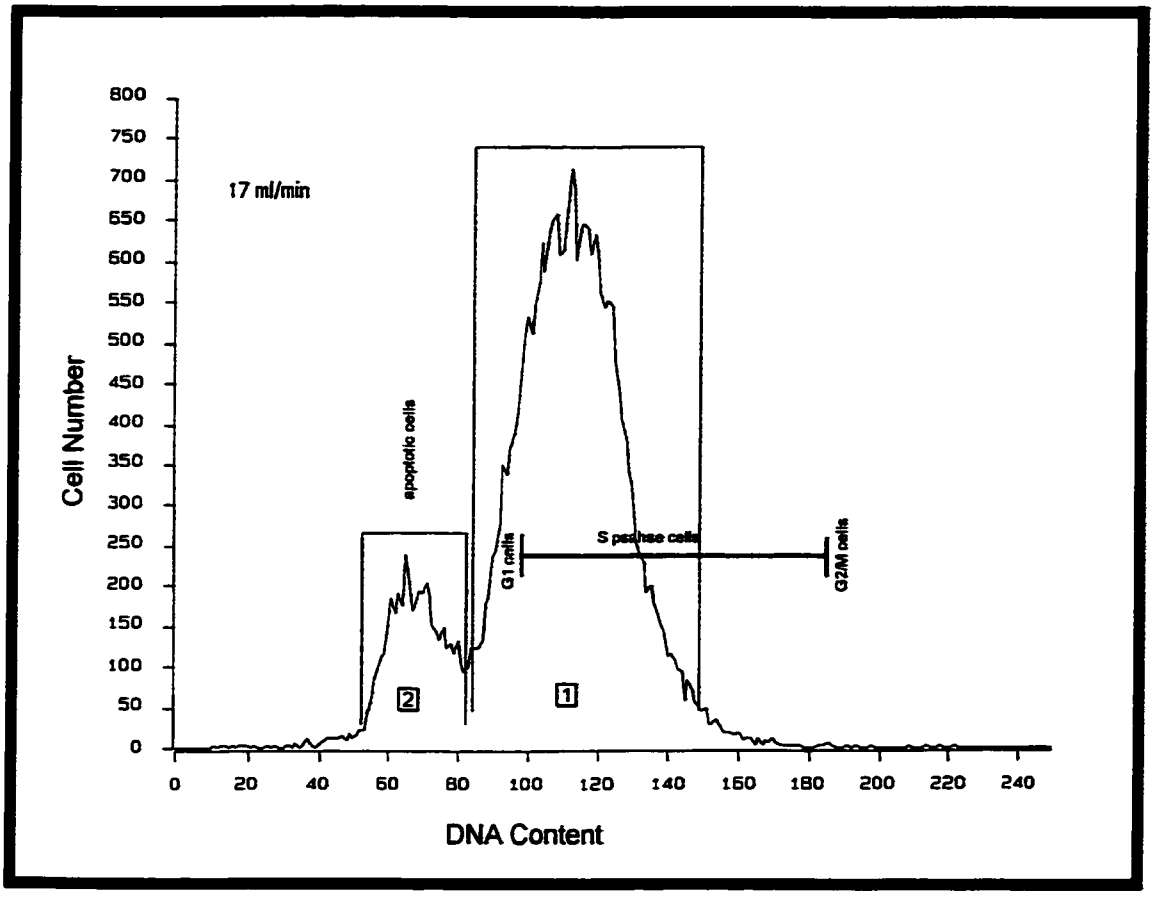

Figure 8-5. Histogram of cells collected at a pump speed of 17 ml/min. The X and Y-axis are as in Figure 8-1. A total of 30,000 cells were analyzed. Region 1 contains 24,536 cells (82% of the total). The peak on the right (region 1) has with a relative DNA content of 114 and a CV of 12, modal value is 113. These cells contain 20% more DNA than found in G_1 cells in Figure 8-2. The cells are 1/5 of the way through S phase replication. The shape of the peak has changed from the earlier peaks, becoming less tightly phased and with a population of S phase cells containing more DNA. The peak on the left (region 2) contains about 14.5% apoptotic cells with a relative DNA content of 69.

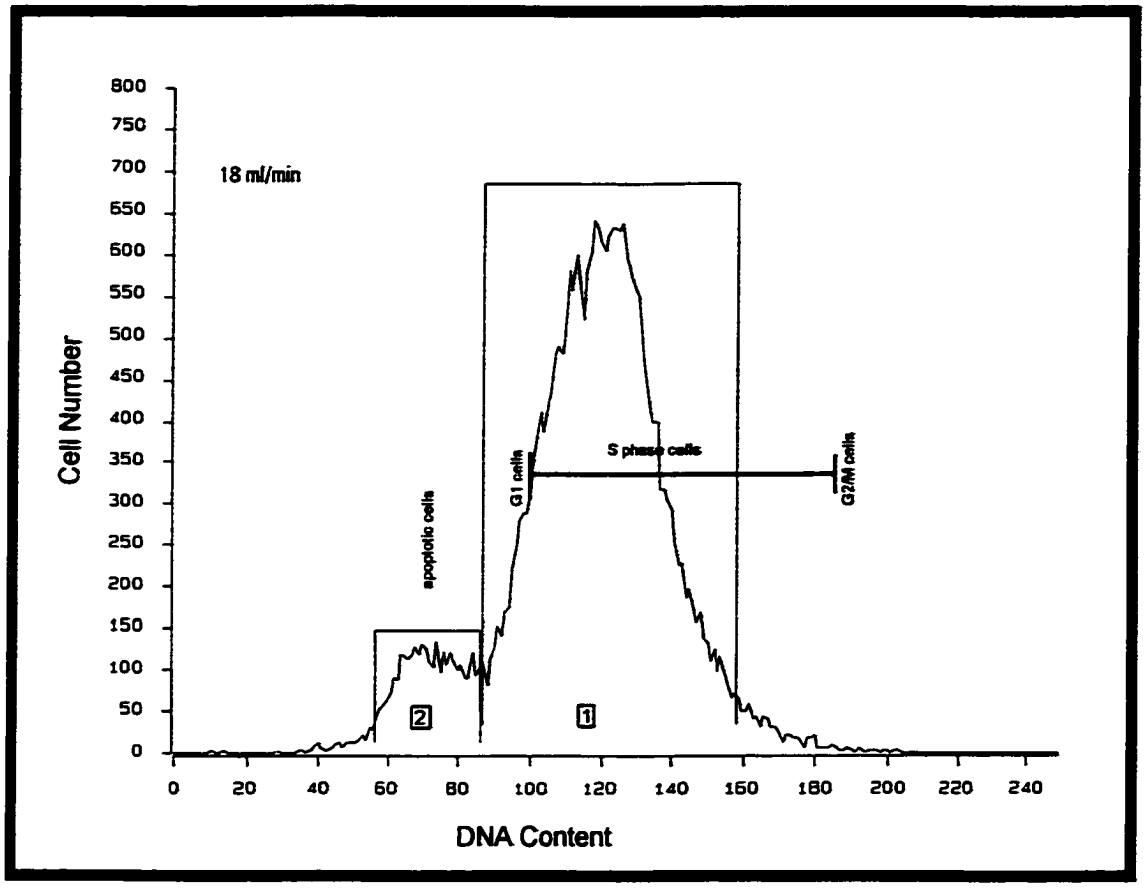

Figure 8-6. Histogram of cells collected at a flow rate of 18 ml/min. The X and Y-axis are as in Figure 8-1. A total of 30,000 cells were analyzed. The peak on the right (region 1) contains 25,663 cells, 85.5% of the total. Region 1 has a relative DNA content of 121 and a CV of 13, modal value is 119. This population has 28% more DNA than the G1 cells in Figure 8-2; therefore the cells are in S phase. The peak is even wider than the previous histograms because as more of the cells come off the elutriator the equilibrium set up in the elutriation chamber becomes more unstable and a wider variation of cells are collected out of the chamber. The peak on the left (region 2) contains 10% apoptotic cells with a relative DNA content of 73.

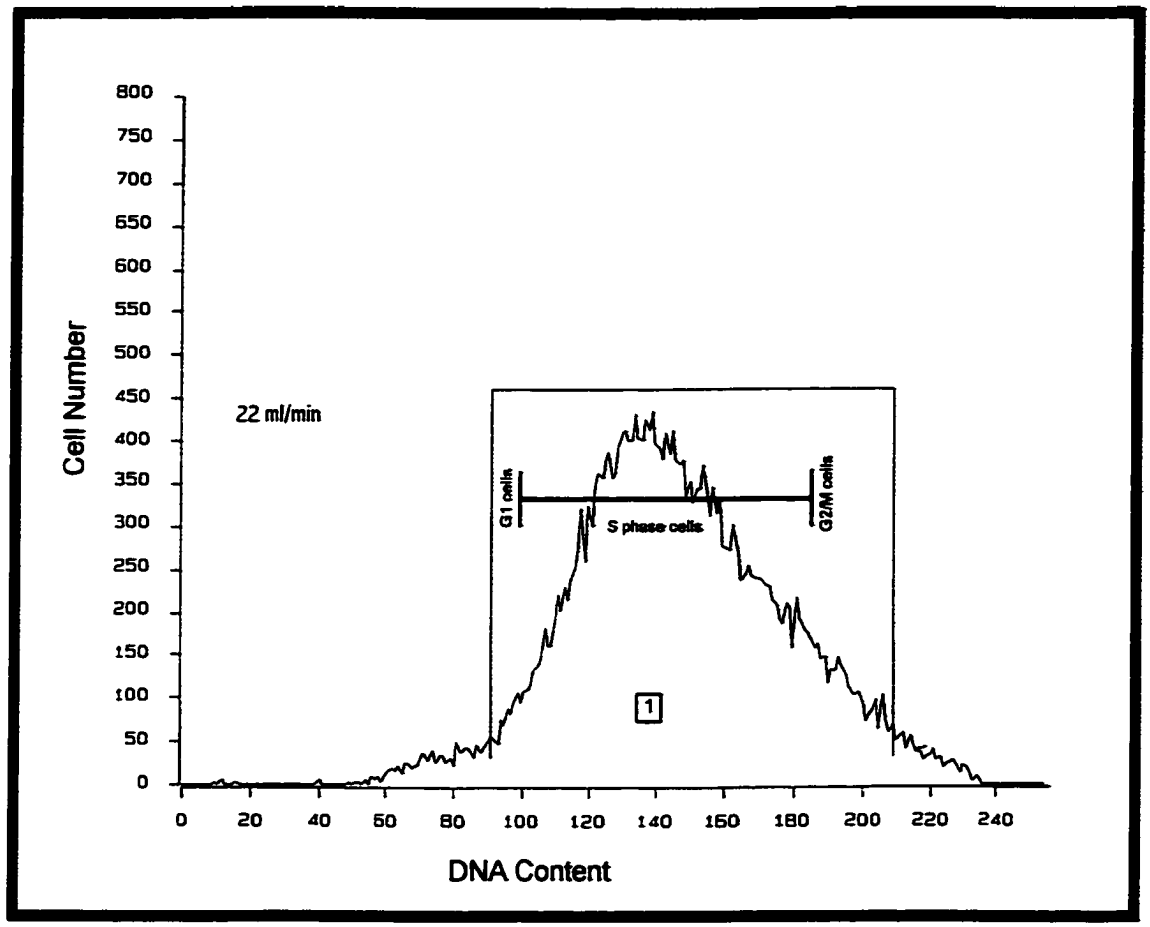

Figure 8-7. Histogram of cells collected at a flow rate of 22 ml/min. The X and Y-axis are as in Figure 8-1. A total of 30,000 cells were analyzed. Region 1 contains 28,018 cells, 93% of the total. This peak has with a relative DNA content of 147 and a CV of 18, the modal value is 140. This value corresponds to mid to late S phase cells according to DNA. The variation in the DNA content shown by the broadness of peak 1 is likely a phenomenon of the loss of the degradation of the separation equilibrium that was set up in the centrifugal elutriation. Sharpness of the peak depends on cell concentration, so as cells are removed, sharpness declines. The equilibrium is lost as the cells are elutriated off and the numbers are reduced. This causes the collected population to contain a more heterogeneous mix of cells. No apoptotic cells are seen in this population.

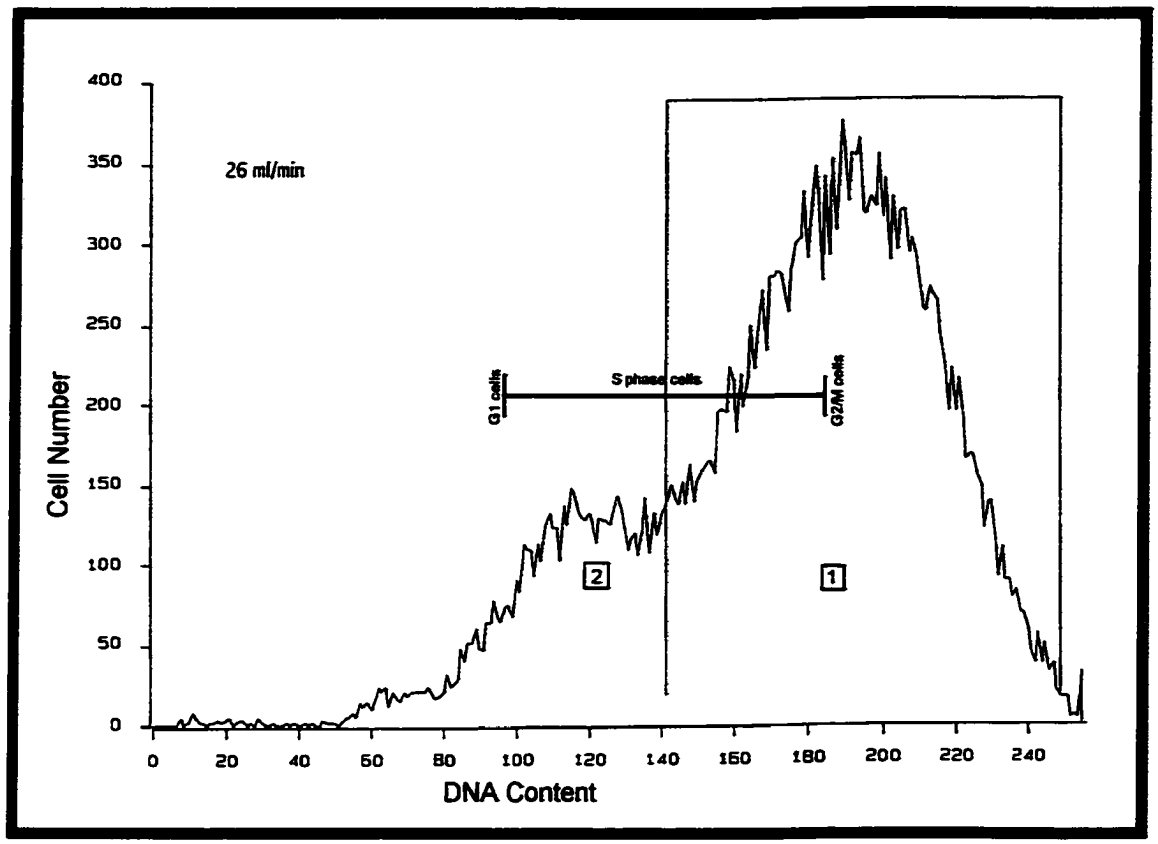

Figure 8-8. Histogram of cells collected at a flow rate of 26 ml/min. The X and Y-axis are as in Figure 8-1. A total of 30,000 cells were analyzed. Region 1 contains 23,332 cells, 78% of the total. This peak has a relative DNA content of 191 and a CV of 13. The modal value is 190 and is also the 2 n amount of DNA for cells in this set of histograms. Therefore most of the cells in this population are in G_2/M. Just to the left of the main peak is a smaller peak or shoulder marked as region 2 with about 20% of the cells. This shoulder contained cells that are still in the late stages of S phase. The variation of the cell size in this sample elutriate is greater than earlier elutriates for reasons discussed.

amount of propidium iodide, a DNA intercalating die. The level of labeling corresponding to a 1 n amount of DNA was arbitrarily assigned a value of 95 for DNA content. In Figures 8-2 to 8-8 a 1 n amount of DNA; the amount of DNA in G_1 cells, is measured at 95 relative units on the flow cytometer histogram. G_2/M cells are known to have a 2 n amount of DNA, double that of the 1 n, and are measured at 190 relative units in this set of histograms. S phase cells would have a DNA content between 95 and 190 depending on how much of the DNA had replicated from 1 n to 2 n in the population of cells. The peak on the left, with a relative of DNA content of approximately 56, consists of cells that were shown to be apoptotic as determined using a Trevigen® (Gaithersberg, MD) TACS™ Annexin V-FITC apoptosis detection kit. These apoptotic cells have less than a 1n amount of DNA. The apoptotic cells were found in all of the cell populations prepared for centrifugal elutriation. Apoptosis was triggered by the cold exposure in cells that were at the transition of logarithmic to stationary growth (Soloff et al., 1987; Nagle et al., 1990). The cells that were not prepared for elutriation and were not on ice did not have a measurable population of apoptotic cells. The apoptotic cells do not appear to affect the results of the flow cytometry but their population is easily seen in the first few samples of cells collected for centrifugal elutriation. How these apoptotic cells arise and how the apoptosis is measured is described in the section detailing the detection of apoptotic cells, and Figures 10-1c and 10-3c.

Figure 8-3 shows the cell collection at a flow rate of 15 ml/min. The peak in Figure 8-3 has moved slightly to the right on the DNA content axis compared to the peak in Figure 8-2, to a DNA content of 103 which means that the population contains some

early S phase cells. The apoptotic peak in Figure 8-3 is still present, but is smaller than the peak in Figure 8-2. The apoptotic cells shown here have a relative DNA content of 64, slightly more than the amount of DNA found in the apoptotic cells in Figure 8-2 and Table 7.

Collection flow rate ml/min	Relative amount of DNA	Coefficient of variance	Relative amount of DNA per cell compared to G_1 cells
14	95	12	1
15	103	10	1.09
16	108	12	1.14
17	114	12	1.20
18	121	13	1.28
22	147	18	1.54
26	191	13	2.0

Table 6. Summary of amount of DNA analyzed by flow cytometry in populations of A_L cells obtained by centrifugal elutriation. Cells that elutriate at a pump speed of 14 ml/min are primarily G_1 cells. As the pump speed is increased, the mean amount of DNA in the elutriated cells increases from 95 relative DNA content to 191 relative DNA content at 26 ml/min. The cells collected at 26 ml/min are primarily in G_2 and M phase cells and have a 2 n amount of DNA.

Figures 8-4 thru 8-8 show that the populations of A_L cells have relatively more DNA as the pump speed is increased to elute larger cells. The cells in Figure 8-8 are primarily G_2/M cells with a 2 n amount of DNA measured with a content of 191 relative units (Table 6). These histograms also show that at later collection points, the width of the peak broadens. This is due to a dilution effect of centrifugal elutriation, and the increasing fluid velocity at higher pump speeds (Grabske, 1978). Centrifugal elutriation

depends on setting up equilibrium within the elutriation chamber (Griffith and Adams, 1982; Applications Data, 1990). As cells are elutriated off, the fluid movement through the chamber becomes more turbulent, the resulting peak on the flow cytometry histogram becomes wider as the cell population becomes more heterogeneous (Grabske, 1978).

Figure	Pump speed ml/min	% Apoptotic cells in the population	DNA per apoptotic cells relative to 1n amount of 95	% DNA apoptotic/normal cells at the same pump speed
8-2	14	30	56	59
8-3	15	18	64	62
8-4	16	13	67	61
8-5	17	15	69	61
8-6	18	10	73	60

Table 7. The percent of apoptotic cells decreased as the centrifugal elutriation collection pump speed is increased. The relative DNA content of the apoptotic cells is about 60 % of the DNA content of the non-apoptotic cells at any collection pump speed.

In Figure 8-1, approximately 30% of the cells were apoptotic (Table 7). As the collection pump speed was increased step wise to 18 ml/min, the percentage of apoptotic cells collected decreased to ~ 10% of the cell population. With a pump speed of 22 ml/min or greater, no apoptotic cells were found. As the collection pump speed increased, cells with higher DNA content (larger cells) were obtained. The cells in the apoptotic peaks in the flow cytometer histograms, Figures 8-2 through 8-6, show progressive increases in the relative DNA content as the pump speed was increased. The relative amount of DNA in the apoptotic cells for the first elutriate at 14 ml/min was 56.

At a pump speed of 18 ml/min, the apoptotic cells collected had a relative DNA measurement of 73. For each of the elutriated volumes, the apoptotic cells found in that population contained about 40 % less DNA than the normal cell population. These apoptotic cells were collected with the other cells at their respective pump speeds; therefore, they were the same volume as the normal cells. However, the apoptotic cells consistently contained about 60 % of the DNA of a normal cell collected at that particular pump speed. These data are consistent with consequences of apoptosis where DNA is lost from the cells (Kerr et al., 1972). In cell cultures, apoptotic cells shrink as they die, in addition to loss of DNA, and cell fragmentation (Kerr et al., 1972; Trump and Berezesky, 1998).

Flow Cytometry Analysis of Incubated Cells

The second method used to characterize the movement of A_L cells through the cell cycle was to isolate populations of early G_1 cells using centrifugal elutriation, and then incubate them so that they progress as a cohort thru the cell cycle. Figure 9-1 is the histogram for the early G_1 cells collected as the first cells off of the elutriator. This histogram shows a tight cohort, i.e. a narrow peak. The 1n DNA content measurement for Figures 9-1 through 9-5 is 78 (Table 8), with the 2 n amounts of 156 relative units. The large, apoptotic peak has a smaller relative DNA content of 45. Consistent with the first set of experiments, the cells in this peak have 60% of the DNA content of the G_1 cells, the same ratio of apoptotic DNA to normal DNA seen in the last section. As will be found in the next section, the majority of these cells are apoptotic cells.

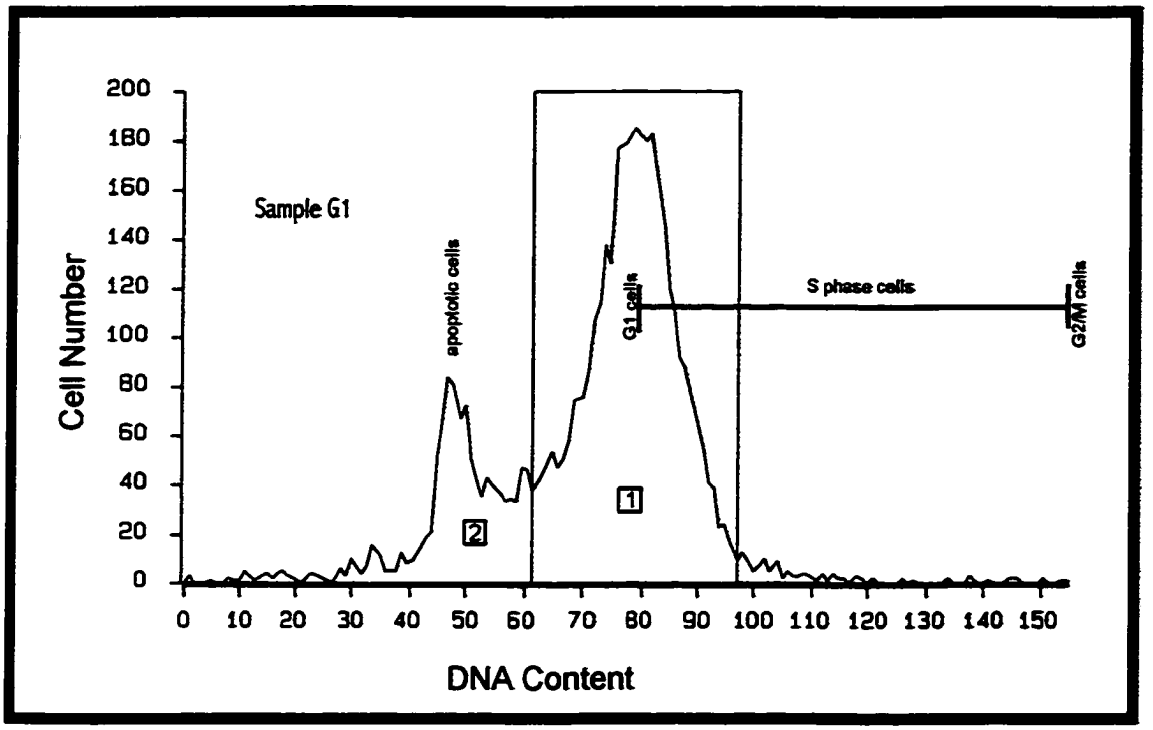

Figure 9-1. Flow cytometry histogram cells obtained by centrifugal elutriation. The X-axis shows the DNA content by measuring the relative amount of the DNA intercalating dye, propidium iodide in each A_L cell and assigning it to "bin", numbered from 0 to 256. The Y-axis gives the number of cells assigned to each data bin. The cells determined to be in early G1 were collected from the centrifugal elutriator and immediately fixed for flow cytometry. The G_1 cells are in bin 78; G_2/M cells are located at 156; S phase cells are located between bins 78 and 156 depending on how much of the DNA has replicated. This histogram consists of 4,724 cells. Region 1 contains about 73% of the total cells analyzed. These cells have a relative DNA measurement of 78 with a coefficient of variance (CV) of 9.7 and a modal value of 78. The cells in region 2 have a relative DNA content of 46 and were shown to be apoptotic.

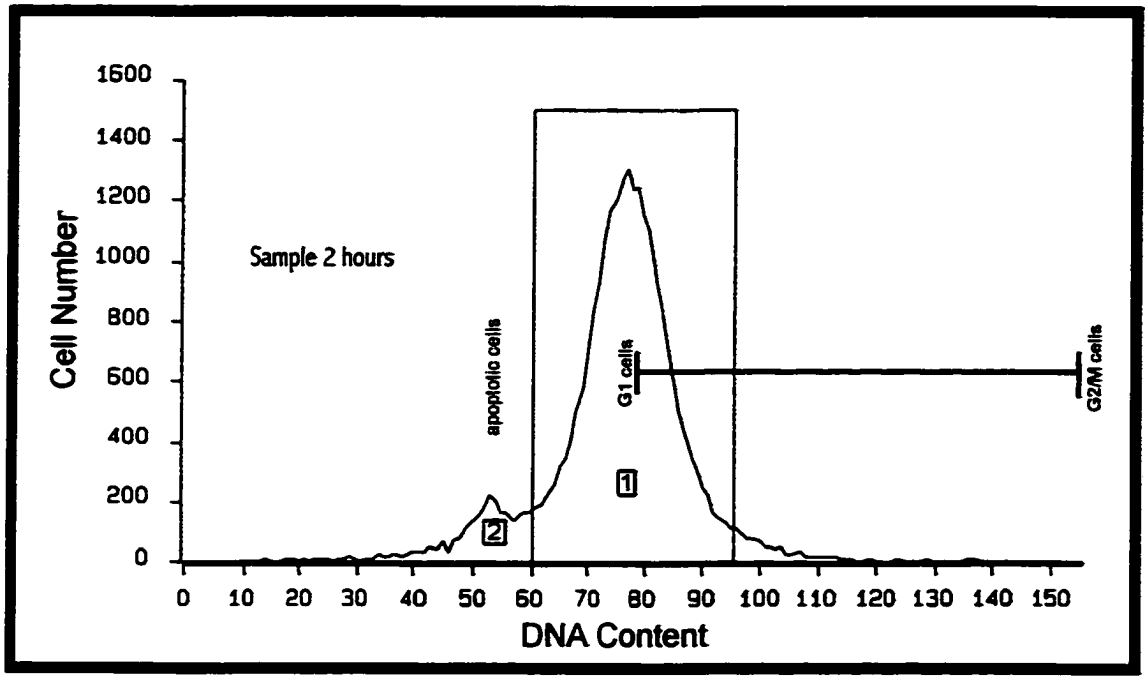

Figure 9-2. Histogram of cells determined by flow cytometry to be in mid-G_1. These cells were separated by centrifugal elutriation as early G_1 cells, the same as the population in Figure 9-1, they were plated on a tissue culture plate and allowed to progress through the cell cycle for two hours before being prepared for flow cytometry. This histogram consists of 26,164 cells. Region 1 contains about 85% of the total cells analyzed. These cells have a relative DNA measurement of 76 with a CV of 9.3, and a modal value of 76. After two hours in growth conditions these cells still contain a 1 n amount of DNA, so they are still in G_1. If the cells had begun to enter S phase the peak would have begun to move to the right. The smaller region 2 consists of apoptotic cells.

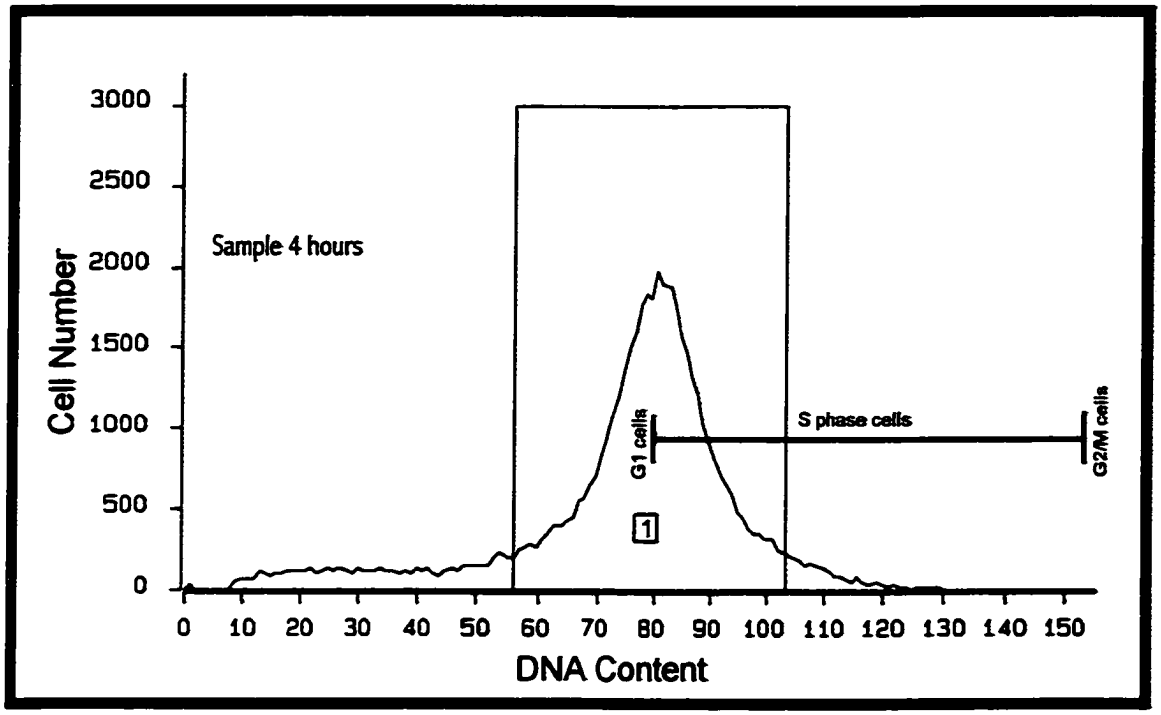

Figure 9-3. Histogram of cells determined by flow cytometry to be in late-G_1. These cells were separated by centrifugal elutriation as early G_1 cells (the same population as Figures 9-1 and 9-2), plated on a tissue culture plate, and incubated for four hours before being prepared for flow cytometry. This histogram consists of 50,000 cells. Region 1 contains about 83% of the cells analyzed. These cells have a relative DNA measurement of 80 with a CV of 12 and a modal value of 80. After four hours of incubation these cells contain a 1 n amount of DNA, therefore they are still in G_1.

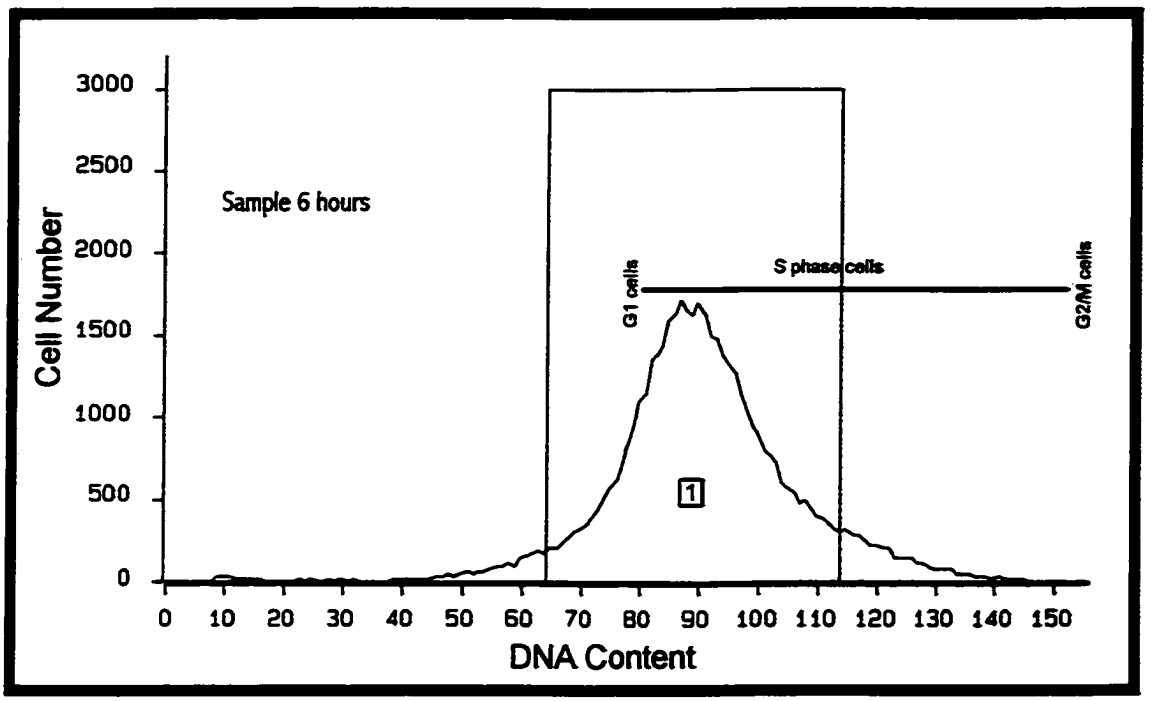

Figure 9-4. Histogram of cells determined by flow cytometry to be in S phase. These cells were from the same population of cells from Figures 9-1 thru 9-3 but they were incubated for six hours before preparing for flow cytometry. This histogram consists of 50,000 cells; region 1 contains 87% of the total cells analyzed. These cells have a relative DNA measurement of 89 with a CV of 12 and a modal value of 86. After six hours of incubation these cells no longer contain a 1 n amount of DNA, the relative amount of DNA has increase as the cells enter into S-phase and begin to replicate DNA. This measures entry time into S phase between 4-6 hours after the early G_1 cells had been plated and incubated. This peak is wider than in the previous figures because of loss of synchrony.

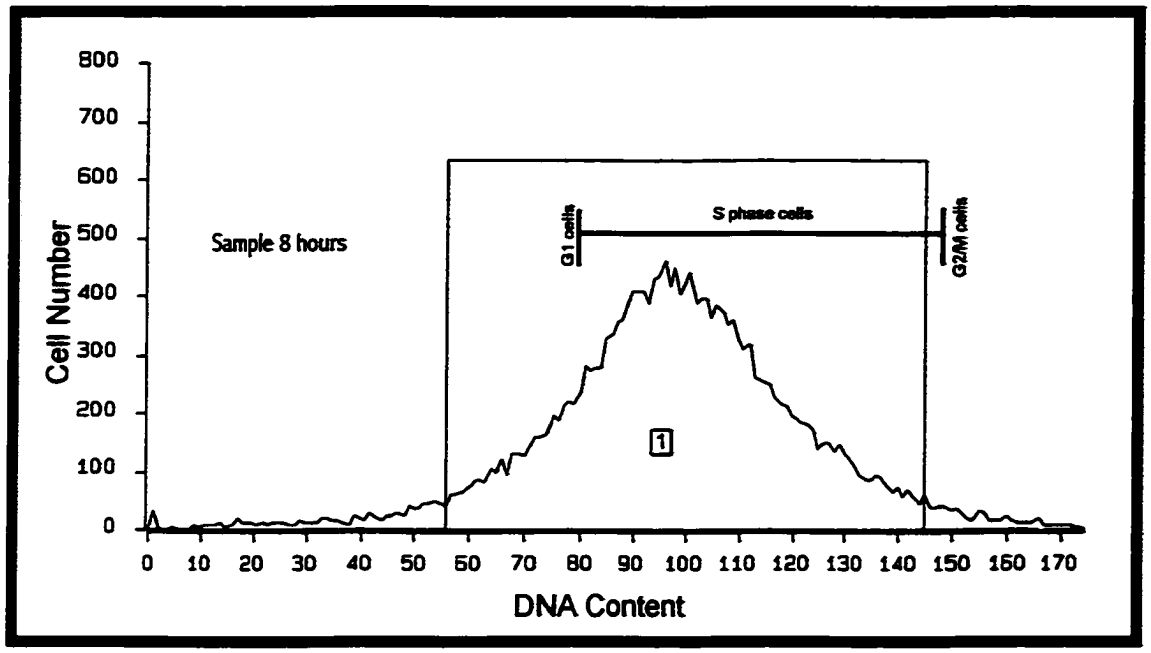

Figure 9-5. Histogram of cells determined by flow cytometry to be in mid-S phase. These cells were collected as in Figure 9-1 and were incubated for eight hours before being fixed for flow cytometry. This histogram contains 21,889 cells; region 1 contains about 92% of the total cells analyzed. These cells have a relative DNA measurement of 98 with a CV of 19 and a modal value of 95. After eight hours of incubation these cells are even farther along in S phase. The shape of the peak demonstrates even greater loss of synchrony of the cells.

Figure	Hours of incubation	Relative mean amount of DNA	Coefficient of variance	Percent increase in DNA
9-1	G_1 0	78	10	0
9-2	2	76	9	0
9-3	4	80	12	2.5
9-4	6	89	12	14
9-5	8	98	19	26

Table 8. Change in amount of DNA/cell in G_1 cells incubated for various times. The cells at 0, 2 and 4 hr have a relative amount of DNA (1n) whereas cells at 6 hr have an increased level DNA and are therefore beginning to enter S phase. By 6 hours the relative amount of DNA per cell has increased by 13% from the G_1 cells. At eight hours the relative amount of DNA has increased to 26% more DNA per cell than in the G_1 cells.

The cells in Figure 9-2 were allowed to progress through the cell cycle for two hours, and then fixed and analyzed by flow cytometry. At 2 hours, the population is still tightly packed, meaning the cells are from a similar volume, and the 1 n value for the DNA content is 76 so that these cells were still in G_1. The apoptotic cell peak that was seen in the G_1 histogram is now much smaller in this population of cells that have progressed two hours thru the cell cycle. The histogram of cells incubated for 4 hours (Figure 9-3) has a mean relative DNA content of 80 which is still well within the coefficient of variance (CV) for the G_1 cells at 0 hr, 2 hr, and 4 hr, thus these cells are solidly in G_1 phase.

Figure 9-4 shows the flow cytometry histogram after the cells incubated for six hours. The cell population shows signs that the cells are moving into S phase. The mean for the cohort on the histogram is an 89 relative DNA content, which is a 13% increase

from the base line of relative DNA content seen at G_1, 2 hr and 4 hr (Table 8). Between 4 and 6 hours after the early G_1 cells were plated, the cell population began to move into S phase. The 6 hr peak is broader than the previous G_1 peaks; this demonstrates that the cells begin to show variances in the rate of their movement through the cell cycle. The cells do not enter into S phase at the same time; therefore some will have more DNA than others causing the peak to spread out. By 8 hours of progression through the cell cycle (Figure 9-5), the cells have moved into mid-S phase. The histogram of the cells at 8 hours shows a peak that has spread out even more compared to the former peaks and the relative DNA content has increased by 26% from the baseline DNA content in the G_1 cells (Table 8). The histograms demonstrate that the elutriated cells start in G_1 and move into S phase between 4-6 hours, the cells also move as a defined peak that gets wider as individual cells move faster or slower through the cell cycle. Pulse labeling with BrdU was used to more accurately determine when the cells entered into S phase.

Apoptosis Measurement

Many of the populations of cells obtained by centrifugal elutriation have less DNA content less than G_1 cells (Figures 8-1 to 8-5, and 9-1 to 9-2). The populations of control cells that were not chilled or elutriated did not show this sub G_1 peak. The histogram in Figure 8-8 illustrates such a population. On the other hand, elutriated G_1 cells that had been re-plated and allowed to progress thru the cell cycle for 4 hours or more did not show the apoptotic peak either. Whereas, G_1 cell populations obtained by elutriation have apoptotic cells (Figure 9-1 thru 9-2). The difference between the control and treatment flow cytometry histograms is that the treatment cells were subjected to ice-

cold temperature when prepared centrifugally elutriated. The sub G_1 peak found in the cells centrifugally elutriated and then fixed for flow cytometry typically contained a 0.6 n amount of DNA. These cells were either cell fragments or apoptotic cells.

A Trevigen TACS Annexin-V FITC test kit was used to test for apoptosis. This kit showed a distinct population of cells that bound annexin V, a phospholipid binding protein. Early apoptotic cells in which the phosphatidylserine has "flipped" from the inner membrane to the outer membrane of the cell bind annexin V, whereas normal cells do not (Fadok et al., 1992; Koopman et al., 1994). The first cell population was collected at a pump speed of 10 to 13.5 ml/min, which is slightly slower than the other populations of cells elutriated. These apoptotic cells elute before normal G_1 cells, because apoptotic cells go thru a pre-lethal change that causes shrinkage of the cells and fragmentation of the DNA (Williamson, 1970; Kerr et al., 1972). At pump speeds between 10 to 13.5 ml/min, the viewing port on the elutriation chamber showed the cell demarcation boundary was almost to the edge of the elutriation chamber (Figure 5b). The cells coming off the elutriator between 10 ml/min and 13.5 ml/min looked, when viewed under a light microscope, to be approximately the same size as the other early G_1 cells. In the first population of elutriated cells collected when the pump speed was increased from 10 ml/min to 13.5 ml/min (Figure 10-1a), 87% of the cells fell in the parameters for G_1 cells; the remainder had a DNA content less than the normal 1 n amount. This smaller peak contains about 38 relative DNA units content compared to 63 units of DNA content for a 1 n amount of DNA in the G_1 cohort, so the relative DNA content of the cells in the smaller peak is about 0.6 n, demonstrating that these cells have lost a significant amount

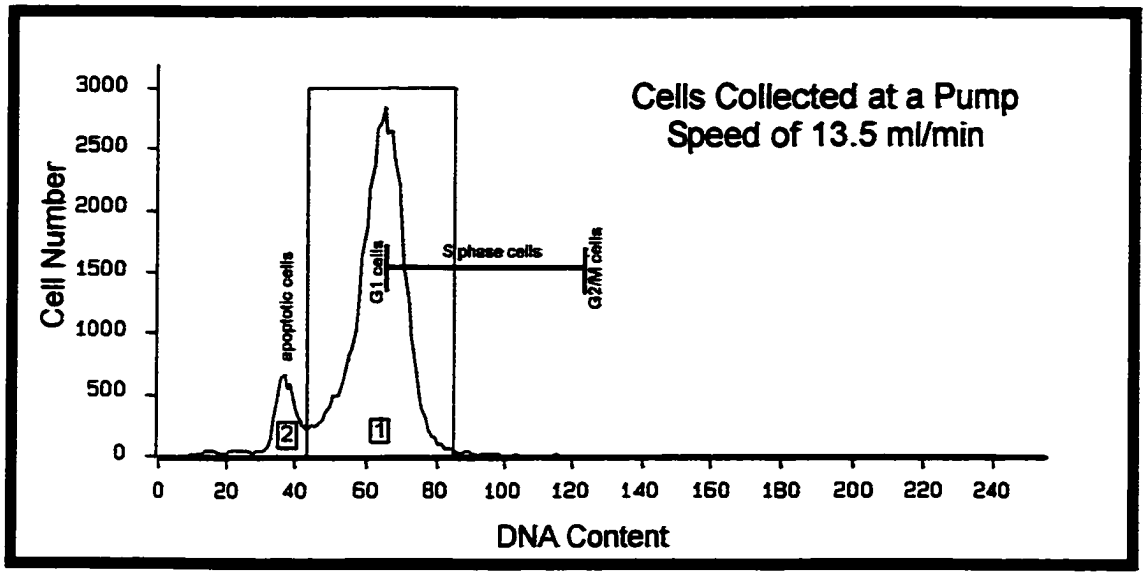

Figure 10-1a. Flow cytometry histogram of cells elutriated at a pump speed of 13.5 ml/min. The axes are as usual, except the 1 n DNA content for the cells is 63 and the 2 n DNA content is 126. This histogram consists of 50,000 cells, 87% of the cells fell in region 1 outlined in the graph and are primarily G_1 cells. The majority of the in region 1 cells have a 1 n DNA content of 63. Peak 2 is seen to the right of peak 1, these cells are primarily apoptotic with a relative DNA content of 38, equal to a 0.6 n amount of DNA.

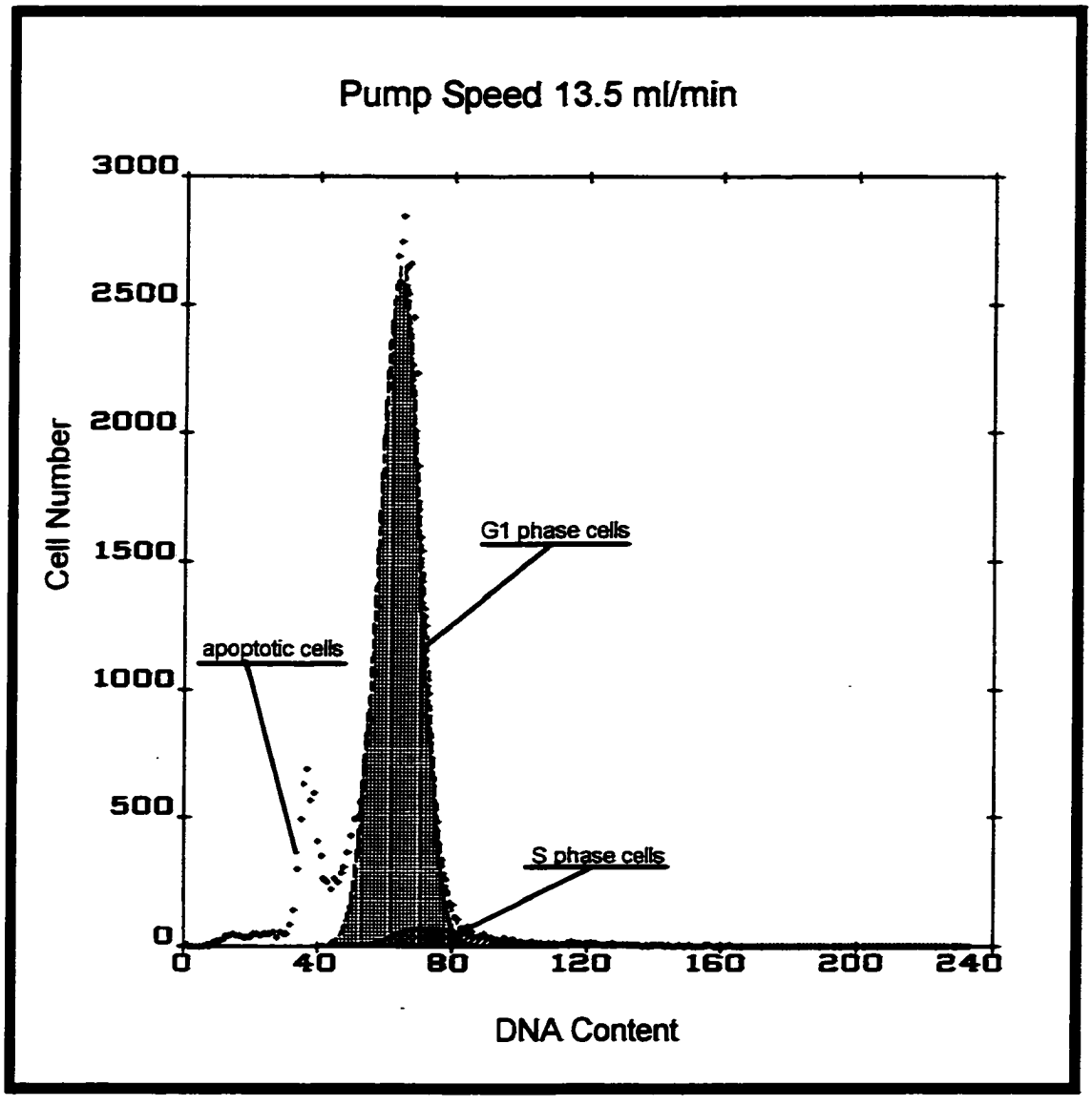

Figure 10-1b. Analysis of the DNA content of cells elutriated at a pump speed of 13.5 ml/min. The mean relative value of DNA content for G_1 cells in this sample is 64 with a coefficient of variance (CV) of 10. 94% of the cells are in G_1; these cells are seen in the checked peak. The mean relative value of DNA content for G_2 cells is 126 with a CV of 10. In this elutriate, a very small percentage of the cells, 0.2% were in G_2, and 5.5% of the cells were in S phase. Apoptotic cells are to the left of the non-apoptotic cells.

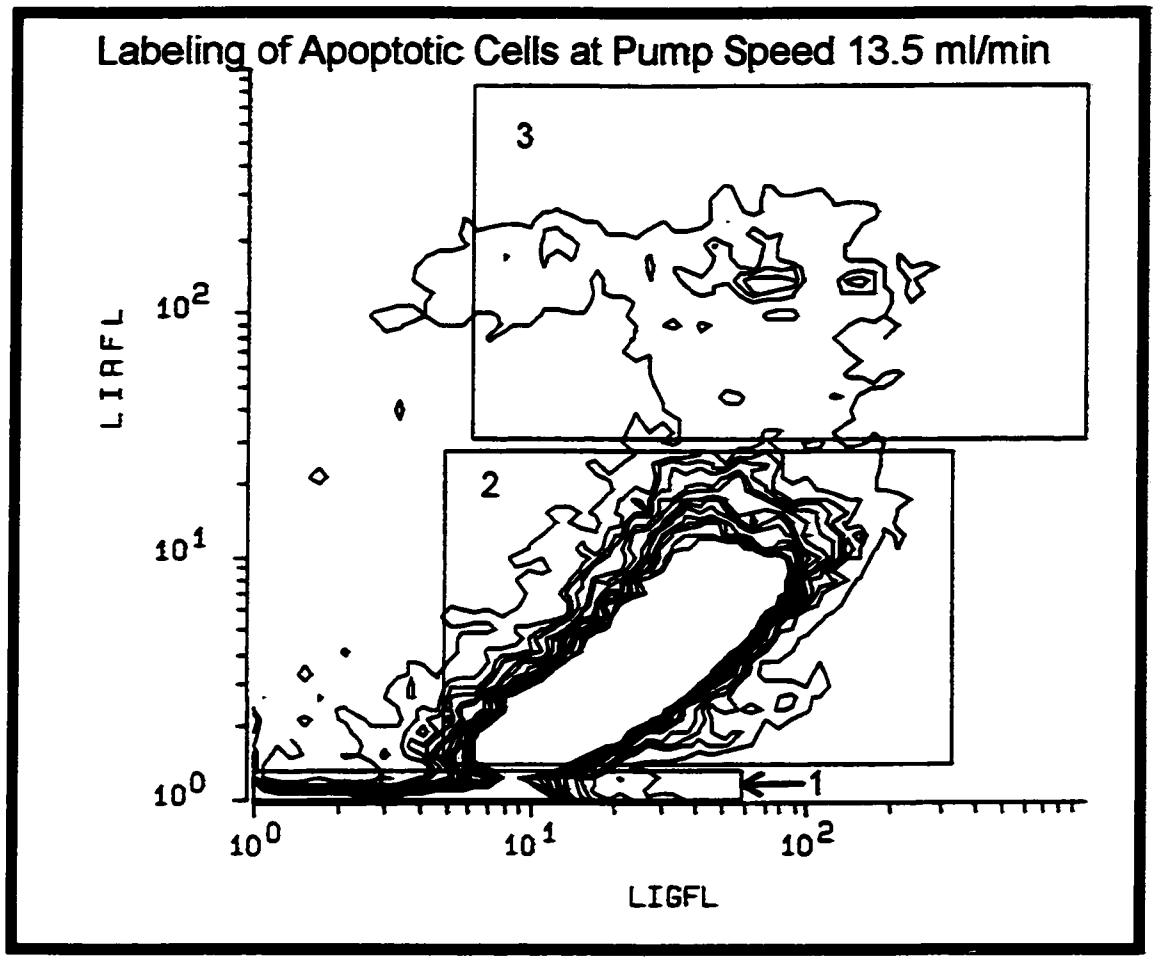

Figure 10-1c. Fluorescence Assisted Cell Sorting plot of binding of Annexin V vs. propidium iodide content in the 13.5 ml/min elutriate. The Annexin V-FITC is shown on the X-axis as the log of the integral green fluorescence and the propidium iodide is on the Y-axis as the log of the integral red fluorescence. For this histogram, 20,255 cells were analyzed and were placed in one of three regions. Region 1 contains 19% of the cells. The cells in region 1 have very little propidium iodide labeling and are low in labeling with Annexin V-FITC, thus their membranes are intact and they are not apoptotic. Region 2 contains 76% of the cells. These cells have relatively more propidium iodide, which means the cell membrane is damaged, and a greater amount of the Annexin V-FITC that is attached to the phosphatidylserine on the outer membrane of the cell. Thus these cells are apoptotic. Region 3 contains 5% of the cells. These cells have even greater amounts of propidium iodide and this is indicative of cells in an advanced state of apoptosis.

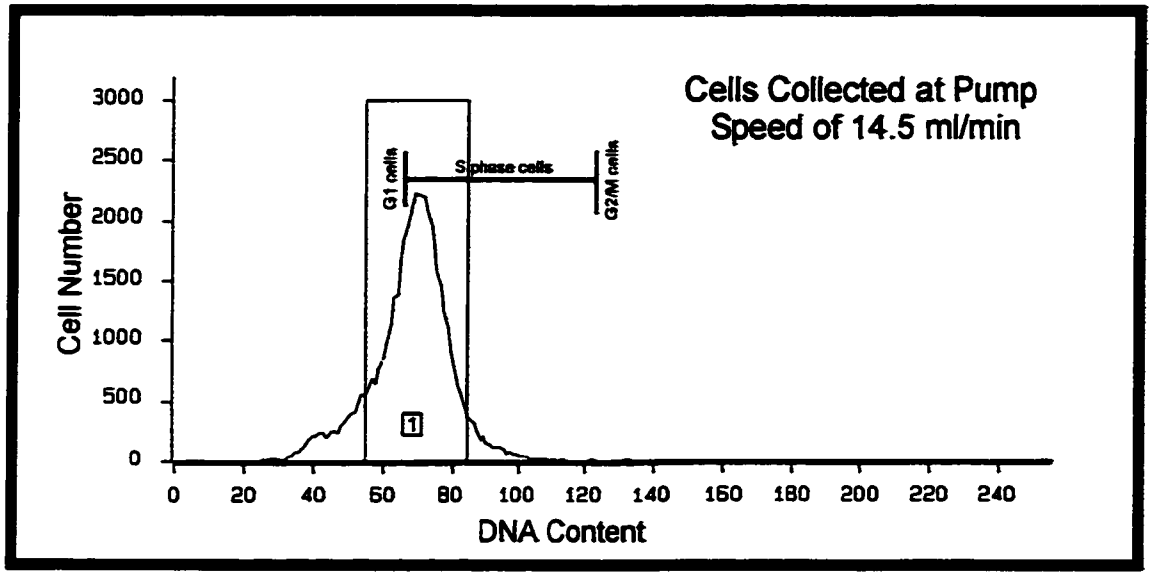

Figure 10-2a. Flow cytometry histogram of cells elutriated at a pump speed of 14.5 ml/min. The axes are as in Figure 10-1a. This histogram consists of 50,000 cells, 80% of the cells (40,000) fell in region 1. These cells have a relative DNA content of 69. The apoptotic peak is much reduced but is still visible at DNA Content of 43.

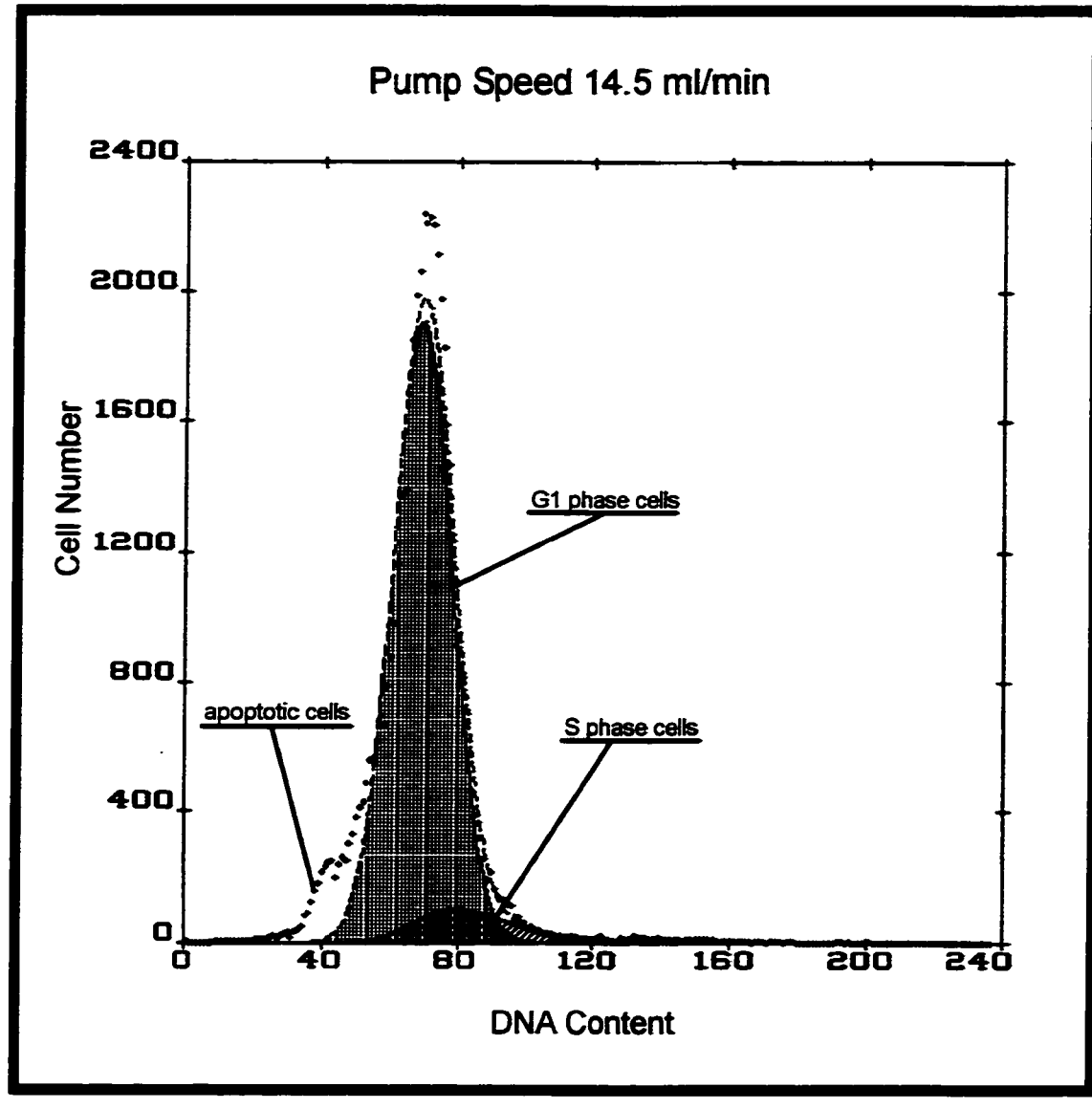

Figure 10-2b. Analysis of the DNA content of cells elutriated at a pump speed of 14.5 ml/min. The mean relative value of DNA for the cells in this elutriate is 69 with a CV of 13. The percentage of cells in G_1 is 91%; these cells are seen in the checked peak. The mean relative value for G_2 cells is 140 with a CV of 13, 1% of the cells are in G_2. The number of cells in S phase has increased to 8%, as shown in the cross hatched peak. The apoptotic cells are to the left of the non-apoptotic cells.

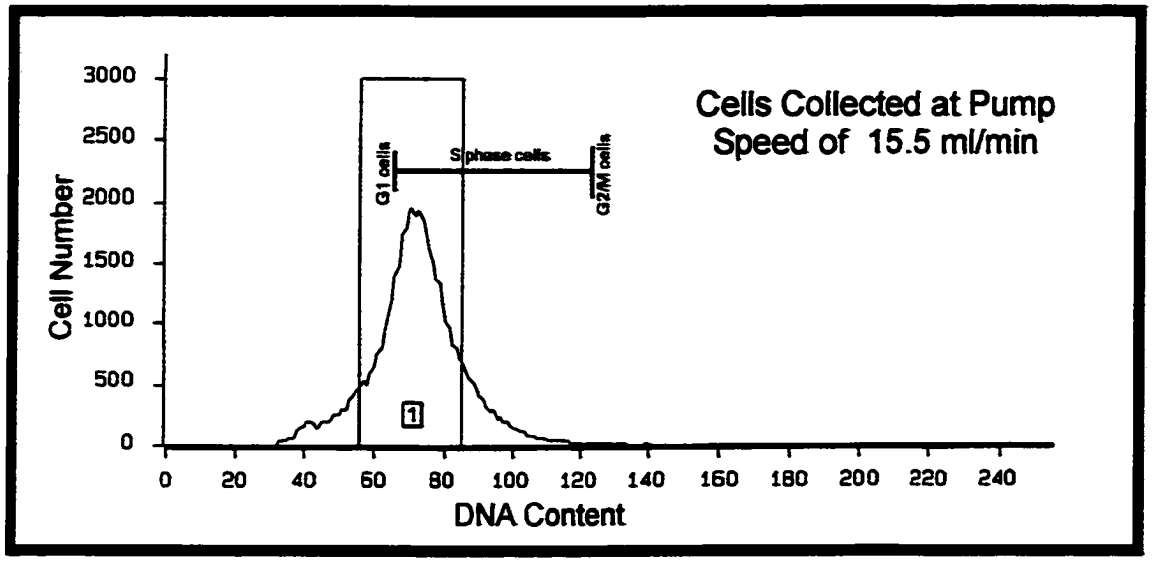

Figure 10-3a. Flow cytometry histogram of cells elutriated at a pump speed of 15.5 ml/min. This histogram consists of 50,000 cells, 75% of the cells fall in region 1. They have a relative DNA content of 71, thus these cells contain more S phase than in Figures 10-1a and 10-2a. The apoptotic peak is seen as a small blip at a DNA content of 43.

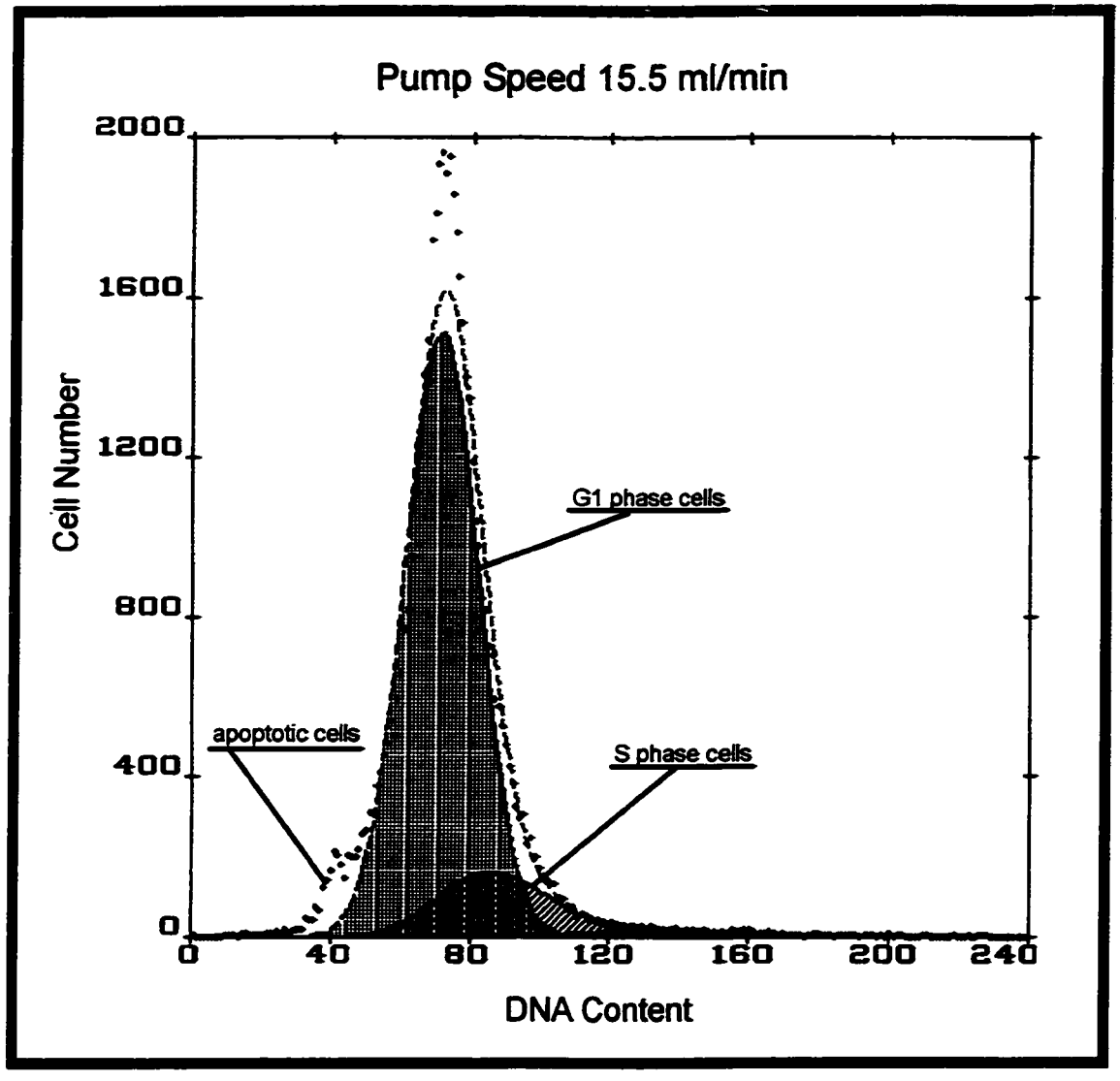

Figure 10-3b. Analysis of the DNA content of cells elutriated at a pump speed of 15.5 ml/min. The mean relative DNA content for G_1 cells in this elutriate is 71 with a CV of 12. The percentage of cells in G_1 is 73%; these cells are in the checked peak. The mean relative value for G_2 cells is 143 with a CV of 12; 1.5 % of the cells were in G_2. The number of cells in S phase was 25%, as seen in the cross hatched peak. The small population of apoptotic cells is to the left of the normal cells.

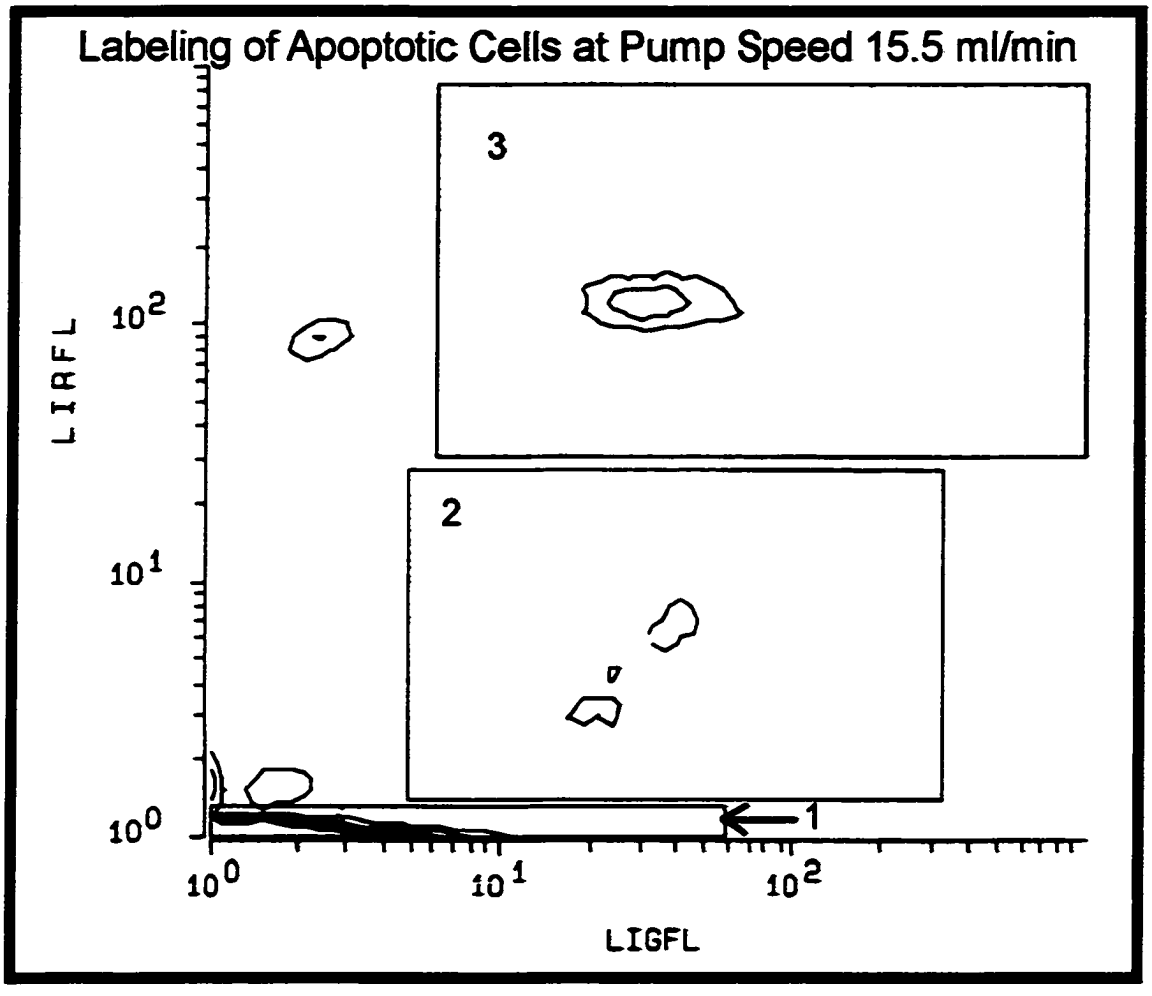

Figure 10-3c. FACS Analysis of the levels of Annexin V vs. propidium iodide content per cell in the 15.5 ml/min elutriate. Very few cells are in apoptosis. The axes are as in Figure 10-1c. In this analysis 57,107 cells were counted and were placed in one of three regions as before. Region 1 contains 83% of the cells, which are viable non-apoptotic cells. Region 2 contains 6% of the cells that are apoptotic. Region 3 contains 7% of the cells that are in an advanced state of apoptosis.

of their DNA. The cell cycle flow cytometry profile for these cells is shown in Figure 10-1b. The cells in this sample have 94% of the cells with a G_1 content of DNA, a few have less than the G_1 content of DNA, and about 5% have more than the G_1 phase content.

The annexin V vs. propidium iodide fluoresce assisted cell sorting (FACS) plot (Figure 10-1c) showed that about 75% of the entire first elutriate collected at a flow rate of 10 to13.5 ml/min consisted of apoptotic cells. The annexin V-FITC is measured on the x-axis and the propidium iodide is on the y-axis. Figure 10-1c has three regions designated. The cells located in the lower left of the plot, region 1; have relatively little annexin-V-FITC labeling indicating that they are normal and not apoptotic. The remaining 81% of the cells fall in region 2 or 3. Thus, the cells that elute between 10 and 13.5 ml/min are 20% normal early G_1 cells with the rest showing apoptotic signs.
At the next elutriation collection, 14.5 ml/min (Figure 10-2a), the apoptotic cell peak at 38 relative DNA content is reduced compared to Figure 10-1b. The primary peak has a relative DNA content of 69 and contains 80% of the cells run through the flow cytometer. The DNA profile for this peak (Figure 10-2b) shows that 91% of the cells were in G_1, and 7.9% of the cells were in S phase.

A substantial population of G_1 cells remain at a pump speed 15.5 ml/min (Figure 10-3a), but the peak is less sharp and starting to show the spreading at it's base characteristic of populations of cells that contain a mixture of G_1 and S phase cells. The flow cytometry analysis shows that this population is 73%, 25%, and 1.5% G_1, S, and G_2 cells respectively. The apoptotic cells are seen as a small peak to the left of normal cycling cells. The fraction of apoptotic cells is decreased in populations elutriated at a

pump speed of 15.5 ml/min compared to the first elutriate at 13.5 ml/min. In the former (Figure 10-3c), 83% of the cells fall in region 1, 5.8% in region 2, and 6.7% in region 3. Thus, the majority of cells in the 15.5 ml/min elutriate are not apoptotic. This result agrees with the data of the flow cytometry shown in Figure 10-3a. Because of this data, G_1 cells collected for later experiments were collected at flow rates from 13 to 15.5 ml/min.

Fluoresce *In-Situ* Hybridization Analysis of BrdU Labeled A_L Cells

FISH analysis was used to determine whether or not the flow cytometry data for the A_L cells entering S-phase was accurate and to analyze the time of replication of human chromosome 11 in S phase. The chromosomes in the control group (Figure 11-1) are cells labeled from 4.5 to 10.5 hr after plating that show extensive red labeling identifying BrdU incorporation. Most of the chromosomes replicated during this time. Figure 11-2 shows the same chromosome spread, but with the blue component removed by computer manipulation to better see the BrdU incorporation. The CHO chromosomes in the chromosome spread show banding patterns of large regions of nearly complete replication. The portions of the chromosome that have not replicated are those that are late replicating portions of the genome, these areas are easily seen by comparing Figure 11-1 and 11-2.

Figure 11-3 is a chromosomal spread of treatment group 1. Treatment group 1 (see Figure 6 for treatment groups) was A_L cells that were pulse labeled with BrdU from 4.5 to 5.5 hours after t_0 (t_0 = time of inoculation of the early G_1 cells that were plated and allowed to progress through the cell cycle). None of these chromosomes show any BrdU

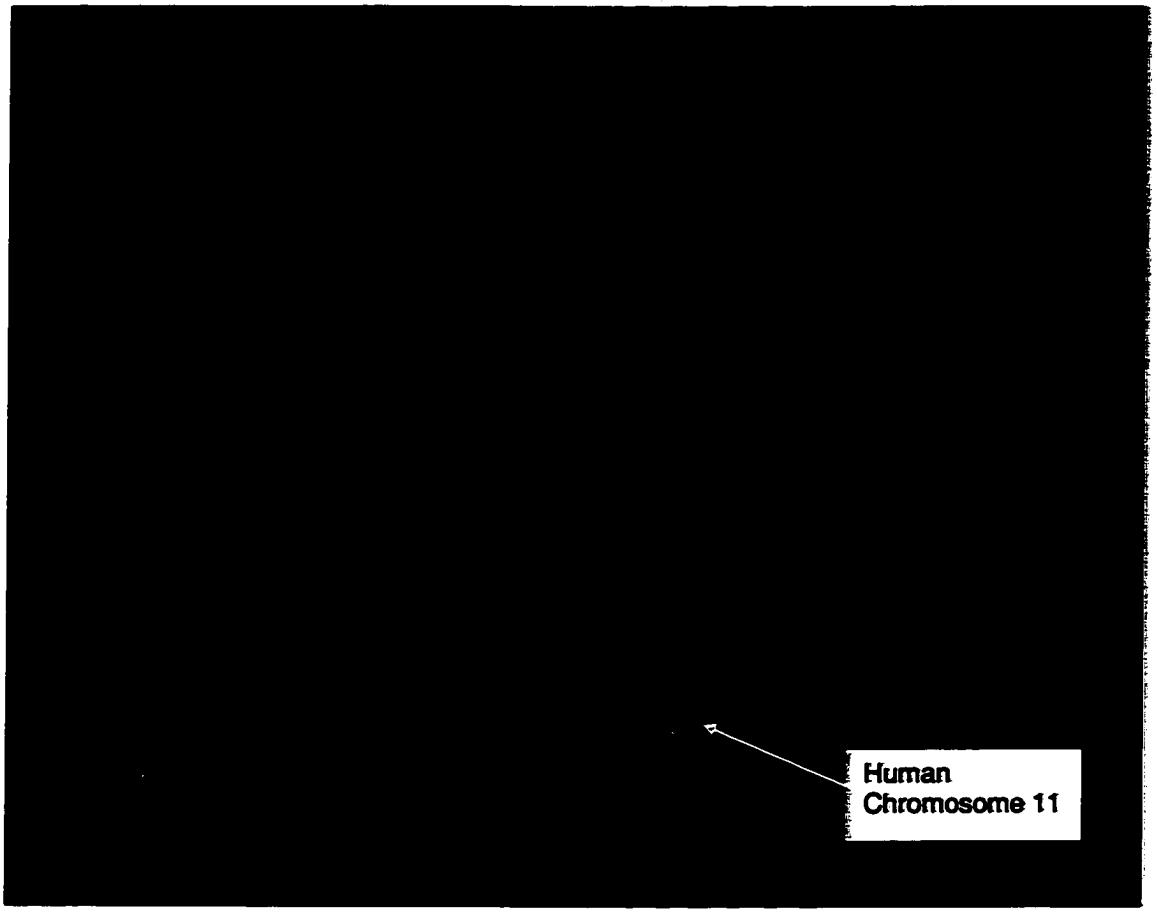

Figure 11-1. Photomicrograph of a chromosome spread of a cell obtained by centrifugal elutriation in early G_1 and labeled with BrdU from 4.5 to 10.5 hr post plating of the G_1 cells. This photo was taken with three different filters (red, green and blue) and the images were combined. This chromosome spread is from the control treatment group. The human chromosome 11 is identified by the green FITC label at its centromere. All chromosomes were labeled with blue DAPI, and BrdU incorporation is labeled with red Texas Red®. The BrdU was labeled with an anti-BrdU antibody secondarily labeled with Texas Red®. The red areas on the chromosomes are areas where BrdU had incorporated in the DNA. The majority of human chromosome 11 has incorporated BrdU by 10.5 hours. The areas that are stained blue had no DNA incorporation and replicated after 10.5.

Figure 11-2. Photomicrograph of a chromosome spread of a cell obtained by centrifugal elutriation in early G_1 and labeled with BrdU from 4.5 to 10.5 hr after plating the early G_1 cells. This is the same photomicrograph as in figure 11-1 with the blue DAPI filtered out. This photo was taken with only two filters (red and green) and the images were combined. Areas where DNA replication occurred are shown as red. The human chromosome 11 was labeled with FITC as described. Comparing figure 11-1 and 11-2 reveals patterns of replication for the chromosomes. Many of the chromosomes show incomplete labeling. These are labeled in very late S phase from during the time 10.5 hr after plating to around 12 hr. However, almost all of chromosome 11 appears to have replicated during this 6 hr interval from 4.5 to 10.5 hr.

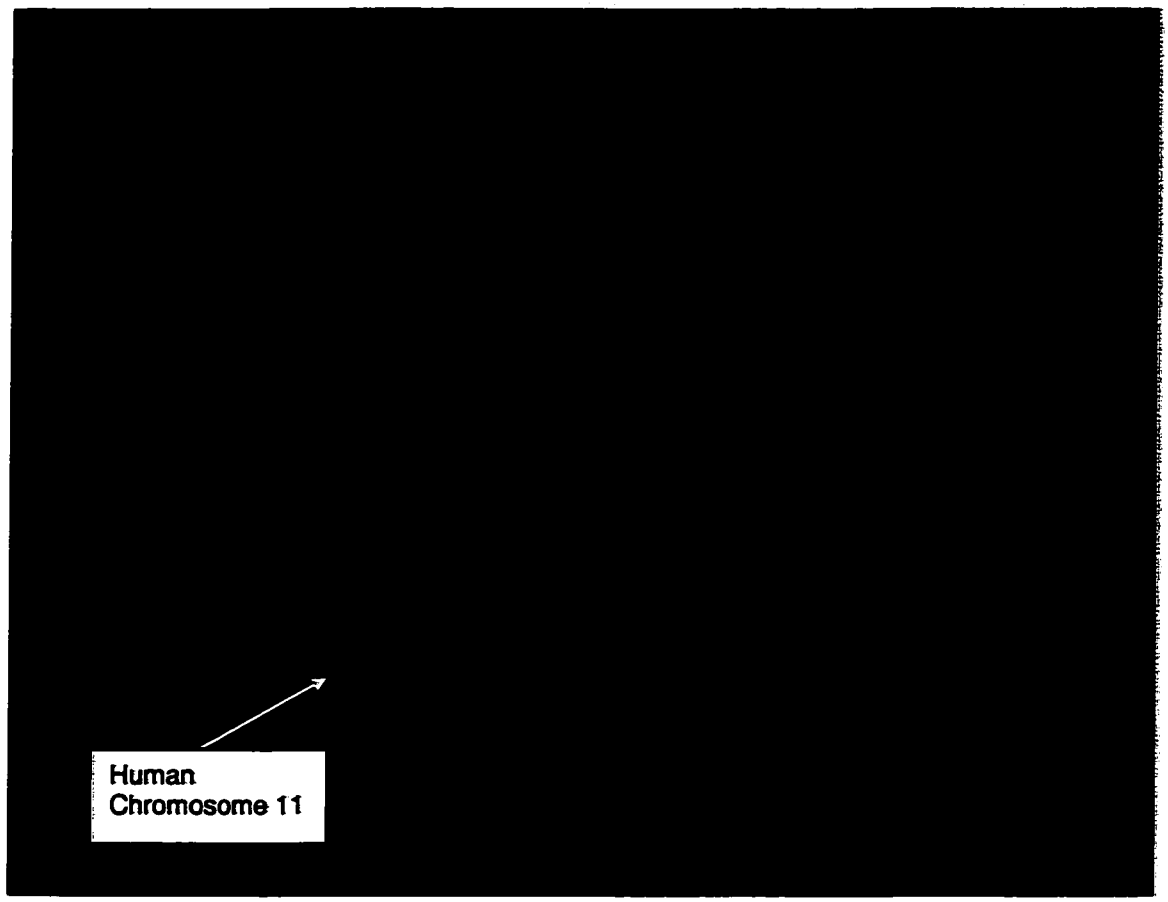

Figure 11-3. Photomicrograph of a chromosome spread from a cell centrifugal elutriated in early G_1, plated, and labeled with BrdU from 4.5 to 5.5 hr after plating. This chromosome spread is from a cell in treatment group 1, where the BrdU was added for 1 hr from 4.5 to 5.5 hr after plating. The absence of red labeling indicates that no DNA replication occurred during this one-hour period showing that up until 5.5 hours after plating the G_1 cells the cell have not entered into S phase.

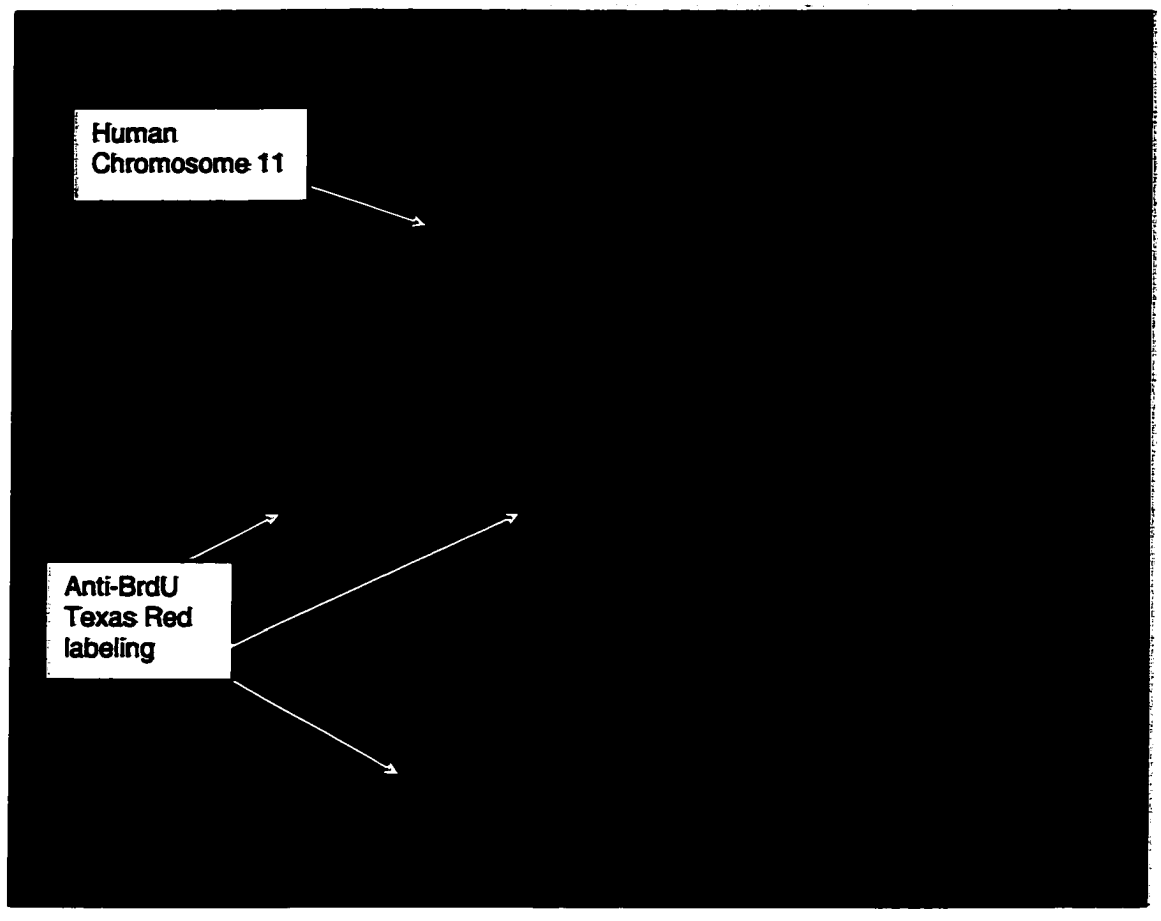

Figure 11-4. Photomicrograph of a chromosome spread of an A_L hybrid cell that had been labeled with BrdU from 5.5 to 6.5 hr after plating centrifugally elutriated early G_1 cells. This chromosome spread is from cells in treatment group 2 where BrdU was added for 1 hr from 5.5 to 6.5 hr after plating. The blue color is DAPI, and the green is the FITC labeling. Small spots of red anti-BrdU antibody with Texas Red® fluorochrome are seen on many of the chromosomes, indicating patches where the DNA replication has occurred. These chromosomes show very little Texas Red® labeling, indicating that they are just entering S phase at 5.5 hours after plating.

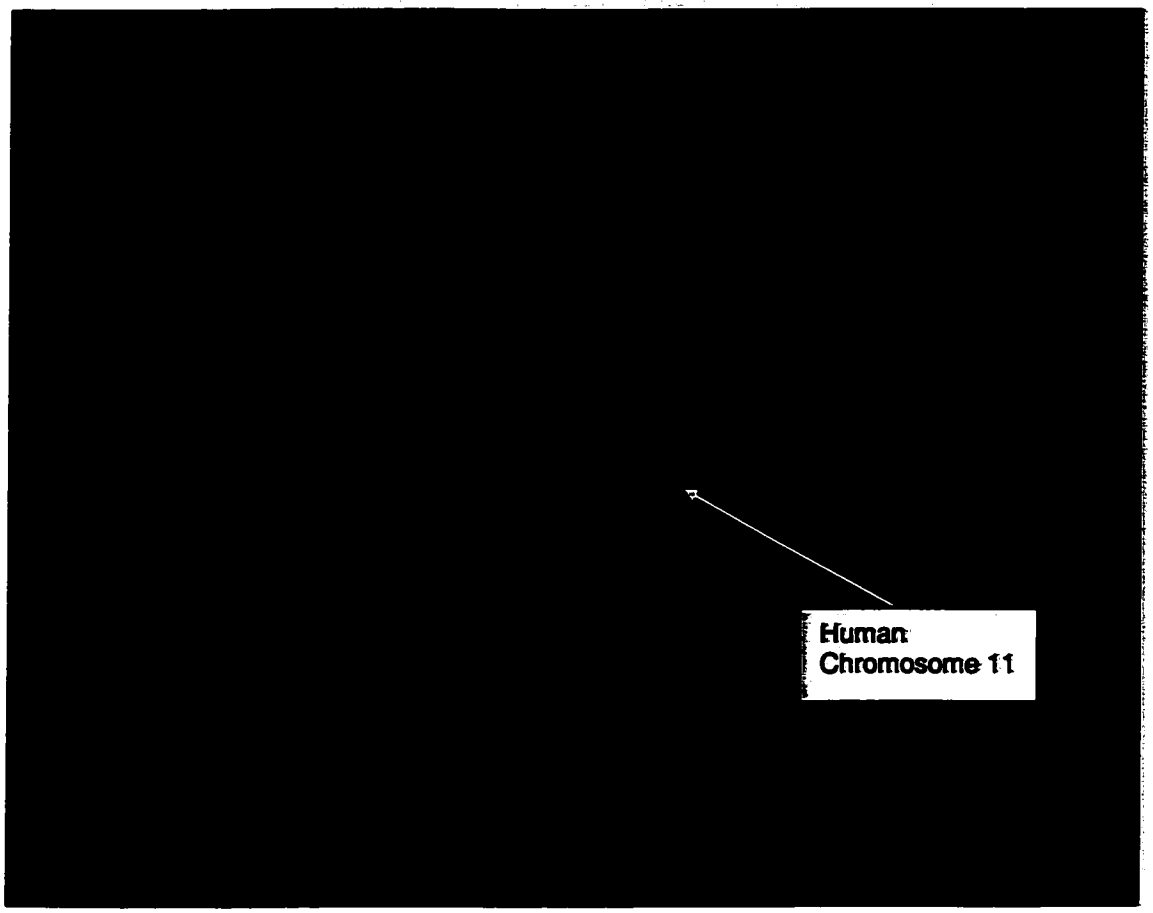

Figure 11-5. Photomicrograph of a chromosome spread of an A_L hybrid cell that had been labeled with BrdU from 7.5 to 8.5 hr after plating centrifugally elutriated early G_1 cells. This chromosome spread is from cells in treatment group 4 where BrdU was added for 1 hr from 7.5 to 8.5 hr after plating. All of the chromosomes are labeled with the Texas Red® anti-BrdU antibody demonstrating DNA replication during S phase. The human chromosome 11 shows very strong red labeling along its entire length, indicating that by 8.5 hours most of chromosome has replicated, whereas many of the CHO chromosomes have not completed replication. Chromosome 11 is an early to mid-replicating chromosome in the A_L cell as it is in human cells (Bickmore and Carothers, 1995).

incorporation or labeling with Texas Red®. Thus, at 5.5 hours after plating, these cells have not yet entered into S-phase.

Figure 11-4 shows treatment group 2 cells that were pulse labeled with BrdU from 5.5 to 6.5 hr after t_0. DNA replication has initiated where the small bright red spots of Texas Red® are located on the chromosomes (see arrows, figure 11-4). Therefore these chromosomes show the beginning of S-phase. This FISH data agrees with the data from the flow cytometry analysis. The data from Figure 9-4, flow cytometry histograms of early-S phase cells, showed that the cells enter into S-phase some time between 4-6 hours post plating. Combining this of data, the flow cytometry histogram and the FISH, narrows the window of DNA replication initiation to between 5.5 to 6 hr after t_0.

Figure 11-5 shows treatment group 4 cells (Figure 6) that were pulse labeled with BrdU between 7.5 to 8.5 hours after t_0. During this time, the human chromosome 11 is extensively labeled with the Texas Red® fluorochrome; CHO chromosomes have various amounts of labeling. The flow cytometry data from Figure 9-5 supports this FISH data that the cells are in the middle of S phase. However, the flow cytometry data does not give any specific insight into when the human chromosome 11 replicates. The short arm of human chromosome 11, where the *CD59* gene is located, is brightly labeled in Figure 11-5, but quantitative measurements of BrdU labeling are difficult to discern on the figures. A method to quantitatively measure the amount of labeling was needed. The method used was to look at a gray scale line-scan of the light emitted from the fluorochromes labeling the chromosomes. This method allows identification of when specific regions of the chromosomes were replicated.

Line-scans of Human Chromosome 11 in A_L Cells

Line-scans were done on human chromosomes 11 from several A_L chromosome spreads. The line-scan provides quantification of the amount of fluorochrome label on individual chromosomes. The line-scan technology involves digitally drawing a line through a chromosome image and quantitatively measuring the intensity of three wavelengths of light; blue, green and red along the length of the line. The chromosome spreads were the same as those used for the FISH. The line-scan data concurs with the FISH images, where the FISH images are brightly labeled; the line-scans show high levels of light. One major advantage of the line-scans is that long and short arms of Human chromosome 11 can be easily distinguished because the position of the centromere can be determined from p82h FITC label (Christian et al., 1998).

Figure 12-1 is a line-scan from the control treatment group of cells pulse labeled 4.5 to 10.5 hr post-plating. The human chromosome 11 is heavily labeled with anti-BrdU Texas Red® that means that this chromosome has gone through most of its replication. The centromere is located at a relative length of 52. The position of the p and q arms can be seen on the graph. The q arm shows labeling in the middle of the long arm. The short arm or the p arm, where *CD-59* is located at 11p13.5, is labeled with Texas Red® along its entire length.

Figure 12-2 is a line-scan from a human chromosome 11 on a A_L chromosome spread pulse labeled 4.5 to 5.5 h after t_0 (same as FISH Figure 11-3). The level of light is equal to background amounts of Texas Red® so that there is essentially no labeling of the human chromosome, thus, there is no BrdU incorporated into the cell at this point in the

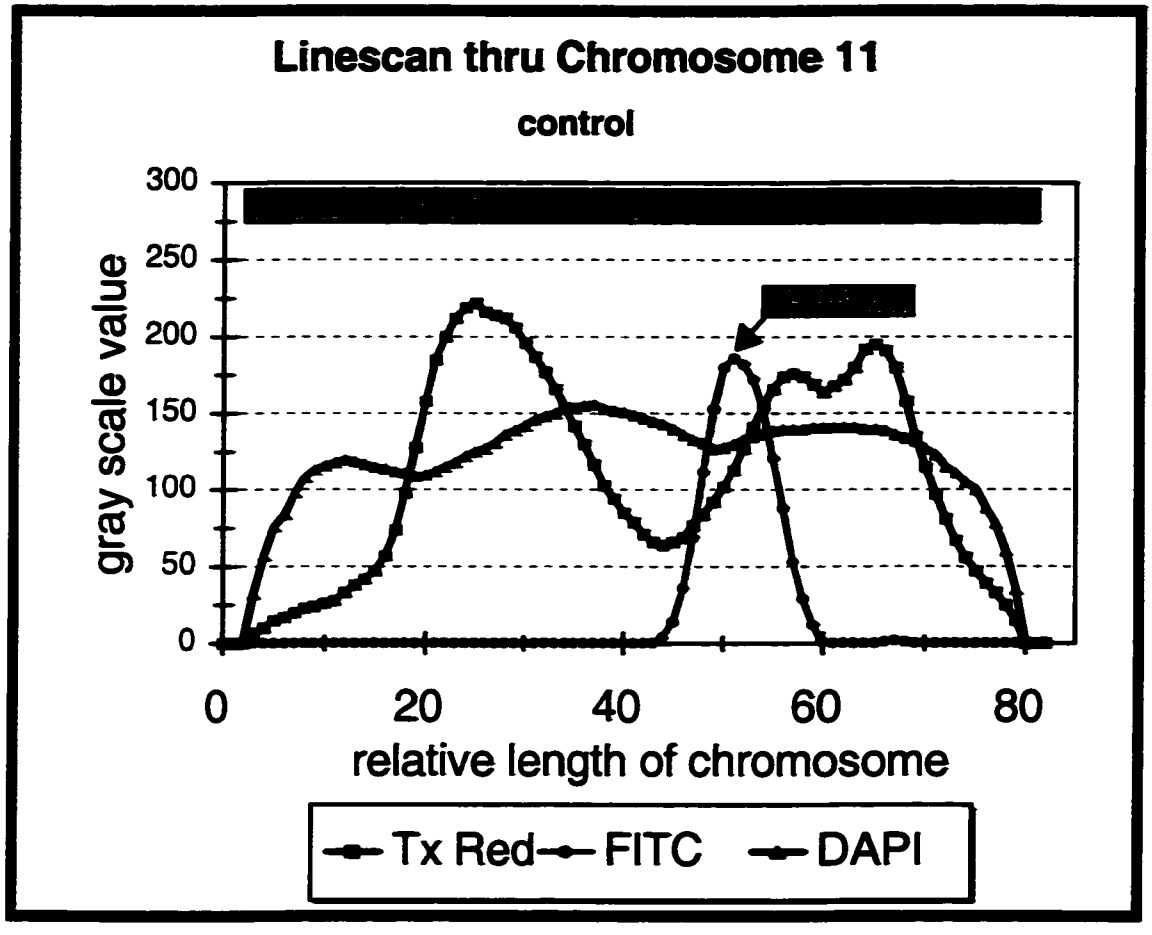

Figure 12-1. Line scan of human chromosome 11 for the control treatment group of elutriated A_L hybrid cells that had been labeled from 4.5 to 10.5 hr after plating. DAPI gives uniformly higher gray scale values ranging from 110 to 160, indicating labeling along the entire chromosome. The centromere is shown by the increase of the value of FITC (green line) from 43 to 60 on the x-axis. The q arm is to the left of the centromere and the p arm is to the right. Texas Red® levels are relatively high, indicating high levels of DNA replication on the p arm of the chromosome (from 50 to 80 on the x-axis) and on most of the q arm (15 to 43 on the x-axis). *CD59* would be located at about 60 on the x-axis (if the chromosome is evenly coiled), and has replicated during this time period. The end of the q arm from about 0 to 17 on the x-axis shows very low levels of labeling with Texas Red®.

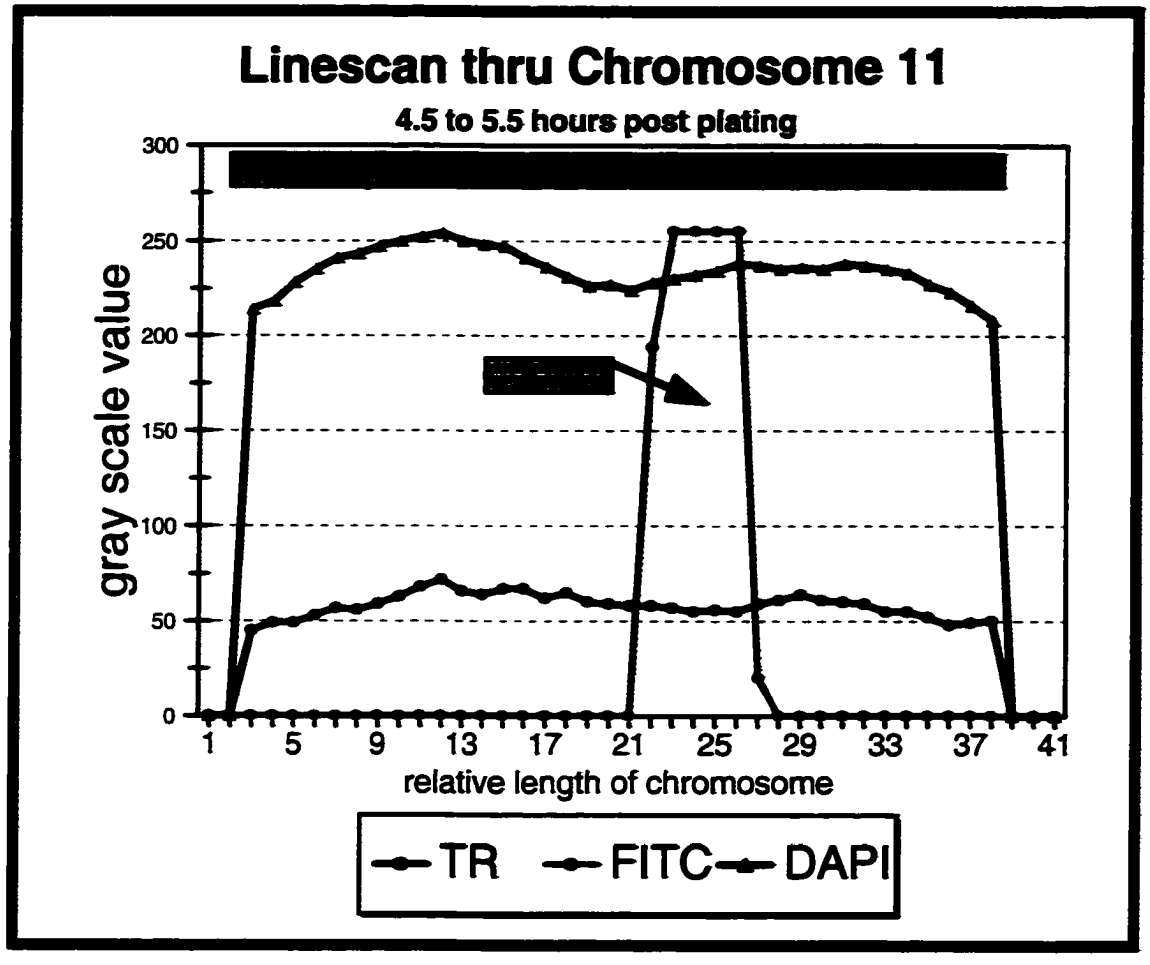

Figure 12-2. Line scan of chromosome 11 for treatment group 1 of A_L hybrid cells that had been labeled with BrdU from 4.5 to 5.5 hr after plating. The centromere was labeled with FITC from position 21 to 29; the p arm is on the right and the q arm on the left. The DAPI gives uniformly high light readings compared to the Texas Red®. The Texas Red® is at the background level over the entire length of the chromosome. Therefore, between 4.5 to 5.5 hr after plating of early G_1 cells no replication was occurring.

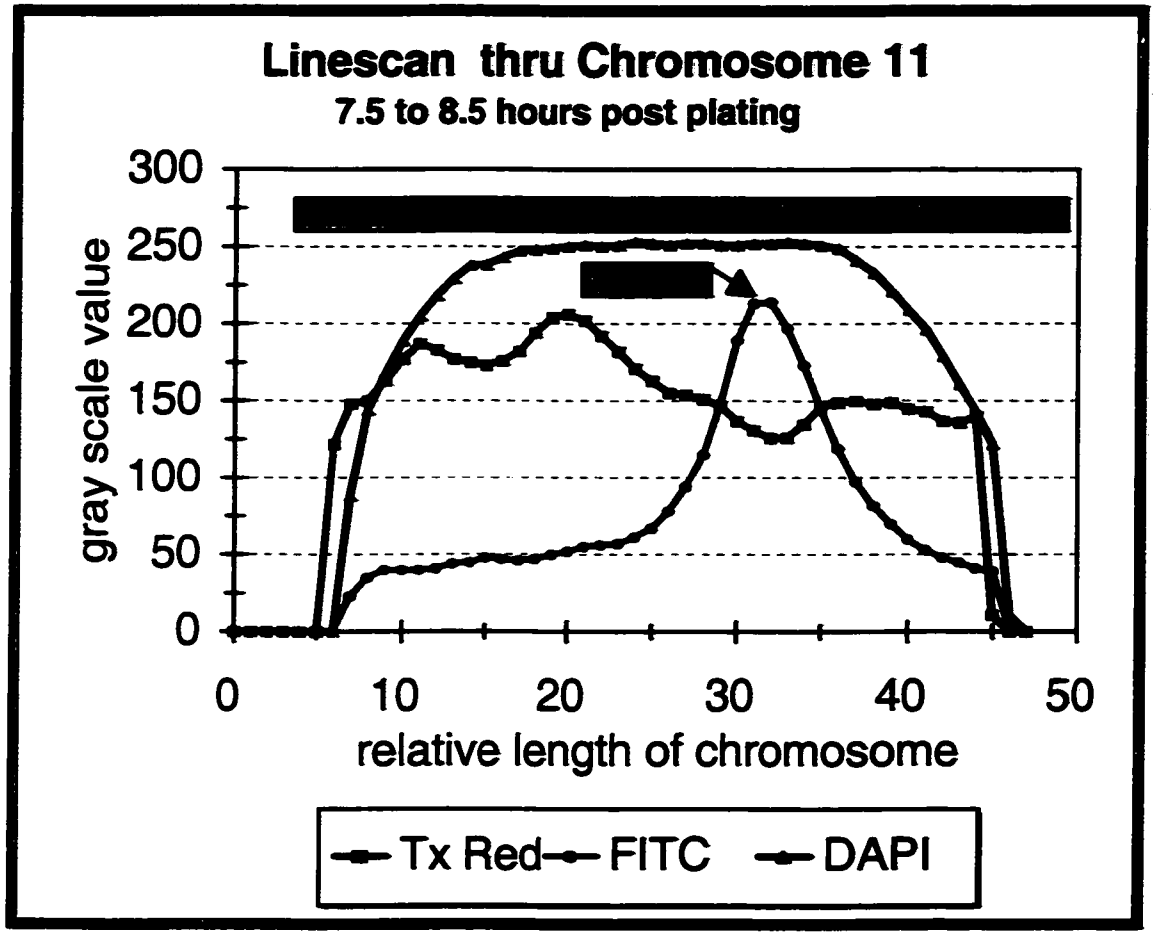

Figure 12-3. Line Scan of chromosome 11 for treatment group 4 of A_L hybrid cells that had been labeled with BrdU from 7.5 to 8.5 hr after plating. The human centromere probe has a FITC peak at position 32. The DAPI gives uniformly high gray scale values along the entire length of the chromosome. The Texas Red® labeling is high throughout the length of the chromosome but is not constant because of incomplete incorporation of the BrdU. This line scan shows that most of the DNA replication of human chromosome 11 is occurring between 7.5 to 8.5 hr after plating of the early G_1 cells.

cell cycle. The position of the p and q arms and the centromere can be seen on the graph from 21 to 28 relative lengths. The chromosome is uniformly labeled with DAPI. From Figure 11-5, the area of the chromosome where the *CD59* gene is located is replicated between 7.5 and 8.5 hr after t_0, the line-scan. Figure 12-3 directly supports the FISH data. The short arm of the chromosome shows the labeling with Texas Red$^{\bullet}$, meaning that the short arm of the chromosome replicated during that hour it was pulsed labeled with BrdU. From Figure 11-5, this chromosome visually appeared to be heavily labeled with Texas Red$^{\bullet}$. Combining the line-scan data and the FISH images, the *CD59* gene is replicated from 7.5 to 8.5 hours after plating early G_1 cells and letting them proceed through the cell cycle. Through the use of flow cytometry and FISH, I have zeroed in on the timing of the replication of the *CD59* gene. The next section will answer the question if irradiation of the *CD59* gene during replication will affect the mutation rate in comparison to irradiating in G_1.

MUTATION STUDIES

Cell Survival Curves for Log Phase Cells Exposed to Gamma Rays at 0 and 8 Hours

Cell killing and mutant induction by ^{137}Cs gamma was measured for A_L cells exposed in log phase, early G_1, and S phase. A survival curve for log phase A_L cells is shown in Figure 13. The surviving fraction for log phase cells exposed to 1.5 Gy was 61% and at 3 Gy the surviving fraction was 27% (Table 9). The mean LD_{50} (lethal dose where 50% of the cells survive) for these cells was 1.8 Gy, and the D_{37}, where 37% of the cells survive was at 2.35 Gy. Figure 14 shows survival curves for early G_1 cells just off the centrifugal elutriation process, S phase cells that were initially early G_1 cells plated

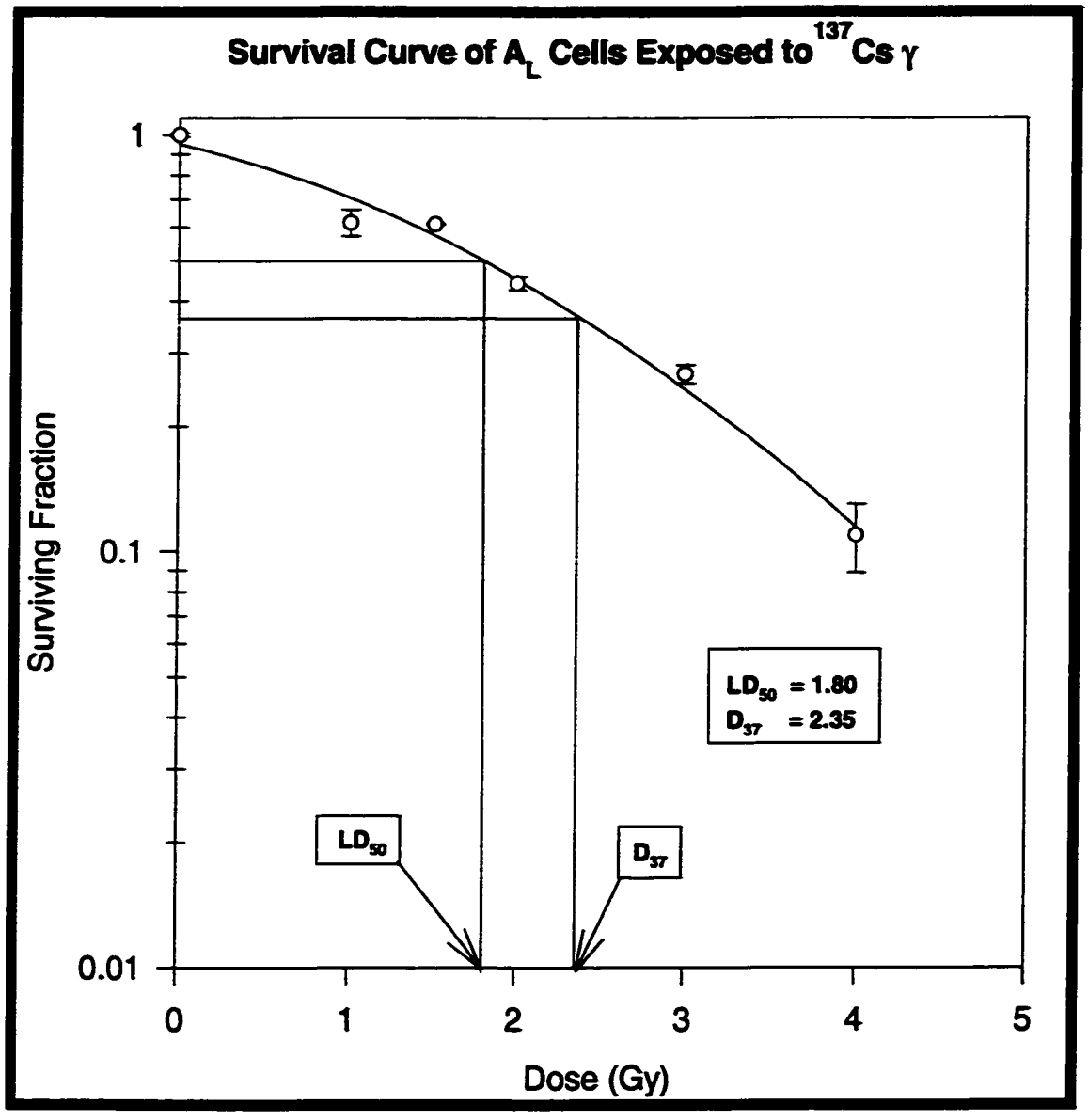

Figure 13. Survival curve of A_L cells exposed to ^{137}Cs gamma. Log phase A_L cells were collected off of tissue culture plates, serially diluted and replated into 60 mm tissue culture plates for irradiation. The LD_{50} for these cells was 1.8 Gy and the D_{37} was 2.35 Gy. Error is the standard deviation for three sets of data.

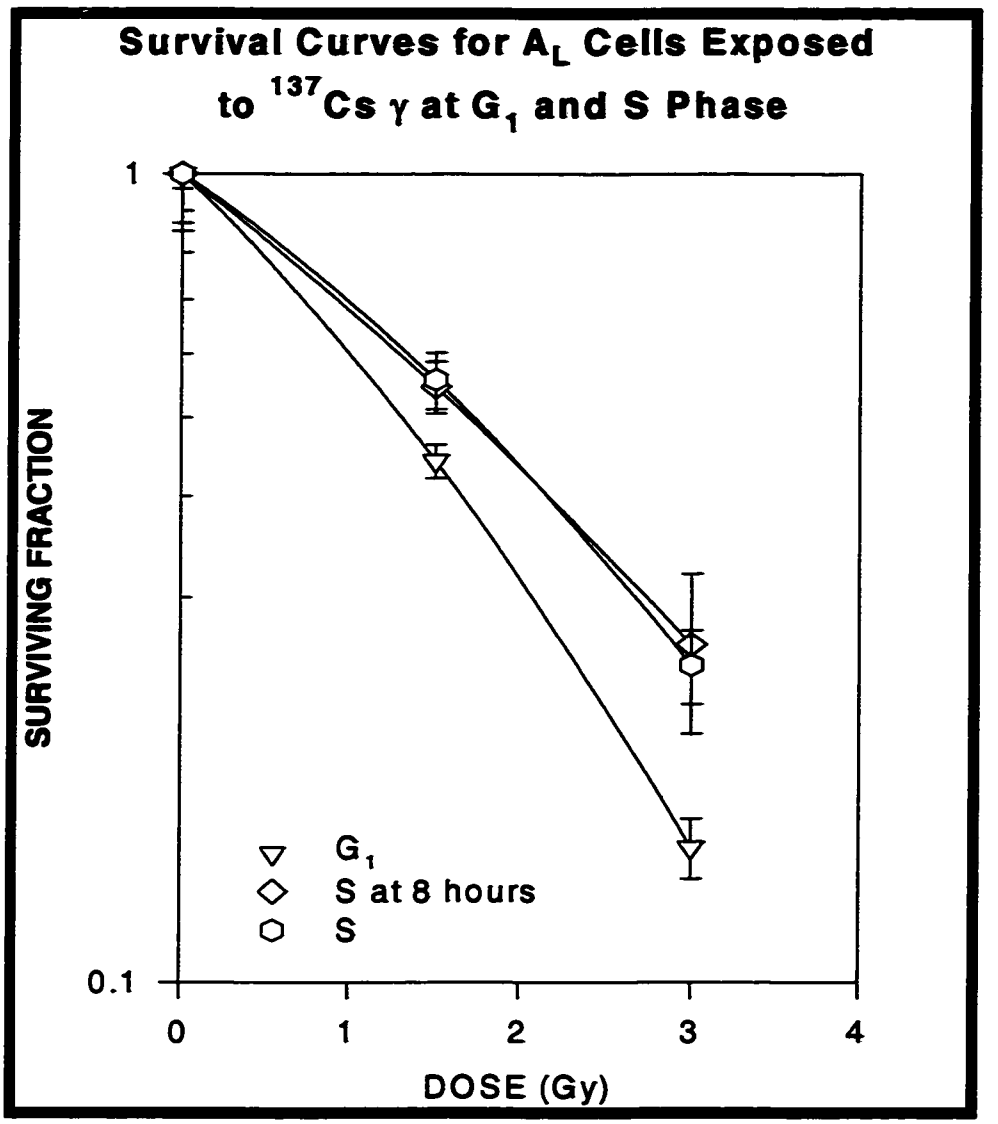

Figure 14. Survival curves for A_L cells exposed to ^{137}Cs gamma at G_1 and S phase. Early G_1 cells were centrifugally elutriated and 3 sets of cells were plated onto tissue culture plates. One set of early G_1 cells was irradiated immediately with ^{137}Cs gamma at 0, 1.5, and 3 Gy, the other set (S at 8 hours) was allowed to progress through the cell cycle for 8-hours in the incubator and then irradiated with ^{137}Cs gamma. Elutriated S-phase cells were also collected at a pump speed of 22 ml/min, plated in tissue culture plates and irradiated immediately with ^{137}Cs gamma. The G_1 cells had a LD_{50} of 1 Gy and a D_{37} of 1.42 Gy. S phase at 8 hours had a LD_{50} of 1.33 Gy and a D_{37} of 1.85 Gy. Elutriated S phase cells had a LD_{50} of 1.42 Gy and a D_{37} of 1.85 Gy. Thus, elutriated S phase cells respond to radiation approximately the same as cells that moved into S phase by incubation.

and allowed to progress through the cell cycle, and S phase cells that were elutriated at a pump speed of 22 ml/min. Early G_1 cells have a lower survival rate and greater killing in an equivalent dose as compared to both log phase and S phase cells (both elutriated S phase and those that were allowed to progress into S phase from early G_1). The G_1 cells irradiated with 1.5 Gy had a surviving fraction of 44 %, and at 3 Gy the surviving fraction was 15% (Figure 14 and Table 9). The S phase survival curve superimposes on the log phase survival curve seen in Figure 13. S phase cells centrifugally elutriated at 22 ml/min, immediately plated, and irradiated at 1.5 Gy has a surviving fraction of 56%. The surviving fraction for these S phase cells at 3 Gy was 25%. The S phase cells allowed to progress from G_1 into S phase had a surviving fraction of 55% at 1.5 Gy, and a surviving fraction of 26% at 3 Gy (Table 9).

Cell Phase	Surviving Fraction 1.5 Gy	Surviving Fraction 3 Gy	LD_{50} (Gy)	D_{37} (Gy)
Log Phase	61%	27%	1.8	2.35
G_1	44%	15%	1	1.42
S at 8 hr	55%	26%	1.33	1.85
S elutriated	56%	25%	1.42	1.85

Table 9. Comparison of surviving fraction, LD_{50}, and D_{37} in A_L cells irradiated with ^{137}Cs gamma during log growth, G_1 phase and S phase. LD_{50} is the dose where 50% of the population dies; D_{37} is the 37% survival rate.

Mutant Induction for G_1 and S Phase Cells

Figure 15 shows the mutant induction for centrifugally elutriated cells that were collected and plated on tissue culture plates. Irradiation with ^{137}Cs γ-rays induced more *CD59* mutants/10^5 survivors in the G_1 phase cells then in the S phase cells. As in the

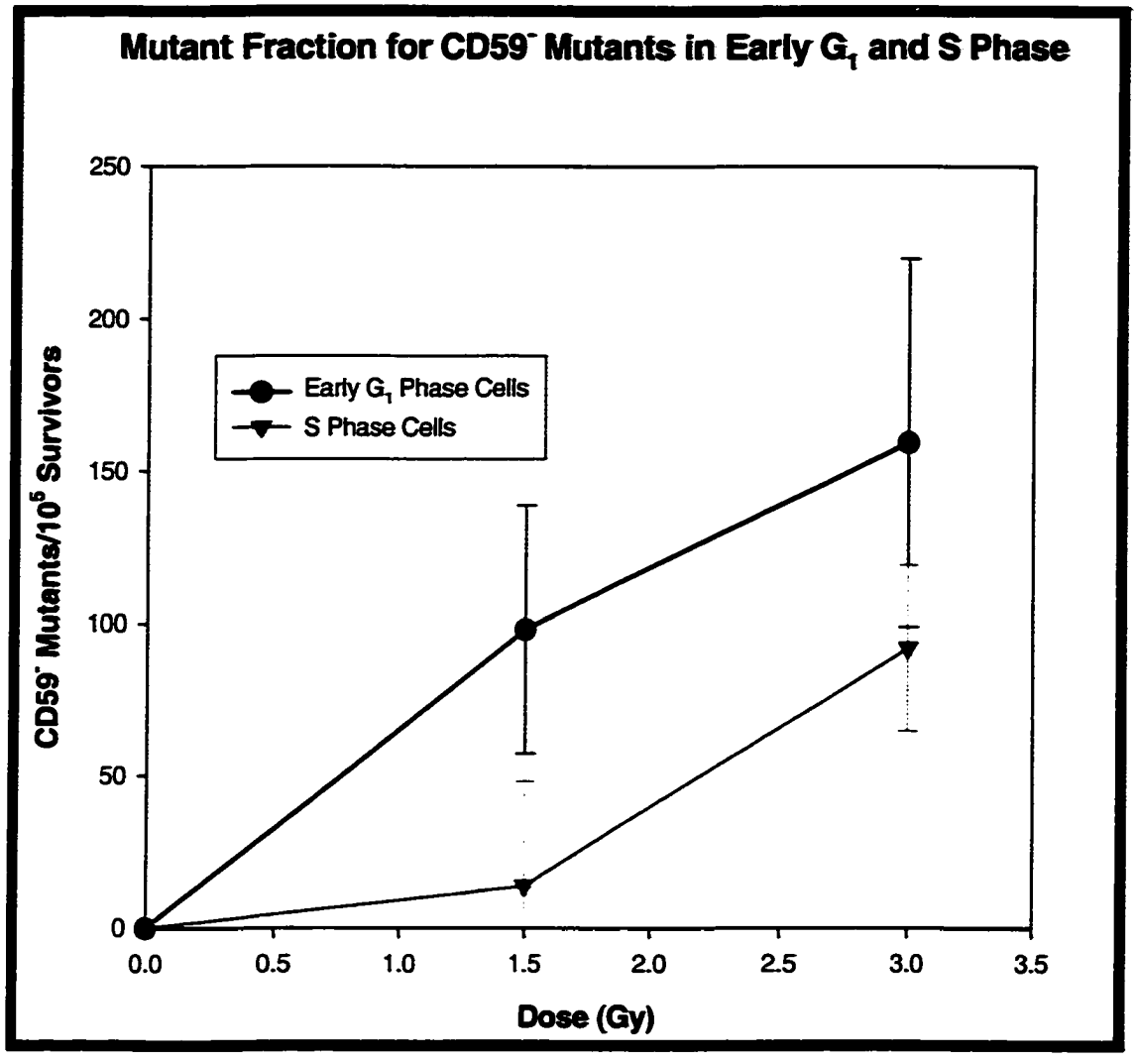

Figure 15. Induced mutant fractions for CD59⁻ mutants cells in early G_1 and S phase. A_L cells were centrifugally elutriated and plated in tissue culture plates. The G_1 cells were irradiated immediately with ^{137}Cs at 1.5 and 3 Gy. The S phase cells were allowed to progress through the cell cycle for eight hours and then were irradiated. The induced mutant fraction for the G_1 cells at 1.5 Gy was $98/10^5$ survivors, and at 3 Gy was $159/10^5$ survivors. S-phase induced mutant fraction was significantly smaller with $14/10^5$ survivors at 1.5 Gy and $92/10^5$ survivors at 3 Gy. The mutant yield, which is the slope of the mutant dose response curve, was 56 induced mutants/10^5 survivors/Gy for the G_1 population and 26 induced mutants/10^5 survivors/Gy for the S phase population.

survival curves, G_1 cells were plated immediately after elutriation and irradiated, whereas S phase cells were plated after elutriation and allowed to progress through the cell cycle for eight hours before being irradiated. With the background level of mutants of $65/10^5$ cells subtracted, the G_1 cells had an induced mutant fraction of $98/10^5$ cells at an irradiation dose of 1.5 Gy and an induced mutant induction fraction of $159/10^5$ cells at 3 Gy (Table 10). The induced mutant fraction for the S phase cells was much less than the G_1 cells. S phase cells had an induced mutant fraction with the background subtracted ($90/10^5$ cells) of $14/10^5$ at a dose 1.5 Gy and an induced mutant fraction of $92/10^5$ cells at 3 Gy. The induced mutant fraction was 85% less for the cells in S phase as opposed to G_1 phase at 1.5 Gy. For 3 Gy, the induced mutants were 42 % less in S phase as compared to G_1 phase. The mutant yield is equal to the slope of the mutant dose response curve. Its value is independent of the pre-existing mutants in the population. The mutant yield for the G_1 cells was $56/10^5$ survivors/Gy and for the S phase cell the mutant yield was $26/10^5$ survivors/Gy. At the time the *CD59* gene is replicating, between 7.5 to 8.5 hr after the early G_1 cells were plated and allowed to progress through the cell cycle, the mutant induction for the gene is much less than the mutant induction in G_1 cells. Survival curves and mutant induction thru the cell cycle of A_L will be discussed in greater detail in Chapter 3.

Cell Phase	Induced Mutant Fraction 1.5 Gy	Induced Mutant Fraction 3 Gy
G_1	$98/10^5$ survivors $\pm$ 40	$159/10^5$ survivors $\pm$ 60
S	$14/10^5$ survivors $\pm$ 34	$92/10^5$ survivors $\pm$ 27

Table 10. Induced mutant fraction for G_1 and S phase A_L treated with ^{137}Cs gamma.

DISCUSSION

Measuring mutant induction in log phase cells has provided valuable information on the effects of different mutagens on cycling cells and the ability of these populations to repair and to survive (Moehring and Moehring, 1977; Liber and Thilly, 1982; Waldren, 1983; Breimer et al., 1986; Adair, 1987; Evans, 1994). However, no completely adequate cell picture exists for mutant induction in non-cycling cells, because the quantity and quality of the damage to cells is not directly measured in mutant assays (O'Neill and Flint, 1985; Chuang and Liber, 1996). Cells exposed to a mutagen must continue through the cell cycle and be able to form colonies to express the mutation (Thilly, 1985). The best method available to measure mutations in different components of the cell cycle is via a synchronized mammalian mutation assay. Using the A_L assay, I evaluated a way to synchronize and measure mutation in different phases of the cell cycle. This chapter focused on defining the parameters of using the A_L assay with synchronized cells. Using flow cytometry, pulse labeling, FISH, and line-scans, I was able to precisely determine the position of the cell in the cell cycle, and then irradiate the synchronized cells at different times in the cell cycle. The mutant assays at G_1 and S showed marked differences in survival and mutant induction. In addition, the A_L assay results are consistent with other researchers' data for mutant induction in different parts of the cell cycle for X-ray and gamma ray.

Cell Cycle Phase Determination

I mapped the timing of cell cycle phases in the A_L cells using flow cytometry, FISH, and line-scans. Approximately 95% of the cells collected with centrifugal

elutriation were in early G_1. The cells were plated and allowed to progress through the cell cycle; the cells reached S phase after 5.5 hours. This was demonstrated in the flow cytometry Figure 8-4 and supported using FISH in figure 10-4. The cells remained in G_1 for about 5.5 hours, providing a window of time to see how G_1 phase cells and perhaps G_0 respond to DNA damage. S phase continued from 5.5 hours through 12.5 to 13 hours, when the cells entered into G_2 and then into mitosis at between16 and 17 hours. The most likely reason for this lag time is the cold treatment of the cells to stop progression through the cell cycle. Compared to a normal CHO cell cycle of about 13 hours, the elutriated A_L cells have a plating delay of about 3 hours from the time they are plated until they begin to progress through the cell cycle. In normal CHO cells, after a period of attachment, G_1 averages 2.5 hours, S phase 7 to 8 hours, and G_2/M about 2.5 hours, so the A_L cells behave like a normal CHO cell (Sinclair and Morton, 1966; Puck et al., 1971; Jones et al., 1975). The cells that were collected by centrifugal elutriation and progressed through the cell cycle, started in a tight cohort, but by the end of the cell cycle, the cells had begun to spread apart as each went through the cell cycle at a slightly different pace. Thus, the cells maintained a tight profile through one cycle to give good results of how the cells respond to mutant induction at G_1 and S phase. It was important to map out the progression of the cell cycle as precisely as possible, so that when the cell survival, mutant induction and mutant spectra are analyzed across the entire cell cycle, I could be confident what phase the cells were in of the cell cycle. Earlier experiments looking at mutant induction in the cell cycle did not thoroughly map the progression of the cells or characterize the position of the cells in the cell cycle with flow cytometry and FISH

(Carver, 1976; Jostes et al., 1980; Tauchi et al., 1993; Chuang and Liber, 1996).

The human chromosome 11 was easily identified in all the FISH chromosome spreads because the centromere on the human chromosome was labeled with FITC. The human chromosome 11 also incorporated BrdU when the DNA replicated during S phase. There was some replication of human chromosome 11 in treatment group 2 which was pulse labeled from 5.5 to 6.5 hours (Figure 11-5). Figure 11-5 shows some replication at the end of the chromosome and at the centromere. However, the majority of the replication for human chromosome 11 occurs between hours 7.5 to 8.5. Figure 11-5 also shows that the human chromosome was replicating during 7.5 to 8.5 hours after plating. To better quantify the labeling of the chromosomes, a line-scan was used to measure the light levels of the chromosomes along their length and to give an accurate measurement of the labeling of the different fluorochromes. The line-scan data provided a unique ability to quantitatively measure labeling of the fluorochromes. This line-scan data concurred precisely with the visual data from the FISH and the flow cytometry data.

Apoptosis Measurement

During the measurement of elutriated G_1 cells for cell cycle analysis with the flow cytometer, I often measured a substantial number of cells in an integral red fluorescence peak that contained less DNA than the G_1 cells. A peak smaller than the G_1 cells would mean one of two things; either the cells had been damaged and produced fragments of cells, or the cells were apoptotic cells and were going through programmed cell death. Because the elutriation process concentrates cells by volume, the smallest cells are collected first, and any cells that have started cell suicide by cutting their DNA and

getting rid of micronuclei and other cellular material would be collected preferentially in the first elutriates. The cells I collected from 10 ml/min to 13.5 ml/min contained a population of G_1 and concentrated apoptotic cells (Figure 10-1c).

The apoptotic peak was only seen when a large population of A_L was farmed, collected, kept on ice, and then elutriated. For each elutriation, a large population of cells was farmed in fifteen 150 mm tissue culture plates. Each plate was seeded with two million cells and allowed to grow for 48 hours. At the end of 48 hours, each plate had approximately 10 million cells. Because of the large number of cells plated, they were not uniformly plated down; areas of the tissue culture plate had denser cell growth than other areas. These dense growth areas contained cells that had moved from logarithmic to stationary cell growth. CHO cells that are in stationary growth, and subjected to temperatures just above freezing, exhibit apoptosis (Soloff et al., 1987). Thus, on these large tissue culture plates, many cells are in stationary growth and apoptosis is initiated when they are exposed to ice-cold temperatures for a short period of time (Nagle et al., 1990). The apoptosis was initiated by the cold treatment to the A_L cells for a period of approximately two hours. The control populations did not have an apoptotic peak. These control cells were grown in the same conditions as the treated cells, but in smaller 100 mm tissue culture plates. This cold treatment did not initiate measurable apoptosis in small control populations of log phase cells grown on 100 mm tissue culture plates, they were collected and processed at the same time, but the cells tended to still be in log growth when collected for flow cytometry.

The apoptotic cells seen in the large centrifugal elutriation runs were not expected.

Peaks of cells with less than a 1 n amount of DNA had not been observed before in flow cytometry histograms of A_L cells. The apoptosis seen in the flow cytometry histograms is just a small portion of the approximately 1-2 X 10^8 A_L cells gathered for each elutriation. Of these cells, 5 to 6 million were collected as early G_1 based solely by size and confirmed as G_1 phase cells by propidium iodide labeling and flow cytometry. A small portion of the cells among the G_1 population were shown as having even less DNA by quantitative staining with propidium iodide. If only 1% of two billion cells are in apoptosis, as many as two million cells could be apoptotic. These apoptotic cells would have cell shrinkage that is common to apoptotic cells, and would be preferentially collected first, when a large cell population is elutriated. Figures 8-1 thru 8-5 show these apoptotic cell populations. The percent apoptotic cells was as high as 30% at the pump speed of 14 mil/min, but the percent of apoptotic cells decreased at each pump speed as shown in Table 7. In addition, Figures 9-1 and 9-2 also show an apoptotic peak, but by 4 hours in the incubator, the population in Figure 9-4 has no apoptotic cells. Centrifugal elutriation served to concentrate these apoptotic cells into a easily collected population, most are smaller than the G_1 cells and are pulled out in the first elutriate or eluted before the first elutriate was ever collected.

The cells collected specifically to check for apoptosis were collected at pump speeds from 10 to 13.5 mil/min, before the cell front reached the elutriation edge (Figure 4). In contrast, normal elutriation collections for G_1 cells were initiated when the cell front was very near the edge of the elutriation line at a pump speed of about 12 ml/min. These apoptotic cells were assayed using the annexin V protocols that showed almost

80% of the population collected was apoptotic (Figure 10-1c). The apoptotic cells in a population can be easily separated by early collection with centrifugal elutriation. If a method was used to initiate apoptosis in a large population, then centrifugal elutriation could be used to concentrate and collect apoptotic cells out of a much larger population of viable cells.

Cell Survival Curves for Log Phase, G_1 and S Phase Cells

The G_1 cells that were collected by centrifugal elutriation remained in a tight cohort through at least one cycle of the cell cycle. All cell cycle phase survival curves and mutant induction measurements were made on newly centrifugally elutriated cells that were irradiated after the appropriate time in the incubator to get to the proper position in the cell cycle. Two cell cycle positions, G_1 and S, were initially evaluated for cell survival curves and mutant induction after exposure to ^{137}Cs gamma and compared to log phase cells.

The cell survival curves were constructed for G_1 cells collected from the centrifugal elutriator at a pump speed of 13-15 ml/min and S phase cells collected at a pump speed of 22 ml/min as well as S phase cells that were plated down as G_1 cells and allowed to progress thru the cell cycle for 8 hours. The cell survival curve for the G_1 cells was significantly different (0.05) than both sets of S phase curves and the log phase curve. This has been seen in other cell assay systems where the cell killing was measured at different points in the cell cycle. The highest cell killing sensitivity has been seen in G_1 in most research looking at cell killing thru the cell cycle due to ionizing radiation (Sinclair and Morton, 1966, Jostes et al., 1980; Berki, 1980; Grdina and Sigdestad, 1992;

Tauchi et al., 1993; Cheong et al., 1994; Evens et al., 1996; Chuang and Liber, 1996, Leonhardt et al., 1997, Leonhardt et al., 2000). Several of the researchers using CHO cells found that the most sensitive time to cell killing was early G_1, followed by later G_1, and then S phase (Jostes et al., 1980; Berki, 1980; Grdina and Sigdestad, 1992). Most of the previous work only measured the cell killing at a few points in the cell cycle. In chapter 3, I take a look at cell survivability due to exposure to gamma rays across several points in the A_L cell cycle.

Mutant Induction for G_1 and S Phase Cells

Mutant Induction for the A_L cells was highest in G_1 phase for both 1.5 and 3 Gy. Mutant induction was measured at zero and eight hours after plating by using 1.5 and 3 Gy of ^{137}Cs gamma rays. These data supports conclusions of other researchers whom have looked at mutant induction thru the cell cycle with ionizing radiation. Several researchers used the HPRT assay to show that the highest mutant induction occurred in G_1; in addition Berki, O'Neill and Flint, and Grdina and Sigdestad were using CHO cells (Berki, 1980; O'Neill and Flint, 1985; Grdina and Sigdestad, 1992; Tauchi et al., 1993; Chuang and Liber, 1996, Leonhardt et al., 1997, Leonhardt et al., 2000). I had hypothesized that the mutant induction would be higher in S phase if the cells were irradiated while they were replicating. This was not supported. The A_L cells replicated the human chromosome 11 between 7.5 to 8.5 hr after plating. During S phase, the DNA is already being broken and rejoined to accommodate replication and winding and unwinding of the DNA. My results suggest that even though the human chromosome is being bombarded with radiation while it is replicating, the mutant induction rate is lower

than the mutant induction that arises is you irradiate the cells in early G_1. It does not matter if the gene is replicating when irradiated. The mutation rates in S phase will be lower because of the differences in repair and proofreading that is occurring while the DNA is replicating. Several different repair mechanisms have shown cell cycle preference with more repairs in S phase (Lavin and Kidson, 1977; Metzer and Iliakis, 1991; Leadon et al., 1996). The DNA breaks caused by gamma radiation are better repaired in S phase than in G_1 because of the innate repair that is already occurring during S phase.

This research is important to establishing and modifying radiation protection standards. In the past, the National Academy of Sciences has stated "If cell stages differ in sensitivity, weigh the data in accordance with the duration of the (sensitive) stage" (NAS, 1972). It appears that the most sensitive stage is G_1, but in cycling cells the G_1 phase may just be a small portion of the cell cycle. In non-cycling cells, the G_1/G_0 phase makes up the majority of the life span of the cells. Mutant induction estimates for ionizing radiation using cycling cells may be 2 to 5 times too low compared to non-cycling cells. On the other hand, a non-cycling cell may not express a mutation until it is induced to begin dividing again. As long as these non-cycling cells remain quiescent, mutant induction remains low, however, if the tissue is damaged and begins to proliferate, mutant induction and a higher cancer risk could be a real possibility.

The next step is to evaluate cell survival and mutant induction throughout the entire cell cycle. How does it vary with each phase in the A_L mutation assay? What are the types of DNA damage, and how can the damage be measure? Does the DNA damage

vary throughout the cell cycle? Are large deletions or small deletion more common, and do they vary thru the cell cycle? As the DNA changes its conformation, will we see differences in the mutant spectra? I will investigate these questions in Chapter 3.

References

National Academy of Sciences, Report of the Advisory Committee on the Biological Effects of Ionizing Radiation. The effects on populations of exposure to low levels of ionizing radiation. 51-71. (1972) Washington D.C., Division of Medical Sciences, National Research Council.

Applications Data. Centrifugal elutriation of living cells. An annotoated bibliography. (DS-534E). (1990) Palo Alto, CA, Beckman Instruments, Inc.

Centrifugal elutriation. (1992) Palo Alto, CA, Beckman Instruments, Inc.

Adair, G. M., Carver, J. H., & Wandres, D. L. (1980) Mutagenicity testing in mammalian cells. I. Derivation of a Chinese hamster ovary cell line heterozygous for the adenine phosphoribosyltransferase and thymidine kinase loci. Mutat.Res. 72: 187-205.

Adair, G. M. (1987) Analysis of mutation at the Chinese hamster APRT locus. In: Mammalian Cell Mutagenesis: Banbury Report No. 28 (Moore, M. M., DeMarini, D. M., de Serres, F. J., & Tindall, K. R., eds.), pp. 183-191. Cold Spring Harbor Press, Cold Spring Harbor, NY.

Aebersold, P. M. (1979) Mutation induction by 5-fluorodeoxyuridine in synchronous Chinese hamster cells. Cancer Res. 39: 808-810.

Ames, B. N. (1989) Mutagenesis and carcinogenesis: Endogenous and Exogenous factors. Environ.Molec.Mutagen. 14 (suppl 16): 66-77.

Ashby, J., Tinwell, H., Glover, P., Poorman-Allen, P., Krehl, R., Callander, R. D., & Clive, D. (1994) Potent clastogenicity of the human carcinogen etoposide to the mouse bone marrow and mouse lymphoma L5178Y cells: Comparison to *Salmonella* responses. Environ.Molec.Mutagen. 24: 51-60.

Bickmore, W. A. & Carothers, A. D. (1995) Factors affecting the timing and imprinting of replication on a mammalian chromosome. J.Cell.Sci 108 (Pt 8): 2801-2809.

Bishop, J. M. (1987) The molecular genetics of cancer. Science 235: 305-311.

Breimer, L. H., Nalbantoglu, J., & Meuth, M. (1986) Structure and sequnce of mutations induced by ionizing radiation at selectable loci in Chinese Hamster ovary cells. J.Mol.Biol. 192: 669-674.

Burki, H. J. & Aebersold, P. M. (1978) Bromodeoxyuridine-induced mutations in synchronous Chinese hamster cells: temporal induction of 6-thioguanine and ouabain resistance during DNA replication. Genetics 90: 311-321.

Burki, H. J. (1980) Ionizing radiation-induced 6-thioguanine-resistant clones in synchronous CHO cells. Radiat.Res. 81: 76-84.

Burki, H. J., Lam, C. K., & Wood, R. D. (1980) UV-light-induced mutations in synchronous CHO cells. Mutat Res 69: 347-356.

Cao, J., Wells, R. L., & Elkind, M. M. (1992) Enhanced sensitivity to neoplastic transformation by ^{137}Cs gamma rays of cells in the G_2-/M-phase age interval. Int.J.Radiat.Biol. 62: 191-199.

Cao, J., Wells, R. L., & Elkind, M. M. (1993) Neoplastic transformation of C3H mouse embryo cells, 10T1/2: cell-cycle dependence for 50 kV X-rays and UV-B light. Int.J.Radiat.Biol. 64: 83-92.

Carey, T. E., Takahashi, T., Resnick, L. A., Oettgen, H. F., & Old, L. J. (1976) Cell surface antigens of human malignant melanoma:mixed hemadsorption assays for humoral immunity to cultured autologous melanoma cells. Proc.Natl.Acad.Sci.USA 73: 3278-3282.

Carver, J. H., Dewey, W. C., & Hopwood, L. E. (1976) X-Ray-induced mutants resistant to 8-Azaguanine. II. cell cycle dose response. Mutat.Res. 34: 465-480.

Cheong, N., Wang, X., Wang, Y., & Iliakis, G. (1994) Loss of S-phase-dependent radioresistance in *irs-1* cells exposed to X-rays. Mutat.Res. 314: 77-85.

Christian, A., McNiel, E., Robinson, J., Drabek, R., LaRue, S., Waldren, C., & Bedford, J. (1998) A versatile image analysis approach for simultaneous chromosome identification and localization of FISH probes. Cytogenet.Cell Genet. 82: 172-179.

Chuang, Y. Y. & Liber, H. L. (1996) Effects of cell cycle position on ionizing radiation mutagenesis. I. Quantitative assays of two genetic loci in a human lymphoblastoid cell line. Radiat.Res. 146: 494-500.

Clermont, Y. (1963) The cycle of seminiferous epithelium in man. Am.J.Anat. 111: 111-129.

Clive, D. (1987) Historical overview of the mouse lymphoma $TK^{+/-}$ assay. In: Mammalian Cell Mutagenesis: Banbury Report 28 (Moore, M. M., DeMarini, D. M., de Serres, F. J., & Tindall, K. R., eds.), pp. 25-36. Cold Spring Harbor Laboratory, Cold Spring Harbor.

Cotton, R. G. (1993) Current methods of mutation detection. Mutat.Res. 285: 125-144.

Crespi, C. L. & Thilly, W. G. (1982) Selection of mitotic Chinese hamster ovary cells from microcarriers. Cell cycle-dependent induction of mutation by 5-bromo-2'-deoxyuridine and ethyl methanesulfonate. Mutat.Res. 106: 123-135.

Croce, C. M. & Klein, G. (1985) Chromosome translocations and human cancer. Sci.Am. 252: 54-60.

Davies, A., Wilson, A. B., Bramley, J. C., Willers, C., Van Heyningen, V., Bickmore, W. A., & Lachmann, P. J. (1995) Identification of MIC 11 antigen as a epitope of the CD59 molecule. Immunology 85: 220-227.

DeMarini, D. M., Brockman, H. E., de Serres, F. J., Evans, H. H., Stankowski, L. F. Jr., & Hsie, A. W. (1989) Specific-locus mutations induced in eukaryotes (especially mammalian cells) by radiation and chemicals: a perspective. Mutat.Res. 220: 11-29.

Dewey, W. C., Furman, S. C., & Miller, H. H. (1970) Comparison of lethality and chromosomal damage induced by X-rays in synchronized Chinese Hamster cells *in vitro*. Radiat.Res. 43: 561-581.

Enninga, I. C., Groenendijk, R. T., van Zeeland, A. A., & Simons, J. W. (1985) Differential response of human fibroblasts to the cytotoxic and mutagenic effects of UV radiation in different phases of the cell cycle. Mutat.Res. 148: 119-128.

Evans, H. H., Mencl, J., Horng, M.-F., Ricanati, M., Sanchez, C., & Hozier, J. (1986) Locus specificity in the mutability of L5178Y mouse lymphoma cells: the role of multilocus lesions. Proc.Natl.Acad.Sci.USA 83: 4379-4383.

Evans, H. H. (1994) The prevalence of multilocus lesions in radiation-induced mutants. Radiat.Res. 137: 131-144.

Evans, H. H., Mencl, J., Ricanati, M., Horng, M.-F., Chaudhry, M. A., Jiang, Q., Hozier, J., & Liechty, M. (1996) Induction of multilocus mutations at the Tk1 locus after X irridation of L5178Y cells at different times in the mitotic cycle. Radiat.Res. 146: 131-138.

Fadok, V. A., Voelker, D. R., Campbell, P. A., Cohen, J. J., Bratton, D. L., & Henson, P. M. (1992) Exposure of phosphatidylserine on the surface of apoptotic lymphocytes triggers specific recognition and removal by macrophages. J.Immunol. 148: 2207-2216.

Fox, M. H. (1994) Flow Cytometry and Cell Sorting Labratory Manual Colorado State University, Ft. Collins, CO.

Goodman, M. F. (1988) DNA replication fidelity: kinetics and thermodynamics. Mutat.Res. 200: 11-20.

Goth-Goldstein, R. & Burki, H. J. (1980) Ethylnitrosourea-induced mutagenesis in asynchronous and synchronous Chinese hamster ovary cells. Mutat.Res. 69: 127-137.

Grabske, R. J. (1978) Separating cell populations by elutriation. Fractions 1: 1-8.

Grdina, D. J. & Sigdestad, C. P. (1992) Chemical protection and cell-cycle effects on radiation-induced mutagenesis. Cell Prolif. 25: 23-29.

Griffith, O. M. and Adams, E. G. A method for obtaining synchronous cells by centrifugal elutriation. DS-594A. (1982) Palo Alto, CA, Beckman Instruments, Inc. Ref Type: Pamphlet

Gustafson, D. L., Franz, H. R., Ueno, A. M., Smith, C. J., Doolittle, D. J., & Waldren, C. A. (2000) Vanillin (3-methoxy-4-hydroxybenzaldehyde) inhibits mutation induced by hydrogen peroxide, N-methyl-N-nitrosoguanidine and mitomycin C but not ^{137}Cs gamma-radiation at the CD59 locus in human-hamster hybrid A_L cells. Mutagenesis 15: 207-213.

Hall, E. J. (1988) Radiobiology for the Radiobiologist Lippencott, Philadelphia.

Han, A. & Sinclair, W. K. (1969) Sensitivity of synchronized Chinese hamster cells to ultraviolet light. Biophysical Journal 9: 1171-1192.

Jones, C., Wuthier, P., & Puck, T. T. (1975) Genetics of somatic cell surface antigens, III. Further analysis of the A_L marker. Somat.Cell Mol.Genet. 1: 235-246.

Jostes, R., Bushnell, K., & Dewey, W. C. (1980) X-ray induction of 8-azaguanine resistant mutants in synchronized CHO cells. Radiat.Res. 83: 146-161.

Josyln, G., Carlson, M., Thliveris, A., Albertsen, H., Gelbert, L., Samowitz, W., Groden, J., Stevens, J., Spirio, L., Robertson, M., Sargeant, L., Krapcho, K., Wolff, E., Burt, R., Hughes, J. P., Warrington, J., Mcpherson, J., Wasmuth, J., Le Paslier, D., Abderrahim, H., Cohen, D., Leppert, M., & White, R. (1991) Identification of deletion mutations and three new genes at the familial polyposis locus. Cell 66: 601-613.

Kaufmann, W. K. & Wilson, S. J. (1994) G_1 arrest and cell-cycle-dependent clastogenesis in UV-irradiated human fibroblasts. Mutat.Res. 314: 67-76.

Kaufmann, W. K. (1995) Cell cycle checkpoints and DNA repair preserve the stability of the human genome. Cancer Metastasis Rev. 14: 31-41.

Kerr, J. F. R., Wyllie, A. H., & Currie, A. R. (1972) Apoptosis: A basic biological phenomenon with wide-ranging implications in tissue kinetics. Br.J.Cancer 26: 239-257.

Koopman, G., Reutelingsperger, C. P., Kuijten, G. A., Keehnen, R. M., Pals, S. T., & van Oers, M. H. (1994) Annexin V for flow cytometric detection of phosphatidylserine expression on B cells undergoing apoptosis. Blood 84: 1415-1420.

Kraemer, S. M. & Waldren, C. A. (1997) Chromosomal mutations and chromosome loss measured in a human-hamster hybrid cell line, A_LC: studies with colcemid, ultraviolet irradiation, and ^{137}Cs-gamma rays. Mutat.Res. 379: 151-166.

Kraemer, S. M., Vannais, D. B., Kronenberg, A., Ueno, A., & Waldren, C. A. (2001) Gamma-ray mutagenesis studies in a new human-hamster hybrid, A_L *CD59(+/-)*, which

has two human chromosomes 11 but is hemizygous for the *CD59* gene. Radiat.Res. 156: 10-19.

Krishnaswamy, G. & Dewey, W. C. (1993) Cell killing and chromosomal aberrations induced in Chinese hamster ovary cells by treating with cisplatin at 41.5 degrees C during the G_1 or late S phase. Cancer Res. 53: 1239-1243.

Lavin, M. F. & Kidson, C. (1977) Repair of ionizing radiation induced DNA damage in human lymphocytes. Nucleic Acids Res. 4: 4015-4022.

Leadon, S. A., Dunn, A., & Ross, C. E. (1996) A novel DNA repair response is induced in human cells exposed to ionizing radiation at the G_1/S-phase border. Radiat.Res. 146: 123-130.

Leonhardt, E. A., Trinh, M., Forrester, H. B., Johnson, R. T., & Dewey, W. C. (1997) Comparisons of the frequencies and molecular spectra of HPRT mutants when human cancer cells were X-irradiated during G_1 or S phase. Radiat.Res. 148: 548-560.

Leonhardt, E. A., Trinh, M., Forrester, H. B., & Dewey, W. C. (1998) Persistent decrease in viability as a function of X-irradiation of human bladder carcinoma cells in G_1 or S phase. Radiat.Res. 149: 343-349.

Leonhardt, E. A., Trinh, M., Chu, K., & Dewey, W. C. (2000) Mutations induced in the HPRT gene by X-irradiation during G_1 or S: analysis of base pair alterations, small deletions, and splice errors. Mutat.Res. 471: 7-19.

Liber, H. L. & Thilly, W. G. (1982) Mutation assay at the thymidine kinase locus in diploid human lymphoblasts. Mutat.Res. 94: 467-485.

Lindahl, T. (1979) DNA glycosylases, endonucleases for apurinic/apyrimidinic sites and base excision repair. Prog.Nucleic Acid Res.Mol.Biol. 22: 135-192.

Lothe, R. A., Fossa, S. D., Stenwig, A. E., Nakamura, Y., White, R., Borrensen, A. L., & Brogger, A. (1989) Loss of 3p or 11p alleles is associated with testicular cancer tumors. Genomics 4: 134-238.

Matsukura, N., Willey, J., Miyashita, M., Taffe, B., Hoffmann, D., Waldren, C., Puck, T. T., & Harris, C. C. (1991) Detection of direct mutagenicity of cigarette smoke condensate in mammalian cells. Carcinogenesis 12: 685-689.

McCormick, P. J. & Bertram, J. S. (1982) Differential cell cycle phase specificity for neoplastic transformation and mutation to ouabain resistance induced by N-methyl-N'-nitro-N-nitrosoguanidine in synchronized C3H10T1/2 C18 cells. Proc.Natl.Acad.Sci.USA 79: 4342-4346.

McGuiness, S., Shibuya, M., Ueno, A., Vannais, D., & Waldren, C. (1995) Mutant quantity and quality in mammalian cells (A_L) exposed to ^{137} gamma radiation: effect of caffeine. Radiat.Res. 142: 247-255.

Meers, P. & Mealy, T. (1993) Calcium-dependent annexin V binding to phospholipids: stoichiometry, specificity, and the role of negative charge. Biochemistry 32: 11711-11721.

Metzger, L. & Iliakis, G. (1991) Kinetics of DNA double-strand break repair throughout the cell cycle as assayed by pulsed field gel electrophoresis in CHO cells. Int.J.Radiat.Biol. 59: 1325-1339.

Miller, R. C., Geard, C. R., Geard, M. J., & Hall, E. J. (1992) Cell-cycle-dependent radiation-induced oncogenic transformation of CH3 10T1/2 cells. Radiat.Res. 130: 129-133.

Mitchell, A. R., Gosden, J. R., & Miller, D. A. (1985) A cloned sequence, p82H, of the alphoid repeated DNA family found at the centromeres of all human chromosomes. Chromosoma 92: 369-377.

Mitchell, B. F. & Tupper, J. T. (1977) Synchronization of mouse 3T3 and SV40 3T3 cells by way of centrifugal elutriation. Exp.Cell Res. 106: 351-355.

Moehring, T. J. & Moehring, J. M. (1977) Selection and characterization of cells resistant to diptheria toxin and *Pseudomonas* exotoxin A: Presumptive translational mutants. Cell 11: 447-454.

Muller, H. J. (1927) Artificial transmutation of the gene. Science 66: 84-87.

Nagle, W. A., Soloff, B. L., Moss, A. J., Jr., & Henle, K. J. (1990) Cultured Chinese hamster cells undergo apoptosis after exposure to cold but nonfreezing temperatures. Cryobiology 27: 439-451.

O'Neill, J. P. & Flint, K. B. (1985) X-Ray inducton of 6-thioguanine-resistant mutants in division arrested, G_o/G_1 phase Chinese hamster ovary cells. Mutat.Res. 150: 443-450.

Olive, P. L. & Balnath, J. P. (1993) Detection of DNA double-strand breaks through the cell cycle after exposure to X-rays, bleomycin, etoposide and ^{125}IdUrd. Int.J.Radiat.Biol. 64: 349-358.

Puck, T. T. & Marcus, P. I. (1956) Action of x-rays on mammalian cells. J.Exp.Med. 103: 653-666.

Puck, T. T., Wuthier, P., Jones, C., & Kao, F. T. (1971) Lethal antigens as genetic markers for study of human linkage groups. Proc.Natl.Acad.Sci.USA 68: 3102-3106.

Puck, T. T. & Waldren, C. A. (1987) Mutation in mammalian cells: Theory and implications. Somat.Cell Mol.Genet. 13: 405-409.

Redpath, J. L. & Sun, C. (1990) Sensitivity of a human hybrid cell line (HeLa X skin fibroblast) to radiation-induced neoplastic transformation in G_2, M, and mid-G_1 phases of the cell cycle. Radiat.Res. 121: 206-211.

Rice, G. C., Dean, P. N., Gray, J. W., & Dewey, W. C. (1984) An ultra-pure in vitro phase synchrony method employing centrifugal elutriation and viable flow cytometric cell sorting. Cytometry 5: 289-298.

Riddle, J. C. & Hsie, A. W. (1978) An effect of cell-cycle position on ultraviolet-light-induced mutagenesis in Chinese hamster ovary cells. Mutat.Res. 52: 409-420.

Ross, M. H. & Reith, E. J. (1985) Histology A Text and Atlas Harper and Row, New York.

Shibuya, M. L., Ueno, A. M., Vannais, D. B., Craven, P. A., & Waldren, C. A. (1994) Megabase Pair Deletions in Mutant Mammalian Cells following Exposure to Amsacrine, an Inhibitor of DNA Topoisomerase II. Cancer Res. 1092-1097.

Sinclair, W. K. & Morton, R. A. (1966) X-ray sensitivity during the cell generation cycle of cultured Chinese hamster cells. Radiat.Res. 29: 450-474.

Soloff, B. L., Nagle, W. A., Moss, A. J., Jr., Henle, K. J., & Crawford, J. T. (1987) Apoptosis induced by cold shock *in vitro* is dependent on cell growth phase. Biochem.Biophys.Res.Commun. 145: 876-883.

Stadler, L. J. (1928) Genetic effects of X-rays in maize. Proc.Natl.Acad.Sci.USA 14: 69-75.

Tauchi, H., Nakamura, N., & Sawada, S. (1993) Cell cycle dependence for the induction of 6-thioguanine-resistant mutations: G_2/M stage is distinctively sensitive to ^{252}Cf neutrons but not to ^{60}Co gamma rays. Int.J.Radiat.Biol. 63: 475-481.

Tauchi, H., Endo, S., Eguchi-Kasai, K., Furusawa, Y., Suzuki, M., Matsuura, S., Ando, K., Nakamura, N., Sawada, S., & Komatsu, K. (1999) Cell cycle and LET dependence for radiation-induced mutation: a possible mechanism for reversed dose-rate effect. J.Radiat.Res (Tokyo) 40 Suppl: 45-52.

Thilly, W. G. (1985) Dead cells don't form colonies: a serious source of bias in mutation assays. Environ.Molec.Mutagen. 47: 255-258.

Tong, C., Fazio, M., & Williams, G. M. (1980) Cell cycle-specific mutagenesis at the hypoxanthine phosphoribosyltransferase locus in adult rat liver epithelial cells. Proc.Natl.Acad.Sci.USA 12: 7377-7379.

Trump, B. F. & Berezesky, I. K. (1998) The reaction of cells to lethal injury: oncosis and necrosis--the role of calcium. In: When Cells Die (Lockshin, R. A., Zakeri, Z., & illy, J. L., eds.), pp. 57-96. Wiley-Liss, New York.

Turman, M., Sanderson, R. J., Waldren, C., & Lehman, J. (1979) Large numbers of highly synchronous tissue culture cells prepared by counter flow centrifugation. J.Cell Biol. 83: 116a (abs.).

Waldren, C. A., Jones, C., & Puck, T. T. (1979) Measurement of mutagenesis in mammalian cells. Proc.Natl.Acad.Sci.USA 76: 1358-1362.

Waldren, C. A. & Jones, C. (1981) Chromosome loss and damage as measured by biological markers. In: Health Risk Analysis: Proceedings of The Third Life Sciences Symposium (Richmond, C. R., Walsh, P. J., & Copenhaver, E. D., eds.), pp. 333-343. The Franklin Press, Philadelphia.

Waldren, C. A. (1983) Mutational analysis in cultured human-hamster hybrid cells. In: Chemical Mutagens: Principles and Methods for Their Detection, Vol. 8 (de Serres, F. J., ed.), pp. 235-260. Plenum Publishing Corp., New York.

Waldren, C. A., Correll, L., Sognier, M. A., & Puck, T. T. (1986) Measurement of low levels of x-ray mutagenesis in relation to human disease. Proc.Natl.Acad.Sci.USA 83: 4839-4843.

Waldren, C. A., Ueno, A., Vannais, D., Bedford, J. S., & Hei, T. (1992) Molecular analysis of chromosomal mutations induced in mammalian cells by high and low dose rate ^{137}Cs gamma rays. In: Low Dose Irradiation and Biological Defense Mechanisms (Sugihara, T., Sagan, L. A., & Aoyama, T., eds.), pp. 339-342. Elsevier Science Publishers B.V., Amsterdam.

Waldren, C. A., Vannais, D. B., Drabek, R., Gustafson, D. L., Kraemer, S. M., Lenarczyk, M., Kronenberg, A., Hei, T., & Ueno, A. (1998) Analysis of mutant quantity and quality in human-hamster hybrid human-hamster hybrid A_L and A_L-179 cells exposed to ^{137} Cs gamma rays or HZE-Fe ions. Adv.Space Res. 22: 579-585.

Waldren, C. A., Ueno, A. M., Schaeffer, B. K., Wood, S. G., Sinclair, P. R., Doolittle, D. J., Smith, C. J., Harvey, W. F., Shibuya, M. L., Gustafson, D. L., Vannais, D. B., Puck, T. T., & Sinclair, J. F. (1999) Mutant yields and mutational spectra of heterocyclic amines MeIQ and PhIP at the S1 locus of human-hamster A_L cells activated by chick embryo liver (CELC) co-cultures. Mutat.Res. 425: 29-46.

Watanabe, M. & Horikawa, M. (1977) Analyses of differential sensitivities of synchronized HeLa S3 cells to radiations and chemical carcinogens during the cell cycle. Part IV. X-rays. Mutat Res 44: 413-426.

Watanabe, M., Suzuki, N., Sawada, S., & Nikaido, O. (1984) Repair of lethal, mutagenic and transforming damage induced by X-rays in golden hamster embryo cells. Carcinogenesis 5: 1293-1299.

White, R. & Caskey, C. T. (1988) The human as an experimental system in molecular genetics. Science 240: 1483-1488.

Williamson, R. (1970) Properties of rapidly labelled deoxyribonucleic acid fragments isolated from the cytoplasm of primary cultures of embryonic mouse liver cells. J.Mol.Biol. 51: 157-168.

Wilson, A. B., Seilly, D., Willers, C., Vannais, D. B., McGraw, M., Waldren, C. A., Hei, T. K., & Davies, A. (1999) Antigen S1, encoded by the MIC1 gene, is characterized as an epitope of human CD59, enabling measurement of mutagen-induced intragenic deletions in the AL cell system. Somat.Cell Mol.Genet. 25: 147-157.

Wood, R. D. & Burki, H. J. (1982) Repair capability and the cellular age response for killing and mutation induction after UV. Mutat.Res. 95: 505-514.

Yang, J. L., Lin, J. G., Hu, M. C., & Wu, C. W. (1993) Mutagenicity and mutational spectrum of N-methyl-N'-nitro-N-nitrosoguanidine in the hprt gene in G_1-S and late S phase of diploid human fibroblasts. Cancer Res. 53: 2865-2873.

Chapter 3

MUTAGENICITY OF ^{137}Cs-γ AT THE *CD59* LOCUS IN A_L HYBRID CELLS IN DIFFERENT COMPARTMENTS OF THE CELL CYCLE

ABSTRACT

Radiation, from exposure to radon or other sources, is a major cause of DNA damage leading to mutation and cancer. Many of the mutation assays used to study radiation effects are based on immortalized mammalian cell lines. Such assays employ restricted target loci in cycling cells which can measure the incidence of certain kinds of mutations, but poorly reflect the situation *in vivo* resting (G_0) cells, or in cells in different compartments of the cell cycle. The advantage of the A_L assay is that it measures both small and chromosomal mutations, from a few base pairs to 1.6 X 10^8 base pairs of DNA. A_L cells are a human X Chinese hamster ovary hybrid containing a single human chromosome 11. On the short arm of chromosome 11 is a gene that encodes for CD59, a surface antigen. *CD59*$^-$ mutants survive an antibody/complement attack that lysis wild-type cells that express the CD59 antigen encoded by the *CD59* gene at 11p13. The human chromosome provides a large, non-lethal target. To study mutant induction in phased cells, we used centrifugal elutriation to obtain large populations of human-hamster A_L cells enriched for G_1, and then allowed them to progress in phase through the cell cycle. Populations were irradiated at specific stages with ^{137}Cs-γ and the number and kinds of mutants were determined. G_1 cells were most susceptible to killing, S phase cells were more resistant, and G_2/M cells had the highest survival. On the other hand, G_1 cells were more mutable (per surviving cell per Gy) than were S or G_2/M phase cells.

Mutant clones were analyzed by Southern blot and multiplex polymerase chain reaction (PCR) to give mutant spectra. At 3 Gy mega-base pair deletions were more frequent than were intragenic mutations in all phases of the cycle. Of the 176 mutants examined for the presence or absence of 12 chromosomal markers on human chromosome 11, 11 mutants (6%) had no discernable damage to the *CD59* gene, 18 mutants (10%) had intergenic CD59 mutations, and the remaining 147 mutants (84%) had deletions larger than 9 mega-base pair (Mbp). The mutant spectra of mutants irradiated at different specific times of the cell cycle were not significantly different from each other as discerned by χ^2 analyses

INTRODUCTION

The study of mutant spectra is important in comparing DNA damage over time and damage to different parts of the chromosome. Mutagenic effects of radiation fractions are additive and the dose response is linear (Grosovsky and Little, 1985; Kronenberg and Little, 1989). From BEIR V (1990), the average annual dose in the USA at sea level is 3.6 mSv, equivalent to 0.36 cGy of gamma radiation. Thus, someone who is 50 years old will have a cumulative dose of 18 cGy. If a person lives at higher altitude, or in an environment with granite rock, is a smoker, has medical procedures using isotopes or X-rays, or regularly flies at high altitudes they may be exposed to significantly higher levels of radiation (Hall, 1994). Current radiation standards were developed from high dose studies in laboratory animals and human radiation exposure, mainly Atomic bomb survivors of Hiroshima and Nagasaki (BEIR V, 1990). Better risk data has been derived from mutation assays developed in mammalian cells. Mammalian mutation assays have shown variation in cell susceptibility to mutant induction at different times in

the cell cycle, as well as differences in the mutant spectra for a specific gene (Burki, 1980; Leonhardt et al., 1997).

Benzer and Freese (1958) first defined the term mutant spectra as the type and location of mutations induced in a specific DNA sequence for a specific mutagen. Studying the mutant spectra caused by different mutagens sheds light on the mechanism of mutagenesis (Miller and Low, 1984; Shibuya et al., 1994; Phillips et al., 1995). Ionizing radiation is known to induce mutants (Muller, 1927). There is, however a lack of data to identify the most frequently occurring kinds of mutations produced by ionizing radiation and even less data on mutational spectra throughout the cell cycle (Okinaka et al., 1994). Studies have shown mutational "hot spots" in individual genes (Tindall et al., 1988; Kunkel, 1990; Okinaka et al., 1994). Mutational "hot spots" in entire chromosomes have been difficult to study because large mega-base pair deletions cannot be evaluated in most mutant assays. The A_L assay provides a method to measure both small intergenic mutations and large mega-base pair deletions (Waldren, 1983; Waldren et al., 1992; Shibuya et al., 1994; McGuinness et al., 1995; Waldren et al., 1999; Wilson et al., 1999). We adapted the A_L CD59$^-$ assay to measure mutant induction of cells in different phases of the cell cycle and analyze their mutant spectra.

Large chromosomal deletions and rearrangements have been implicated as much as smaller types of mutations in the cancer process (Croce and Klein, 1985; Bishop, 1987). In addition, large mutations caused by ionizing radiation have been implicated in tumor formation by causing specific chromosomal aberrations (Yunis, 1983; Sandberg et al., 1988; Rowley, 1990). However, large mutations have been very difficult to study by

standard mutation assays, and very few studies have looked at large mutations and their spectra at different points in the cell cycle. Much is known about how ionizing radiation induces mutants in cultured mammalian cells, but there are still questions about how radiation effects cells in different compartments of the cell cycle (BEIR V, 1990). Prior studies have looked at mutant spectra in CHO and human *HPRT*⁻ mutants using Southern or PCR analysis to measure the presence or absence of 9 exons (Morgan et al., 1990; Nelson et al., 1994; Bao et al., 1995; Suzuki and Hei, 1996; Schwartz et al., 2000). The HPRT⁻ assay is effective in looking at large mutations up to and larger than the *HPRT* gene (up to 1 Mbp). However, deletions beyond the flanking region of the *HPRT* gene tend to be lethal because vital genes are lost. Morgan et al. (1990) found that X-irradiated CHO cells have a non-random distribution of mutations that suggests certain areas of the DNA are more sensitive than others to X-ray induced mutants. Human TK6 cells irradiated with X-rays and assayed for *HPRT*⁻ tend to have more deletions than spontaneous mutants, which have mainly small mutations (Nelson et al., 1994). X-rays and gamma rays have a tendency to cause more and larger deletions when measured with the HPRT⁻ assay than spontaneous deletions in cells. Furthermore, higher doses of radiation cause a larger number of clones with complete *HPRT* gene loss than smaller doses (Bao et al., 1995; Suzuki and Hei, 1996; Schwartz et al., 2000). The HPRT assay has provided information on intragenic mutant spectra and in some cases mutant spectra beyond the *HPRT* gene, but the study of very large deletions is limited with the HPRT assay.

To study mutagenic effects to cells in different components of the cell cycle, I

used centrifugal elutriation to obtain populations of cells in specific regions of the cell cycle to produce nearly pure populations of phased cells. The cells were irradiated with ^{137}Cs gamma and assayed for mutant induction using the A_L assay. The A_L assay was described in Chapter 1. Briefly, the power of the A_L *in vitro* assay system is that it detects both small and large mutations with great sensitivity. It is at least 100-fold more sensitive per cGy to the mutagenic activity of ionizing radiation than such standard assays as the Chinese hamster ovary (CHO) hypoxanthine guanine phosphoribosyl transferase (HPRT) assay, and >1000-times more sensitive than the bacterial Ames test (Ames, 1971). This sensitivity makes it possible to quantify the activity of small, non-lethal doses of a mutagen down to the very low levels of exposure that most human populations are exposed. The A_L assay has been used to detect damage by ionizing radiations such as ^{137}Cs gamma rays, X-rays, HZE Fe nuclei, α-particles (as found in the decay of radon), neutrons, protons, N nuclei; non-ionizing radiations (254 nm and 308 nm UV light); direct alkylating agents (MMS, EMS); and indirect mutagens like benzo[a]pyrene metabolites (Waldren et al., 1999). The A_L assay was the first to demonstrate that asbestos was in fact a mutagen (Hei et al., 1992) that the chemotherapeutic agent Amsacrine was highly mutagenic (Shibuya et al., 1994), but that obstetrical ultrasound was not mutagenic (Ritenour et al., 1991).

The A_L hybrid cell line contains a normal set of CHO chromosomes plus a single copy of human chromosome 11. Its production by hybridization and its properties and use in mutation assays has been described (Waldren, 1983; Waldren et al., 1986; Puck and Waldren, 1987; Matsukura et al., 1991; Shibuya et al., 1994). Human chromosome 11

encodes a series of human cell surface antigens that provide excellent markers for mutant induction. We have mainly used the antigen CD59 for mutation studies. It has previously been reported that the CD59 antigen and the *CD59* gene is the same as the S1 antigen (Wilson et al., 1999). Wild type A_L cells espressing the CD59 antigen are quantitatively killed when exposed to a monoclonal anti-CD59 antibody and particular rabbit serum complement. Mutations involving the *CD59* gene of any kind (intragenic or multilocus) cause loss of expression of the CD59 antigen. These mutant cells live to form colonies. Thus, a mutation is measured by counting mutant colonies as a function of dose of mutagen. Mutant clones can be selected and their genotype investigated by using southern or PCR analysis with the dozens of mapped probes available for human chromosome 11 (Shibuya et al., 1994). The development of chromosome 11 maps and markers of specific genes enables the study of the mutagenic effect of numerous classes of mutagens across the entire length of human chromosome 11. Figure 1 shows a human chromosome 11 map that consists of approximately 160 mega-base pairs and delineates the gene markers used in this research to determine if chromosomal damage, rearrangement, or deletions have occurred.

As shown in Chapter 2, A_L cells are most sensitive to radiation killing in G_1 and less so in S phase. CHO cells may be as much as 10-times more resistant to killing in S than in G_1, M, and G_2 (Sinclair, 1969). The reasons for this change in sensitivity is not known, but the DNA is in different configurations in each of these phases, and the DNA repair capabilities and mechanisms vary greatly during the different phases of the cell cycle (Chuang and Liber, 1996; Yu et al., 1999; Wood et al., 2001). Mutant induction

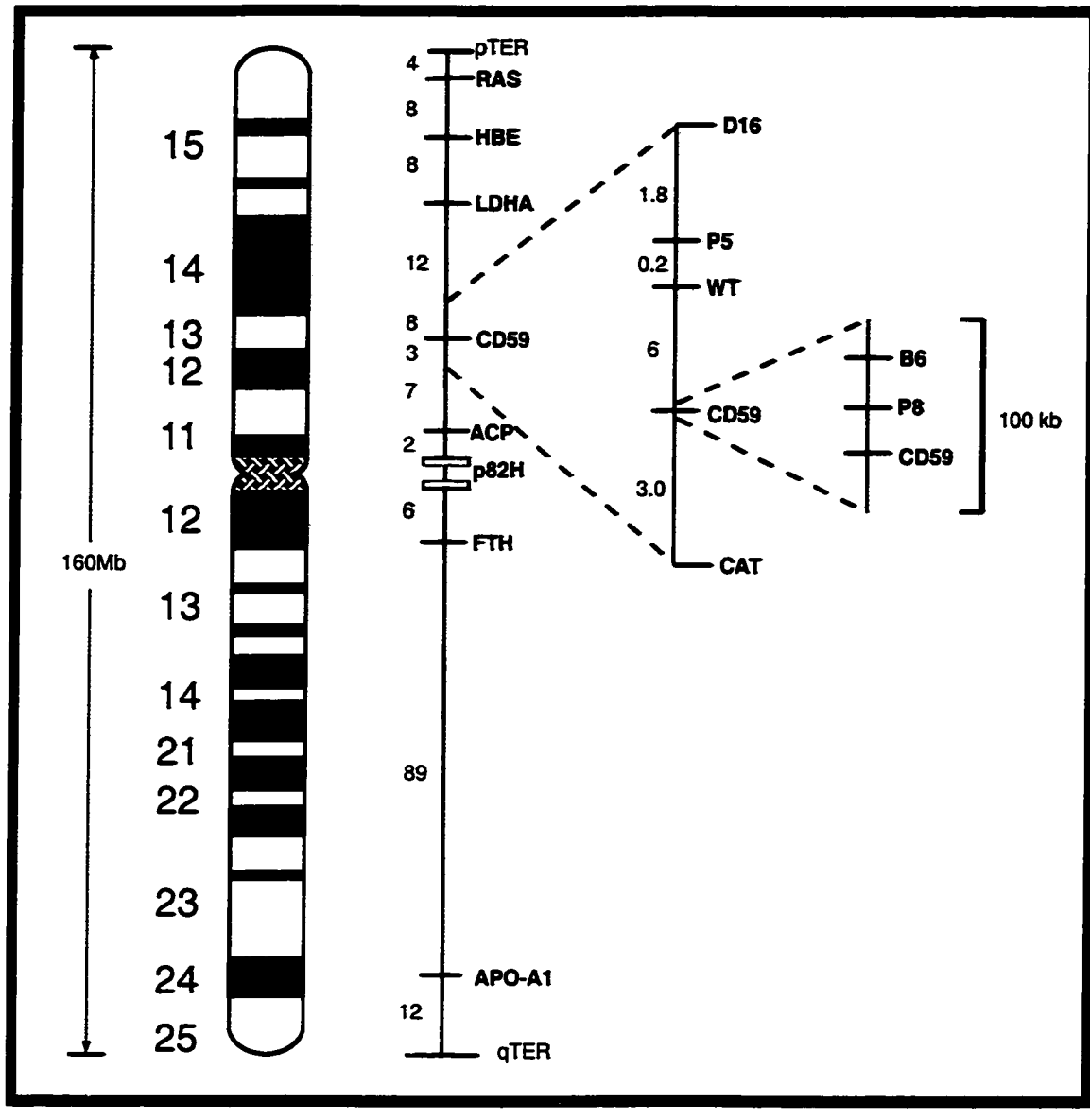

Figure 1. Diagram of human chromosome 11. CD59 is located at 11p13.5. The vital hostage locus is located near RAS. The length of human chromosome 11 is 160 Mb. The other markers are shown in relation to CD59. D16, P5, P8, WT (Wilms' tumor), B6, and CAT (catalase) are all located at 11p13. LDHA (lactate dehydrogenase-A) is at 11p14-p15; HBE (hemoglobin) is located at 11p15, while RAS (H-*ras*) is at 11p15.5. ACP (acid phosphatase-2) is located at 11p11. P82H is an alphoid repeat found at the centromeres of all human chromosomes. FTH (ferretin) is found at 11q13 with APO-A1 (apolipoprotein A1) found at 11q24 (Mitchell et al., 1985; Hei et al., 1992; Shibuya et al., 1994; McGuinness et al., 1995; Waldren et al., 1999). Note: this chromosome 11 has not rearranged during its time in the A_L hybrid and was in fact chosen as the reference human chromosome 11 for the human genome project (Shows et al., 1996). The A_L human chromosome 11 also repairs ionizing induced damage as effectively as chromosome 11 in normal human cells (Fouladi et al., 2000).

also varies throughout the cell cycle. Mutant induction is greater in G_1 than in S. What is not known are the mutation spectra generated by gamma rays in each of these phases? Does the size of the deletion change depending on where the cell is in the cell cycle, or do we find simple or complicated deletions? It is the aim of this chapter to characterize that damage and the corresponding mutant spectra for each phase of the cell cycle.

MATERIALS AND METHODS

Experimental Design

A_L cells were grown to large numbers, 1-2 X 10^8 for centrifugal elutriation (Figure 2), and the early G_1 cells were collected for survival curve and mutation induction measured at different points in the cell cycle. Early G_1 cells were plated on tissue culture plates and allowed to progress through the cells cycle until they were irradiated. After irradiation, the plated for the survival curves were kept in the incubator for eight days and were then fixed and counted. The cells used for mutant induction measurement were maintained in log phase growth for ten days until challenged with anti-CD59 antibody described in Chapter 2. After 10 days, individual clones (4 to 5 per tissue culture plate) were collected from the mutation assays and maintained in log phase growth until there were enough cells to isolate a large quantity of DNA; the plates were fixed, stained and counted. The DNA from the cultured clones was then analyzed using PCR and southern blotting to determine the mutant spectra of the individual clones.

Cell Culture Techniques

The variant of A_L cells used in this study were the AM2, derived from A_L AND-6 cells with human O-6 methylguanine-methyl transferase in a hygromycin construct

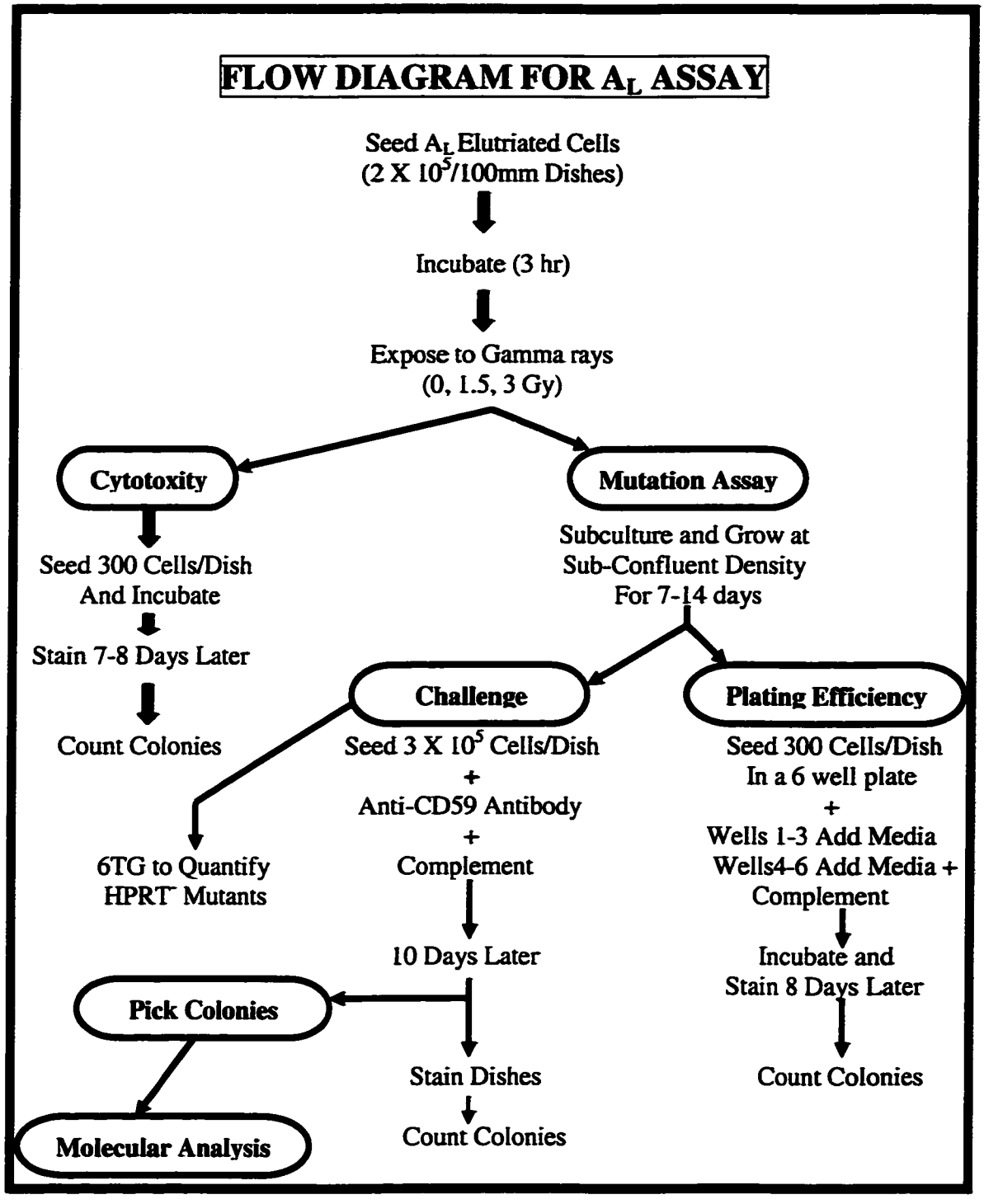

Figure 2. Flow diagram for the A_L assay.

lipofected into the cells (Gustafson et al., 1997). Cells were grown as described in Chapter 2. Briefly, asynchronously growing Chinese hamster ovary/human A_L cells were maintained in exponential growth in mono-layer with Ham's F-12 (Ham, 1965) medium (Atlanta Biologicals, Norcross, GA) supplemented with 0.001 M L-glutamine (Sigma, St. Louis, MO), 50 u/ml penicillin and 50 mcg/ml streptomycin (Gemini Bio-Products, Calabasas, CA), 0.02 M HEPES at pH 7.4 (Amersham Life Science, Cleveland, OH), 4% fetal bovine serum (v/v) (Gemini Bio-Products, Calabasas, CA), and 3% Newborn bovine calf serum (v/v) (Summit, Fort Collins, CO). Cells were grown in tissue culture plates in a humidified atmosphere of 5% CO_2/95% air. To obtain the large number of cells needed for elutriation, 8 to 10 150 mm tissue culture plates were plated with 2 X 10^6 cells in 20 ml of media and incubated until they were nearly confluent. The cells were then sub-cultured and transferred to 12 to 15 150 mm culture plates with 7 X 10^6 cells plated in 20 ml of media each, and incubated for 16-24 hours. These plates reached confluence with a large proportion of newly divided cells. Newly divided cells were seen in the microscope as rounded-up cells in a nearly confluent layer. The cells were harvested with trypsin and all media and rinses were saved, giving a total yield of between 1 X 10^8 and 2 X 10^8 cells. To prepare for injection into the elutriator, the cells were centrifuged at 400 X g and re-suspended in 3-5 ml of ice-cold complete F-12 media. The cells were kept on ice through the centrifugal elutriation process to prevent their progressing through the cell cycle.

Centrifugal Elutriation

Centrifugal Elutriation was described in Chapter 2. Briefly, cells were collected by trypsinization and separated into G_1 populations by centrifugal elutriation on a

Beckman JM-5 elutriator rotor mounted in a J2-21 centrifuge. To insure a sterile transit for the cells through the tubing and elutriator, 150 ml of 95% ice-cold ethanol was run through the apparatus, followed by 150 ml of sterile ice cold water, then the ice-cold cell loading buffer (non-supplemented F12). MasterFlex tubing 6485-16 (PharMed) was used, which is suitable for using with cell culture when sterilized by autoclaving. The 3-5 ml of harvested cells were slowly injected into the apparatus over a period of 1-2 minutes. The cells were injected into the Beckman JE-6B rotor set at a speed of 2000 RPM, at 4°C for a two hour elutriation, with an initial pump speed of 7 ml/min set on the MasterFlex L/S reversible drive pump. Once the cells entered the elutriation chamber, after approximately 2 minutes, they reached equilibrium and a cell demarcation line was established at about 0.5-1 cm from the edge of the elutriation chamber (Chapter 1, Figure 4). The vast majority of the cells were behind the line arranged in a gradient with the smallest cells (the newly divided G_1 cell) at the front of the line, followed by progressively larger cells to the outside aspect of the elutriation chamber. The buffer flow rate was gradually increased to a pump speed of 12 ml per minute. Gradually increasing pump speed moved the cell demarcation line closer to the where the cells were eluted and collected. The G_1 cells eluted in the collected fraction at a pump speed of 12.5 -13.5 ml per minute. The early G_1 cells were collected in 3-4 fractions by incrementally increasing the pump speed by 1 ml/min. Collected cells were plated and irradiated at the appropriate times. The collected G_1 fraction was maintained on ice until the fraction could be centrifuged and counted. Cells were then plated in duplicate on 100 mm plates for irradiation. Portions of the cells were fixed in 70% ethanol for flow cytometer

analysis to confirm the compartment of the cell cycle (Data as shown in Chapter 2).

Irradiation for Survival Curves

Cell survival was determined at different phases of the cell cycle by irradiating the cells with gamma rays at 0, 2, 4, 6, 8, 10, 12, 13, 14, 15, 16, 17, and 18 hours post plating. At each treatment time, three 60 mm plates with 600 cells each were irradiated with 1.5 Gy, 3 plates with 1000 cells each were irradiated with 3 Gy, and 3 plates with 3000 cells each were irradiated with 6 Gy to determine survival throughout the cell cycle. The cells were irradiated with ^{137}Cs gamma rays from a Shepard and Associates Mark I Model 68A cavity gamma irradiator containing 6000 Ci of ^{137}Cs (Glendale, CA) at a dose rate of approximately 0.85 Gy/min. The tissue culture plates were mounted on a rotating platform during irradiation to ensure uniformity of the dose. Dosimetry was done by T. C. Patel using a Victoreen Condenser R-meter and Harshaw TLD lithium fluoride chips. Once the cells were irradiated, they were incubated and left undisturbed for eight days to develop into colonies. The plates were fixed with a fixative containing 3% acetic acid and 8 % ethanol and were stained with crystal violet. The colonies were counted manually. Survival curves were constructed by plotting surviving fraction (number of colonies/cells plated) vs. the dose.

Irradiation for Mutant Induction

Cells were irradiated as described at 0, 2, 4, 6, 8, 10, 12, 13, 14, 15, 16, 17, and 18 hours after plating to induce mutants. Zero hour G_1 cells were plated on 100 mm tissue culture plates and irradiated immediately. To irradiate the other cells as they progressed thru the cell cycle, the cells were plated, put into the incubator, and allowed to progress

through the cell cycle for the appropriate time. The control un-irradiated log-phase cells were plated in duplicate at a density of 2 X 10^5 cells per plate. Cells receiving 1.5 Gy of dose were plated with a density of 4 X 10^5 cells per plate, while cells receiving 3 Gy were plated at a density of 6 X 10^5 cells per plate. The cells were irradiated with ^{137}Cs gamma rays from a Mark I gamma irradiator (Glendale, CA) at a dose rate of approximately 0.85 Gy/minute. After irradiation, the cells were placed in a 37^{0}C incubator with 5% CO_2 and maintained in log phase growth for 10 days to allow expression of mutations, recovery from growth lag due to treatment, and to allow the *CD59*$^-$ mutants to clear their cell surface of the CD59 antigen.

Mutation Assay and Determination of *CD59*$^-$ Mutant Yields

After 10 days. *CD59*$^-$ mutants were selected by a complement mediated cytotoxicity assay as described in Chapter 2 (Figure 2). For each irradiated treatment and control group, 2 X 10^5 cells were plated in triplicate onto 100 mm tissue culture plates. The cells were allowed to attach in 7 ml/plate of challenge media; Ultra Culture (Bio Whittaker, Walkersville, MD), 2 % Fetal Calf Serum (v/v), P/S, and 0.001 M L-Glutamine and were incubated at 37^{0}C for 3 hours to recover from trypsinization and attach to the surface of the tissue culture plate. For each irradiation treatment and control, a 6-well plate, with 35 mm wells was seeded with 300 cells to determine cloning efficiency. After 3, hours a mixture of 2.0% rabbit serum complement from Dutchland Laboratory (Denver, PA) [with 0.05 human serum added to the rabbit serum volume to prevent complement-only killing of cells] and 0.2% lethal E7.1 monoclonal antibodies against the CD59 antigen in challenge media were added to the treatment and control

plates. The challenge media, complement, and human serum were added to one-half of the plating efficiency plates. The other three wells in each 6-well plate were inoculated with the challenge media and 300 cells as a control to monitor for complement killing. The 6-well plates were returned to the incubator for 8 days and were then fixed with 3% acetic acid and 8% ethanol in water, stained with crystal violet, and counted. The treatment/mutation assay plates were returned to the incubator for 10 days to allow for colony development. Mutation assay plates were taken out and surviving colonies were selected for sub-cloning by using cloning cylinders and trypsin removal of single clones, the rest of the cells were then fixed, stained, and counted to determine mutant induction.

Mutation Assay and Determination of *HPRT* Mutant Yields

The HPRT mutation assay was accomplished to look at the induction of mutants throughout the cell cycle at the *HPRT* loci and compare/contrast the results to the A_L assay. The same cells that were used for the A_L *CD59*$^-$ mutation assay; those that had been maintained in log-phase growth for at least ten days after treatment were used for the HPRT mutation assay. The HPRT assay was done by plating 2 X 10^5 cells on five 100 mm tissue culture plates for each control and irradiation treatment group. The cells were plated in 10 ml of supplemented F12 media containing 40 μM 6 thioguanine as described (Hei et al., 1988; Hei et al., 1992). The plates were returned to the incubator at 37^0C/5% $C0_2$ in air to form colonies. After 12, days the colonies were fixed with standard fixative, stained with crystal violet, and counted. A plating efficiency series of 3 plates for each treatment and control was also seeded with 300 cells per plate and the cells were allowed to grow into colonies for eight days and were then fixed, stained, and counted.

Mutant Selection

Four to five clones were picked randomly from each $A_L CD59^-$ tissue culture plate and sub-cloned into 35 mm tissue culture plates. When these plates were confluent after about seven days they contained approximately 2 X 10^5 cells/plate. These plates were farmed into 60 mm plates until they reached confluence (6 X 10^5 cells) at which time the 60 mm plates were sub-cultured into four 60 mm plates and allowed to become confluent. For each clone, three plates were harvested for their DNA and used in PCR and Southern analysis and the forth plate of cells were collected and frozen in 50% media and 50% cryoprotective Medium (Bio Whittaker, Walkersville, MD) and kept at -70^{0}C in case they were needed in the future. DNA harvest was done using a genomic DNA miniprep described by Miller et al. (1988).

Mutant Spectra Determination

Mutation deletion maps for human chromosome 11 were generated using PCR and Southern blots. The PCR primers used were for specific introns of the human gene so as not to amplify the homologous hamster DNA. Gene markers that were screened for by PCR, some by multiplex include: LDHA, lactate dehydrogenase; H-RAS, a proto-oncogene; WT (Wilms' Tumor), a tumor suppressor gene; CAT (catalase); and APO-A1 located at 11q23. The second method used to determine marker presence or absence was by Southern blotting. These markers include: HBE, (hemoglobin), D16, P5, P8, ACP (acid phosphatase), p82H (a centromeric probe), and FHT, (ferritin heavy chain) (Shibuya, et al. 1994).

Polymerase Chain Reaction Analysis of *CD59*⁻ Mutants

PCR was carried out as described (Hei et al., 1992; Shibuya et al., 1994; McGuiness et al., 1995; Zuh et al., 1996; Hei et al., 1997). Oligonucleotide primers used for PCR detection of markers includes the genes and exons listed in Table 1 and the primer sequences listed in Table 2.

Gene	Abbreviation	Product Size (bp)	Reference
RAS	RAS	110	Capon et al., 1983
APOA-1	APOA1	192	Karathanasis et al., 1983
Wilms' Tumor	WT9	220	Pelletier et al., 1991
LDHA	LDHA	523	Smith et al., 1993
CAT	CAT	563	Quan et al., 1986
CD59 exon 1	CD59X1	87	Wilson et al., 1999
CD59 exon 2	CD59X2	205	Wilson et al., 1999
CD59 exon 3	CD59X3	300	Wilson et al., 1999
CD59 exon 4	CD59X4	401	Wilson et al., 1999

Table 1. Human gene PCR primer names and amplicon size on chromosome 11 used to detect the presence or absence of the gene in A_L.

PCR for APO-A and RAS were done in a multiplex 20 µl volume, as described by Innis et al. (1990), using an ice-cold master mix of 1.25 mM deoxynucleotide triphosphate mixture (0.2 mM, final concentration), 10 µM of each primer (1 µM, final concentration), distilled water, 10X Stoffel fragment buffer (10 mM KCl-10mM Tris-HCl, final concentration), 25 mM $MgCl_2$ (1.5 mM, final concentration), 0.1% gelatin

(0.01% final concentration), 10 mM β mercapto-ethanol (1.0 mm final concentration), and 0.3 µl of 10 units/µl AmpliTaq DNA Polymerase (Stoffel fragment; Perkin Elmer Cetus, Norwalk, CT). One µl of sample and/or control DNA (0.2 µg each) were pipetted into the thermocycler reaction tubes containing 19 µl of the master mix using aerosol-resistance tips. The reaction mix was overlaid with sterile mineral oil, and the tubes were thermocycled in a Hybrid Limited OmniGene TR3 (National Labnet Co., Woodbridge, NJ) with the following profile, Program 1: 94^0C, 5-min time delay cycle; 31-step cycles consisting of 94^0C for 45 seconds, 45 seconds at 55^0C, and 45 seconds at 72^0C, after 31 cycles the tubes were held at 72^0C for 20 minutes. Once finished, the samples were stored at 4^0C, 10µl of sample were then loaded on a 2% agarose gel made with 1X Tris-acetate/EDTA electrophoresis buffer, 1.5% NuSeive GTG Agarose and 0.5% Seakem LE Agarose (FMC BioProducts, Rockland, ME) and run on an horizontal gel electrophoresis apparatus (Bio-Rad Laboratories, Richmond, CA) at 60 V for 4 hours, then stained with ethidium bromide, and examined using UV light transillumination.

PCR conditions for the multiplex of WT9 and CAT markers were similar. An ice-cold master mix containing 1.25 mM deoxynucleotide triphosphate mixture (0.2 mM, final concentration), 10 µM of each primer (1 µM, final concentration), distilled water, Qiagen 10X buffer (Qiagen INC., Santa Clarita, CA), Qiagen 25 mM $MgCl_2$ (2.5 mM, final concentration), Qiagen 5X Q solution (0.5X, final concentration), and 5u/µl of Qiagen Taq DNA polymerase (0.5u/µl, final concentration). Nineteen µl of the ice-cold master mix was added to each tube and one µl of the sample and control DNA (0.2 µg each) were pipetted and overlaid with mineral oil as described above. The tubes were

thermocycled with the following profile, Program 2: 94^{0}C, 5-min time delay cycle; 27-step cycles consisting of 94^{0}C for 45 seconds, 45 seconds at 57^{0}C, and 45 seconds at 72^{0}C, after 27 cycles the tubes were held at 72^{0}C for 20 minutes. PCR Conditions for the LDHA were similar to protocols for WT9 and CAT, except a higher concentration of Qiagen 5X Q solution (1X, final concentration), and 5u/μl of Qiagen Taq DNA Polymerase (1u/μl, final concentration) were used. The thermocycler was set for Program 2 as described above.

PCR Analysis of Intragenic Mutations in *CD59*

The analysis of cells lacking only *CD59* on human chromosome 11 was done using multiplex PCR. Four *CD59* PCRs, one for each exon was done in one PCR reaction tube for each clone that was *CD59*$^-$only. The PCR reaction was done in a 20 μl volume. The ice-cold master mix contained 1.25 mM deoxynucleotide triphosphate mixture (0.2 mM, final concentration), 4 mM of each primer (0.1 mM, final concentration), distilled water, Invitrogen 5X buffer M (Carlsbad, CA; containing 300 mM Tris-HCl, 75 mM $(NH_4)_2SO_4$, 1.5 mM $MgCl_2$, at pH 10), Qiagen (Valencia, CA) 5X Q solution (1X final concentration), and 5u/μl Biolase DNA Polymerase (Intermountain Scientific, Bountiful, UT; 0.5u/μl, final concentration). The master mix was pipetted into thermocycle tubes, 0.2 μg of sample or control DNA was added, 20 μl of light mineral oil was overlaid, and the samples were run on thermocycle program 2. PCR product was run on a 5% MetaPhor Agarose gel (FMC BioProducts, Rockland, ME) at 20V for 8 hr, stained with ethidium bromide, and examined using UV light transillumination.

Gene	5'							3'
RAS-F	ATG	ACG	GAA	TAT	AAG	GTG	GTG	
RAS-R	TCT	ATA	GTG	GGG	TCG	TAT	TCG	
APOA1-F	CCT	AAA	GCT	CCT	TGA	CAA	CT	
APOA1-R	TTC	TTC	TGG	AAG	TCG	TCC	AG	
WT9-F	GGA	ATT	GAA	TTT	CAT	TCC	ACA	ATA
WT9-R	GGA	ATT	CCT	CAC	TGT	GCC	CAC	ATTG
LDHA-F	TAG	TGT	TCC	TTG	CAT	TTT	GGG	
LDHA-R	ATC	CCA	GGA	TGT	GAC	TCA	CTG	
CAT-F	AAA	CAG	AAT	GCG	ATT	CAC	ACC	
CAT-R	ATT	AAG	CCA	TGA	CGG	TGC	TC	
CD59X1-F	CTG	GAG	CGA	AAG	AAT	GCG		
CD59X1-R	TTC	GGG	CCT	TCT	TAC	CTG		
CD59X2-F	TTG	AGA	CAA	CCA	GCA	GTC		
CD59X2-R	TAA	GAA	GGG	AGT	TCA	TGG		
CD59X3-F	GGA	AGT	ATA	CCA	CAA	GTT	GC	
CD59X3-R	GCC	TAA	TGA	GGA	TTA	CAG	TG	
CD59X4-F	ACA	AGT	GTA	TAA	CAA	GTG	TTG	G
CD59X4-R	TCC	CTG	CAA	ACA	GGA	CTG		

Table 2. PCR primer sequences used for gene detection in A_L cells.

Southern Analysis of *CD59*⁻ Mutants

Southern blot analysis was performed by standard method according to the method of Maniatis et al. (1982) with modifications by our lab (Shibuya et al., 1994; Waldren et al., 1999). Genomic DNA was extracted from *CD59*⁻ clones by the genomic DNA miniprep described previously. The DNA was digested with EcoRI (Biolabs,

Beverly, MA) for 5 hr at 37^0 in a buffer specified by the supplier. The DNA fragments were separated by electrophoresis in a 0.75% agarose gel in a horizontal gel electrophoresis apparatus (Bio-Rad Laboratories, Richmond CA) for 16 hours at 20V in Tris-acetate/EDTA electrophoresis buffer. The DNA samples were then transferred for 4+ hours to charged Hybond N+ Nucleic Acid Transfer Membranes (Amersham Life Science, Cleveland, OH) by alkaline Southern blotting using a BIOS blotting apparatus (New Haven, CT). The nylon filters were washed in 5X saturated saline phosphate EDTA (SSPE) [an aqueous solution of 3.6% (w/w) NaCl, 0.5% (w/w) $NaH_2PO_4{\cdot}H_2O$, and 0.1% (w/w) EDTA], and stored at 4^0C until ready to hybridize. The nylon filters were loaded into hybridization tubes with 5X (SSC) saturated saline citrate [an aqueous solution of 3.6% (w/w) NaCl and 0.5% (w/w) sodium citrate], 5% Denhardt's solution, 2.5% SDS, and 20 μg/ml denatured salmon sperm DNA with a total volume of 9 ml per tube. The filters were allowed to pre-hybridize for 1-4 hours at 65^0C in a hybridization incubator (Robbins Scientific, Sunnyvale, CA). DNA probes were random prime labeled using a kit from Boehringer Mannheim (Mannheim, Germany) with [^{32}P]dCTP to greater than 10^8 cpm/μg and added at a final concentration of 10^6 cpm/ml in the hybridization tubes containing the filters. Sources of DNA probes were as described (Shibuya et al., 1994; McGuinness et al., 1995). After 16 hours of hybridization at 65^0C, the filters were washed twice in 2 X SSPE plus 0.1% SDS for 10 minutes and then washed again at 65^0C for 15 minutes in 1 X SSPE plus 0.1% SDS and dried. The nylon filters were exposed with intensifying screens to high performance autoradiography film (Hyperfilm-MP; Amersham, Cleveland, OH) at -70^0C for 24 to 72 hours as needed for exposure, and

developed in a Kodak M35A X-OMAT Processor (Eastman Kodak, High Plains, NY). The presence or absence of bands was judged visually. The bands for human and CHO alleles were discerned in comparative Southern analysis between A_L and CHO genomic DNA controls. The DNA deletion in each clone was determined by the presence or absence of the PCR and Southern marker as describe above and shown in Figure 1.

Statistical Analysis

All of the data for the survival curves and for the mutant induction for the cell cycle were calculated as means and the standard error of the mean. Differences in mutant spectra for $CD59^-$ between the treated groups in different phases of the cell cycle and control groups were analyzed by χ^2 analyses. A P-value of 0.05 or less between groups was considered to be significant.

RESULTS

Survival Curves for A_L Cells Irradiated at Different Times in the Cell Cycle

The surviving fraction of A_L cells exposed to 1.5, 3, and 6 Gy ^{137}Cs gamma throughout the cell cycle in four-hour intervals is shown in Figure 3. The survival data fit well to a second order log-linear curve. The LD_{50} is the lethal doses where 50% of the cells die. The D_{37} is the dose where 37% of the cells survive. The cells irradiated in early G_1 are the most sensitive to cell killing followed by late G_1, S and then G_2/M phase. Figure 4 shows the surviving fraction for cells at different points in the cell cycle exposed to 1.5 and 3 Gy ^{137}Cs gamma every two hours after the early G_1 cells were plated. These data, compiled from five experiments, show that G_1 cells had a lower survival rate in an equivalent dose as those cells in S, G_2, and G_2/M phase. The LD_{50} and the D_{37} for the

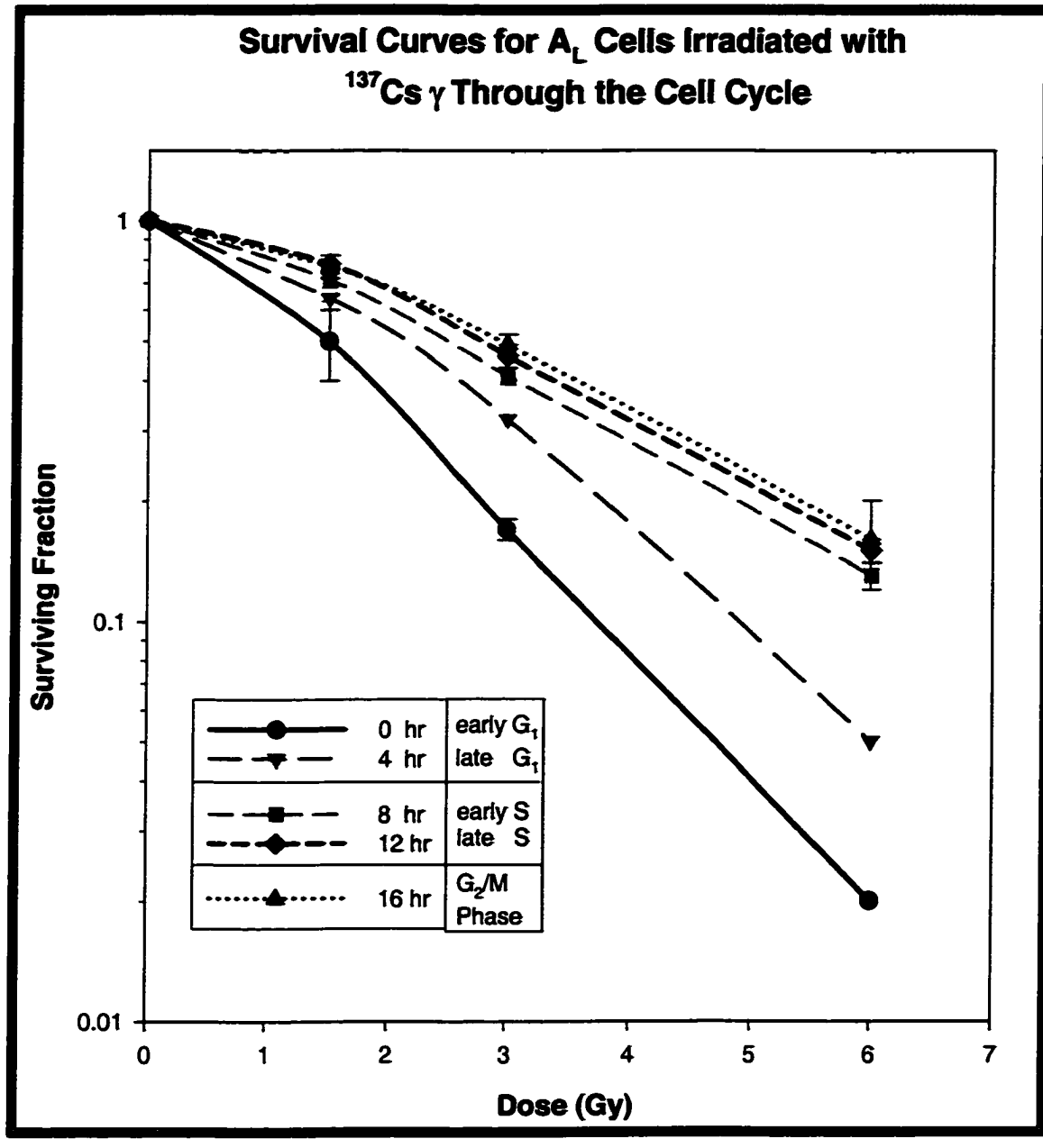

Figure 3. Survival curves for A_L cells exposed to ^{137}Cs gamma rays at different stages of the cell cycle. Early G_1 cells were centrifugally elutriated and cells were plated onto tissue culture plates. Populations of cells were irradiated at 4 hour intervals. The LD_{50} for the curves from 0 to 16 hr were 1.5, 2.1, 2.5, 2.8, and 2.9 Gy. The D_{37} for the curves were 2, 2.7, 3.33, 3.66, and 3.8 Gy. Cells in early G_1 are most sensitive, S phase cells are more resistant and G_2/M have approximately the same survival as the late S phase cells.

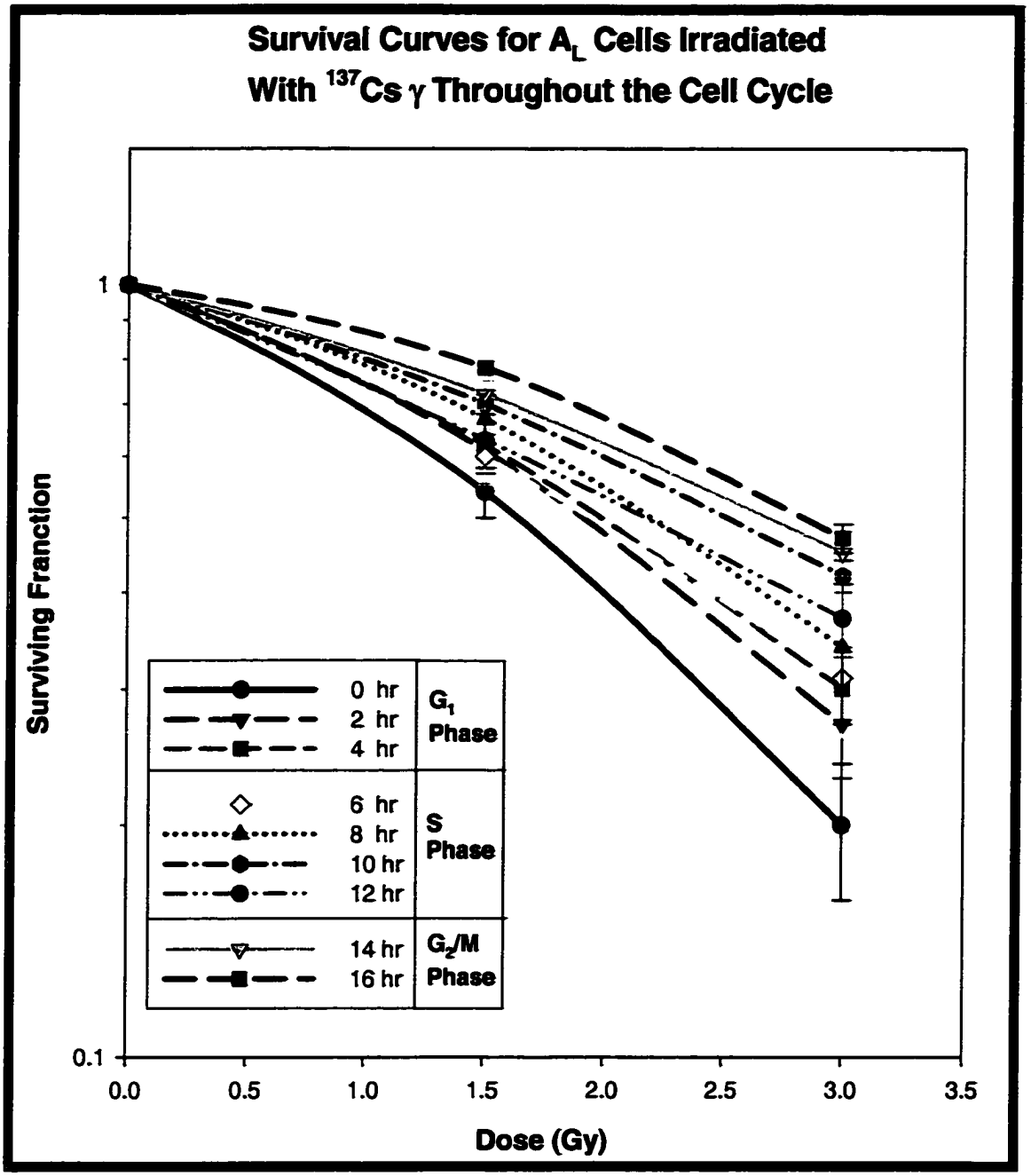

Figure 4. Survival curves for populations of A_L cells irradiated at specific times through the cell cycle with ^{137}Cs gamma rays. These curves were combined from the data of five experiments. The early G_1 cells are the most sensitive. S phase cells are more resistant than G_1, and G_2/M cells have more resistance than S phase cells. The LD_{50} and D_0 for these curves are in Table 3. These survival curves were done with the same cells from the $CD59^-$ mutant induction curves in Figure 6 and 7.

curves in Figure 4 are shown in tabular format in Table 3 below. Figure 5 shows the data from the curves in Figure 4 plotted as surviving fraction vs. time of irradiation at 1.5 and 3 Gy. In this format it is easier to see the relationship of the change in surviving fraction vs. time. The survival curves throughout the cell cycle maintain the same 2nd order log linear shape.

Time of Irradiation after G_1 cells were plated (hr)	Cell cycle phase	LD_{50} (Gy)	D_{37} (Gy)	Mutant Fraction/LD_{50}
0	early G_1	1.6	2.0	129
2	mid G_1	1.9	2.4	141
4	late G_1	2.0	2.6	87
6	early S	2.0	2.6	65
8	mid S	2.2	2.8	63
10	Mid S	2.5	3.3	45
12	late S	2.2	3.0	39
14	G_2	2.7	3.5	32
16	G_2/M	2.8	3.5	42

Table 3. LD_{50} and D_0 for the survival curves for A_L cells in Figure 4. Lethal dose for 50% of the population (LD_{50}) is the dose where 50% of the population will survive. D_{37} is defined as the dose where 37% of the population survives.

Induction of *CD59*⁻ Mutants at Different Parts of the Cell Cycle

Mutant induction for A_L *CD59*⁻ was measured at different points in the cell cycle from 0 to 16 hours after plating of early G_1cells. Figure 6 shows the mutants induced with 3 Gy of ^{137}Cs γ-rays compared to the LD_{50} at each time of irradiation. The LD_{50} was lowest for the G_1 cells and increased as the cells moved through the cell cycle until nearing the S/G_2 border where the LD_{50} dropped and then increased again at 13 hours. To normalize the mutants for the cell differences in surviving fractions at the irradiation time, the mutants/10^5 were divided by the dose to give the mutant yield in mutants/Gy.

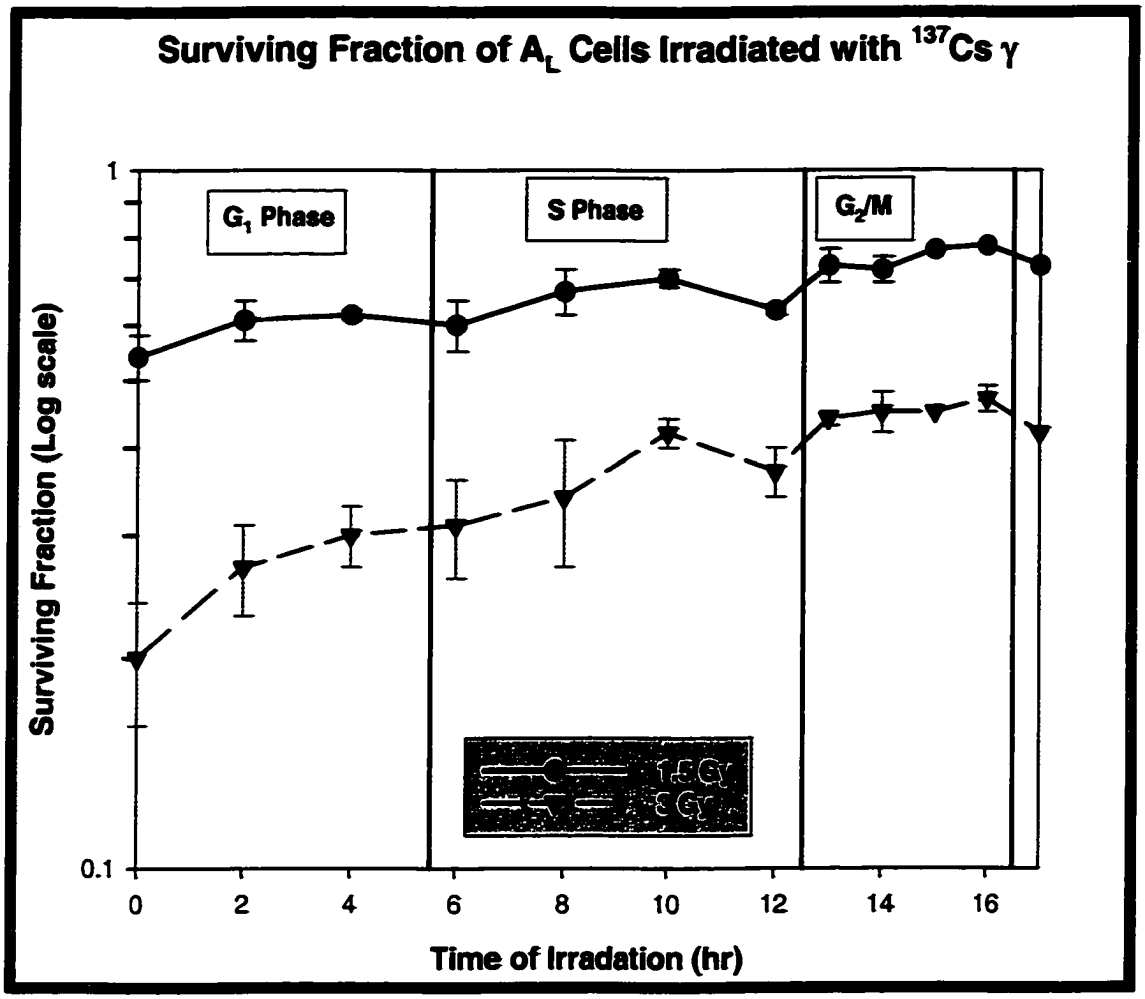

Figure 5. Surviving fraction of A_L cells irradiated with 1.5 and 3 Gy ^{137}Cs gamma rays. Early G_1 cells were centrifugally elutriated, plated, allowed to progress through the cell cycle, and were irradiated at the appropriate time. The difference in the surviving fraction for 1.5 and 3 Gy is greatest in G_1 at 0 and 2 hr with a difference of 0.34, which is a D_0 of 4.4 Gy. The smallest difference is for cells irradiated at 12 hr, with a difference of 0.26, which is a D_0 of 5.8 Gy. These data shows that the mean lethal dose is lower in G_1 than in S phase. The surviving fraction may change through the cell cycle but the shapes of the survival curves remain the same. Data is combined from five experiments.

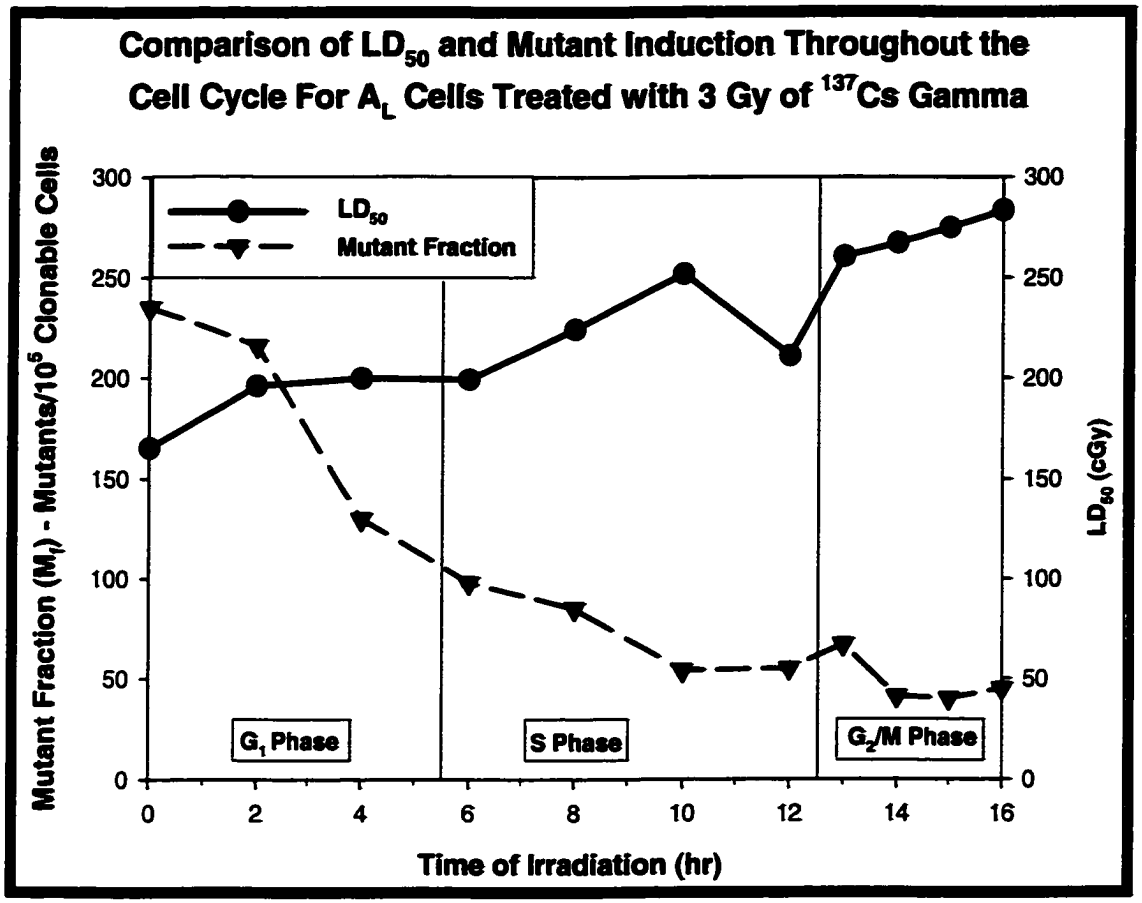

Figure 6. LD_{50} and *CD59*$^-$ mutant induction through the cell cycle for AL cells treated with 3 Gy of 137Cs gamma rays. Through the cell cycle the LD_{50} tends to increase from G_1 phase cells through to the G_2/M phase cells. Conversely, the *CD59*$^-$ mutants induced in the cell cycle are the highest in G_1 and decrease as the cell progress through the cell cycle.

The mutant yield was then multiplied by the LD_{50} at each irradiation point to determine the mutant fraction per LD_{50} as shown in Figure 7. The mutants induced per LD_{50} were greatest at the 2 hour irradiation point in G_1 and decreased through the cell cycle until late S phase, 10 hours after plating. The induced mutant fractions increase at the S/G_2 border, which coincided with the decrease in the LD_{50}. The numbers of mutants induced decrease in G_2 and G_2/M and then begin to rise again as the cell begin to move into G_1. The induced mutants during the replication of *CD59* remained consistent with the other S phase times of irradiation. No increase in mutants was seen when the *CD59* gene was irradiated in S phase (eight hr time of irradiation).

Induction of HPRT Mutants at Different Parts of the Cell Cycle

The cells that were prepared for the A_L *CD59*$^-$ were also used for the *HPRT* assay. The induction of *HPRT* mutants in various stages of the cell cycle was about 100 fold less than were the levels of *CD59*$^-$ mutant induction. This has been shown previously for CD59$^-$ and HPRT (Burki, 1980; Waldren, 1983; Shibuya et al., 1994). Figure 8 shows the HPRT mutant induction at different points in the cell cycle. The highest mutant induction was in early G_1 and decreases through G_1, then increases at the G_1/S border. The mutant induction drops again in S phase and remains low until the S/G_2 border where it rises and then drops again in G_2.

Mutation Spectra of *CD59*$^-$ clones

Multiplex PCR and Southern analysis was used to determine the size and types of mutations caused by ^{137}Cs gamma on the human chromosome 11. The marker genes used are shown in Figure 1. The PCR primers and conditions were chosen to amplify the

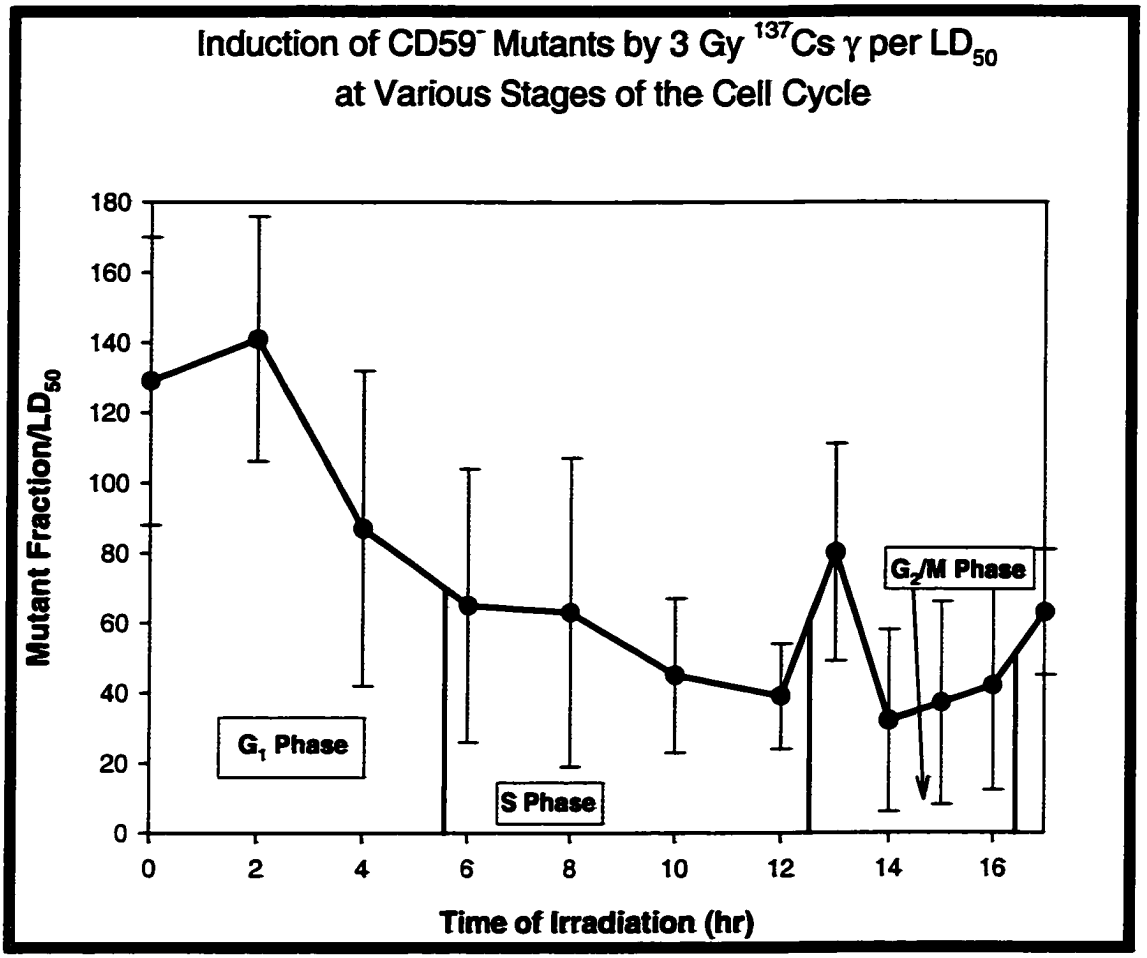

Figure 7. CD59⁻ mutant fraction per LD_{50}. The mutant induction data from Figure 6 mutants/10^5 clonable cells was used to determine the mutant yield at each time of irradiation to give mutants/Gy. Mutant yield was then multiplied by the LD_{50} to determine the mutant fraction per LD_{50} value on the y-axis. The x-axis is the time of irradiation measured from plating early G_1 cells. This data takes into account the variation in cell killing at each point measured in the cell cycle. The highest mutant induction was in early G_1 at the 2 hr point. Mutant fraction per LD_{50} decreased until late S where it rose steeply and then fell. The rise in mutant fraction per LD_{50} seen at the 17 hr point is caused when the cells move into G_1 again. During the replication time of the CD59gene, there is no spike in the mutant fraction /LD_{50}.

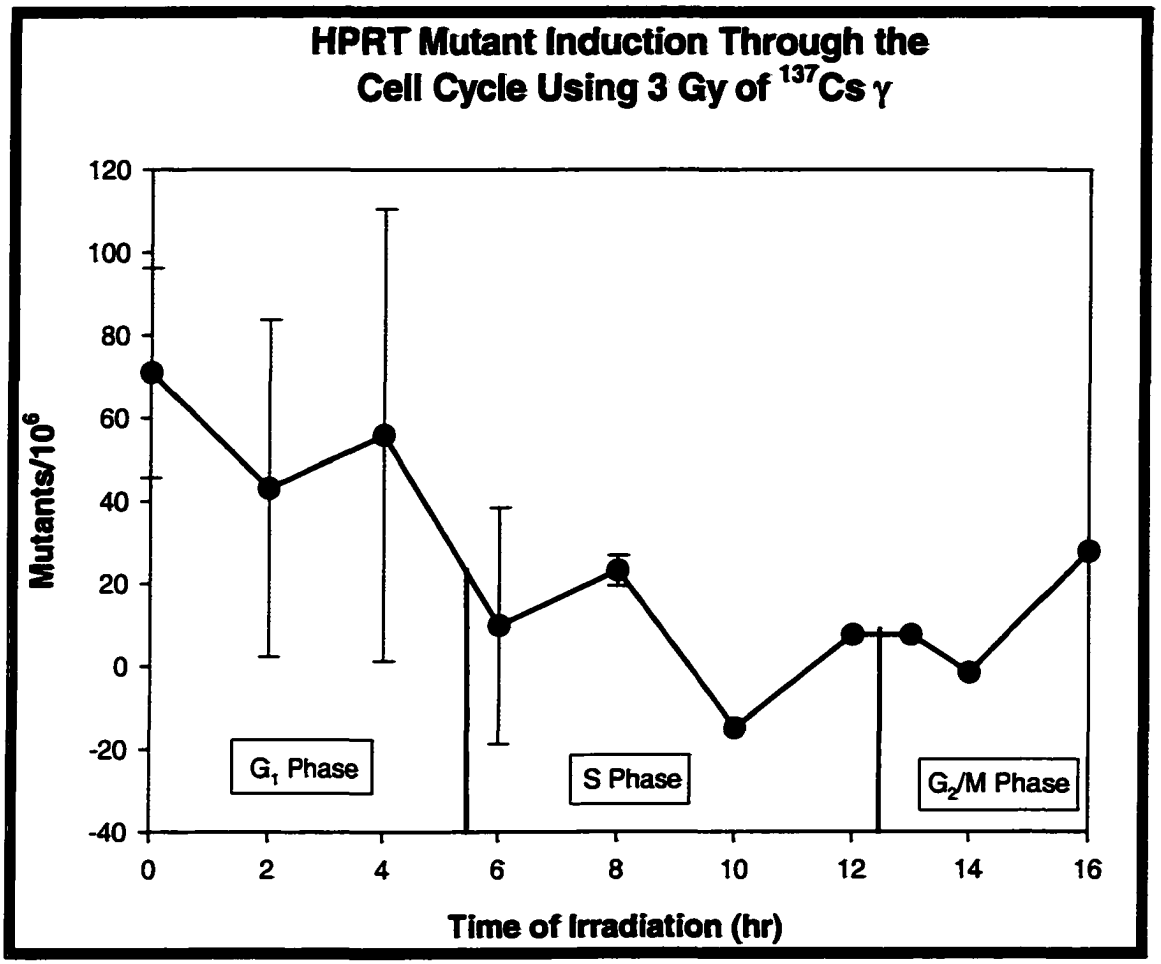

Figure 8. Mutant induction throughout the A_L cell cycle measured with the HPRT assay. A_L cells were centrifugally elutriated, plated, and then irradiated as in Figure 7 for the A_L assay. The x-axis is the time of irradiation from plating the early G_1 cells. The y-axis is mutants/10^6 selected by growing A_L cells in 6-thioguanine to select $HPRT^-$ mutants. Mutant induction is highest in early G_1 and drops at the 2 hr point. Mutant induction increases in late G_1. During S phase the mutant induction is lower than G_1 phase. There is a slight increase in mutation at 12 to 13 hr after plating as seen also with the $CD59^-$ mutant assay, Figure 7. Mutant induction remains low in G_2 and then increases at the G_2/M border. This data is the combination of three experiments.

human gene and not the CHO genes. Table 4 shows the mutational spectra of $CD59^-$ exposed to ^{137}Cs gamma throughout the cell cycle. The mutants were defined into 43 classes each successively with one less gene marker distal from CD59. Only a few of the classes predominated in the mutant spectra, classes 1 ($CD59^-$ only, up to a 9 Mb pair deletion), 11, 12, 19, 21, 24, 26, and complicated. The size of these deletions for each class is given in column 2 on Table 4. Two points on the chromosome show significantly more breaks than any other loci. These "hot spots" involve several of the mutant classes. Mutant classes 10, 11, 12, 24, and 38 have a break between D16 and LDAH, these classes include 74/161 (46%) mutants. Another "hot spot" for breaks in chromosome 11 is found in mutant classes 4, 5, 7, 11, 19, and 21 between CAT and ACP with 62/161 or 38.5% of the mutant clones. Approximately 10% of the total of phased cell mutants are "complicated" mutations that involve loss of non-antigous markers, the rest of the mutations are simple continuous deletions. The mutant clones in each class irradiated at different points in the cell cycle (columns 15 –24) were not significantly different from each other; therefore, the mutants were pooled by cell cycle phase for analysis.

Table 5 shows the mutant induction in cell cycle phases and compares the total from the phased cells with non-irradiated control (spontaneous) mutants and log phase cells irradiated with 3 Gy ^{137}Cs gamma. The control cell mutants (column 21) and the total of phase mutants (column 19) were significantly different for 11 mutant classes; however, the high dose rate (HDR) gamma log phase cells (column 22) were significantly different at only 3 mutant classes. There are significantly more mutants in the HDR gamma for mutant classes 9, 12, and 20 than the same classes for the total phased cells.

Table 4. Spectra of *CD59*$^-$ mutants from populations of A_L cells exposed to ^{137}Cs gamma at different points of the cell cycle. The absence or presence of marker genes along human chromosome 11 in each mutant was determined by multiplex PCR or Southern analysis. The assignment and definition of the 43 mutation classes are in the first two columns. Class number in the first column, size of the mutation in mega-base pairs (Mbp) is in the second column. Columns 3-14 list the gene markers that were screened for in the assay. Gene markers present define a given class of mutants, the gray shaded plus under a marker means it was present and the white shaded minus that the marker was absent from the mutant. The 43rd class of mutants is called "complicated". These mutants show variable presence and absence of the chromosome 11 markers. Blank boxes in columns 15 through 24 mean no clones for that mutant class at that time. The green columns 15-17 are the number of mutant clones that had a particular class of mutation in G_1 phase, blue columns 18-21 are S phase, orange columns 22-23 are G_2 phase, and the red column 24 is G_2/M. Column 25 is the total of columns 15-24. Column 26 is the total for log phase cells used as non-irradiated control cells. The mutant classes in the total column that were found significantly different via χ^2, $p < 0.05$ were classes 1, 11, 12, 19, 21, 24, 26, and complicated (highlighted in purple). None of the clones in each class thru the cell cycle, columns 15-24, were found to be significantly different from each other. Twenty-four mutants (14.9%) were class 1 CD59$^-$ only; therefore, this class includes intergenic mutants and mutants up to 9 Mbp. All other mutants (137/161) irradiated with ^{137}Cs gamma had Mbp mutations.

Chromosome 11 Markers														Number of CD59⁻ Clones in Each Mutant Class at Various Times in the Cell Cycle						
1	2	3	4	5	6	7	8	9	10	11	12	13	14	15	16	17	22	23	25	26
Class #	Size (Mb)	RAS	HBE	LDHA	D16	P5	WT	CD-59	CAT	ACP	p82H	FTH	APO	0hr	2hr	10hr	13 hr	14 hr	Total	Log phase
1	9	+	+	+	+	+	+	-	+	+	+	+	+	1	1	2	1	4		5
2	9.2	+	+	+	+	+	-	-	+	+	+	+	+							
3	11	+	+	+	+	-	-	-	+	+	+	+	+							
4	16	+	+	+	+	+	+	-	-	+	+	+	+	1	1				2	
5	16	+	+	+	+	+	-	-	-	+	+	+	+	1					2	
6	18	+	+	+	+	+	+	-	-	-	+	+	+			1			2	
7	18	+	+	+	+	-	-	-	-	+	+	+	+			2			3	
8	18	+	+	+	+	+	-	-	-	-	+	+	+							
9	20	+	+	+	+	-	-	-	-	-	+	+	+							
10	23	+	+	+	-	-	-	-	+	+	+	+	+						2	1
11	24	+	+	+	-	-	-	-	-	+	+	+	+	1	1	2	2	1		2
12	24	+	+	+	-	-	-	-	-	-	+	+	+	2	2	2	2	2		
13	26	+	+	-	-	-	-	-	+	+	+	+	+	1				1	4	
14	30	+	-	-	-	-	-	-	+	+	+	+	+							
15	31	-	-	-	-	-	-	-	+	+	+	+	+							
16	32	+	+	+	+	+	+	-	-	-	-	+	+					1	1	
17	38	+	+	+	+	+	-	-	-	-	-	+	+	1					1	
18	38	+	+	+	+	-	-	-	-	-	-	+	+							1
19	39	+	+	-	-	-	-	-	-	+	+	+	+	1	1	2	2	2		
20	40	+	+	-	-	-	-	-	-	-	+	+	+	1	1	1			2	
21	43	+	-	-	-	-	-	-	-	+	+	+	+		2		1	3		
22	46	-	-	-	-	-	-	-	-	+	+	+	+							
23	46	+	-	-	-	-	-	-	-	-	+	+	+			1		1	2	
24	48	+	+	+	-	-	-	-	-	-	-	+	+		1	2		1		2
25	50	-	-	-	-	-	-	-	-	-	+	+	+							
26	52	+	+	-	-	-	-	-	-	-	-	+	+	2	1	1				1
27	54	+	-	-	-	-	-	-	-	-	-	+	+	1	1	1			3	
28	58	-	-	-	-	-	-	-	-	-	-	+	+							
29	113	+	+	+	+	+	+	-	-	-	-	-	+							
30	113	+	+	+	+	+	-	-	-	-	-	-	+	1	1	1				
31	115	+	+	+	+	-	-	-	-	-	-	-	+							
32	125	+	+	+	-	-	-	-	-	-	-	-	+							
33	125	+	+	+	+	+	+	-	-	-	-	-	-							
34	127	+	+	+	+	+	-	-	-	-	-	-	-							
35	127	+	+	+	+	-	-	-	-	-	-	-	-		2				2	
36	135	+	+	-	-	-	-	-	-	-	-	-	+			1			1	
37	139	+	-	-	-	-	-	-	-	-	-	-	+		1	2			2	
38	143	+	+	+	-	-	-	-	-	-	-	-	-						3	
39	147	-	-	-	-	-	-	-	-	-	-	-	+							
40	148	+	+	-	-	-	-	-	-	-	-	-	-					1	2	
41	155	+	-	-	-	-	-	-	-	-	-	-	-							
42	160	-	-	-	-	-	-	-	-	-	-	-	-							
43		Complicated												2	1	2	0	2		4
													Total =	19	21	16	8	19	161	16

Table 5. Spectra of CD59$^-$ mutants from populations of A_L cells exposed to 3 Gy of ^{137}Cs gamma in different cell cycle phases. The first 14 columns are as in Table 4. Markers present and absent define a given class of mutants, the gray shaded (+) means a marker was present, (-) that it was absent. The green column number 15, are the pooled G_1 phase clones irradiated from 0-4 hr after the early G_1 cells were plated, the blue column, number 16 are the pooled S phase clones irradiated from 6 to 12 hr, the orange column, number 17 are pooled G_2 phase clones irradiated 13-14 hr, and the purple column number 18 is for G_2/M cells irradiated at 16 hr. The yellow column number 19 is the total of columns 15-18. Column 20 is the total for log phase cells. Column 21 is pooled historical data for log phase cells from several experiments in the Waldren lab. Column 22 is pooled historical data for cells exposed to high dose rate gamma (0.85 Gy/min). Eleven classes of the historic control cells shown in purple in column 21; classes 1, 4, 9, 10, 11, 12, 19, 21, 24, 26, and complex were significantly different than the same mutant classes in total phased cells (yellow column 19). The classes shown in pale blue in column 22 (γ HDR 3 Gy); classes 9, 12, and 20 were significantly different than the same mutant classes in the total phase cells (yellow column 19). The un-irradiated log phased control cells in column 20 show no difference in the frequency of mutants for the historical control cells (column 21).

Chromosome 11 Markers															*CD59*⁻ Clones in Each Class							
															γ HDR 3 (Gy)							
1	2	3	4	5	6	7	8	9	10	11	12	13	14		15	16	17	18	19	20	21	22
Class #	Size (Mb)	RAS	HBE	LDHA	D16	P5	WT	CD-59	CAT	ACP	p82H	FTH	APO		G1/Prom		G2 Phase		Total Phased Cells	Log Phase Control	Control	γ HDR 3 Gy
1	9							-									5		24	5		12
2	9.2						-	-													3	
3	11					-	-	-													3	2
4	16							-	-										2			2
5	16						-	-	-										2		1	2
6	18							-	-	-									2		1	3
7	18					-	-	-	-										3		1	3
8	18						-	-	-	-											2	
9	20					-	-	-	-	-												
10	23				-	-	-	-											2	1		2
11	24				-	-	-	-	-								3		26	2		9
12	24				-	-	-	-	-	-							4		14			
13	26			-	-	-	-	-									1		4		2	1
14	30		-	-	-	-	-	-														
15	31	-	-	-	-	-	-	-														
16	32							-	-	-	-						1		1			1
17	38						-	-	-	-	-	-							1		2	
18	38					-	-	-	-	-	-									1	1	1
19	39			-	-	-	-	-	-								4		21			3
20	40			-	-	-	-	-	-	-									2			
21	43		-	-	-	-	-	-	-								4		8			
22	46	-	-	-	-	-	-	-	-													
23	46		-	-	-	-	-	-	-	-							1		2		1	
24	48				-	-	-	-	-	-	-						1		9	2		
25	50	-	-	-	-	-	-	-	-	-												
26	52			-	-	-	-	-	-	-	-								9	1		
27	54		-	-	-	-	-	-	-	-	-								3			
28	58	-	-	-	-	-	-	-	-	-	-											
29	113							-	-	-	-	-										
30	113						-	-	-	-	-	-										
31	115					-	-	-	-	-	-	-										
32	125				-	-	-	-	-	-	-	-									2	
33	125							-	-	-	-	-	-								1	
34	127						-	-	-	-	-	-	-									
35	127					-	-	-	-	-	-	-	-						2		3	
36	135			-	-	-	-	-	-	-	-	-							1		1	
37	139		-	-	-	-	-	-	-	-	-	-							2			
38	143				-	-	-	-	-	-	-	-	-						3		2	5
39	147	-	-	-	-	-	-	-	-	-	-	-										
40	148			-	-	-	-	-	-	-	-	-	-				1		2			
41	155		-	-	-	-	-	-	-	-	-	-	-									
42	160	-	-	-	-	-	-	-	-	-	-	-	-									
43	n/a	Complicated															2		16	4		2
		Total =													50		27		161	16	153	73

The log phase control cells (column 20) from the study were not significantly different than the historic control mutants in column 21. There are no significant differences using χ^2 analysis in mutant induction within specific mutant classes at different points in the cell cycle when the time phased mutants were combined into their cell compartments (columns 15 to 18, Table 5).

Analysis of Intragenic Mutations in the human *CD59* gene of A_L Cells

CD59$^-$ mutants that retained all of the outside markers were analyzed by multiplex PCR of the four exons of *CD59*. A total of 161 mutant clones that were irradiated at various points in the cell cycle were selected for gene marker analysis, 24/161 of these clones were missing CD59 only. Five out of 16 clones from the log phase control population of cells selected were *CD59*$^-$ only. The multiplex PCR for the 5 log phase clones and the 24 cell cycle clones is shown in Figure 9. All of the log phase clones; lanes 5-9 are missing one or more exons of CD59, but they all have at least one exon. Thus, these spontaneous mutant clones are all intergenic mutants. None of the 19 clones picked for the 0 hr early G^1 cells were CD59$^-$ only. Each of the other times of irradiation had one or more clones that were CD59$^-$ only. Thirteen of the 24 cell cycle clones that were CD59$^-$ only were missing one or more exons for *CD59* (Figure 10). Five of these 13 cell cycle clones were missing all of CD59; lanes 10, 14, 16, 29, and 33 have no exons that were amplified via PCR. These five mutant clones could have deletions up to 9 Mbp, the size of a deletion between WT and CAT. Eleven of 24 mutant clones had all exons that amplified with PCR, lanes 12, 15, 17-18, 30-32, and 34-37. Thus, out of a total of 176 clones selected, 11 (6%) had all markers and also had all exons for CD59.

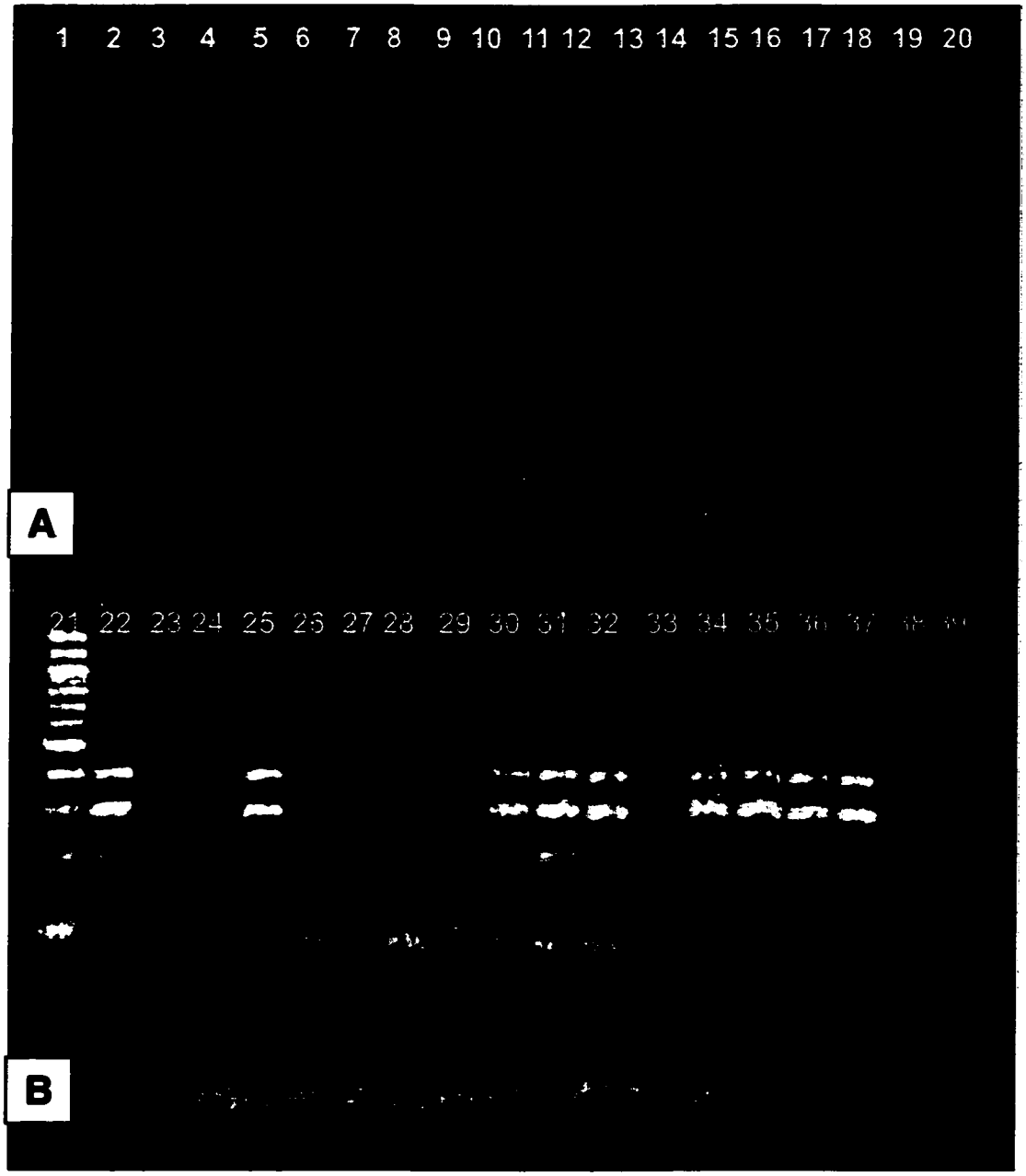

Figure 9, A and B. Multiplex PCR analysis of CD59$^-$ mutant clones missing no other markers, in A_L cells irradiated with 3 Gy ^{137}Cs gamma. A 100 bp molecular weight ladder was run in lanes 1 and 21. A_L DNA was extracted and run in lanes 2 and 22 showing CD59 exons 1-4 (87 bp, 205 bp, 300 bp, and 401 bp respectively). CHO cell DNA was run in lane 3 and 23, and a negative control (no template) in lane 4 and 24. Lanes 5-9 were log phase control cells. Lanes 10-20 and 25-37 were irradiated A_L cells selected with the E7.1 antibodies using the AL assay; lanes 10-14 were irradiated at 2 hr, 15-16 at 4 hr, 17-19 at 6hr, 20, 25-27 at 8 hr, 28-29 at 10 hr, 30 at 12 hr, 31 at 13 hr, 32-35 at 14 hr, and 36-37 at 16 hr.

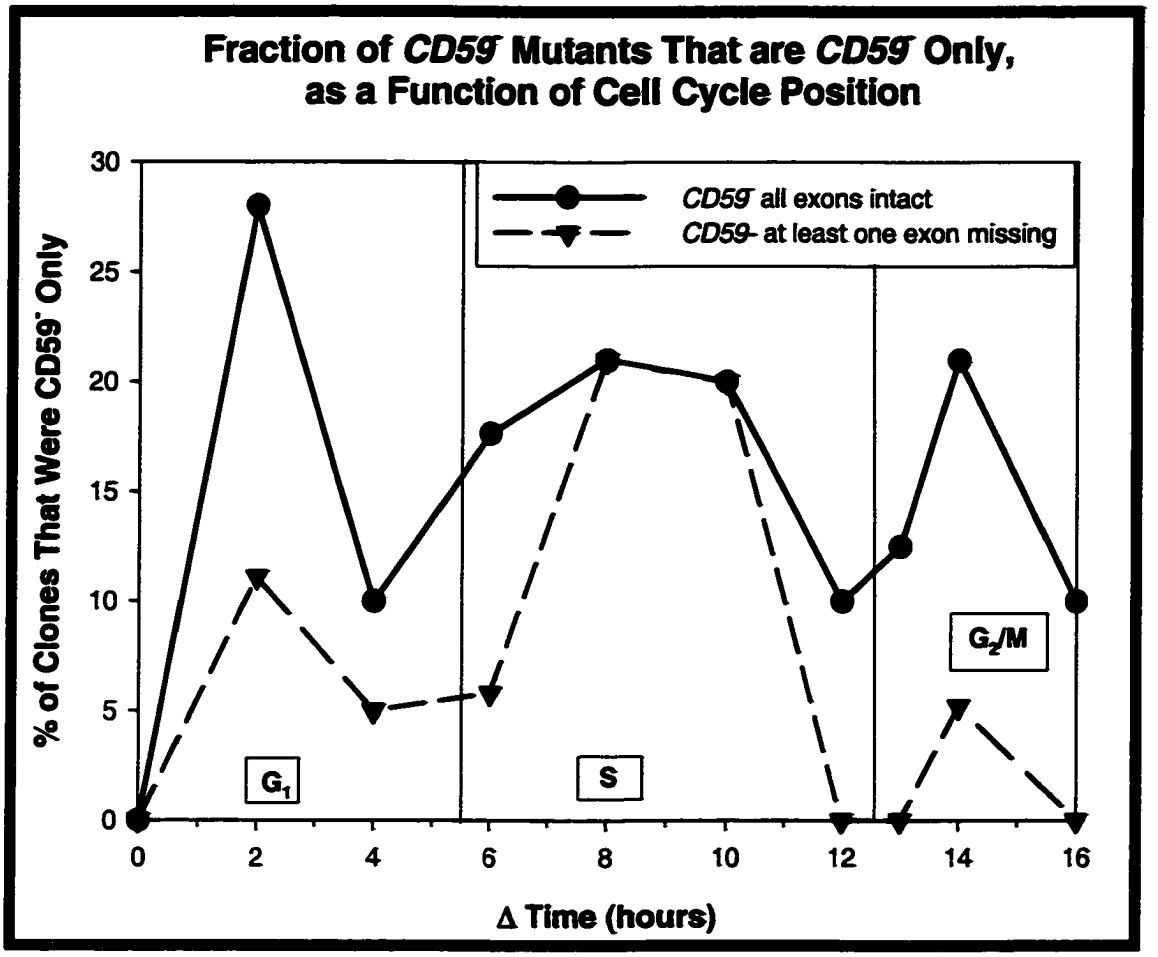

Figure 10. Fraction of *CD59*⁻ mutants that were *CD59*⁻ only (CD59⁻ only = *CD59*⁻ clone that has all other outside markers). The x-axis is the time of irradiation from when the early G_1cells were plated. The percentage of the CD59⁻ only clones from the total clone population at each time is shown on the y-axis. The solid black line represents 24 mutant clones out of a total of 161 that were *CD59*⁻ only at various times in the cell cycle. The dashed red line represents the clones from the population of *CD59*⁻ only clones that were missing one or more of the exons for *CD59*. Out of the population of 24, 13 had one or more of the exons of *CD59* missing. Thus, only 6% of the total irradiated clones had intact *CD59* according to the PCR of the *CD59* exons. These 11 clones with all the *CD59* exons intact could be point mutations or a mutation in a CHO gene needed for *CD59* expression.

These cells either had mutations that were non disruptive to the PCR, had a point mutation, or were missing one of the many genes require to express the GPI anchored CD59 on the cell surface (Kinoshita et al., 1997).

DISCUSSION

Several of the questions raised in the introduction are addressed by this research. The sensitivity to cell killing and mutant induction by ^{137}Cs gamma varies at different points in the cell cycle, but mutant induction does not follow the same pattern through the cell cycle when A_L cells were assayed for HPRT compared to CD59. The specific mutant class (column 1 and 2, Tables 4 and 5) induced by irradiation at each time in the cell cycle is not significantly different within the mutant class. Pooling the mutant clones for each mutant class into cell phases did not show any significant differences within the mutant class for different compartments of the cell cycle. The complicated deletions (mutant class 43) were not significantly different between the cell cycle phases. However, there were significantly more complicated deletions between the historical control cells and the total cells irradiated at different points in the cell cycle. Chromosome damage occurs with ionizing radiation, and the data clearly demonstrates that irradiation at 3 Gy with ^{137}Cs gamma generates many more large deletions than intergenic lesions to the DNA. Thus, in A_L cells irradiated with 3 Gy ^{137}Cs gamma rays, more mutants are induced in G_1 than in S or G_2/M; however, the mutants produced have the same mutant spectra within each mutant class through the cell cycle and the mutations tend to be large Mbp deletions. In addition, the number of mutant classes for irradiated cells through out the cell cycle agrees much more closely with the historic high dose rate

log phase gamma mutant spectra than with the control spontaneous mutation spectra.

Mutant Induction in *CD59* and *HPRT*

The HPRT mutation assay was done with A_L cells in conjunction with the CD59 assay because much data exists for HPRT at different times in the cell cycle. The mutant induction was different at the two loci at different points in the cell cycle, but this was not unexpected. The pattern of *HPRT*⁻ mutant induction in the A_L cells through the cell cycle is similar with the mutant induction in CHO at the *HPRT* locus done with X-rays by Burki (1980). Burki found that the mutants induced by HPRT tended to increase at the G_1/S border, this concurs with the HPRT data with A_L cells in Figure 8. Differences in mutant spectra are also seen with the HPRT assay in different cell types such as WTK1 cells and TK6 cells irradiated with the same dose (Phillips et al., 1995). Leonhardt et al. (1997) found that mutant induction was approximately 4-fold higher when cells were irradiated in G_1 compared to S phase. There are similarities in the shape of the mutant induction with the HPRT and CD59 assays with a minor difference at the G/S border; however the A_L $CD59^-$ assay is approximately 100-fold more sensitive than the HPRT in the same cell.

Spontaneous vs. Radiation Induced Mutants

The A_L cells irradiated with 3 Gy ^{137}Cs gamma had more large deletions than the spontaneous control cells. Others have found that ionizing radiation increases the fraction of total deletions of a gene. Suzuki and Hei (1996) found that *HPRT* total gene deletion increased by more than two-fold with ^{137}Cs gamma rays, and that the induced mutants suffered larger deletions compared to spontaneous mutants. Bao et al., (1995)

showed that deletions were the predominant mutation recovered and large deletions are the main kind of deletion for TK6 cells assayed at the *HPRT* locus for low linear energy transferred (LET) X-rays. These deletions span the entire *HPRT* gene and tend to extend into flanking regions of the gene. X-ray induced mutants were also two fold higher than spontaneous mutants. Okinaka et al. (1993) reported that of the ionizing radiation induced clones selected, 93.75% had partial or total deletions of the *HPRT* gene. Schwartz et al. (2000) found 3 times more deletion mutations than point mutations when cells were irradiated at 3 Gy. They suggested that the dose response for small deletions arose from single events, and the higher doses that cause larger deletions were due to two independent events. I showed in this research that mega-base pair deletions are much more frequent than intragenic mutations in all phases of the cycle. The control spontaneous mutants and the total of phase mutants were significantly different in 11 mutant classes; however, the high dose rate (HDR) gamma log phase cells were significantly different in only 3 mutant classes.

Pattern of Mutant Spectra

The A_L cells that were irradiated with ^{137}Cs gamma were significantly different than the control cells (spontaneous mutants). The mutations were defined into 43 classes, but only a few of the classes dominated. Mutant classes 10, 11, 12, 24, and 38 have a break between D16 and LDHA; these classes include 74/161 (46%) mutants. Another "hot spot" for breaks was found in mutant classes 4, 5, 7, 11, 19, and 21 between CAT and ACP; these classed include 62/161 (38.5%) mutants. The individual mutant classes throughout the cell cycle, produced by irradiating every two hours, showed no significant

differences within the mutant class. Others have reported mutation "hot spots" and non-random damage to cells. Morgan et al. (1990) found that the damage from ionizing radiation results in non-random damage to the chromosomes. Okinaka et al. (1993) reported a radiation specific mutational "hot spot" in exon 3 of *HPRT*. Because the size of the human chromosome in A_L is 160 Mbp, and the chromosome is not essential for cell survival except for a hostage gene near RAS, the entire chromosome provides a canvas to look for large deletion "hot spots" (McGuinness et al., 1995).

Measure of Intragenic mutations

Clones that were selected using the E7.1 antibody and were shown to have all exons for *CD59* present may have had mutations outside of the PCR amplicons that resulted in the CD59 antigen non-expression. To determine this, the *CD59* gene could be sequenced to determine the extent of the loss of the *CD59* genetic material. In addition, other PCR primers could be developed to cover more of the CD59 DNA that contains 27 kb of DNA in 4 exons, encoding a mRNA of 1.2 kb. Rapid PCR light cyclers could be used to screen for point mutations on the exons using existing or new primers. The light cyclers are able to measure PCR products in a quantitative manner. At the end of the PCR cycles, the temperature of melting of the amplicons may be measured. Single base pair changes would result in a minor shift of the melting point because of a change in the hydrogen bonding.

Repair at Different Times in the Cell Cycle

Differences in mutation induction may be linked to repair pathways in different phases of the cell cycle. Over 130 repair genes have been described (Wood et al., 2001).

Many of these repair enzymes work in different parts of the cell cycle due to their activation by cyclin dependent kinases (Yu et al., 1999). Mismatch repair enzymes are active and work to repair DNA during replication and recombination (Wood et al, 2001). The structure of the chromatin must at times allow and control access to DNA during gene transcription. Many chromatin-remodeling complexes are known and are active at different times (Vignali et al., 2000). One of the reasons that we get such high mutant induction in A_L cells irradiated in early G_1 may be due to the fact that just after mitosis the DNA is still tightly packed and repair enzymes may not have access to the damage. Leonhardt et al. (1998) demonstrated that repair is preferential in S in human bladder carcinoma cells. They showed that residual damage in progeny persisted longer in S phase irradiated cell than in G_1 cells. In looking for the mechanism of this differential, they found 10-fold more errors in the mRNA from G_1 cells irradiated with 6 Gy than with irradiated S phase cells. Using reverse transcriptase PCR, they found more splice errors and deletions preferentially induced during G1 (Leonhardt et al., 2000). Other repair enzymes such as Ku, which functions in DNA repair, varies widely through the cell cycle (Novac et al., 2001). Variations in mutant spectra may be explained with regards to the state of DNA repair, DNA replication, and transcription that exists among these phased populations, and may affect the cells susceptibility to mutation and ultimately carcinogenesis.

Relevance of Cell Cycle Mutation Measurement to Radiation Risk

Both epidemiology data from actual exposures and radiobiological data based on laboratory experiments should be used for determining risk from radiation exposure.

Mutant assays can provide some the necessary laboratory studies to elucidate types of DNA damage and repair pathways. To understand the damage from ionizing radiation and the cell risk, researchers need to look at metabolic processes initiated during the life of the cell, what repair enzymes are activated, and at what time. We need to understand the damage pathways and what is happening at the chromosomal and nucleic acid level, what their state of condensation is, and what is the repair capability of the cell is in different cell cycle phases. With most of our body cells, if they are in G1 or G_0, then they are in danger of accumulating more damage and thus more mutations. If we are more susceptible to DNA damage because our cells are primarily in G_1, then radiation risk assessment and recommended dose limits for individuals may be dangerously high.

References

National Academy Press (1990) Health Effects of Exposures to Low Levels of Ionizing Radiation: BEIR V.,pp. 1-421., Washington, D.C.

Ames, B. N. (1971) The detection of chemical mutagens with enteric bacteria. In: Chemical Mutagens: Principles and Methods for Their Detection (Vol. 1) (Hollaender, A., ed.), pp. 267-288. Plenum Press, New York.

Bao, C. Y., Ma, A. H., Evans, H. H., Horng, M. F., Mencl, J., Hui, T. E., & Sedwick, W. D. (1995) Molecular analysis of hypoxanthine phosphoribosyltransferase gene deletions induced by alpha- and X-radiation in human lymphoblastoid cells. Mutat.Res. 326: 1-15.

Benzer, S. & Freese, E. (1958) Induction of specific mutations with 5-bromouracil. Proc.Natl.Acad.Sci.USA 44: 112-119.

Bishop, J. M. (1987) The molecular genetics of cancer. Science 235: 305-311.

Burki, H. J. (1980) Ionizing radiation-induced 6-thioguanine-resistant clones in synchronous CHO cells. Radiat.Res. 81: 76-84.

Capon, D. J., Chen, E. Y., Levinson, A. D., Seeburg, P. H., & Goeddel, D. V. (1983) Complete nucleotide sequences of the T24 human bladder carcinoma oncogene and its normal homologue. Nature 302: 33-37.

Chuang, Y. Y. & Liber, H. L. (1996) Effects of cell cycle position on ionizing radiation mutagenesis. I. Quantitative assays of two genetic loci in a human lymphoblastoid cell line. Radiat.Res. 146: 494-500.

Croce, C. M. & Klein, G. (1985) Chromosome translocations and human cancer. Sci.Am. 252: 54-60.

Fouladi, B., Waldren, C. A., Rydberg, B., & Cooper, P. K. (2000) Comparison of repair of DNA double-strand breaks in identical sequences in primary human fibroblast and immortal hamster-human hybrid cells harboring a single copy of human chromosome 11. Radiat.Res. 153: 795-804.

Grosovsky, A. J. & Little, J. B. (1985) Evidence for linear response for the induction of mutations in human cells by x-ray exposures below 10 rads. Proc.Natl.Acad.Sci. USA 82: 2092-2095.

Gustafson, D., Trotter, B., Snead, D., & Waldren, C. (1997) Expression of human O^6-methyl guanine methyl transferase (MGMT) in post replication repair (PRR) deficient CHO-UV-1 cells: compensation for hypersensitivity to methylating and ethylating agents but not to mitomycin C. Somat.Cell Mol.Genet. 23: 9-17.

Hall, E. J. (1988) Radiobiology for the Radiobiologist Lippencott, Philadelphia.

Ham, R. G. (1965) Clonal growth of mammalian cells in a chemically defined medium. Proc.Natl.Acad.Sci.USA 53: 288-293.

Hei, T., Piao, C. Q., He, Z. Y., Vannais, D., & Waldren, C. A. (1992) Chrysotile fiber is a strong mutagen in mammalian cells. Cancer Res. 52: 6305-6309.

Hei, T. K., Hall, E. J., & Waldren, C. A. (1988) Mutation induction and relative biological effectiveness of neutrons in mammalian cells. Radiat.Res. 115: 281-291.

Hei, T. K., Wu, L.-J., Liu, S.-X., Vannais, D., Waldren, C., & Randers-Pehrson, G. (1997) Mutagenic effects of a single and an exact number of alpha particles in mammalian cells. Proc.Natl.Acad.Sci.USA 94: 3765-3769.

Innis, M. A., Gelfand, D. H., Sninsky, J. J., & White, T. J. (1990) PCR Protocols: A Guide to Methods and Applications Academic Press, San Diego, CA.

Karathanasis, S. K., Zannis, V. I., & Breslow, J. L. (1983) Isolation and characterization of the human apolipoprotein A-I gene. Proc.Natl.Acad.Sci.USA 80: 6147-6151.

Kinoshita, T., Ohishi, K., & Takeda, J. (1997) GPI-anchor synthesis in mammalian cells: genes, their products, and a deficiency. Journal of Biochemistry 122: 251-257.

Kronenberg, A. & Little, J. B. (1989) Molecular characterization of thymidine kinase mutants of human cells induced by densely ionizing radiation. Mutat.Res. 211: 215-224.

Kunkel, T. A. (1990) Misalignment-mediated DNA synthesis errors. Biochemistry 29: 8003-8011.

Leonhardt, E. A., Trinh, M., Forrester, H. B., Johnson, R. T., & Dewey, W. C. (1997) Comparisons of the frequencies and molecular spectra of HPRT mutants when human cancer cells were X-irradiated during G_1 or S phase. Radiat.Res. 148: 548-560.

Leonhardt, E. A., Trinh, M., Forrester, H. B., & Dewey, W. C. (1998) Persistent decrease in viability as a function of X irradiation of human bladder carcinoma cells in G_1 or S phase. Radiat.Res. 149: 343-349.

Leonhardt, E. A., Trinh, M., Chu, K., & Dewey, W. C. (2000) Mutations induced in the HPRT gene by X-irradiation during G_1 or S: analysis of base pair alterations, small deletions, and splice errors. Mutat.Res. 471: 7-19.

Maniatis, T., Fritsch, E. F., & Sambrook, J. (1982) Molecular cloning: a laboratory manual. Cold Spring Harbor Laboratory, Cold Spring Harbor, NY.

Matsukura, N., Willey, J., Miyashita, M., Taffe, B., Hoffmann, D., Waldren, C., Puck, T. T., & Harris, C. C. (1991) Detection of direct mutagenicity of cigarette smoke condensate in mammalian cells. Carcinogenesis 12: 685-689.

McGuinness, S., Shibuya, M., Ueno, A., Vannais, D., & Waldren, C. (1995) Mutant quantity and quality in mammalian cells (A_L) exposed to ^{137} gamma radiation: effect of caffeine. Radiat.Res. 142: 247-255.

Miller, J. H. & Low, K. B. (1984) Specificity of mutagenesis resulting from the induction of the SOS system in the absence of mutagenic treatment. Cell 37: 675-682.

Miller, S. A., Dykes, D. D., & Polesky, H. F. (1988) A simple salting out procedure for extracting DNA from human nucleated cells. Nucl.Acids Res. 16: 1215-1219.

Mitchell, A. R., Gosden, J. R., & Miller, D. A. (1985) A cloned sequence, p82H, of the alphoid repeated DNA family found at the centromeres of all human chromosomes. Chromosoma 92: 369-377.

Morgan, T. L., Fleck, E. W., Poston, K. A., Denovan, B. A., Newman, C. N., Rossiter, B. J., & Miller, J. H. (1990) Molecular characterization of X-ray-induced mutations at the HPRT locus in plateau-phase Chinese hamster ovary cells. Mutat.Res. 232: 171-182.

Muller, H. J. (1927) Artificial transmutation of the gene. Science 66: 84-87.

Nelson, S. L., Giver, C. R., & Grosovsky, A. J. (1994) Spectrum of X-ray-induced mutations in the human hprt gene. Carcinogenesis 15: 495-502.

Novac, O., Matheos, D., Araujo, F. D., Price, G. B., & Zannis-Hadjopoulos, M. (2001) In vivo association of Ku with mammalian origins of DNA replication. Mol.Biol.Cell 12: 3386-3401.

Okinaka, R. T., Anzick, S. L., Oller, A., & Thilly, W. G. (1993) Analysis of large X-ray-induced mutant populations by denaturing gradient gel electrophoresis. Radiat.Res. 135: 212-221.

Okinaka, R. T., Anzick, S. L., and Thilly, W. G. Denaturing gradient gel electrophoretic analysis of specific exons of the HPRT gene from X-ray induced mutant populations. Chadwick, K. H., Cox, R., Leenhouts, H. P., and Thacker, J. 151-156. 1994. The Netherlands, European Comission of Radiation Protection. Molecular mechanisms in radiation mutagenesis and carcinogenesis.

Pelletier, J., Bruening, W., Kashtan, C. E., Mauer, S. M., Manivel, J. C., Striegel, J. E., Houghton, D. C., Junien, C., Habib, R., Fouser, L., Fine, R. N., Silverman, B. L., Haber, D. A., & Housman, D. (1991) Germline mutations in the Wilms' tumor suppressor gene are associated with abnormal development in Denys-Drash syndrome. Cell 67: 437-447.

Phillips, E. N., Xia, F., Kelsey, K. T., & Liber, H. L. (1995) Spectra of spontaneous and X-ray-induced mutations at the *hprt* locus in related human lymphoblast cell lines that express wild- type or mutant p53. Radiat.Res. 143: 255-262.

Puck, T. T. & Waldren, C. A. (1987) Mutation in mammalian cells: Theory and implications. Somat.Cell Mol.Genet. 13: 405-409.

Quan, F., Korneluk, R. G., Tropak, M. B., & Gravel, R. A. (1986) Isolation and characterization of the human catalase gene. Nucl.Acids Res. 14: 5321-5335.

Ritenour, E. R., Braaton, M., Harrison, G. H., Ueno, A., Gadd, M., Manco-Johnson, M., Parker, R. D., Shih, S., & Waldren, C. A. (1991) Absence of mutagenic effects of continuous and pulsed ultrasound in cultured (A_L) human-hamster hybrid cells. Ultrasound in Med.& Biol. 17: 921-930.

Rowley, J. D. (1990) Recurring chromosome abnormalities in leukemia and lymphoma. Semin.Hematol. 27: 122-136.

Sandberg, A. A., Turc-Carel, C., & Gemmill, R. M. (1988) Chromosomes in solid tumors and beyond. Cancer Res. 48: 1049-1059.

Schwartz, J. L., Jordan, R., Sun, J., Ma, H., & Hsieb, A. W. (2000) Dose-dependent changes in the spectrum of mutations induced by ionizing radiation. Radiat.Res. 153: 312-317.

Shibuya, M. L., Ueno, A. M., Vannais, D. B., Craven, P. A., & Waldren, C. A. (1994) Megabase pair deletions in mutant mammalian cells following exposure to Amsacrine, an inhibitor of DNA Topoisomerase II. Cancer Res. 1092-1097.

Shows, T. B., Alders, M., Bennett, S., Burbee, P., Cartwright, P., Chandrasekharappa, S., Cooper, P., Courseaux, A., Davies, C., Devignes, M.-D., Devilee, P., Elliott, R., Evans, G., Fantes, J., Garner, H., Gaudray, P., Gerhard, D. S., Gessler, M., Higgins, H., Hummerich, H., James, M., Lagercrantz, J., Litt, M., Little, P., Mannens, M., Munroe, D., Nowak, N., O'Brien, S., Parker, N., Perlin, N., Reid, L., Richard, C., Sawicki, M., Swallow, D., Thakker, R., Van Heyningen, V., van Schothorst, E., Vorechovsky, I., Wadelius, B., Weber, B., & Zabel, B. (1996) Report of the fifth international workshop on human chromosome 11 mapping (1996). Cytogenet.Cell Genet. 74: 1-56.

Sinclair, W. K. Dependence of radiosensitivity upon cell age. Proceedings of the Carmel Conference on Time and Dose Relationship in Radiation Biology as Applied to Radiotherapy, 97-107. 1969. Upton, NY, BNL Report 50203 [C-57].

Smith, M. W., Clark, S. P., Hutchinson, J. S., Wei, Y. H., Churukian, A. C., Daniels, L. B., Diggle, K. L., Gen, M. W., Romo, A. J., Lin, Y., & . (1993) A sequence-tagged site map of human chromosome 11. Genomics 17: 699-725.

Suzuki, K. & Hei, T. K. (1996) Mutation induction in gamma-irradiated primary human bronchial epithelial cells and molecular analysis of the HPRT$^-$ mutants. Mutat.Res. 349: 33-41.

Tindall, K. R., Stein, J., & Hutchinson, F. (1988) Changes in DNA base sequence induced by gamma-ray mutagenesis of lambda phage and prophage. Genetics 118: 551-560.

Vignali, M., Hassan, A. H., Neely, K. E., & Workman, J. L. (2000) ATP-dependent chromatin-remodeling complexes. Mol.Cell Biol. 20: 1899-1910.

Waldren, C. A. (1983) Mutational analysis in cultured human-hamster hybrid cells. In: Chemical Mutagens: Principles and Methods for Their Detection, Vol. 8 (de Serres, F. J., ed.), pp. 235-260. Plenum, New York.

Waldren, C. A., Correll, L., Sognier, M. A., & Puck, T. T. (1986) Measurement of low levels of x-ray mutagenesis in relation to human disease. Proc.Natl.Acad.Sci.USA 83: 4839-4843.

Waldren, C. A., Fouladi, B., Braaton, M., Parker, R. D., & Vannais, D. (1992) The use of human repetitive DNA to target selectable markers into only the human chromosome of a human/hamster hybrid cell Line (A_L). Somat.Cell Mol.Genet. 18: 417-422.

Waldren, C. A., Ueno, A. M., Schaeffer, B. K., Wood, S. G., Sinclair, P. R., Doolittle, D. J., Smith, C. J., Harvey, W. F., Shibuya, M. L., Gustafson, D. L., Vannais, D. B., Puck, T. T., & Sinclair, J. F. (1999) Mutant yields and mutational spectra of heterocyclic amines MeIQ and PhIP at the S1 locus of human-hamster A_L cells with activated by chick embryo liver (CELC) co-cultures. Mutat.Res. 425: 29-46.

Wilson, A. B., Seilly, D., Willers, C., Vannais, D. B., McGraw, M., Waldren, C. A., Hei, T. K., & Davies, A. (1999) Antigen S1, encoded by the MIC1 gene, is characterized as an epitope of human CD59, enabling measurement of mutagen-induced intragenic deletions in the AL cell system. Somat.Cell Mol.Genet. 25: 147-157.

Wood, R. D., Mitchell, M., Sgouros, J., & Lindahl, T. (2001) Human DNA repair genes. Science 291: 1284-1289.

Yu, Z., Chen, J., Ford, B. N., Brackley, M. E., & Glickman, B. W. (1999) Human DNA repair systems: an overview. Environ.Molec.Mutagen. 33: 3-20.

Yunis, J. J. (1983) The chromosomal basis of human neoplasia. Science 221: 227-236.

Zhu, L. X., Waldren, C. A., Vannais, D., & Hei, T. K. (1996) Cellular and molecular analysis of mutagenesis induced by charged particles of defined LET. Radiat.Res. 145: 251-259.